JPRS-CST-94-014
24 August 1994

FOREIGN BROADCAST INFORMATION SERVICE

JPRS Report

Science & Technology

China

Science & Technology
China

JPRS-CST-94-014 CONTENTS 24 August 1994

Science and Technology

Science and Technology Policy

Academy of Elite Engineers Established in Beijing *[CHINA DAILY, 4 Jun 94]* 1
State Allocates $54 Billion To Modernize 'Bottleneck' Industries *[CHINA DAILY, 2 Jun 94]* 1
China Puts Efforts on Intellectual Property Rights Protection *[CHINA DAILY, 23 May 94]* 2
China Deepening Science and Technology System Reform
[Beijing ZHONGGUO HUANJING BAO, 5 Apr 94] 3
Levels of High-Tech Industries Investment and Management Mechanism
[Xia Mu; KEYAN GUANLI, No 1, Jan 94] 4
Protecting China's S&T Secrets Said Critical *[YUNNAN RIBAO, 7 May 94]* 9
The Joint Stock System in China's High-Tech Industry Development *[KEJI RIBAO, 11 Apr 94]* .. 12

Advanced Materials and Superconductivity

Newest Reports on Nanomaterials 14
Fe-Matrix Nanocrystalline Alloys
[Liu Xuedong, Hu Zhuangqi, et al.; KEXUE TONGBAO, Vol 39 No 5, 1-15 Mar 94] 14
DSC Analysis of Mo, Mo_2N, Ti, TiN Nanoscale Solids
[Zhu Yong; KEXUE TONGBAO, Vol 39 No 5, 1-15 Mar 94] 16
Ultrahigh-Melting-Point Nanoscale Metal Carbides
[Liu Lin, Li Bing, et al.; KEXUE TONGBAO, Vol 39 No 5, 1-15 Mar 94] 17
Growth, Spectral Characteristics of Halite ZnO Nanoparticles
[Zou Bingsuo, Wang Bin , et al.; KEXUE TONGBAO, Vol 39 No 6, 16-31 Mar 94] 20
Preparation, Thermal Stabilization of β-Sn Ultrafine Powder
[Yang Wenping, Xue Desheng, et al.; KEXUE TONGBAO, Vol 39 No 6, 16-31 Mar 94] 23
W/Si, WSi_2/Si, W/TiN Nanoscale Multilayer Films
[Liu Wenhan, Zhou Lingyun, et al.; KEXUE TONGBAO, Vol 39 No 7, 1-15 Apr 94] 25
Size Dependence on Ferroelectric Phase Transition in $PbTiO_3$ Nanoscale Particles
[Zhang Peilin, Jiang Bin, et al.; GUISUANYAN XUEBAO, No 2, Apr 94] 27
World's First Low-Cost Process for Making Kg-Class Metallic Nanomaterials Invented
[Yuan Xiaoyang; KEJI RIBAO, 18 Jun 94] 32
Study of High-Speed CVD for C/C Composite: High-Speed Directional Diffuse Technology
[Luo Ruiying, Yang Zheng, et al.; GAO JISHU TONGXUN, No 2, Feb 94] 32
Microstructure, Interface of SiCp/Al Composites
[Geng Lin, Yao Zhongkai, et al.; GAO JISHU TONGXUN, No 4, Apr 94] 34
Preparation of TiC-Ni_3Al Matrix Composites by SHS Technique
[Mei Bingchu, Yuan Runzhang; GUISUANYAN XUEBAO, No 2, Apr 94] 37

Aerospace

HK Aerospace Firm To Be Link to Overseas Market *[Liu Weiling; CHINA DAILY, 6 Jun 94]* 41
Transfer of Aerospace Technology to Civilian Sector Still Needs 'Catalyst'
[Guo Xiao; JINGJI RIBAO, 10 Apr 94] 42
Beijing Aeronautical Technology Research Center Profiled
[Wu Qingrong; GUOJI HANGKONG, No 5, May 94] 43

Biotechnology

World's First Attenuated Live Encephalitis Vaccine Developed *[JIAN KANG BAO, 13 May 94]* .. 44
New Bone Grafting Material Developed *[JIAN KANG BAO, 8 May 94]* 44
Cloning of Hepatitis D Genome Said Successful *[Beijing JIAN KANG BAO 20 Apr 94]* 44

China Becomes World's Largest Vaccine-Producing Nation
[Beijing JIAN KANG BAO 26 Apr 94] 44
Ciba-Geigy To Expand Business in China *[CHINA DAILY 7 Jun]* 44
Results in Genetic Research Said Fruitful *[CHINA DAILY, 3 Jun 94]* 45
New Diagnostic Method To Detect Cancer in Early Stage Developed
[CHINA DAILY, 3 Jun 94] 45
Hangzhou To Become Base for Biotech Research *[CHINA DAILY, 30 May 94]* 46

Computers

Efficient Implementation on YH Supercomputers of Library for Large Sparse Linear Algebraic Iterations
[He Xinfang, Hu Qingfeng, et al.; GUOFANG KEJI DAXUE XUEBAO, Mar 94] 47
Digital Logic Design Expert System Unveiled *[Li Wei; KEJI RIBAO, 16 Jun 94]* 51
Neural Information Processing System Certified
[Zhang Ling; ZHONGGUO KEXUE BAO, 24 Jun 94] 51

Lasers, Sensors, Optics

Latest Reports on Optical Computing 51
Optical Image Fuzzy Associative Memory
[Zhang Shuqun, Chen Caisheng; ZHONGGUO JIGUANG, Mar 94] 51
Full-Permutation Nonblocking Double Omega Interconnection Network
[Luo Fengguang, Xu Jun et al.; ZHONGGUO JIGUANG, Mar 94] 52
Equivalent Optically Interconnected Perfect Shuffle/Exchange Network
[Luo Fengguang, Cao Mingcui et al.; HUAZHONG LIGONG DAXUE XUEBAO, Mar 94] . 53
Nonblocking Banyan Four-Port Switching Network
[Li Hongpu, Cao Mingcui et al.; GUANGXUE XUEBAO, Apr 94] 54
Associative Memory with "Cat" Self-Pumped Phase Conjugator
[Zhang Jingwen, Zhao Hua et al.; GUANGXUE XUEBAO, Apr 94] 54
Fabrication of Microlens Array Using Photosensitive Glass
[Luo Fengguang, Cao Mingcui et al.; GUANGXUE JISHU, May 94] 56
Growth, Holographic Storage Properties of Ce: Fe: $LiNbO_3$ Crystal
[Li Minghua, Jia Xiaolin et al.; GUISUANYAN XUEBAO, Apr 94] 56

Microelectronics

0.6-Micron $TiSi_2$ Polycide LDD MOS Process Studied, 31-Stage Ring Oscillator Fabricated
[Xu Qiuxia, Gong Yiyuan et al.; BANDAOTI XUEBAO, May 94] 57
Chinese R&D of Microactuators Compared to U.S., Japanese Levels
[Cai Hegao, Sun Lining, et al., GAO JISHU TONGXUN, May 94] 57
Domestically Made Flat-Panel VFDs Compared With Imported Displays
[Ruan Shiping; YIQI YIBIAO XUEBAO, No 2, May 94] 59
Wuxi Microelectronics Expansion Passes Acceptance Check
[Gao Lihua; JISUANJI SHIJIE, 6 Jul 94] 60
Nation's First LED Chip Production Line Operational
[Luo Laiping; ZHONGGUO DIANZI BAO, 11 Jul 94] 60

Telecommunications

Newest Reports on Information Highway 61
AT&T Co-Hosts Telecom Clinic *[Liu Weiling; CHINA DAILY, 12 Jul 94]* 61
Communications Ministry To Build Info Highway
[Gao Jin'an; CHINA DAILY, 20 Jul 94] 61
New Telecom Provider To Build Own Network *[Pei Jianfeng; CHINA DAILY, 25 Jul 94]* .. 62
Beijing-Taiyuan-Xian Fiber Optic Cable Trunk Line Construction Begun
[Jiang Guoqiang; ZHONGGUO DIANZI BAO, 17 Jun 94] 63
Beijing-Wuhan-Guangzhou Fiber Optic Cable Trunk Line Construction to Begin Soon
[Chen Bingguang; RENMIN RIBAO OVERSEAS EDITION, 19 Jul 94] 63
Shanghai Firm, AT&T to Jointly Construct Intelligent Buildings
[Qian Weihua; WEN HUI BAO, 28 Jun 94] 63

Three Gorges Development Corp. to Get "Intelligent Building" HQ
[Song Yi; JISUANJI SHIJIE, 6 Jul 94] 63
Chongqing to Build 800-MHz Trunking Communications System
[Yu Ruming; ZHONGGUO DIANZI BAO, 4 Jul 94] 63
General Instruments Corp. Supplies DigiCipher Technology
[Wang Yong; CHINA DAILY, 11 Aug 94] 64

Physics

Selective Photoionization of Isotopic Atoms via Pulsed Lasers
[Dai Changjian, Yu Changjiang; WULI XUEBAO, Mar 94] 64
Soft X-ray Lasing in Neon-Like Germanium Plasma Produced by Double-Pulse Laser of Lower Energy
[Huang Wenzhong, Zhang Qiren, et al.; QIANG JIGUANG YU LIZI SHU, Vol 6 No 2, May 94] 66
Microwave Pulse Generation by Photoconductive Switching
[Yang Zixiang, Miao Tieying, et al.; QIANG JIGUANG YU LIZI SHU, Vol 6 No 2, May 94] 66
Particle Simulation of Dual-Beam Side-Shot Vircator
[Wang Zhixiong, Guo Yonghui, et al.; QIANG JIGUANG YU LIZI SHU, Vol 6 No 2, May 94] ... 66
Numerical Calculation of REB Diode, Experimental Research
[Zhang Dong, Yang Dawei, et al.; QIANG JIGUANG YU LIZI SHU, Vol 6 No 2, May 94] 66
Performance Improvements of 3.3 MeV LIA
[Deng Jianjun, Ding Bonan, et al.; QIANG JIGUANG YU LIZI SHU, Vol 6 No 2, May 94] 66
Experimental Investigation of Large-area Diode for Hundred-joule KrF Laser
[Ma Weiyi, Wang Youtian, et al.; QIANG JIGUANG YU LIZI SHU, Vol 6 No 2, May 94] 67
Lanzhou Heavy Ion Accelerator Achieves Maximum Design Targets
[Song Wenjie; ZHONGGUO KEXUE BAO, 20 May 94] 67

Energy

National Developments

Figures in on Power Production for First Half of '94
[JINGJI RIBAO [ECONOMIC DAILY], 7 Jul 94] 68
Closer Ties With French Power Up Electricity Industry
[Chang Weimin; CHINA DAILY (Economics), 7 Jul 94] 68
Outlook for Nation's Electric Power Summarized
[Huang Xi; ZHONGGUO DIANLI, No 4, 5 Apr 94] 68
Suggestions for Development of Clean Coal Technologies
[Zhang Mingyao, Li Daji, et al.; DONGLI GONGCHENG, Vol 14 No 2, 14 Apr 94] 70
Foreign Investment Helps Ease Energy Bottleneck in Fujian
[Chen Yong; FUJIAN RIBAO, 30 Mar 94] 74
Work Begins on Main Portion of Three Gorges
[Shi Yongfeng, Jin Min; RENMIN RIBAO OVERSEAS EDITION, 25 Apr 94] 74

Power Network

Inner Mongolia—Hebei Transmission Line *[Wang Sheng; NEIMENGGU RIBAO, 23 Feb 94]* 75

Hydropower

700MW Generators for Three Gorges *[Xiang Datian; SICHUAN RIBAO, 22 Apr 94]* 75
Prospects for Hydropower Development in Sichuan
[Cao Hong, Xiong Dabin; SICHUAN RIBAO, 12 May 94] 75
Tianhuangping: 'Regulator' for East China Power Grid
[Tang Huiching, Zhang Kecheng; ZHEJIANG RIBAO, 1 Jun 94] 76
Hydropower Development in Northwest Hubei
[Yuan Zhenghong, Huang Xing; RENMIN RIBAO OVERSEAS EDITION, 6 Jul 94] 77
Xizang To Have 1 Million Kilowatts in Installed Capacity by End of Century
[Zhang Dan, Duo Qiuong; RENMIN RIBAO OVERSEAS EDITION, 27 Jun 94] 78
Pubugou: Another Massive Station on the Dadu River *[SICHUAN RIBAO, 5 Jul 94]* 78

Thermal Power

Haibowan Power Plant Goes Into Commercial Operation
[Li Kexin; NEIMENGGU RIBAO, 23 Feb 94] 78
U.S.-China Joint Investment in Shanxi Power Plant *[Du Jucai; SHANXI RIBAO, 13 Apr 94]* 78
Sichuan Develops First 330MW Generator Simulation System
[Xiao Su; SICHUAN RIBAO, 27 Apr 94] 78

Coal

Guizhou Set for Large-Scale Exploitation of Coal Resources
[Chen Zhiqiang; RENMIN RIBAO OVERSEAS EDITION, 28 Apr 94] 79
Ningxia Sets Record for Newly Installed Capacity
[Sun Bo; RENMIN RIBAO OVERSEAS EDITION, 2 May 94] 79
Underground Gasification: 'Second Generation' Coal Mining Method
[Gu Derun, Wang Jien; ZHONGGUO KEXUE RAO, 9 May 94] 80
China's Coalbed Methane Resources and Their Exploitation
[Li Yuwei; ZHONGGUO DIZHI, No 4, 13 Apr 94] 80

Oil and Gas

Joint Development of Northern Shaanxi Oil Resources *[He Dao; SHAANXI RIBAO, 15 Apr 94]* .. 85
Modern Pipeline Planned for Sichuan Basin *[Zhou Zeshan; WEN HUI BAO, 4 May 94]* 85
Dagang: New Life for Aging Oil Field
[Man Xuejie, Cong Wenzi; RENMIN RIBAO OVERSEAS EDITION, 3 Jun 94] 86
Development Stepped Up in Western South China Sea
[Chen Bingguang; RENMIN RIBAO OVERSEAS EDITION, 8 Jun 94] 86
Headway in East China Sea Oil Exploration
[Man Xuejie; RENMIN RIBAO OVERSEAS EDITION, 7 Jun 94] 86
China National Petroleum Corporation Opens New Laboratory
[Jiao Nianyou, Zhang Hongmei; RENMIN RIBAO, 13 Jun 94] 87
Prospects for Natural Gas Exploration in Yinggehai Basin
[Zu Jiaqi; TIANRANQI GONGYE [NATURAL GAS INDUSTRY], No 2, 25 Mar 94] 87

Nuclear Power

Conceptual Design of 200MW Nuclear Heating Plant
[Wang Dazhong, Lin Jiagui, et al.; HE DONGLI GONGCHENG, Vol 14 No 4, 15 Aug 93] 93
Inherent Safety Features of 200MW Nuclear Heating Reactor
[Zhang Zuoyi, Gao Zuying, et al.; HE DONGLI GONGCHENG, Vol 14 No 3, 15 Jun 93] 98

Alternative Energy

Direction of Biogas Digester Development Analyzed
[Zhu Jianxiang; XIN NENGYUAN, Vol 16 No 5, 5 May 94] 103

Science and Technology Policy

Academy of Elite Engineers Established in Beijing

40101008C Beijing CHINA DAILY in English 4 Jun 94 p 1

[Article by He Jun: "Academy of Elite Engineers Established in Beijing"]

[Text] An academy of elite engineers has been founded to rally the country's talent and enhance its modernization drive, it was announced yesterday.

And 96 specialists were appointed to the new body, the Chinese Academy of Engineering (CAE), by the government at the academy's inaugural meeting yesterday.

President Jiang Zemin said the new academy will help to realize veteran leader Deng Xiaoping's idea that science and technology are the "number one forces of production."

The appointees will elect the first leaders and approve a CAE constitution during a six-day conference held at Zhongnanhai, the headquarters of the Chinese central government.

A nationwide trawl for more CAE academicians will start after the conference, which is running in tandem with that of the Chinese Academy of Sciences (CAS). The establishment of the CAE will greatly enhance the initiative of engineers across the country and improve the levels of research, design, construction and operation, Jiang said.

Jiang met with the members of the two academies before the conference, accompanied by six other top Chinese leaders—Li Peng, Qiao Shi, Li Ruihuan, Zhu Rongji, Liu Huaqing and Hu Jintao.

He encouraged the two academies to work together closely to modernize science and technology.

He hoped that the close co-operation between China's engineering and science circles would enhance the country's international competitiveness and contribute to the progress of mankind.

The next 60 years would be a historic era for China, Jiang said.

In order to achieve economic progress, social development and general wealth and prosperity China needs to rely on Deng Xiaoping's theory of building socialism with Chinese characteristics and the basic principles of the Party, as well as the scientific and technological progress, he said.

The country's reforms aimed to develop productive forces, he said, which meant developing science and technology.

Premier Li Peng stressed that the on-going reform of the scientific system aimed to help the development of the socialist market economy.

The new system would realize the co-ordinated development of economy, science and technology and society, Li said.

Zhou Guangzhao, President of CAS, encouraged top scientists to provide more suggestions about the country's development.

The central government has invited CAS to give advice on drafting the Ninth Five-Year Plan (1995-2000) and a long-term plan by 2010, according to Zhou.

The academic activities organized by CAS should be more open to society and pay more attention to economic and social issues, he said.

The incumbent 535 CAS academicians will select the first batch of foreign academicians to be appointed to CAS during the conference.

Zhu Guangya was appointed president of the inaugural conference of the CAE.

State Allocates $54 Billion To Modernize 'Bottleneck' Industries

40101008B Beijing CHINA DAILY in English 2 Jun 94 p 1

[Text] China has invested 468 billion yuan ($54 billion) to modernize industry during the first three years of the Eighth Five-Year Plan.

During this 1991-93 period, the government's investments increased at an average annual rate of 38.2 percent, according to a senior official.

Spending has already outpaced the amount invested in the entire previous five-year period (1986-90), when the government provided about 400 billion yuan ($46 billion).

Investments focused on expanding production of State-owned enterprises, the ECONOMIC DAILY quoted Xu Penghang, Vice-Minister of the State Economic and Trade Commission, as saying.

Xu told a national conference on technical innovation in Wuxi, Jiangsu Province, that the government has made great efforts to modernize industry, and thus improve efficiency, the paper reported yesterday.

About 60 percent of the funding was used to develop new products, cut energy consumption and improve product quality.

China gave priority to developing the so-called "bottleneck" industries: Energy plants, producers of raw materials, transport and telecommunications.

Last year, the country poured 111 billion yuan ($12.7 billion) into these industrial areas, more than half of the total for the year.

To maximize the impact, investors took into account inflation, fluctuating foreign exchange rates and investment taxes.

Xu said the country also gave special attention to imports that involved new technology, research and development. The government also monitored what impact imports had on the public's buying habits and how much had to be done to adjust imported equipment to Chinese industrial needs.

During the last two years, the country spent $2.5 billion importing 1,000 industries, including production of video recorders, advanced textile machinery, automobile engines and compressors for air conditioners.

At the beginning of the 1990s, China selected six large industrial cities: Shanghai,, Tianjin, Shenyang, Wuhan, Chongqing and Harbin, for pilot reforms of large and medium-sized State-owned enterprises.

A total of 28.3 billion yuan ($3.3 billion) were spent in the last three years on 1,015 projects in these cities, and 674 of them have been completed. Modernization generated 7.7 billion yuan ($880 million) in additional profits, including $1.5 billion in foreign sales.

China Puts Efforts on Intellectual Property Rights Protection

40101008A Beijing CHINA DAILY (Opinion) in English 23 May 94 p 4

[Article by Huang Zhiling: "China Puts Efforts on Intellectual Property Rights Protection"]

[Text] Protecting intellectual property from unauthorized use is growing in importance in the international community.

And as the value of such arts and scientific goods rise, no place in the world is safe from intellectual fraud.

China was a late-arriver to the protection of intellectual property arena. It only became interested in patent, trademark and copyright issues after its reform and open policy was adopted in the late 1970s.

But within 15 years, it has established a comprehensive legal system for intellectual property protection, said delegates to the International Symposium Intellectual Property Protection held in Beijing over the weekend.

"Intellectual property protection was put on the agenda of Chinese legislators soon after the country decided to adopt the reform and open policy in 1979," said Guo Shoukang, professor of law at the Chinese People's University, who has participated in the drafting of all major intellectual property laws.

China began drafting the Trademark Law in 1979. And since 1982, it has passed the Trademark Law (1982), the Patent Law (1984), the Copyright Law (1991) and the Anti-Unfair Competition Law (1993).

Dr Arpad Bogsch, Secretary-General of the World Intellectual Property Organization (WIPO), said last year, "In the history of intellectual property, China has made these achievements at a speed second to none."

In 1992 and 1993, China revised its Patent Law and Trademark Law respectively. The revised laws bring China's protection of patent and copyright closer to international standards.

In the revised Patent Law, the scope of patentable technologies has been enlarged and the duration of patent rights extended.

"It includes everything except scientific discoveries, rules and methods of mental activities, methods for the diagnosis and treatment of diseases, animal and plant varieties and substances obtained through nuclear fusion," said Ma Lianyuan, deputy director of the Patent Office.

"The duration of patent rights for inventions used to be 15 years. Now it is 20 years," said Ma.

In the revised Trademark Law, harsher penalties have been introduced for violators of trademarks.

The maximum sentence for people counterfeiting registered trademarks used to be three years. But now infringers can be given a sentence ranging from three to seven years. And they will also be fined.

"The penalties are more severe than in other countries," said Li Bida, deputy director of the Trademark Office of the State Administration for Industry and Commerce (SAIC). China has also played an active role in international conventions.

Just when it was setting up its patent system in March 1980, China applied to join the WIPO, and became a member three months later.

"Since then, China has joined many international organizations, including the Paris Convention for the Protection of Industrial Property, the Madrid Agreement on International Registration of Trademarks, the Berne Convention for the Protection of Literary and Artistic Works, the Universal Copyright Treaty and the Patent Co-operation Treaty," said Liu Jiyang, secretary-general of the Chinese Intellectual Property Society.

Li gave an example of trademark protection to illustrate China's determination to protect intellectual property in compliance with domestic laws and the regulations of international organizations.

THE READERS' DIGEST monthly, launched in 1981 by the Gansu Provincial People's Publishing House, was popular with Chinese readers.

Informative and entertaining, it was a top-selling Chinese magazine with a circulation of more than 1 million.

But it never registered its trademark in China. READERS' DIGEST of the United States, on the other hand, had registered in the country.

"The Gansu Publishing House changed the magazine's name to READERS last year in compliance with the ruling by the Trademark Review and Adjudication Board under the Trademark Office of the SAIC," said Li.

He added that the government has been firm in cracking down on the counterfeiting of registered trademarks.

And many Chinese officials have advocated the severe punishment of counterfeiters.

Ren Jianxin, president of the Supreme People's Court, called for penalties for the manufacturing and sales of counterfeited products to be more severe.

Death sentences should be passed on those who deserve it, and anyone who obstructs the fight against counterfeiting must also be punished regardless of who they are, said Ren.

Li described two cases in which China's local administrations for industry and commerce protected foreign trademarks.

In January 1989, the Shenzhen Municipal Administration for Industry and Commerce in Guangdong Province punished six local firms which counterfeited and sold "IBM" computers.

In August 1992, the Guangzhou Municipal Administration for Industry and Commerce in Guangdong penalized a local firm which made nearly 28,000 fake American Polo T-shirts.

"All the counterfeited trademark products were destroyed. The two firms were made to pay fines totalling 1.7 million yuan ($195,000) and 300,000 yuan ($34,000). The fines exceeded the amount of money they had earned as a result of the bogus goods," said Li.

Two years ago China held the first national telephone conference on fighting against counterfeiting registered trademarks.

"In the year following the conference, more than 3,000 people were arrested for counterfeiting registered trademarks, five of them were sentenced to life imprisonment and four were executed," said Li.

Between 1986 to 1993, courts in China handled 3,505 cases involving intellectual property crimes—1,783 involved patent rights, 1,168 copyrights and 554 trademarks.

Last July, the Beijing Higher People's Court and the Beijing Intermediate People's Court set up the country's first intellectual property division in their courts. Since then, higher people's courts and intermediate people's courts in five provinces and eight cities in the country have set up their own intellectual property divisions.

"Those who commit intellectual property offenses must be dealt as criminals and punished accordingly," said Xiao Yang, Minister of Justice.

At the moment, only civil cases can be brought against copyright infringers, while criminal cases are only brought against trademark violators.

"Copyright pirates should be dealt with by the criminal courts," said Xiao.

China Deepening Science and Technology System Reform

94P60291 Beijing ZHONGGUO HUANJING BAO in Chinese 5 Apr 94 p3

[Article by Pan Hongtao [3382 3163 3447]]

[Text] A new plan to implement China's S&T system reform, the 'Implementation Point of Adopting Socialist Market Economy Development and Deepening System Reform', has been jointly released by the State Science and Technology Commission and the State System Reform Commission. The goal of the plan is to implement the the "Agenda 21" strategy, to modernize the research institute system, to develop scientific research organizations that are beneficial to society, and to reform integrated experimental zones that are closely tied to social development. The plan will enhance the integration of S&T and the economy.

Point: It contains eight parts and 34 articles. The eight parts are: overall strategy and measures, to promote restructuring of S&T system and redistribution of S&T personnel, to foster and develop technology market and information market, to vigorously develop civilian S&T enterprises, to promote regional comprehensive reform and development, to create favorable environment for S&T personnel, to promote further opening to the outside world on S&T; to further perfect macroscopic adjustment and control system and S&T legislation system.

Point: Before year 2000, China will map out a basic framework for the new system, which means to form a modern research and development (R&D) system, and to establish an operational mechanism for scientific research and conversion of S&T results. Microscopically, China will establish a modern research institute system, a modern S&T enterprise system and an army of S&T personnel to meet the demands for next century. Macroscopically, China will establish a S&T management system and perfect S&T policy and legislation systems.

Point: China will promote deeper reform based on governmental development strategy that includes the six measures listed in the "Social Development Research, Solution of Problems Encountered in the Economic Development and Environmental Pollution, and

Improvement of Overall Social Development in the Implementation of Agenda 21" and to accelerate integration of S&T and economic development. In term of the establishment of non-profit and socially beneficial research institutes, Article 9 of the plan calls for establishing 5-10 testing bases, which will, under the support of state policy, solicit contributions from whole society and donations from foreign countries to raise their fundings for further development. Article 9 also calls for exploring a mode for developing China's civilian S&T organizations.

Point: Where, Article 22 calls for promoting reforms of integrated experimental zones to meet the needs for social development, to provide guidance for a cordinated development of S&T, economy, society and environment and to enhance Chinese people's quality and standard of living. Article 23 calls for promoting the establishment of high- and new-tech industrial development zones and 'Spark Plan' technology aggregration zones, carrying out concurrent reform and development of the integrated experimental zones for the needs of social development, focusing on mapping out trans-century development strategies, establishing high-tech industrial development belts, natural resources-rich industrial development belts and technology business and trade zones on the border based on S&T conditions, resources, and environmental superiority of the coastal regions, border zones, sectors along rivers and areas along main highways and railroads.

Levels of High-Tech Industries Investment and Management Mechanism

94FE0576A Beijing KEYAN GUANLI [SCIENCE RESEARCH MANAGEMENT] in Chinese
Vol 15 No 1, Jan 94 pp 50-55

[Article by Xia Mu [1115 3668], Jiangsu Province, Yancheng Suburban Regional Committee]

[Text] This paper analyzes levels of investment in China's high-tech industries, examines questions concerning investment trends and the investment structure, addresses enforcement in investment management, perfecting investment laws, and provides suggestions for establishment of mechanisms for investment risks and safeguards.

(I)

Although conversion of China's high- and new-technology results to industrial production started out late and small scale, it has developed rather rapidly. The establishment of local economic and technology development zones and S&T organizational system reforms, particularly, have set the conditions for China's high-tech industrialization. This is most evident in the growth and increasing momentum of investments. There are now nearly 10,000 high-tech enterprises and projects in China; investments are up to around 50 billion yuan, and the annual value of industrial output is over 100 billion yuan. In respect of investment levels, there are six divisions overall.

1. State Investments

This mainly refers to investments directly raised and allocated for high-tech projects listed by the state government, and designated loans from special central banks. State investments make up about 10 percent of all investments, and although not large, they occupy a commanding position. One is that the scale of investment is quite large, in general they are in the range of several tens of millions of yuan, some in the hundreds of millions, many in the billions. The second one is that the investment level is high. Most state-level investments are concentrated in the leading technologies, the international front-runners, and domestic pioneer projects. The Beijing positron collider, Wuxi Huajing microelectronics project, and Wuhan rolled-steel technology transformation project are all at or above the advanced world level of late-80s or early-90s, and they will be very instrumental in China's industrial modernization.

2. Local Investments

These are mainly funds raised by prefectural and municipal governments or bank-financed projects that are planned and listed by the provinces, municipalities and regions. There are more local investment projects than national ones, but they are smaller in scale and their investment levels are comparatively lower. High-tech projects under local investments are concentrated mainly in economic and technical development zones along the coasts and rivers. Typically they are under state policy, locally funded, develop at their own expense for their own gain, such as the state-listed high-tech Torch belts including Jiangsu Su-Xi-Chang Zone, the new technology enterprise projects concentrated in the Zhu Jiang Delta Zone, and the fast-rising Shandong Jiaozhou Bay Zone for marine bio-tech industries. They are all state-policy directed, locally financed and developed, and successful. The local investments draw support from schools of higher learning and research units, and depend on urban economic strengths for the development, therefore the high-tech industries get fertile input, and not only do they form local high-tech industrial specialties, but also are outlets for S&T potential, and stimulate combined production-study-research activities.

3. Enterprise Investments

These are mainly what the enterprises can raise by themselves and borrow from foreign creditors. Generally there are two types of investments from enterprises in high technology, one being changes and improvements in traditional industries. Traditional industries still make up 80 percent of the whole economy, but they are technologically backward, they are deficient in talent, money, materials and performance, they lack drive, and

it is impossible for them to realize any rapid growth, nor are they suitable for modernized production. As a result, many enterprises take their own money, and reform traditional processes and backward technology to get them on the high-tech track, and raise their capabilities and quality. The Nanjing Radio Factory is an example: In recent years it raised its own funds, and, throughout, delved into research-manufacturing. It imported a video-recorder production line, a large-screen and multi-system colored-TV production line, and a high-quality TV-satellite receiver system production line, so that this enterprise, which was an old radio electronics enterprise, could be converted to high-tech product development and become a domestic high-tech pioneer, a top gun among electronics enterprises.

4. Foreign Commercial Investments

Foreign commercial and foreign Chinese investors are also changing history and getting into China's high-tech industries, and there are now over 3,000 investors in enterprises and projects. Primarily, there are three forms of such commercial investments, one being direct investment into Chinese high-tech enterprises; for example, Japan, Hong Kong, Europe and America make up the bulk of the investors in Chinese opto-electronics, communications, chemicals, and electronics industries. Another is foreign commercial projects and investments involved in the development of Chinese high-tech industries, like the Nanjing, Wuhan, and Xi'an fiber-optic cable, programmable communications, magnetic-disk technology, high-strength carbon fibers, and medical and bio-engineering projects, all of which are brought in and funded by foreign commercial interests. Yet another is foreign funds used by the Chinese government and business for the development of high-tech industries, which have really helped speed up building of economic and technical development zones in various places.

5. Investments From Schools of Higher Learning and Scientific Research Organizations

The solid and plentiful S&T achievements of China's schools of higher learning and research units also have demonstrated creativity and profitability. As educational and scientific research system reforms progressed, many institutions of higher learning and scientific research units joined in the economic construction effort. They actively participated in the development of high technology, and supplied the armament for converting S&T production strength into economic power, and many high-tech enterprises have made use of their achievements. The famous Beijing Legend Group, Beijing University's Fangzheng ["Founders"] Group, Nanjing University's Biochemical Group, and MMEI 14th Institute's Huaning Electronics Group are all examples of groups whose S&T achievements have been industrialized. The Huaning Group was entrusted by the 14th Institute of MMEI to develop satellite communications, cable TV, large-screen displays, and their associated special devices, and other high-tech products, which have already reached or approached international advanced levels, and have reached an annual production value of over 300 million yuan. The 18-man Nanjing University's Biochemical Plant earned over 1.5 million yuan per man-year, and it has become an important nursery for China's fine chemicals industry.

6. Combined Investments

There are two forms of combined investments: One is two or more units jointly investing in operating some high-tech industry. This includes corporate persons in joint ventures with corporate persons, and joint ventures between corporate persons and natural persons (including privately managed enterprises and those operated by individuals), and Sino-foreign joint ventures. For example, a Chinese character computer-output software was developed through a joint venture of a Beijing scientific research institute that invented a Chinese character-card technology and a Beijing high-tech investment corporation. Their product is now capturing 60 percent of China's software market, and they are starting to export the product. Another is the floating of securities. When state, local, enterprise and scientific research groups find themselves unable to independently complete certain high-tech projects, then they sell securities to domestic and foreign economic and industrial departments, to the general public and individuals to raise money to stay in business, and they also sell discount shares for investing in facilities and technologies.

As China's reforms progress and the market economy develops, the forms of investment in high-tech industries will also develop and change, and the levels will get higher, and that will be helpful to improving industries and the economy, to raising the technical content of products, and making enterprises more competitive at home and abroad. The Shenzhen high-tech industries and their export volumes make up about 30 percent of the overall volumes in export and trade, and besides their absolute growth value, they stimulate improvements in the product structure and increase earnings from exports. According to Shenzhen Economy and Trade Department, the upsurge of high-tech enterprises throughout the city, the change in levels of investment, and the growth in trade benefits are at their highest level ever, and that is putting Shenzhen's economic development in top shape.

(II)

There is no doubt that the investment picture for Chinese high-tech industries is making history, but it is still far behind the daily-changing world scene. The big problem is that the level of investments and the investment structure are not totally sound, they are scattered, redundant, monopolistic, the foreign input level is low, and the foreign funds are not used well. Hereafter, investors in high-tech industries should pay attention to two questions.

1. Pay Closer Attention to Direction of Investment

Making a strategic course-correction toward intensive investment and practical development of high-tech industry the present options.

(1) The direction should be toward a mix of domestic and foreign funds and away from domestic dominance in funding. Investments in Chinese high technology are predominantly internal, and foreign funds are comparatively little used. This has to do with the fast-profits mentality of investors and Chinese perceptions. Foreign investors are mainly after fast bucks from labor-intensive industries and products, and the mid- to low-grade machine and electronics industries and products, and where investments would be large and long-range, they have distinct doubts about the risks in high-tech industries, and there is fear of policy changes that may affect investment returns. There is a great need to go after foreign investments, and the issue of publicizing policy and changing mind sets has to be dealt with. Policies must be dynamic, sustainable, and stable to interest foreign investors in taking a chance on Chinese high-tech industries. It must be recognized that high-tech industries development in the world is so fast that the turnover of technology is increasingly evident. Those high-tech industries that do not go after foreign funds for their development will be losing opportunities and stunting their industrial and technological advancement. It also must be recognized that the key is strong laws, good procedures, and legal protection of intellectual property rights. If China can solve those two problems, then foreign investments will pour in. Now, transnational corporations are keying their investments on the Asian Pacific area, and China is a hot spot for foreign commercial interests. The various localities and departments must seize the opportunity to cooperate with major foreign financial and banking groups and transnational corporations, and get foreign commercial investors more interested in technology-intensive industries and products instead of labor-intensive things, and that will raise the development curve for China's high-tech industries.

(2) Transform monopolies into corporations. Under the planned economic system China's industrial economy was mainly state-owned. In line with that, former investments in high technology and the management authority were mainly concentrated in the national economic sector. In practice it demonstrated that this monopolistic form of economy has restricted investments into high technology, and prevented faster techno-economic development. Fundamental changes are now taking place in China's economy as the planned economy is being replaced by a market economy, and the investment situation is changed commensurately. The government cannot willy-nilly invest in every project that comes along, and many projects must depend on local, departmental, and entrepreneurial sources for their funding. High-tech industries are technology-intensive and investment-intensive industries. Their investments will have to command somewhere around one-half of the total investment scene in China in the future (developed countries are generally about 70 percent, the United States is 80 percent). That is to say, they will need about several hundred billion yuan every year, and that is a big sum. The central and local governments alone will not be able to come up with such astronomical figures, so what it will take is a multi-level multitude of investors: domestic and foreign, central and local, public and collective, private and individual; and while working to get the most out of national and foreign commercial investors, the public and private management and funding potential must be ferreted out, and the maximum value has to be gotten out of those funds. Private holdings in the specialized banks around the country are up to 1 trillion yuan, which is generally referred to as the big tiger, who, once he gets out of his cage, could be bad news. But, if this tiger can be brought into the big industries, including the high-tech industries, which urgently need to be developed, then that tiger can be turned into good news, the investment crunch can be eased, the intransigent industrial structure can be improved to a great extent, and the techno-economic level can be raised.

(3) Change scattered investments into concentrated investments. Scattered investments and redundant construction are a malignancy in China's economic development. There is a lot of independence in the market economic system, which will definitely make the problem worse. This problem also exists in high-tech industry investments. Provincial, municipal, and regional enterprises are clamoring for these projects, and often there are several enterprises engaging in the same project. This creates wasteful competition, and leads to redundant and superfluous industrial activity. This sort of piling on fritters away financial power and materials, and creates wasteful internal competition in the country, provinces, and cities. Therefore, investments must be more concentrated and redundancies be reduced in the high-tech industries, especially in the provinces and cities where there is too much redundancy.

(4) Transform micro into macro. Because of the large investments required, high-tech enterprises start out on a small scale, and gradually accumulate and grow, and that accords with the general law of an industrial economy. But, looking at it on a world scale, industries in advanced countries have broken through this law and start out with large investments and large-scale management. According to the U.S. Boeing Corporation researchers, high technology has its risks, and basically there is no risk in mature technology, so more factories invest in it, and hundreds of companies can spring up in a single night. But, high-tech industries have high cost per unit, and if they work on a grand scale with high volumes of output, and if sales are brisk, then the cost per unit is reduced, and contrarily, it is increased. Therefore, when making their investments, many enterprises think in terms of scale, or when they reach a certain point then they go to broad scale. This way has more competitive

strength, and eventually they can force out weaker enterprises. China's high-tech industries are mostly small scale, some having invested only several 10,000 yuan, their product volume is small and their costs high, their market command is deficient, and they lack competitive strength. The ultimate goal for high-tech industrial development in China must be to invest in scale, intensify management, build group structures, and globalize the market. Investors in key projects, besides using state and local organization funds, should make full use of the financial ability of specialized banks, extend their network into the international arena, get on track with international financial elements, win over more construction funds, and as far as possible, create the conditions for large investments. They must think big in the technology industry.

2. Focus on the Question of Investment Structure

There are three aspects that need attention here. One is starting out high. At present, a good portion of the listed high-tech industrial projects are neither high nor new; they are high-tech alright, but they are not broad in application, have low market potential and do not have future development value. But policy makers have been ignorant and ill-informed investors have invested blindly and taken unwarranted losses. For this reason, in selecting high-technology items, there must be some technical evidence of their value, and they should be shooting for advanced international levels, setting new domestic standards, opening the way to genuine high technology, and have inherent enticements for higher investments. Second is being selective in importation of equipment. China's high-tech industries are lagging behind industrially developed countries and a lot of technology and facilities have to be imported. In the past, many imported projects were successful, but there are plenty of others that did not pan out for a host of reasons, but mainly it was because the imported facilities failed the test. According to the most recent findings of the State Auditing Office, 40 percent of the 1,401 technology reform projects that have been examined do not live up to expected design requirements, and they have borrowed over 2 billion yuan in Asian Bank loans (which represents only a small part of the total for the whole country), and imported facilities make up a major portion of that. Investment requirements for developing high technology are high, and if they cannot get the maximum benefit out of those investments, then the losses for the state, localities and enterprises will be great, so the level of advancement and reliability of imported facilities must be carefully watched. Third is that products must have wide marketability. Large product volumes, faster product sales and investment returns are the key to raising investment returns. The products have to get a foothold in domestic market, international markets have to be opened up, high-tech product exports have to be exported, and efforts must be made to get more foreign exchange for China.

(III)

Under the conditions of China's market economic system, precedents must be given to larger, multi-channeled, multi-level, higher standard investments, and larger organizational systems. Then, a whole set of relevant measures such as investment management, legal protection, risks insurance must come into place.

1. Investment Management Should Be Strengthened First

The minute the high-tech projects are listed, the question of investment management looms. Actions to strengthen investment management, and the scope of management are important conditions for assuring the success of high-tech projects.

On the world scene, because of the special nature of high-tech industries, the governments and relevant departments of the various countries are mindful of the investment management of projects. Generally speaking, high-tech projects and their investments are programmed on the national, county, and city levels, and for important projects, the governments provide not only policy advice and guidance, but also watch over the control of techno-economic actions. As far as factory production and market management and sales, distinctions are made according to the product conditions, and tax and trade policies are issued to make needed adjustments and set standards. In China, after implementing the market economic system, not only was the Enterprise Law put into effect giving full authority to enterprises, necessary controls were also strengthened according to the particulars of the high-tech industry. As respects the development of investment management in high-tech industries, there are four links that must be understood.

(1) Business management is the principal link. Business management includes high-tech development planning, revising policy, macroadjustment, extending credit, policy consultation, resource allocation, information and guidance. Business management layers include central and ministerial committees and corporations, special banks, and the various local participants. In principle, local planning and policy decisions should comply with the overall central scheme of things to avoid major redundancies. But giving consideration to local situations and giving business management some leeway to plan and manage according to local needs is also important. It must be emphasized that managing businesses does not mean running monopolies, but it is cooperating, serving and guiding to prevent the recurrence of the "father and son" type of arrangements of the past.

(2) Group management is a key link. The wave of the future in industrial economic development is the forming of techno-economic groups, which combine large and small enterprises to develop economies of scale. The establishment and management of high-tech enterprise groups should therefore be emphasized. Group management means group elements and enterprise components getting involved in steering group

development, project selection, pooling funds, building enterprises, distributing profits and resolving conflicts. At the heart of group management is the creation of an excellent corps of managers in the organizational structure by bringing representatives of the various investors and members into group management. The ultimate aim is to make full use of the activism of the various economic entities to build on strengths and eliminate weaknesses, join forces in a flagship enterprise, and get tough in the international market.

(3) The corporate entity is a main link. An enterprise is a corporate entity for organizing production and management. From formulating plans, selecting projects, to handling investments and getting products on the market, all are done by the corporate enterprise entity. The key to managing a corporate entity is to have fully independent management authority. Any economic and technical activity, which follows the guidance of state laws and industrial policies, and direction of group development, should be determined by the enterprises. Of course, group corporations and investors have the right to intervene in any irregular economic practices or profit motivation on the part of corporate entities.

(4) On-site management is also an important link. Abroad, on-site management is said to be fundamental to investment payoff. The most glaring and most easily overlooked item in Chinese enterprises today is on-site management. Undelineated investment, negative cash flow, and production delays are all closely linked to indifferent and unstandardized on-site management. A sound management responsibility system, selection of competent managers, improving basic-level management offices, and raising the quality of personnel are the keys to strengthening on-site management. And, at the same time, advanced management experience should be brought in, better management procedures should be worked out, and modern management facilities should be built to make them suitable for high-tech industries.

2. Investment Laws Must Be Perfected

The market economy is an economy governed by laws. High-tech investment should be governed by the laws. Economically developed countries that are developing high-tech industries and paying close attention to investments and profits, do this through sound legal systems, policies, and clearly defined property rights relationships. Although the control structure in China in the past tended to be impractical, it was clear about property rights; public enterprises were state owned and collective enterprises were owned collectively. But now, with the implementation of multi-channeled investments and group management, property rights relationships tend to get muddled, especially the haphazard allocations, which often lead to lopsided profits that not only hurt state property, but also infringe on the real profits of other economic entities. Under present conditions, more attention is paid to non-state-owned entities while state-owned components are ignored, which brings unsecured national revenues. At the same time, because of excessive government interference and faulty guidance and management, investments and profits are not appealing, which also directly or indirectly affects investor's profits all round. Therefore, clearly defined property rights relationships, a good property rights system, and the management of enterprises in accordance with property rights laws, are important to guaranteeing the protection of the basic profits of investors, and they are essential for a robust development of high-tech industries.

It is the experience of European and American countries that high-tech enterprises start out with standard and contractual property rights terms to avoid any conflicts, and to protect the profits of all parties. In China, the key will be to formulate a scientifically sound property rights system amenable to delineating investment particularities and property rights relationships. In the process of strengthening property rights, extra attention must be given to intellectual property rights, especially in transfer of technology and trademark registration; they are particularly important to a healthy development in the high-tech industries.

Tax law is also a vital issue. China has many of them, such as the preferential policies for reduced taxation, especially at the local level where there are competitive three- to five-year tax exemption policies, which are highly voluntary, for getting schools of higher learning and research department projects and foreign commercial investments. National monetary tax revenues have been reduced as a result, causing serious macro-deficits, and precarious local financial situations. In reality, piecemeal tax reductions are not a good way to stimulate economic development. Developed countries do not give advantages to enterprises (including high-tech enterprises and foreign investors), and there is no such thing as arbitrary reduction, they only provide favorable investment environment. So, if China wants to develop high-tech industries, there have to be good tax laws, stronger supervision of tax laws, curbs on the local phenomena of arbitrary relaxation of taxation. This goes for high-tech industries as well: while providing good environment, and where there is a need to give policy advantages, the basic-level tax enforcement departments will be allowed to give certain specific measures of flexibility, without ignoring national interests by letting local profits impinge on state, departmental or foreign profits, otherwise the value of high-tech industrial development to building up the strength of the country will be lost.

3. Once Again, There Has To Be an Investment Risks Insurance System

Investments for high-tech projects are usually quite large, and foreign enterprises generally use about 20 percent of their sales for their high-tech product R&D expenses, and China's should be still higher. There is also some uncertainty about what the high-tech industries are coming up with and what the market wants, which often can lead to economic failure or the possibility of losing investments. There are risks on high-tech investments. Minimizing risks can protect investments and profits, and is also an important way to support high-tech industrial development. High-tech investment-risk funds could be set up with state and local governments paying part, scientific research departments and schools of higher learning paying part from their technology transfer charges, with part of it coming from sales of manufacturing enterprises and marketing elements; other channels could also be taken to raise funds for setting up risk foundations to reimburse investment losses for important technological developments. All national scientific research projects and developmental projects, and enterprises that have their own world-class projects or are involved in new technologies of significance to the country that encounter setbacks and incur losses, and, after having had their risk circumstances evaluated by experts are finally judged to be important to the advancement of national S&T, may then have part of their losses reimbursed by the national or local risk foundation. A form of social insurance could also be implemented, all high-tech enterprises or projects requesting bank loans could buy insurance from an insurance organization and take advantage of the ability of the society to relieve the risks and losses in high-tech industries. Yet another approach is to establish investment-risk corporations or common-investment foundations. Specialized banks, stock markets, and market funds can be used for social amalgamated funds, or joint-stock forms of invese of investment could be used, or ownership shares in enterprises taking over technology could be used to get high profits. These methods have been adopted in such places as Shenzhen and Shanghai and they are getting good results.

Protecting China's S&T Secrets Said Critical

946B0097A Kunming YUNNAN RIBAO in Chinese 7 May 94 p 6

[Article by He Xie [0149 0533]: "Leakage of China's S&T Secrets: An Alert"; from the "Societal Reportage Competition"]

[Text] The competition in science and technology and the fact that science and technology represent wealth indicate the extreme importance of protecting S&T secrets. The conflict between protection of secrets and theft of secrets is steadily intensifying. In the last few years, foreign S&T spies have increased their efforts and activities in China, but because Chinese officials lack a strong secrecy-mindedness in science and technology, they have been unable to guard effectively against the theft of secrets by foreign S&T spies. In addition, they often give secrets away inadvertently, with the result that disclosure of S&T secrets is becoming common, and many of China's advanced processes and research results that are unique in the world have been stolen or otherwise obtained by foreigners, which has caused China great economic loss.

Theft of the "Four Ancestral Secret Methods"

In the course of its history, China, one of the four great ancient civilizations, has created many advanced processes unparalleled elsewhere in the world, which not only have brought prestige and pride to many generations of Chinese, but also have been a steady source of wealth. In recent years, however, many of these technologies, which have been declared national secrets, have been stolen by foreign S&T species, so that the superior ancient products and national treasures bequeathed to us by the motherland have been stolen one by one. The most striking such cases are the internationally important theft of the four "secret ancestral methods."

1. Anhui Xuan Paper.

Xuan paper, produced in Jing County, Anhui Province, has long been famous as the "thousand-year paper" or the "king of papers." In 1915 it won a gold medal at the Panama International Exposition. The meticulous traditional process for making it was declared an S&T secret by Anhui Province in 1985. For years, many foreigners, especially one Japanese company, had coveted the process

for making Xuan paper, and S&T spies were often sent toep;bal;j Xuanzhou to look around. Eventually, the spies noticed a truck bearing the trade mark of the Xuan paper plant in Jing County and began to tail it. When the plant authorities heard of this activity, they realized that visitors with bad intentions had come and resolutely refused their request to visit the plant. In addition, they ordered that the company's trade mark be removed from all trucks to prevent them from being tailed. But the S&T spies were tremendously resourceful and persistent. When they heard that there was a plant in Zhejiang Province that provided support to the Xuan paper plant in Jing county, they at once headed to Zhejiang: there was more than one way to skin a cat. When the Japanese visitors arrived, the officials of the plant in Zhejiang welcomed them, and in the expansive atmosphere of Sino-Japanese friendship, they freely gave the spies the manufacturing process that they had long coveted, telling them every important secret detail down to the concentration of the alkali solution used to boil the starting materials. So that nothing would be unclear, at parting, the plant officials also gave the visitors samples of sandalwood bark, rice husks, and wisteria bark. The Japanese spies departed satisfied. After their departure, the plant in Zhejiang did not receive any good news about future cooperation or an influx of capital: but it was announced somewhere in the Japanese media that in the production of Xuan paper, "Anhui was number 1, Japan number 2, Zhejiang number 3, and Taiwan number 4." The secret of the manufacture of Xuan paper, which had been guarded since the distant past, was finally divulged to the world by the present generation.

2. Enamel cloisonn.

Enamel cloisonné is another one of China's finest products, which sells very well on international markets. A law-breaking Japanese company not only was attracted by the excellence of the process, but also coveted its growing market. When Sino-Japanese relations were restored, it sent S&T spies to China to visit the cloisonné plant. The plant officials had no suspicion that the visitors were thieves; they warmly and generously permitted them to videotape the entire manufacturing process. When the Japanese spies returned home, they immediately set about copying the process. But there were still a few steps that did not work, so they went back to the plant for a second visit. Their Chinese hosts, still unsuspecting, continued to let them steal the secret technique in broad daylight. They patiently explained the details of the processes until everything was clear. But the visitors that had been so warmly welcomed were a source of calamity: 2 years later, the price of the traditional enamel cloisonné that had earned China foreign exchange plummeted. The plant authorities suddenly realized that Japanese-produced cloisonné was cutting heavily into the world market.

3. Silk.

The harness bells of camels along the ancient Silk Road made Chinese silk famous throughout the world and brought wealth to China. Another Japanese company had long been interested in Chinese silk. Externally, the silk manufacturing process seemed simple: place the silkworms on mulberry leaves to feed, then wait until they produce the silk and spin their cocoons. But the whole secret was in unwinding the fine, precious silk threads. In order to acquire this technique, the Japanese country sent a delegation to China, formally inviting the plant's engineers to visit Japan to teach them the silk-making technique. They knew that the Chinese side would refuse, but they prolonged their stay in China, used both soft tactics and persistence, and sent spies everywhere to find out the secrets of silk-making. Once they had obtained the entire technique, they pulled up stakes and went home. Not long after, Japan became the world's number-two silk-producing country.

4. Longxu Alpine Rush Mats.

The Longxu alpine rush mats, produced in a certain Chinese province, have a long history. In the Qing dynasty they were an object of tribute suitable for an emperor. They were first exported in 1953 and were sold in Japan, Hong Kong, Malaysia, Italy and elsewhere. They were recognized as a "unique Chinese handicraft product" at the Leipzig World Handicraft Exposition and were included among Chinese products that were exempt from inspection. The Longxu mats were exported in large numbers and earned China a great deal of foreign exchange.

The fame and wealth of the mats attracted Japanese S&T spies. In the early 1980's, a certain Japanese corporation sent its representatives on a special trip to the province to visit the mat factory and gather information. They inspected the production flow line, were told the details of the process, and took pictures. Within 3 month of their return home, the Japanese built a machine that replaced the manual beating of the rushes.

Subsequently, the Japanese stopped importing Longxu mats from the Chinese province and began to compete with China on world markets. Chinese exports of the mats dropped steadily: by 1985 they had fallen 70 percent from the 1979 figure. The Japanese now have monopolized the international market for Longxu mats, and the Chinese factories that produced them for export have now been closed.

Lessons, anguish, and grief: We must not fail to keep a sharp eye on S&T spies.

Ulterior Motives Behind a Fine Facade

There is a Chinese catch-phrase that runs, "the yellow weasel paying a New Year's visit to the chickens"; the implied final phrase is, "with evil intent." This "paying a New Year's visit" is the pretext. Similarly, when foreign S&T spies come to China to steal secrets, they too adopt all manner of high-sounding pretexts or guises that allow deceit and confer legality, making their objectives difficult to see through and forestall.

Story 1: A U.S. Company's Ulterior Motives. Parker pens, produced in the United States, are an elegant product and are known throughout the world. But China's Yingxiong and Jinxing pens are the world's best in one respect, namely, a polishing technique that enables them to keep their luster. The Parker pen company wanted this technique, so two vice presidents used the guise of a visit and exchange of experience to find out about it. To their surprise, they found that the plant was entirely open to visitors. Elated, they took out their cameras, openly photographing the structure of the Chinese polishing machine and the operations that were performed. They then returned home satisfied, having reaped a splendid harvest.

Story 2: A German Delegation's Pretext. A German delegation visited China on a pleasure trip. This was good. Translators and guides were provided. But as the trip progressed, things seemed odd: when the group visited Beijing, it did not want to visit the Ming Tombs; at Loyang, it did not visit the Longmen Caves; in Chengdu, it ignored the Dujiang Pool; at Leshan, it did not go to see the Buddha statue; and at Hangzhou it was not interested in West Lake. What was going on?

Actually, under the guise of a pleasure trip, the group had come to China to steal valuable botanical specimens. The head of the delegation was a botanist and had been given this assignment. His only interest was plants, and everywhere he went, his only wish was to visit botanical gardens and collect samples and seeds.

After collecting everything assigned, the group was ready to return home successful. But as they were leaving the country, they were stopped by customs officials, who had been alerted by the authorities. A detailed check of all members of the delegation revealed that their camera cases, their clothing, notebooks, envelopes, plastic bags, and plastic boxes contained specimens and seeds of 94 different plants, along with 6 terraria. In accordance with customs regulations, these were confiscated, thus preventing the loss of Chinese wild plant resources to outsiders and preserving national sovereignty.

Although these plant specimens were kept in China, there have been innumerable instances when secrets could not be kept. One example is the earth-shaking disclosure of the secret process for producing the amino acid cystine. China developed the process independently, and the cystine that it produced was highly regarded in international markets and earned a great deal of foreign exchange. As the fame of the product spread and the profits increased, wave after wave of S&T spies came to China under a variety of pretexts, such as observation, fact-finding, arranging for joint operations, or placing orders, and attempted to visit the plant and steal the secret. The plant authorities were unsuspecting and were insufficiently secrecy-minded; they not only warmly welcomed the visitors, but let engineers explain the process in detail and allowed the visitors to observe the production process. The visitors returned home satisfied and rapidly turned their knowledge into production capabilities. Not long afterwards, the cystine market no longer exclusively belonged to China: everyone had the product for sale. Chinese sales of course plummeted, and there has been grievous economic loss.

Handing Over Secrets Leads to Later Regrets

In their dealings with foreign countries, whether during exchange activities, in discussions, when writing papers, or when presenting gifts, as a result of insufficient secrecy-mindedness, Chinese personnel often unintentionally leak important economic and technical secrets.

In particular, as a result of a period of erroneous propaganda guidance, some S&T personnel have focused on fame and wealth and have given insufficient thought to protecting secrets; before obtaining patents in order to stake a claim on future markets, out of a desire to be "first in the world," they have hastened to publish their results in domestic or foreign journals or to present them at international science and technology conferences. But the result has been serious leakage of technological secrets. When the two-step fermentation process for producing vitamin C was developed in China, experts evaluated it as a major national-level S&T innovation. It was a research result that was greatly needed by humanity and that had extensive potential markets. Representatives of the world's two largest vitamin C-producing countries, Switzerland and the United States, heard about the technique and visited China, bidding against each other and offering large sums for the patent. But just a week after their bidding competition for the patent had reached its highest intensity, a small journal caused them to shake hands and agree with each other. Both groups returned home satisfied, with neither of them having bought the patent. The reason was that the journal had published the details of the entire process,

including the individual steps of the preparation, the amounts of the ingredients, and the like, so that anyone with even a slight knowledge of chemistry could use the article as a recipe. Thus, no one was willing to pay a large sum of money to buy the patent. At an international conference of silkworm specialists, to the surprise of the Chinese participants, the Japanese entertained them especially lavishly. Later they found out that this was a gesture of gratitude: in a technical journal, the Chinese had fully revealed the details of the preparation and administration of a drug for treating an epidemic disease of silkworms and had even included their findings on the source of the disease. The Japanese had been frustrated by their inability to control the disease, but the Chinese experts had generously given them what they needed so that they solved their problem without effort. This was why the clever Japanese were unusually lavish in entertaining the Chinese representatives.

Secrets may be stolen by spies, handed over by enemy agents, or leaked by S&T personnel; but in addition, some leadership cadres have unintentionally provided secrets in the form of gifts to foreign visitors, thus giving the visitors a great advantage. On one occasion, a high official presented French visitors with a pig of the Meishan breed, the best in Zhejiang Province, thus allowing French pig breeders to bypass 20 years of research. Recently, with increasing international interest in asparagus, representatives of many countries came to China to discuss purchasing it. But Chinese officials actually presented the visitors with samples of several varieties whose export is prohibited, including the Loulu and Lilu varieties. Although it was later realized that these gifts were too valuable, the foreigners had long since departed.

In the 1950's, China unstintingly supplied the Soviet Union with more than 700 varieties of soybeans, without compensation. In the 1960's, China made a swine fever vaccine based on the chemically weakened virus unconditionally available to the countries of Eastern Europe. In the 1970's, China again generously gave away soybean varieties, this time to the US; the Americans then used them as a genetic stock to rectify the critical degeneration of US soybean varieties, which enabled US soybeans to recover their domination of world markets. Today, 20 years later, despite being a major agricultural country, China still has no presence on world soybean markets, while US producers dominate the markets. China not only has suffered a grievous economic loss, but also has been embarrassed. And who is to blame? If we had known, we would have acted differently.

The world is a vast marketplace, and in the intense market competition, whoever gains control of an advanced technology first will be able to dominate the market. Similarly, whoever gets hold of his competitor's scientific and technological information can eliminate the competitor's unique advantage, uncover his secret methods, and circumvent him. In turn, those who let the secrets out are in a position described by another catchphrase, "the dumb man eating goldthread root": the interpretation is, "unspeakable bitterness." As Bruce Hurston, a member of the information protection committee of the US Industrial Security Association, puts it, "Someone who has been harmed by industrial spies is like a person who has contracted a venereal disease: he has been harmed but is not eager to talk about it."

When a sheep has been lost, it is still not too late to mend the pen. This memorandum has been written in response to frequent leakage of China's S&T secrets, in the hope that it will induce people at all levels to take the subject seriously and to conscientiously strengthen propaganda and education regarding the protection of secrets, thus leading to an increase in secrecy-mindedness and to effective self-protection.

The Joint Stock System in China's High-Tech Industry Development

94FE0641A Beijing KEJI RIBAO [SCIENCE AND TECHNOLOGY DAILY] in Chinese 11 Apr 94 p 3

[Article by Zhang Xiaoyuan [1728 2556 0626], System Reform Office, State Science and Technology Commission: "The Joint Stock System in the Development of China's High Technology Enterprises"]

[Excerpt] The enterprise system under which the high technology enterprises operate must assure that high-technology results suitable for conversion to commodities, for development into industries, and for sale on international markets, as well as essential funds and materials, can be rapidly and effectively organized without ownership constraints so that conditions favor enterprise development; they must assure that the great risks involved in the creation of high-technology enterprises can be spread around in optimum fashion; and they must assure that the high-technology and new-technology enterprises have full autonomy in production management, can use the market as a guide in their efforts to survive and grow, and can make their entry onto the international stage via multiple channels and in multiple forms. The joint stock system is a modern enterprise system that is in accordance with these requirements and that is used throughout the world.

In September of 1991, the State Science and Technology Commission and the State Commission on Reform of the Economic System jointly issued the "Decision on Advancing the Reform of High-Technology Industrial Development Zones and Promoting the Development of High-Technology Enterprises," which expressly stated that "Once their property relationships and creditor relationships are put in order, enterprises may organize themselves in such forms as partnerships, cooperative enterprises, limited-liability corporations, and limited-liability joint stock corporations. Mutual stock ownership by corporations is encouraged, and corporations may hold controlling interest in other corporations; we encourage the purchase of stock in intellectual property such as patents and engineering results, the provision of

systematic guidance to enterprise employees in the purchase of stock, and active efforts to attract stock purchases by foreign capital. Shares of stock may be transferred and circulated by over-the-counter exchange." After this decision was issued, some localities drafted local laws and regulations and began spot experiments with the system. In early 1992, after the publication of Comrade Deng Xiaoping's important talk during his southern visit, the pace of reform was accelerated nationwide. In September of 1992, the State Commission on Reform of the Economic System issued the "Standard Opinion on Joint Stock Companies," which resulted in the beginning of spot experiments with stock ownership nationwide. Pursuant to this standard opinion, in November 1992 the State Science and Technology Commission and the State Commission on Reform of the Economic System jointly issued a document dealing with the characteristics of high-technology enterprises, entitled "Provisional Rulings on Some Issues Related to the Creation of High-Technology and New-Technology Lim ited Liability Joint Stock Corporations in the State High-Technology Development Zones," which laid down the following special provisions.

Regarding the persons that start such corporations, the document specified that in the case of large and medium-size high-technology enterprises recognized by the State Science and Technology Commission, subject to approval from the cognizant bodies, the founder may be a single person. This provision makes it easier for large and medium-size enterprises under various ownership systems in the development zones to accelerate their conversion to joint-stock form. Second, the rulings expanded the range of organizations permitted to be founders of high-technology joint stock limited liability corporations by expressly specifying that, with the approval of the State Commission for Reform of the Economic System and the State Science and Technology Commission, both corporate entities outside China and foreign-capital corporations inside China may become corporate founders, provided that they transfer high technology to the company or exchange the technology for stock shares of value equivalent to the appraised value of the technology.

Regarding the purchase of technology stock, the provisional rulings specified that with the special permission of the corporate oversight departments, the total appraised price of invisible property may constitute up to 30 percent of a corporation's charter capital. Thus the percentage of high-technology joint stock corporations' shares that are purchased with technology may be higher than in the case of other joint stock enterprises. The technology for which the shares are purchased must of course be carefully examined in each specific case: it must be the core technology of the company's main products, and it must meet the high-technology standards issued by the State Science and Technology Commission. Certificates of ownership and of value appraisal must be issued.

As regards the demarcation of property rights, in view of the fact that in the past a few enterprises were set up with a rather complex property structure, the document specified that when an existing high-technology enterprise is reorganized as a corporation, it must define the property rights of the original enterprise, and in cases where ownership is hard to apportion, the property may be temporarily invested in the corporation as corporate stock for management purposes.

As regards protection of the legitimate interests of enterprise pioneers, creators and founders, the document specifies that when existing high-technology enterprises are converted to corporations, after examination by the cognizant departments, and contingent upon unanimous approval of the registered employees of the original enterprise, the enterprise may award personal shares to those of the corporation's scientific and technical personnel who made major contributions to creating the original enterprise. In other words, they may be awarded founder's shares. This provision helps to increase the cohesiveness of the enterprise and protects and promotes the development of the corporation and the optimum use of its intellectual resources.

The issuance of the temporary rulings created a nationwide legal basis for the promotion of the stock ownership system in high-technology companies in the development zones and marked the change from policy promotion of this system to standardized implementation measures. When the State Science and Technology Commission and the State System Reform Commission jointly issued the temporary provisions, they also selected three enterprises in the development zones for direct spot experimentation with the stock ownership system. These enterprises were: the Peite Joint Stock Corporation (Group), of Chengdu; the Longyuan Industrial Corporation, of Beijing; and the Changchun High-Technology Corporation (Group).

Encouraging high technology enterprises to engage in system innovation will be an important component of the advancement of reform in the development zones for some time to come. Continuing to promote the stock ownership system will be the key factor. The activities being undertaken by the State Science and Technology Commission this year include the following.

—Further improving legislation regarding the creation of high-technology joint stock companies in the development zones and bringing the legislation into line with the Law on Corporations.

—Continued support for the conversion of qualified existing science and technology enterprises in technology development zones throughout the country to the joint stock system, and resolution of some difficulties involving inefficient enterprise ownership systems, the lack of long-term development impetus, and self-imposed constraints.

—The making of recommendations to the countrywide certification and inspection committees in which several high-technology enterprises that have completed

system reform are identified as candidates for spot experiments in the public issue of stock; an effort is being made to accomplish the objective this year, and new investigations are being conducted in order to support further improvement of the operating mechanisms of high-technology enterprises, the expansion of society's fund-raising channels, and the establishment of a modern enterprise system.

—The making of recommendations to the countrywide certification and inspection committees in which several privately owned high-technology enterprises that have completed system reform are identified as candidates for spot experiments in the issuance and foreign sale of stock, and the development of new means of internationalizing China's high-technology enterprises.

The efforts to develop the joint stock system in the technology development zones are sure to make major progress in 1994.

Advanced Materials and Superconductivity

Newest Reports on Nanomaterials

Fe-Matrix Nanocrystalline Alloys

946B0109A Beijing KEXUE TONGBAO [CHINESE SCIENCE BULLETIN] in Chinese Vol 39 No 5, 1-15 Mar 94 pp 411-413

[Article by Liu Xuedong [0491 1331 3639], Hu Zhuangqi [5170 1104 7784], and Ding Bingzhe [0002 3521 0772] of the State Key Laboratory for Rapid Solidification Nonequilibrium Alloys (RSA) of the Institute of Metals Research (IMR) of the Chinese Academy of Sciences (CAS), Zhu Jie [2612 3381] of the International Materials Physics Center of CAS, and Jiang Jian [1203 0256] of IMR of CAS, Shenyang, 110015: "Boundary Defect Structures, Mechanical Properties of Fe-Matrix Nanocrystalline Alloys"; MS received 18 Jan 93, revised 6 Sep 93]

[Text] Positron-lifetime spectrum results show that two types of defects exist along the grain boundaries of large nanocrystalline (crystal size: 1 nm to 100 nm) alloys prepared by the amorphous crystallization method.[1] These two types are: the free volume type and nanoscale microhole.[2] The former is smaller than a monohole, and the latter has the size of several monoholes generally existing at the intersection of several boundaries. In comparison, the free volume type is a shallow trapping potential, but could amount to 90 percent of the total defects. It is worth noting that as the crystals coarsen, the size and density of microholes will change considerably, hence, predictably, the microhole defect will greatly affect the grain-boundary structure and properties of nanocrystalline material. At present, there are very few reports on this subject.

An amorphous $(Fe_{0.99}Mo_{0.01})_{78}Si_9B_{13}$ (atomic percent) strip of 5mm width and 27μm thickness is made by the single-roll rapid-solidification method. The X-ray diffraction test proves that the quenched sample is amorphous. Samples in prepared condition and in annealed condition are tested for positron-lifetime spectra with a fast-coincidence ORTEC system. A time resolution of 230ps is used under our test conditions. A 3.7 x 10^5Bq ^{22}Na source is sandwiched between the two specimen groups. Each group consists of five specimen layers. The microhardness H_v is measured with a Vickers hardness tester with a load of 50g and cycle time of 10s.

Figure 1 shows the amorphous alloy DSC (differential scanning calorimetry) curve (Perkin-Elmer, DSC-2) at the constant-temperature increase rate of 20K/min. During the heating process, two crystallization exothermic peaks, at 841K and 858K, appear on the curve, respectively. The area ratio of these two peaks is 10:1. The annealing temperatures for crystallization treatments are in the range of 833K-1023K, and the annealing time is one hour for all temperatures. Annealing is conducted in a tube furnace with argon as protection gas. Both the X-ray diffraction test and the transmission electron microscope (TEM) examination indicate that the annealed samples are all crystallized. The grain size is measured with a TEM. Table 1 shows the averaged sample grain sizes resulting from different annealing temperatures.

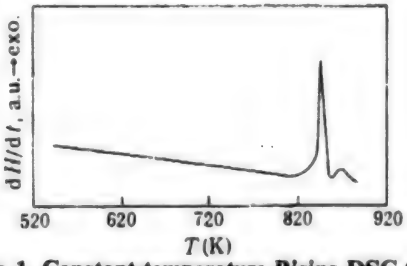

Figure 1. Constant-temperature Rising DSC Curve. (Temperature rising velocity: 20K/min)

Table 1. Average Grain Sizes at Different Annealing Temperatures

T_a (K)	833	853	873	893	913	1023
Average value of D (nm)	17	25	40	55	70	200

Each crystallized sample is given the three lifetime fits. Since the long-lifetime τ_3 originates from the surface effect of the sample and its source,[2] and does not reflect the structural signal of the sample interior, τ_3 is ignored in the following analysis. Furthermore, since the average grain size is generally much smaller than the positron's averaged diffusion distance ($L+$ = 100 nm) in a perfect crystal, the thermalized positrons can rapidly diffuse to the grain boundary where they are trap-annihilated.

Figure 2 shows the plots of how the grain growth affects the short-lifetime τ_1, the intermediate-lifetime τ_2, and

the intensity ratio I_1/I_2 of Fe-Mo-Si-B alloy. In these plots, τ_1 and τ_2 show the volume of the free-volume type defects and the volume of the microhole defects, respectively. Figure 2a shows that when the averaged grain size D increases from 17 nm to 70 nm, the changes of short-lifetime τ_1 are quite small. However, when the average value of D = 200 nm, τ_1 drops significantly. This observation indicates that when the averaged grain size $D < 100$ nm, the free-volume type defects are relatively stable; in contrast, the change of microhole defects is much greater, as shown in Figures 2b and 2c. Obviously, when the average value of D = 55 nm τ_2 reaches it highest value (282 plus or minus 12 ps), and I_1/I_2 also reaches the maximum value (17.0) at this point. Therefore, during crystal growth, the microhole defects aggregate and grow. At the average value of D = 55 nm, each defect empty volume reaches its maximum, but the total defect quantity reaches its minimum. With further grain coarsening, the volume of each microhole gradually decreases, and the total defect quantity quickly increases. When the average value of D = 200 nm, I_2 reaches as high as 12.7 plus or minus 1.0 percent. For this experiment, τ_2 varies in the range of 240 ps to 290 ps, which corresponds to a hole group composed of 5 to 9 monoholes.[3] The aforesaid analysis indicates that the microhole type defect is very sensitive to grain growth, and reflects in a nonmonotonic variation. It is worth noting that the microhole type defects at the grain boundary can be considered as a structural element in the Fe-Mo-Si-B nanoscale crystal material, owing to the fact that these defects continue to exist in a crystal grain during its growth from 17 nm to 70 nm, as well as within a concentration change from 8 percent to 13 percent. Therefore, it is believed that the microhole type defect will have great influence on nanoscale material properties.

Recently, research on nanoscale alloy microhardness has drawn great interest, mainly because the emergence of nanoscale crystal makes it possible to study the deformation mechanism of crystals with grain sizes in the nanometer range. Interestingly, an abnormal Hall-Petch relation in the nanoscale crystal material has been discovered independently by both Gleiter[4] and Lu Ke et al.[5] Therefore, crystal size is unlikely the only factor that influences material strength or hardness. Other factors such as grain boundary structure, etc. may affect or modify the mechanism of strength variation.

Based on this consideration, we measured the microhardness H_v of Fe-Mo-Si-B nanoscale crystal material as shown in Figure 2d. The data of microhardness measurement show that when the average value of $D < 55$ nm, the decrease of crystal size reduces the material hardness. This result is similar to that in references 4 and 5. But when the average value of $D > 55$ nm, the microhardness decreases with increase in the grain size. Hence, for the Fe-Mo-Si-B polycrystalline alloy, H_v variation produces a critical phenomenon, and the critical point is the average value of D = 55 nm. At this point, H_v reaches as high as 10 plus or minus 0.3 GPa. The interesting point is that the variations of intermediate-lifetime τ_2

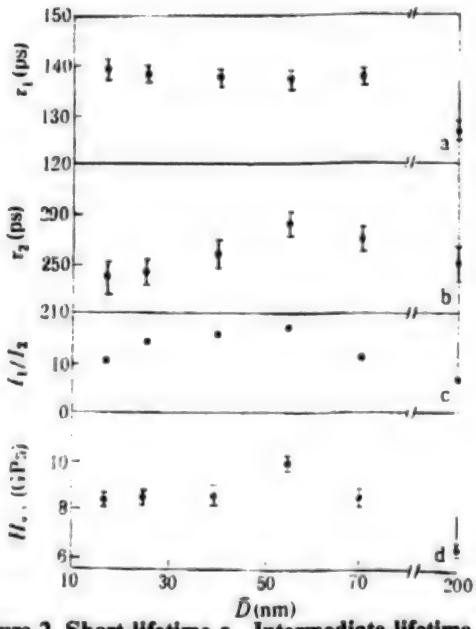

Figure 2. Short-lifetime τ_1, Intermediate-lifetime τ_2, Intensity Ratio I_1/I_2, and Microhardness H_v vs. Average Grain Size D for Fe-Mo-Si-B Nanocrystalline Alloy

and the intensity ratio I_1/I_2 are the same as the variation of H_v, when the grain size changes. When the average value of D = 55 nm, the microhole volume inside the material is the largest and the microhole density is lowest; the corresponding material hardness reaches as high as 10 plus or minus 0.3 GPa. These results show that for Fe-Mo-Si-B nanocrystal alloy, H_v magnitudes depend not only on the crystal size, but also the interface structure. The contribution of nanoscale hole defects on the interfaces to material hardness must not be overlooked. When the average value of $D < 55$ nm, the fact that H_v decreases with decrease in the crystal size is probably due to the volume reduction of the microholes on the interfaces and the decrease of the resistance from the dislocation movement.

In conclusion, for Fe-Mo-Si-B nanoscale crystal, the change of crystal size will induce obvious change of boundary-defect structure, especially the change of microhole type defect, and, consequently, will induce the change of material properties such as hardness, etc., which are related to material microstructures. The study of the formation and development of microholes and their effects on other material properties is in progress.

References

1. Lu, K., Wang, J.T., Wei, W.D. J. APPL. PHYS., 1991, 69(1): 522-524.

2. Sui, M.L., Lu, K., Deng, W. et al., PHYS. REV. B, 1991, 44(12): 6466-6471.

3. Schaefer, H.E., Wurschum, R.W., PHYS. LETT., 1987, 119A: 370-372.

4. Chokski, A.H., Rosen, A., Karch, J. et al., SCR. METALL., 1989, 23(10): 1679-1684.

5. Lu, K., Wei, W.D., Wang, J.T., SCR. METALL., 1991, 24(12): 2319-2323.

DSC Analysis of Mo, Mo_2N, Ti, TiN Nanoscale Solids

946B0109B Beijing KEXUE TONGBAO [CHINESE SCIENCE BULLETIN] in Chinese Vol 39 No 5, 1-15 Mar 94 pp 469-470

[Article by Zhu Yong [2612 0516] of the Institute of Solid State Physics (ISSP), CAS, Hefei, 230031: "DSC Analysis of Mo, Mo_2N, Ti, TiN Nanoscale Solids," funded by NSFC; MS received 22 May 93, revised 16 Sep 93]

[Text] Nanoscale solid material is a new solid material with a gas-like structure. Its structure shows neither long-range order nor short-range order.[1] Generally it is made by pressing ultrafine particles (nanoparticles) into a shape which is then formed into a block material under a condition that keeps the surfaces very clean. The interfaces occupy a large portion (as high as 30 percent to 50 percent) of the block, because of the ultra-fineness of the particles. When the pressed block becomes solid, the particles' original free surfaces become interfaces. This type of structure gives the material many significant characteristics and superior properties. From the thermodynamics point of view, this is a metastable structure.

The samples are prepared with a locally made Type IAC-1 nanoscale solid material manufacturing apparatus utilizing the apparatus' capability of direct-current magnetron sputtering cold condensation and in-situ pressing. The working chamber is first evacuated to a vacuum of 4 x 10^{-4} Pa, and then the circulating gas is introduced until a specific pressure is reached. For the preparation of nanoscale solid Mo or Ti, 0.5 Pa high-purity argon is introduced; and for the preparation of Mo_2N or TiN, first 0.2 Pa high-purity argon and then 0.5 Pa high-purity nitrogen. The cold trap is cooled with liquid nitrogen. Direct-current voltage is applied between the target and the cold trap. After the cold trap has collected a specific amount of powder, the powder is removed with a scraper and sent to the in-situ pressing device for pressing at 1.5 GPa. The prepared sample for analysis is in disc shape, 8 mm in diameter, and 0.5 mm to 2 mm thick.

Transmission electron microscope (TEM) and X-ray diffraction (XRD) analyses are conducted on samples. The particle sizes of samples made by the aforesaid method range between 5 nm and 8 nm. DSC is conducted with a Perkin-Elmer Type DSC-2 differential scanning calorimeter. The scanning rate is 40K/min, and the temperature is from room temperature to 1000K. Figures 1 to 4 show the DSC analysis results for four specimens. The figures show that each nanoscale solid curve, within the range from room temperature to 1000K, displays two kinds of peaks: at the low end of temperature, exothermic peaks; and at the high end, endothermic. In the same temperature range, the nanoscale Mo_2N curve displays no endothermic peak but two exothermic peaks, an indication that the exothermic reaction is caused by two different factors. Each of the other three nanoscale solids has one single exothermic peak only, which can be considered as a compound peak. The TEM shows that the particle sizes of the nanoscale solid materials virtually remain unchanged beyond the range of temperatures where the exothermic peaks form. Therefore, we can essentially exclude the factor of grain-growth, which ordinarily contributes to the formation of exothermic peak. Normally, low-temperature annealing is a method to eliminate residue stress. In this experiment, the residue stress induced in the nanoscale solid during pressing is eliminated through temperature increase in the process. By analyzing the X-ray diffraction results, we can see that there are two factors causing the formation of exothermic peaks: the stress relief, and presumably, the relaxation of atoms on the grain boundary. The reasoning behind this is that when two particles adhere to each other through external pressure, the original free surfaces become material interfaces. Since the environment of atoms on the free surface is quite different from that of atoms in the interface, the required energy of these two atom groups differs. It is very difficult to alter the energy states by outside pressure; however, proper temperatures can achieve the change. This is the process of relaxation of interface atoms induced by rising temperature, also an energy release process, and a process in which the atoms transform from the higher-energy metastable state to the lower-energy metastable state. Similarly, the exothermic peak shows in the DSC analysis. As to the endothermic peak, due to the temperature range limitation, the curve for nanoscale solid Mo_2N does not display endothermic peaks as the other three nanoscale solid materials do. The endothermic peak of nanoscale Ti solid is a compound peak. The endothermic peaks of the nanoscale Mo and TiN solids are closer to being typical, which only indicates that the formation of each peak is caused mainly by one factor. All the materials are nanoscale solids, and their particle size differences are quite small. However, metallic titanium, especially in its ultrafine powder form, is a superior gas absorbent, or has very strong gas absorbability. During heating, a portion of the energy changes the quantity and the state of the absorbed gas. As the temperature continues to increase, another portion of energy turns the interface atoms to a molten state. At this point the crystals become nuclei and grow. This is the reason why after the endothermic peak temperature, the crystal growth is clearly observed. It also explains why after specimen annealing, all grain boundaries in the interfaces are identical under the TEM observation.[2,3] Titanium has very strong gas absorbability and adsorbability, whose effects are distinctively reflected on the endothermic peak. Yet, the absorbabilities and adsorbabilities of Mo and Ti have much weaker effects on their nanoscale materials. This is the main

reason why the endothermic peak configuration of titanium is widely different from those of the Mo and Ti materials. The corresponding temperatures of the lowest value of the endothermic peak and the highest value of the exothermic peak are listed as follows:

minimum value: $t_{Ti} < t_{Mo} < t_{TiN} <$ the average value of t_{Mo2N},

maximum value: $T_{Ti} < T_{Mo} < T_{TiN}$,

where the average value of t_{Mo2N} is the mathematically averaged value of the corresponding temperatures of the two exothermic peaks. Obviously, the equation is in agreement with the melting points of the materials.

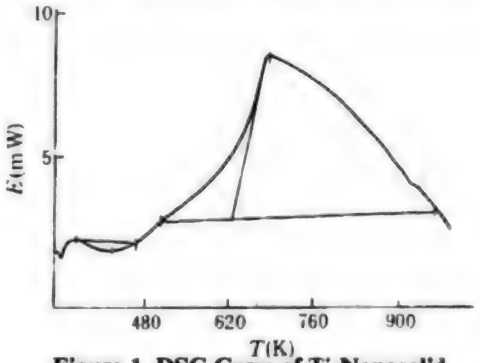

Figure 1. DSC Curve of Ti Nanosolid

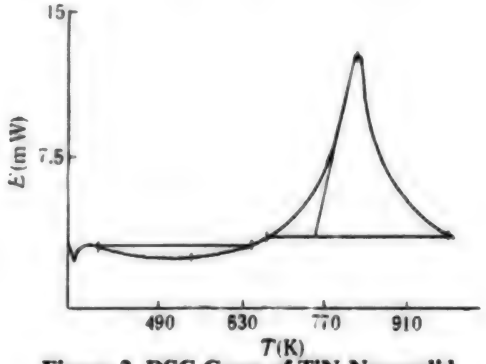

Figure 2. DSC Curve of TiN Nanosolid

In conclusion, since the nanoscale solid material is a material of metastable structure, its stability changes once it is heated. Therefore, its stability is related to the original material's melting point. DSC analysis of each material displays exothermic and endothermic peaks. Exothermic peaks are induced by the residue stress relief and the relaxation of interfacial atoms; endothermic peaks are induced by interfacial adsorption and state change, as well as grain-boundary melting.

References

1. Zhu, X., Birringer, R., Herr, U. et al., PHYS. REV., 1987, B35: 9085.

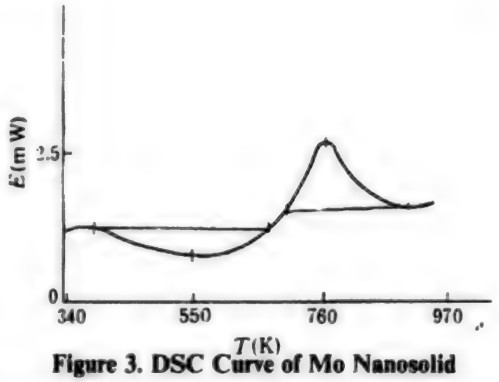

Figure 3. DSC Curve of Mo Nanosolid

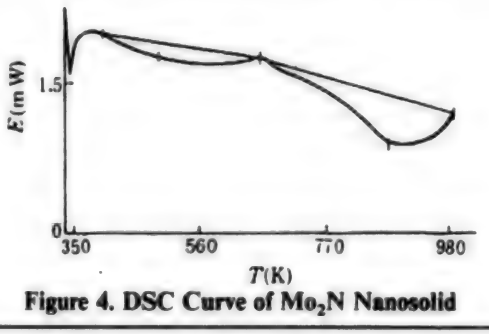

Figure 4. DSC Curve of Mo_2N Nanosolid

2. Wunderlich, W., Ishida, I., Maurer, R., SCRIPTA MET. ET MATER., 1990, 24: 403.

3. Thomas, G.J., Siegel, R.W., Eastman, J.A., SCRIPTA MET. ET MATER., 1990, 24: 201.

Ultrahigh-Melting-Point Nanoscale Metal Carbides

946B0109C Beijing KEXUE TONGBAO [CHINESE SCIENCE BULLETIN] in Chinese Vol 39 No 5, 1-15 Mar 94 pp 471-474

[Article by Liu Lin [2692 2651], Li Bing [2621 0365], Ding Xingzhao [0002 2502 0340], Ma Xueming [7456 1331 7686], and Qi Zhenzhong [2058 7201 0022] of the CAS ISSP, Hefei, 230032, and Dong Yuanda [5516 6678 6671] now with the Materials Science and Engineering Department, Shanghai University of Technology: "Ultrahigh-Melting-Point Nanoscale Metal Carbides Prepared by Mechanical Alloying Method," funded by NSFC; MS received 12 Apr 93, revised 20 Sep 93]

[Text] Nanoscale material is a new type of material developed in the 1980s. The material has gained the attention of materials scientists because its interfacial atoms occupy a considerably large portion of the total, and consequently, the nanoscale material demonstrates unique physical and chemical properties. At present, most nanoscale materials are made with the gas condensation-method,[1] which has low efficiency, lower powder

production rate, and high cost, especially for high-melting-point metals or alloys. These drawbacks limit research on nanoscale material structure and properties as well as its application. Mechanical alloying offers a new way to prepare nanoscale materials. The low-temperature solid-state reaction can be achieved by mechanical energy with a high-energy ball mill. The method can prepare materials with new structures which cannot be made with conventional methods.[2,3] Since Shingu et al.[4] first reported on nanoscale Al-Fe alloys produced by mechanical alloying, many different nanoscale metals and alloys have been developed.[5,6]

Metal carbide materials with good high-temperature thermal stability and mechanical properties have a broad industrial application future. Because most of the metal carbides have very high melting points, they cannot be made with a conventional melting method, and it is even more difficult to make nanoscale material the conventional way. This paper presents ultrahigh-melting-point carbide materials (TaC, NbC, and WC) made with a high-energy ball mill from basic element powders. The structural changes of the powder mixes during ball milling are studied with X-ray diffraction tests, scanning electron microscope (SEM), and transmission electron microscope (TEM).

I. Experiment

Powders of graphite, tantalum, niobium, and tungsten, each of 99 percent plus purity, are mixed together according to the atomic ratio $M_{50}C_{50}$ (M = Ta, Nb, W). The powder mix is loaded in a 120 ml steel can with argon as protection atmosphere. WC balls (diameter = 12 mm) are used. The weight ratio of balls to powder mix is 18:1. The powder is milled with a "planet" type high-energy ball mill. At each specific stage, the specimen is collected under argon protection for structural analysis.

X-ray diffraction tests are conducted with a Philip PW 1700 X-ray diffractometer, with a KαCu radiation source. Sample topography is observed both with an Amary-1000B SEM and a Joel-200CX TEM. The crystal size and the microstrain of milled specimens are analyzed by the configurations of the X-ray diffraction line (this experiment adopts the single-line method). In the line configuration analysis, the diffraction peak shape is measured by step-by-step scanning. The step interval and counting time are $2\theta = 0.02°$ and $t = 40$ s, respectively, to assure that the intensity count at the maximum peak is not less than 10^4. The $K\alpha_2$ line is eliminated with the Rachinger method in order to obtain the diffraction from $K\alpha_1$ only. All the instrumental errors are corrected in reference to the diffraction spectrum of a standard specimen tested under the same condition. It is generally believed that the configuration of an x-ray diffraction peak can be expressed with the Voigt function,[7] which can be viewed as the convolution of the Cauchy function and the Gauss function. Normally, sample-induced peak broadening is caused by the combination of grain-size refining and microstrain. The broadening by grain size is described by the Cauchy function; and that by microstrain, by the Gauss function. Based on the separately obtained peak-broadening values by the Cauchy function and the Gauss function, the corresponding grain size and the microstrain magnitude can be calculated (for detailed calculation method, see reference [8]).

II. Results and Discussion

Figure 1 shows the X-ray diffraction results of these three specimens (TaC, NbC, and WC), after each of them has gone through 110 hours (h) of ball-milling. The diffraction tests show that the products from all the ball-milled powder mixes are their corresponding carbides. Table 1 shows the X-ray line shape analysis of each ball-milled specimen. The grain sizes of all three carbides are around 10 nm, and relatively large microstrain exists in all specimens. The microstrain is mainly caused by crystal lattice distortion from severe mechanical impact during the milling process.

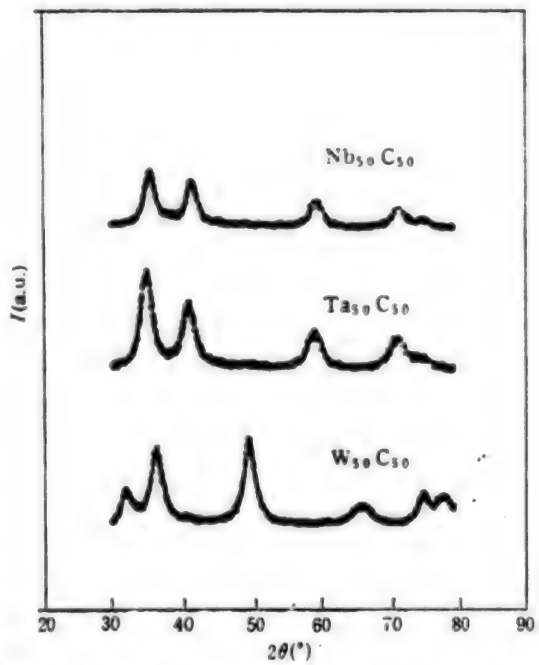

Figure 1. X-ray Diffraction Results of Different Powder Mixes After 110 h Ball-milling

Table 1. Analysis Results of Curve Configurations of Ball-milled Samples

Sample	Crystal Size (nm)	Strain (%)
$Nb_{50}C_{50}$	10.0	1.32
$Ta_{50}C_{50}$	10.2	1.32
$W_{50}C_{50}$	7.2	1.44

Figure 2 shows the X-ray diffraction results of Ta-C powder mix after milling for various length of time. After 10 h milling, all the C peaks disappear, and all the Ta peaks lose some of their intensities, and widen. The fact that Ta peaks

have no obvious shifts indicates that C atoms have not formed a solid solution with Ta. The disappearance of C peaks is probably an indication that the C particles are encased in the Ta particles which have a stronger absorption coefficient; as a result, it is difficult for X-rays to penetrate. After 20 h milling, TaC compounds with f.c.c. [face-centured cubic] structure are formed, and they coexist with some Ta particles. After 60 h milling, all the Ta peaks disappear, which indicates that the transformation of Ta and C powder elements to TaC is essentially complete. After 110 h further milling, X-ray diffraction does not reveal any structural change except some TaC peak broadenings. All this indicates that the TaC compound is stable.

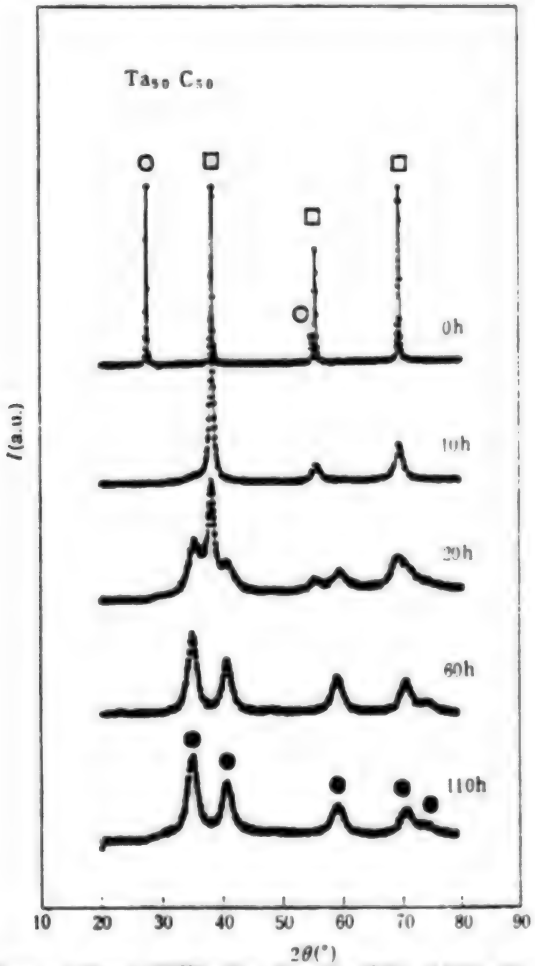

Figure 2. X-ray Diffraction Results of Ta-C Mix after Different Milling Times

Figure 3 shows the SEM results after different periods of ball-milling. During the first few hours, the powders agglomerate in large plate-shape particles, then the plates break down gradually. After 60 h milling, the particles become spherical and distribute uniformly. The particle size is 1 μm. To study particle interior structural detail, TEM observation is conducted. Figure 4 shows the TEM dark-field photo and the electron diffraction pattern of the corresponding area of the sample after 60 h milling. Figure 4(a) shows that the particle in the milled specimen is composed of many ultrafine crystallites with sizes from 10 nm to 30 nm. The electron diffraction pattern is attributed to the f.c.c. structure of TaC. The specimen after 110 h milling displays particles with grain size of 10 nm, which coincides with the X-ray diffraction result.

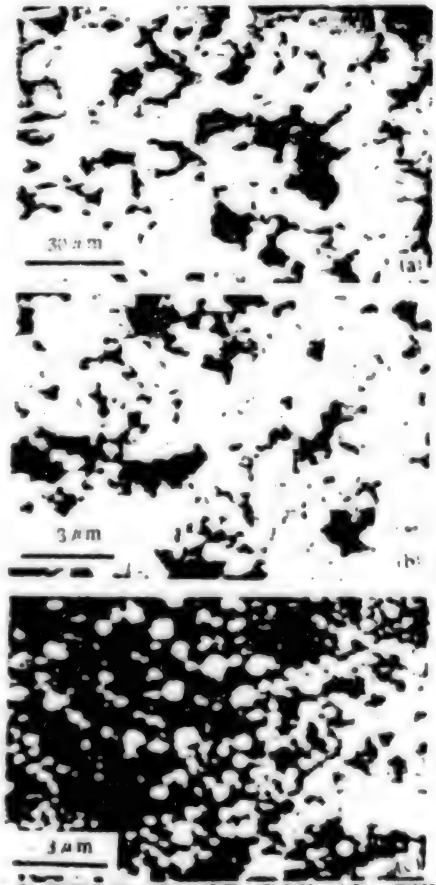

Figure 3. SEM Results of Ta-C Mix After Different Milling Times. (a) 5 h, (b) 20 h, (c) 60 h.

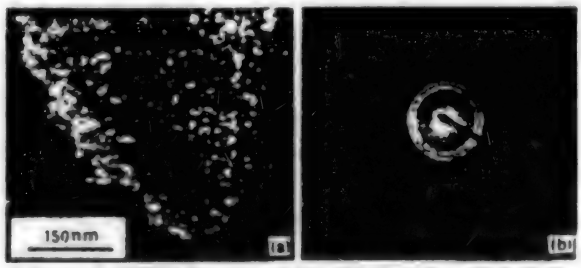

Figure 4. TEM Results of Ta-C Mix After 60 h Ball Milling. (a) Dark field image. (b) Selective area electron diffraction.

All metal carbides have high melting points. The melting points of TaC, NbC, and WC in this experiment are 3825°C, 3600°C, and 2600°C, respectively.[9] To prepare compounds with these structures by the gas-phase cold precipitation method is very difficult. Through high-energy ball-milling of element powders at room temperature, we have successfully prepared these metal carbides, whose refined crystalline particle size is around 10 nm. It is generally believed that the phase change in mechanical alloying is through the mutual diffusion between the elements. This is similar to the solid solution reaction of multi-layered films.[10] In the C-M (M = Nb, Ta, or W) alloy system, graphite particles break easily and become finer due to their plate-type structure. The fine graphite particles are encased in the interface of plastic metal powders. Consequently, the short-life C peaks completely disappear due to ball-milling. With continued milling, the particles become further refined, the number of interfaces increases, and the composition becomes more uniform. Due to the defect accumulation and the increase of interface density, the system energy is raised, which enables the atomic diffusion to proceed fully, and eventually achieve the alloying reaction.

In conclusion, through high-energy ball-milling of element powders, we have successfully prepared carbide compounds NbC, TaC, and WC, of nanoscale structures. Therefore, mechanical alloying is believed to be an effective method to prepare high-melting-point nanoscale materials.

References

1. Gleiter, H., Zarquardt, P., Z. METALL., 1985, 75: 262.

2. Koch, C.C., Gavin, O.B., Mckmacy, C.G. et al., APPL. PHYS. LETT., 1983, 43: 1017.

3. Schultz, L., Wecker. J., Hellstern, E., J. APPL. PHYS., 1987, 61: 3583.

4. Shingu, P.H., Huang, B., Nishitani, S.R. et al., PROC. MET. ALLOYS, Supp. to TRANS. JPN INST. MET., 1988, 29: 3.

5. Fetch, H.J., Hellstern, E., Fu, Z. et al., METALL. TRANS., A, 1990, 21: 2333.

6. Oehring, M., Bormamn, R., MATER. SCI. ENG. A, 1991, 134: 1330.

7. Keijser, Th.H., Langford, J.I., Mittemeijer, E.J. et al., J. APPL. CRYST., 1982, 15: 308.

8. Xiao, K.Q., Dong, Y.D., He, Y.Z., MODERN PHYS. LETT., B, 1989, 3: 313.

9. Brandes, E.A. (ed), Smithell's Metals Reference Book, Robert Hartnoll Ltd., England, 1983.

10. Petzoldt, F., Scholz, B., Kunze, H.D., MATER. LETT., 1987, 5: 280.

Growth, Spectral Characteristics of Halite ZnO Nanoparticles

946B0109D Beijing KEXUE TONGBAO [CHINESE SCIENCE BULLETIN] in Chinese Vol 39 No 6, 16-31 Mar 94 pp 499-501

[Article by Zou Bingsuo [6760 3521 6956] now with the CAS Institute of Physics, Beijing 100080, Wang Bin [3769 2430], Tang Guoqing [3282 0948 1987], Zhang Guilan [1728 2710 5695], and Chen Wenju [7115 2429 7467] of the Research Institute of Optics of Nankai University, Tianjin 300071: "Formation and Spectral Characteristics of Rocksalt ZnO Nanoparticles"; MS received 27 May 93, revised 20 Sep 93]

[Text] ZnO (hexagonal wurtzite structure) is an important II-VI compound for semiconductors, and can be useful in many ways. Its optical properties have produced many results.[1] Thirty years ago, the transformation of ZnO to rocksalt (halite) structure under 9.5 GPa pressure was reported.[2] Recently, the postulation[3] is that the ZnO rocksalt structural phase is likely to have unique optical and transport properties which can be used in semiconductor devices. However, no details have been reported. This paper presents the first rocksalt ZnO nanoparticles prepared via chemical synthesis. Their chemistry and structural characteristics display properties clearly similar to those of nanoparticle Cu_2O, which is an exciton-type semiconductor within the exciton limit. Rocksalt ZnO has good stability, which makes it a potential new optical material.

1. Experimental Method

ZnO(R) ([R: rocksalt],[W: wurtzite]) nanoparticles are chemically prepared according to the following flow diagram:

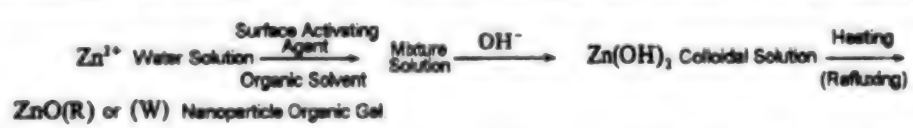

Transmission electron microscope (TEM) examination shows that the ZnO(R) nanoparticles prepared by this method have spherical shape, with a size of 4 nm. The product's absorption spectrum is obtained with a Shimadzu Type UV240 spectro-photometer; its fluorescence spectrum and excitation spectrum, with a Hitachi F4000 fluorophotometer; and its infrared transmitting spectrum, with a Nicolet Type 170 SX infrared spectrometer. From these experiments, a few new unreported phenomena have been observed.

II. Results and Discussions

Figure 1 shows the absorption spectra of ZnO(W) and ZnO(R) nanoparticles. The absorption starting point of ZnO(R) shifts much closer to the red wavelength than that of ZnO(W). And for ZnO(R), there is a distinct absorption in the visible-light region. This notable change of the ZnO(R) shift is caused by changes of the system's electron structure.

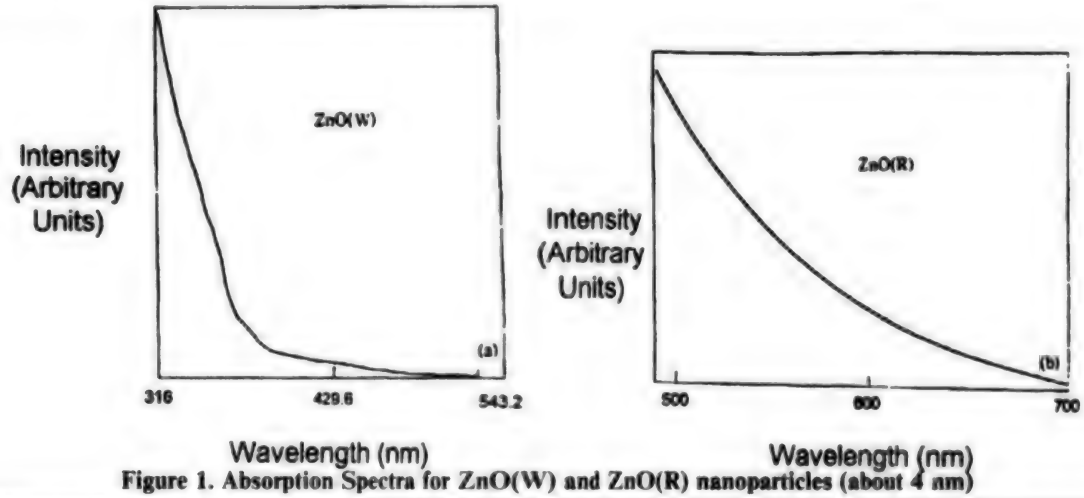

Figure 1. Absorption Spectra for ZnO(W) and ZnO(R) nanoparticles (about 4 nm)

In ZnO(W), the $4sp^3$ orbit and O2*p* orbit form a valance band for Zn^{2+}, and the coordination number for oxygen is four. The 3*d* orbit of Zn^{2+} almost does not participate in the forming of the valance bond. At this moment, the optical bandgap is 3.4 eV. While in ZnO(R), the hybridized $3d$-$4sp^3$ orbit and the O2*p* orbit form a valance band for Zn^{2+} and the coordination number for oxygen is six. In this case, the 3*d* electrons of Zn^{2+} strongly participate in the bond formation; consequently, the covalence character is stronger, and the bonding length is shorter than those of ZnO(W). From theoretical calculation, the direct bandgap is 2.36 eV[3], far smaller than the bandgap of ZnO(W).[4] These calculated values are essentially consistent with the absorption spectrum results.

During the preparation process, the last step is heating (refluxing). When the temperature is below 250°C, the product is colorless transparent ZnO(W) nanoparticles. When the temperature is well above 250°C, the product becomes dark-red ZnO(R) nanoparticles, which do not revert to ZnO(W) by cooling to room temperature. In fact, the ZnO(R) phase structure already exists in the surface relaxation state of ZnO body phase.[5] Therefore, thermal transformation to the ZnO(R) phase promoted by a surface modifier (surface active agent) may have occurred in the ZnO(W) nanoparticle. From the above, the contribution of the surface polarization effect deserves attention.[6] The strengthening of interface polarization will induce the occurrence of a self-trapped state (the self-trapped state of electrons, holes, and phonons). When the non-linear couplings of electrons and phonons are reinforced to a certain degree, the structure becomes unstable;[7] phase transformation occurs, and consequently, the material optical properties will change.

Figure 2 shows the photoluminescence spectra and the excitation spectra of ZnO(R) nanoparticles with stearic acid as surface modifier. It shows that ZnO(R) nanoparticles have many resonance exciton radiation jumps:

(1) 350-445 nm violet series;

(2) 450-510 nm blue series;

(3) 510-580 nm yellow series;

(4) 580-650 nm orange series.

The excitation spectrum of ZnO(R) is entirely like the exciton structure of Cu_2O nanoparticles,[8] and each exciton jumping energy is clearly isolated. Cu_2O and ZnO(R) are similar because they have the same valance-band electron state and structural symmetry, and the sizes of their effective electron masses are relatively closer. The only difference is that ZnO has a larger split of revolving orbit coupling, which means that there is a slightly greater difference in the optical jumping energy between the blue series and the violet series.

Jaffe et al.[3] utilized the *ab initio* calculation-related Hatree-Fock model to calculate the electron structure of ZnO(R) and obtained the values of direct bandgap (2.36 eV) and indirect bandgap (1.36 eV). In Figure 1, the 500 nm absorption in the low-energy spectrum portion is possibly contributed by the indirect jumps. In nanoparticles, optical jumps may also occur during the indirect bandgap jump,[8,9] which is contributed by the quantum limit effect and the dielectric limit effect. Consequently, in ZnO(R) nanoparticles, a radiation jump with an absorption energy at 500 nm is also distinctly observed

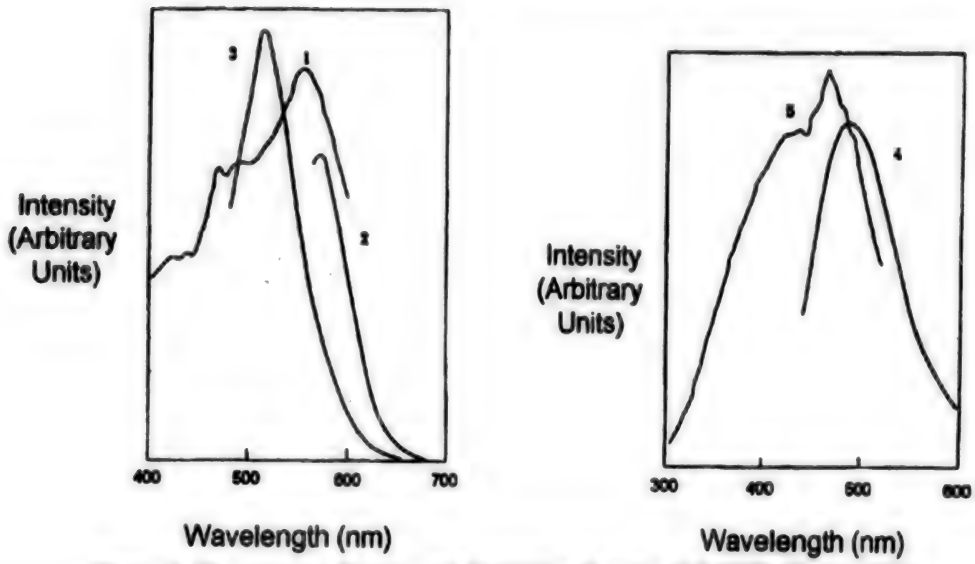

Figure 2. Fluorescence Spectra and Excitation Spectra of ZnO(R) Nanoparticles

(Figure 2). At this moment, the electron-phonon coupling reinforced by the interface polarization can also promote the occurrence of this process, as shown in the infrared spectrum.

Figure 3 shows the infrared transmission spectrum of ZnO(R) nanoparticles. The Zn^{2+} related vibration mode below 300 cm^{-1} forms the strongest absorption peak. The infrared bandgap occurs below the lowest vibration mode. The highest vibration mode shifts slightly to the blue. However, the Zn^{2+} vibration (lower than 300 cm^{-1})[10] is almost undetectable in the ZnO(W) nanoparticle infrared spectrum. These observations directly prove: (1) the existence of intense electron-phonon mutual reaction in the system; and (2) the bond-forming effect of the Zn^{2+} 3*d* electrons in the valance electron band. These two facts explain the obvious strengthening of the vibration mode related to Zn^{2+}. Further theoretical description of these changes is necessary.

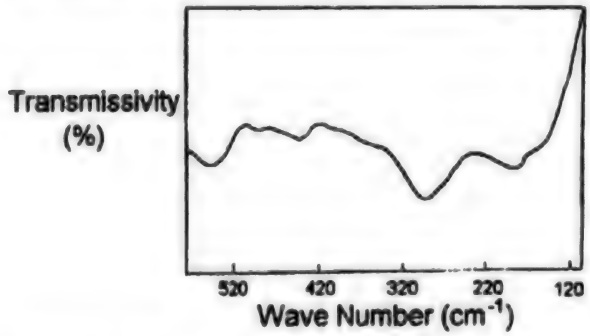

Figure 3. Infrared Transmission Spectrum of ZnO(R) Nanoparticles

In conclusion, this paper first presents the optical spectrographic characteristics and the electron structure features of ZnO(R) nanoparticles. The experiment shows that ZnO(R) is a new material, having an exciton semiconductor property with good stability, and will definitely have an important influence on the properties and applications of nonlinear optical materials.

References

1. Butkhuzi, T.V., Geogobiani, A.N., Ye, Z.U., et al., "Luminescence of Wide-band Semiconductors" (ed. Galanin, M.D.), Nova Science Publishers, New York, 1990, 167-216.

2. Bates, C.H., White, W.B., Roy, R., SCIENCE, 1962, 137: 993-996.

3. Jaffe, J.E., Pandey, R., Kunx, A.B., PHYS. REV. B, 1991, 43: 14030-14036.

4. Liang, W.Y., Yoffe, A.D., PHYS. REV. LETT., 1968, 20: 5-9.

5. Skinner, A.J., Lafemina, J.P., PHYS. REV. B, 1992, 45: 4557-4562.

6. Banyai, L., Cilliot, J.P., et al., PHYS. REV. B, 1992, 45: 14136-14144.

7. de Bodas, E.L., Hipplito, O., PHYS. REV. B, 1983, 27: 6110-6123.

8. Zou Bingsuo, et al., KEXUE TONGBAO [CHINESE SCIENCE BULLETIN], 1993, 38(18): 1649-1651, [in Chinese] [translated in full in JPRS-CST-94-002, 24 Feb 94 pp 9-11].

9. Takagahara, T., Takeda, K., PHYS. REV. B, 1992, 46: 15578-15583.

10. Hayashi, S., Nakamori, N., Kanamori, H., J. PHYS. SOC. JPN. 1979, 46: 176-183.

Preparation, Thermal Stabilization of β-Sn Ultrafine Powder

946B0109E Beijing KEXUE TONGBAO [CHINESE SCIENCE BULLETIN] in Chinese Vol 39 No 6, 16-31 Mar 94 pp 509-511

[Article by Yang Wenping [2799 2429 1627], Xue Desheng [5641 1765 0524], Zhou Rongjie [0719 2837 3381], and Li Fashen [2621 4099 0135] of the Department of Physics, Lanzhou University, Lanzhou 730000: "Study of Preparation, Thermal Stabilization of β-Sn Ultrafine Powder"; funded by NSFC and the Natural Science Foundation of Lanzhou; MS received 2 Aug 93, revised 20 Nov 93]

[Text] Ultrafine-powder research is at the leading edge of current materials science development. Ultrafine powder has great application potential in the fields of catalysis, powder metallurgy, biomedical science, and other high-tech areas. It has gained increasing attention.

Ultrafine powders of Fe, Co, Ni, and their alloys are prepared by a gas-phase evaporation process, and have been studied by numerous means.[1] However, research on metallic Sn ultrafine powder has had no significant progress. We have used differential thermal analysis (DTA), thermal gravimetric analysis (TGA), X-ray diffraction, transmission electron microscope (TEM), and in addition, the Mossbauer Effect (ME)—a microprobing tool—to study the thermal stability and oxidation of β-Sn ultrafine powder in the atmosphere, as well as the local properties of β-Sn and its oxides in ultrafine powder. These properties are compared with those of the Sn bulk material.

I. Experiment

The β-Sn ultrafine powder is prepared by gas-phase evaporation in argon (99.99 percent purity). At the completion of evaporation, nitrogen is introduced for passivation of the ultrafine-powder surfaces. High-melting-point metal molybdenum (Mo) is used for the heating source. Complete metallic atomic emission spectrum (AES) analysis shows that the Mo content in the final ultrafine powder is less than 0.3 percent. An EM-400T TEM is used to study the powder topography and size; a photo is shown in Figure 1. The prepared β-Sn ultrafine powders are clearly spherical and in different sizes, averaging 25 nm. TGA and DTA are conducted with a DuPont-1090 analyzer. The temperature range for TGA analysis is 20°C-1050°C; and that for DTA, 20°C-600°C. The temperature is increased at the rate of 10°C/min. Every minute, 50 ml of compressed air is introduced. Based on the thermal analysis results, a few representative heat-treatment temperatures are selected. The samples are heat-treated individually in air at 190°C, 240°C, 400°C, 600°C, and 800°C at a 10°C/min increase rate. The powder structure of untreated samples and samples treated under the various temperatures are measured with a D/MAX-RB X-ray spectrometer with Cu-Kα radiation. The ME measurements are conducted with a sine-wave-driven Mossbauer spectrometer. The intensity of the radiation source ^{119}Sn is 5 mCi [millicuries]. An α-Fe foil is used to calibrate the speed. The isomer shifts are in reference to SnO_2. For comparison, the Sn bulk material is also measured with ME.

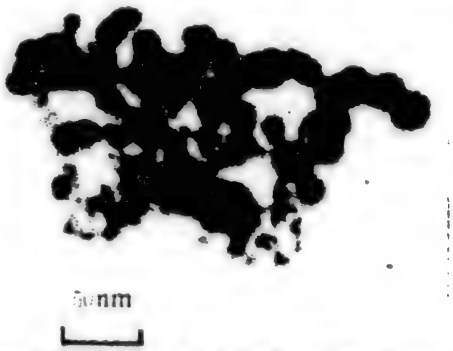

Figure 1. TEM Photo of β-Sn Ultrafine Powder

II. Results and Discussions

2.1 DTA and TGA

To study the ultrafine powder stability in air, DTA is used to find its phase-change condition. The DTA spectrum (Figure 2) shows that an exothermic peak appears at 220°C, which indicates a phase change at that point. When the temperature is above 220°C, the curve variation is not significant and the thermal effect is not apparent. The purposes of TGA are to observe the thermal stability of ultrafine powder within a chosen temperature range, and to chose the proper heat-treatment temperature based on the curve. Figure 3 shows the TGA spectrum of ultrafine powder. It shows that the mass change begins at 220°C. The change is very pronounced. At 800°C, the mass tends to be stabilized.

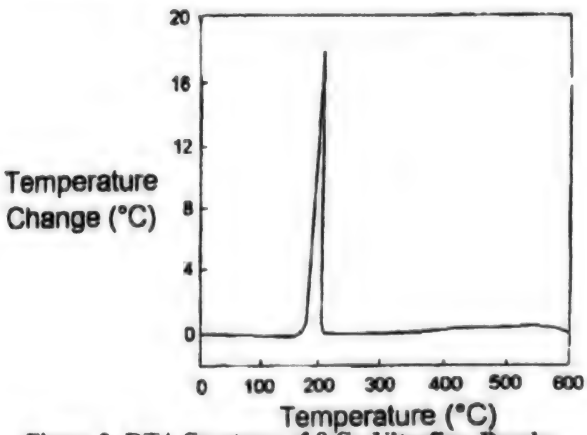

Figure 2. DTA Spectrum of β-Sn Ultrafine Powder

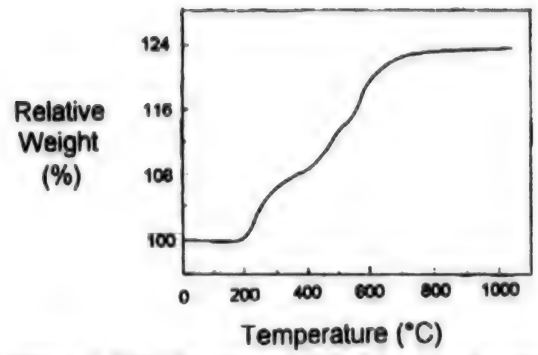

Figure 3. TGA Spectrum of β-Sn Ultrafine Powder

2.2 X-Ray Diffraction

Figure 4 shows the X-ray spectrum of the prepared β-Sn ultrafine powder. Four stronger peaks appear at $2\theta = 30.64°$, 32.02°, 43.84°, and 44.90°, respectively, which correspond to the [200], [101], [320], and [211] diffraction peaks of the β-Sn bulk material. The relative spectrum line intensities are 100:80:35:62, which coincide well with the relative intensities of β-Sn bulk material, which are 100:90:34:74. The spectrum also shows that the sample phase contains only one composition, an indication that the prepared ultrafine powder is made of tetragonal β-Sn only.

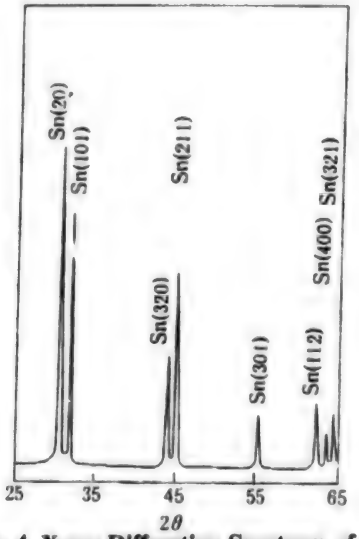

Figure 4. X-ray Diffraction Spectrum of β-Sn Ultrafine Powder

2.3 Mossbauer Spectrum

For local measurement, ME is adopted to study the local environment and its changes in relation to temperature. Figure 5 shows the room-temperature ME spectra of the untreated Sn ultrafine powder and specimens after heat treatment at 240°C, and 800°C, respectively. The room-temperature ultrafine parameters of the samples after different heat treatments are shown in Table 1. The spectrum of the untreated Sn ultrafine powder reveals that besides the single β-Sn peak of the principle phase, a small amount of SnO_2 (double-peak)[2] exists in the sample. It is possible that oxygen, an impurity in the N_2 passivating gas, has oxidized the ultrafine-powder surface. The oxide does not appear in the X-ray spectrum because the relatively small amount of oxide and its loose structure achieve no complete crystal formation. At room temperature, the ratio for the recoilless fractions of Sn and SnO_2 can be expressed in the following relations:[3]

$$f_{Sn} / f_{SnO2} = 0.11.$$

From the relative areas under the SnO_2 spectrum curve and under the Sn sub-spectrum curve, SnO_2 content is estimated to be below 0.3 percent. The isomer shift (IS) of the ultrafine powder increases as compared with that of the bulk material. The difference is caused by the space lattice imperfections, which make the average Sn-Sn atom distance in the powder larger than that in the bulk material. This is proven by the fact that under high pressure the isomer shift of the β-Sn bulk material decreases with increased pressure.[4] Figure 5 and Table 1 show that as the heat treatment temperature increases, SnO and SnO_2 covering the β-Sn powder surface are formed; then the SnO_2 content increases monotonically. But SnO reaches its maximum content at 240°C; from then on it gradually diminishes until it vanishes at 800°C while the sample transforms to SnO_2 completely. The TGA curve reveals that the mass starts to change when the temperature exceeds 220°C. After 800°C, it can be assumed that the mass has transformed to SnO_2, which coincides with the ME result.

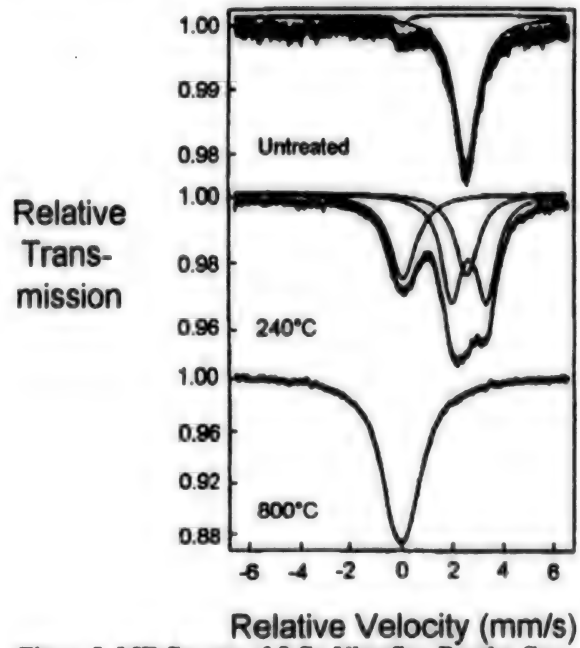

Figure 5. ME Spectra of β-Sn Ultrafine Powder Samples: Untreated (Upper), Treated at 400°C (Middle) and 800°C (Bottom)

Table 1. Ultrafine Parameters of Samples at Room Temperature and Treated at Different Temperatures

		Ultrafine Powder (Room Temperature)	190°C	240°C	400°C	600°C	800°C	Bulk Material
Isomer shift (mm/s)	Sn	2.53	2.54	2.57	2.58			1.68
	SnO		2.96	2.66	2.65	2.62		2.70[3]
	SnO_2	0.01	0.03	0.08	0.03	0.00	0.00	0.00
Quadrupole Split (mm/s)	SnO		1.94	1.36	1.39	1.69		1.32[3]
	SnO_2	0.00	0.03	0.23	0.31	0.50	0.57	0.56[2]
Line Width (mm/s)	Sn	1.08	1.07	1.10	1.58			0.66
	SnO		0.42	0.95	0.87	1.13		0.90[3]
	SnO_2	0.38	1.24	1.24	1.04	1.25	1.51	1.10[3]
Relative Intensity (%)	Sn	97.5	86.0	23.2	23.5			
	SnO		1.9	48.8	44.4	11.0		
	SnO_2	2.5	12.1	28.0	32.1	89.0	100.0	

References

1. Du Youwei, Wu Jian, Lu Huaixian et al., JOURNAL OF APPLIED PHYSICS, 1987, 61: 3314-3316.

2. Zhang Dauyuan, Wang Dazhi, Wang Genmiao et al., MATERIALS SCIENCE AND ENGINEERING, 1991, B8: 189-192.

3. Gauzzi, F., Maddalena, A., Princip, G. et al., "Applications of the Mossbauer Effect," 1985, 3: 919-923.

4. Moller, H.S., ZEITSCHRIFT FUR PHYSIK, 1968, 212: 107-121.

W/Si, WSi_2/Si, W/TiN Nanoscale Multilayer Films

946B0109F Beijing KEXUE TONGBAO [CHINESE SCIENCE BULLETIN] in Chinese Vol 39 No 7, 1-15 Apr 94 pp 594-596

[Article by Liu Wenhan [0491 2429 3352] of the Univ. of Science & Technology of China's (USTC) Basic Physics Center (BPC) and Open Laboratory for Structural Analysis (OLSA), Zhou Lingyun [0719 0407 0061] of OLSA, Wu Liwen [0124 0632 2429] and Zhang Yuheng [1728 5940 1854] of BPC, Hefei 230026, and Xu Zhenjia [6079 2182 0857] of OLSA and the CAS Institute of Semiconductors, Beijing 100083: "Properties and Thermal Stabilities of W/Si, WSi_2/Si, W/TiN Nanoscale Multilayer Films" funded by NSFC and OLSA at USTC; MS received 27 Oct 93]

[Text] In the last 20 years, the rapid development of synchrotron-radiation light sources has offered a superior light source for the soft X-ray band. This is because ordinary optical reflection makes it impossible to use the transmission component in the soft X-ray band. Additionally, because of the particular structures and properties of the grating monochromator used for ultraviolet band and the crystal monochromator used for X-ray band, these monochromators have limited use for the soft X-ray band. As to multilayer films composed of periodic nanoscale layers of light or heavy elements (or other low/high electron density layers), Bragg diffraction can obtain higher reflexiveness and better energy (wavelength) resolution in the soft X-ray band. Furthermore, recent technological development has made it possible to produce multilayers film with alternate layers of heavy/light elements such as Mo/Si, W/Si, W/C, etc. by sputtering technology,[1-3] thus the soft X-ray band application is provided with new optical materials.

However, when these multilayer films are used in the strong synchrotron-radiation light beams, their thermal stabilities have to be understood.[4] Research by Jiang et al.[5] and Dupuis et al.[6] shows that due to interface diffusion and reaction, multilayer films of Mo/Si, or W/Si after heat treatment form silicides ($MoSi_2$, WSi_2), which shorten the multilayer periods and decrease the Bragg peak intensities; on the other hand, the W/C multilayer periods increase with increase in annealing temperature. These are the factors that limit the utilization of these films. To improve the stability of multilayer films, this investigation replaces W in W/Si with WSi_2; uses TiN to replace Si in W/Si; or uses TiN as the barrier between W and Si layers. The bi-layer and multilayer films with WSi_2/Si, W/TiN, and W/TiN/Si compositions are prepared by the magnetron sputtering method. The characteristics of the film-forming process and film reactions to annealing are studied with transmission electron microscope (TEM) and X-ray diffraction (XRD).

1. Experiment

Films with compositions of W, WSi_2, TiN, and Si, respectively, are prepared with ultrahigh-vacuum magnetron sputtering equipment. Single-element targets are used for sputtering W and Si films; and WSi_2 compound target, for WSi_2 film. TiN film is sputtered with Ti target in argon atmosphere through reaction with N_2, which is introduced in the process. The sputtering speeds are: W: 10 nm/min, WSi_2: 9 nm/min., Si: 3 nm/min, and TiN: 10 nm/min. For TEM observation, the bi-layer film is sputtered on a freshly cleaved single NaCl crystal chip. A 10 nm α-Si film is first sputtered on the NaCl substrate, and then W, WSi_2, and

TiN films are separately sputtered. Each film has four different types of thickness: 1 nm, 2 nm, 4 nm, and 8 nm. The multilayer films are prepared the same way except that a single-crystal Si(111) chip, or freshly cleaved NaCl single crystal is used as substrate. The films on the two substrates are sputtered at the same time. The multilayer films are of the following compositions: W(15 nm)/Si(50 nm)/W(15 nm)/Si(30 nm)/substrate (referred to as W/Si multilayer film in this paper); three-period film, WSi_2(20 nm)/Si(20 nm) (WSi_2/Si multilayer film); two different types of three-period W/TiN films (W/TiN multilayer film); and W/TiN/Si/TiN/W/TiN/Si (the TiN layer is either 10 nm or 4 nm thick; however, only one thickness is used per sample). The two bi-layer films, W/Si and WSi_2/Si, are sputtered on Si substrates, respectively. The thickness of the α-Si layer is 200 nm. Each of the W and WSi_2 layers is 10 nm, 50 nm, or 100 nm. Samples with NaCl as substrates are used for TEM observation. Their maximum annealing temperature is 600°C. Samples with Si(111) as substrates are used for XRD analysis. Their maximum annealing temperature is 900°C. All the annealings are conducted in a vacuum annealing furnace with a background vacuum of 3×10^{-3} Pa, at a constant annealing temperature for half an hour.

The sputtered samples and annealed samples are measured with XRD and observed with TEM. The crystal and chemical compound formations as well as phase changes are determined by the peak positions and intensities on the XRD curve. The particle size and uniformity are observed with TEM topography. Selected area electron diffractions (SAED) are used to determine the crystallization, chemical compound formation, and phase change of samples.

2. Film-Formation Characteristics

Figure 1 shows respectively the TEM topographs of W/Si, WSi_2/Si, and TiN/Si bi-layer films (a, b, and c, respectively) and their SAED graphs (a', b', and c', respectively).

Xiu Lisong et al.[7] have reported that the Si film sputtered on the NaCl substrate is a continuous, uniform, amorphous film, and there is no contrast in the TEM topograph. Therefore, TEM topograph shows only the characteristics of W, WSi_2, and TiN films in the W/Si, WSi_2/Si, and TiN/Si bi-films.

As shown in TEM topograph, the nanoscale W film grows in the island mode. The islands in the 1 nm and 2 nm films are all connected, and those in the 4 nm films are very well connected (Figure 1). When the W layer is 8 nm, the contrast in the TEM topograph is much sharper. The innermost fuzzy ring in the SAED graph is from α-Si. The fact that the other diffraction rings become narrower with increase in W film thickness indicates that the grains grow with increasing film thickness.

Figure 1. TEM Photos of 4 nm W, WSi_2, TiN Films

Figure 1(b) shows that the contrast displayed in the TEM topography is very small. The variation of film thickness has little effect on the topograph and the electron diffraction photo. Obviously, the growing process of WSi_2 is different from that of W film. It is possible that when the W and Si atoms are simultaneously sputtered from the target, they form into atomic clusters either before they reach the substrate or as soon as they precipitate on the substrate; hence, they lose their transition capability, and precipitate on the substrate as a uniform microcrystalline film at the very beginning.

The TEM topograph of 1 nm TiN practically does not show any contrast, and the TEM topographs of 2 nm, 4 nm, or 8 nm TiN respectively display uniformly distributed black spots. During the course of TiN film growth from 1 nm to 8 nm, the electron diffraction rings on their corresponding electron diffraction graphs change gradually from a uniform continuous mode to a discontinuous mode. This indicates that during the growth of TiN film thickness, the crystals gradually follow a preferred orientation. Obviously, the growing process of TiN film is different from that of W film. TiN atom clusters are formed during the sputtering process as a result of the Ti and N reaction. After their precipitation on the substrate, the atom clusters lose the transition capability and form a uniform and continuous polycrystalline film.

3. Annealing Behavior

All the samples have been analyzed by XRD and SAED before and after annealing. Table 1 shows the sample phase changes as the annealing temperature changes.

Table 1. Annealing Temperatures and Sample Phases

	Not Annealed	480°C	580°C	650°C	700°C	800°C	900°C
W/Si	W	W *h*-WSi_2(500°C)[a]	W *h*-WSi_2(600°C)[a]	W *t*-WSi_2	W *t*-WSi_2	W *t*-WSi_2	*t*-WSi_2[b]
WSi_2/Si	*h*-WSi_2 microcrystalline	*h*-WSi_2 grain growth	*h*-WSi_2	*h*-WSi_2 *t*-WSi_2 W	*t*-WSi_2 W	*t*-WSi_2[b]	*t*-WSi_2
W/TiN	W cubic TiN[a]	No change before 850°C					
TiN/Si	Cubic TiN[a]	No change before 600°C					
W/TiN/Si	W cubic TiN[a]	No change before 850°C					Wcubic TiN[c]

Note: (a) Have signals in electron dispersion analysis, but no signal in XRD; (b) W phase still exists in 50 nm, 100 nm W/Si and WSi_2/Si bi-layer films, other samples do not have W phase; (c) weak *t*-WSi_2(002) peak appears in 4-nm-thick TiN sample.

For W/Si multilayer film, the formation of *h*-WSi_2 is observed at 500°C annealing. At 650°C, *t*-WSi_2 starts to form. At 900°C, except for the 50-nm- and 100-nm-thick W/Si bi-layer films, W layer has completely reacted with Si forming WSi_2. This indicates that at high temperature, due to the strong mutual diffusion of W and Si, the reaction that forms WSi_2 not only occurs on the interface, but also spreads some 10 nm beyond. For WSi_2/Si multilayer film, *h*-WSi_2 microcrystals start to grow at 480°C; their transformation to *t*-WSi_2 begins at 650°C, and at this same temperature W crystals segregate out. The W crystals then disappear at 800°C. The appearance of W phase at 650°C is due to the departure of actual film composition from WSi_2, and then W atoms move along the WSi_2 grain boundaries and aggregate to W crystals. At high temperature, the Si atoms in the Si layer diffuse strongly into WSi_2 layer. The Si atoms combine with W crystallites forming additional WSi_2, which causes the disappearance of W phase. These phenomena explain that the diffusions of W and Si in WSi_2 are very strong. Although there exist the phase change of *h*-WSi_2 to *t*-WSi_2 and the W and Si diffusion in WSi_2, no interface reaction occurs. Hence, the thermal stability of WSi_2/Si multilayer film is better than that of W/Si, especially at temperatures below 480°C.

TiN is a very stable compound. Compressed W and TiN powder mix does not react until around 2100°C.[8] In this investigation, results of the annealings of TiN/Si, W/TiN, and W/TiN/Si multilayer films reveal that nanoscale TiN film is also very stable and does not react with W and Si at the interface up to 900°C. Therefore, W/TiN and W/TiN/Si multilayer films are multilayer film materials with superior thermal stability. They can be used as optical component materials in the strong synchrotron-radiation soft X-ray band.

Acknowledgment: The authors are grateful to Zhou Guien and Zhang Shuyuan for their TEM and XRD measurements.

References

1. Spiner, E., AIP Conf. Proc., 1988, 75: 124.

2. Barbee, T.Y., OPT. ENG., 1986, 25: 898.

3. Spiller, E., Grebe, K., Golab, L., SPIE, 1989, 1160: 66.

4. Ziegler, E., Lepetre, Y. Schuller, I.K. et al., APPL. PHYS. LETT., 1986, 48: 20.

5. Jiang, Z., Liu, W., Wu, Z., J. APPL. PHYS., 1989, 65: 196.

6. Dupuis, V., Ravet, M.T., Tets, C. et al., J. APPL. PHYS., 1990, 68: 3348.

7. Xiu, L.S., Wang, B., Liu, W.H. et al., SOLID STATE COMM., 1992, 83: 1.

8. Suppl, W., "Gmerlin Handbook," Vol. A2, 1987.

Size Dependence on Ferroelectric Phase Transition in $PbTiO_3$ Nanoscale Particles

946B0093A Beijing GUISUANYAN XUEBAO [JOURNAL OF THE CHINESE CERAMICS SOCIETY] in Chinese Vol 22 No 2, Apr 94 pp 141-146

[Article by Zhang Peilin [1728 3099 7207], correspondent, Jiang Bin [1203 2430], and Zhong Weilie [6945 4850 3525] of the Physics Department of Shandong University, Jinan, 250100; Ma Jiming [7456 1323 6900] and Cheng Humin [4453 5706 3046] of the Chemistry Department, Beijing University; Yang Zhaohe [2799 0340 5440] of the Institute of Crystal Materials of Shandong University; and Li Lixia [2621 7787 7209] of the Experimental Center, Shandong University: "Size Dependence on Ferroelectric Phase Transition in $PbTiO_3$ Nanoscale Particles"; MS received 3 Sep 92]

[Text]

Abstract

This paper reports the effect of $PbTiO_3$ nanoscale particle (nanoparticle) size on ferroelectric phase transition. The nanoparticles, with sizes ranging from 20 nm to 200 nm, are prepared by the sol-gel process. The soft-mode frequency decreases with the decrease of particle size, as measured by Raman scattering at room temperature. The axial ratio c/a is measured by X-ray diffraction and approaches 1 as the particle size of nanoscale powder

gets smaller. The phase transition temperature is determined by the specific heat anomaly of the particles. As the particle size becomes smaller, the phase transition temperature drops, while the dispersiveness of phase transition increases. The relationship of phase transition temperature T_c and particle size D (in nm units) can be expressed by the empirical formula: $T_c(D) = 766 - 256/(D-8.8)$ (K), where 766K is the phase transition temperature of bulk $PbTiO_3$, and 9.1 nm is the critical size below which ferroelectricity disappears.

1. Introduction

Nanoparticles exist in the transition zone between microscopic particles and the macroscopic body, and possess a series of new distinctive physical and chemical characteristics. Research on the effect of nanoparticle size on particle properties has become highly important in material science. Lead titanate is a typical ferroelectric body. It has a high Curie point, strong spontaneous polarization, and low dielectric constant, and has been widely studied in bulk form. Developing new ferroelectric functional materials, such as the ferroelectric nanoparticles used as zero-dimension ["quantum dot"] active constituents of precision composite functional materials,[1] requires further study of the relationship between the properties and the sizes of $PbTiO_3$ nanoparticles.

To simplify the parameters of the study of this relationship, the nanoparticles must fulfill these two conditions: the size distribution must be extremely narrow, and the mutual reaction among particles must be at a minimum, meaning that particles are practically in isolation. These two conditions could not be obtained for earlier research; however, recently, great progress in the technology of preparing composite oxide nanoparticles has satisfied the two conditions. Under these conditions, Ishikawa et al.[2] and Uchino et al.[3] studied the relationship of phase transition temperature and particle size of $PbTiO_3$ nanoparticles and of $BaTiO_3$ nanoparticles, respectively.

Because the experimental samples are all in a powder state, not densely pressed block or sintered body, the powder's electric properties cannot be directly measured. Currently, two methods are mainly used: Raman scattering[2] and X-ray diffraction.[3] They respectively utilize ferroelectric soft-mode frequency and axial ratio c/a to determine the phase transition temperature.

This study investigates $PbTiO_3$ nanoparticles prepared with a sol-gel method. For the first time, a specific heat anomaly method is used to study the changes of ferroelectricity of nanoparticles in relation to the change of particle sizes. The ferroelectric soft-mode frequencies and axial ratios at room temperature are also measured. Results obtained from the decrease of phase transition temperature when the particle size becomes smaller are preliminarily discussed from the soft-mode aspect.

2. $PbTiO_3$ Nanoparticles, and Particle Size Measurement

The $PbTiO_3$ nanoparticles are prepared with a sol-gel method. First lead amylate is prepared and the solvents (ethylene glycol methyl ether, 2-ethoxyethanol, and isopropanol) are purified. Then the $PbTiO_3$ nanoparticles are prepared as follows:

(1) $Pb(OA)_2$-$3H_2O$ is heated to dissolve into 2-ethoxyethanol; the reaction is refluxed at 180°C.

(2) The solution is distilled to form the dehydrated $Pb(OA)_2$ and 2-ethoxyethanol solution.

(3) 2-ethoxyethanol and butyl titanate are added in the solution and formed lead titanium organic compound and butyl acetate.

(4) The mixture is heated to remove butyl ester acetate, until lead titanium organic compound is the only residue.

(5) At specified temperature and atmosphere, a proper amount of ethylene glycol biethyl ether and water (HNO_3) are added to form sol.

(6) The sol is heated to various specific temperatures and soaked at each specific temperature for a proper period (generally about 2h), and then $PbTiO_3$ nanoparticles of different sizes are formed.

The measurement of $PbTiO_3$ nanoparticle size is based on the magnitude of the broadening of peaks in the X-ray diffraction spectra. For the nanoparticle sample, these three factors cause the diffraction peak to widen: instrument parameters, particle size, and microstrain. The peak broadening caused by instrument parameters can be corrected from a known standard sample. The broadening caused by particle size and microstrain can be explained by the following equations:[4]

$$\delta_{si} = \frac{K\lambda}{L_{hkl} \cdot \cos\theta} \qquad (1)$$

$$\delta_{st} = 4\left|\frac{\Delta d}{d_{hkl}}\right|\tan\theta \qquad (2)$$

where K is the Scherrer constant, generally assumed to be 1; λ, wavelength; θ, diffraction angle; L_{hkl} the dimension perpendicular to the (hkl) crystal planes; d_{hkl}, the distance between planes; and Δd, the average deviation of d_{hkl} caused by stress. The broadening by particle size causes the peak to form a Gaussian distribution; and by microstrain, Cauchy distribution. When both the above broadening factors exist, the relationship of the integrated width δ with δ_{si} and δ_{st} is expressed by the following equation:

$$\frac{\delta_{si}}{\delta} = 1 - \left(\frac{\delta_{st}}{\delta}\right)^2 \qquad (3)$$

Substituting (1) and (2) into (3), we obtain:

$$\left(\frac{\delta}{\tan\theta}\right)^2 = \frac{K\lambda}{L_{hkl}}\left(\frac{\delta}{\tan\theta \cdot \sin\theta}\right) + 16\left(\frac{\Delta d}{d_{hkl}}\right)^2 \qquad (4)$$

In the straight-line plot of $(\delta/\tan\theta)^2$ against $\delta/(\tan\theta \times \sin\theta)$, the slope represents the particle size and the intercept represents the microstrain. When the particle size is smaller than 100 nm, the grain size measured by the X-ray diffraction method is more accurate.[5] And, the grain size as determined by X-ray diffraction is the averaged value in which the relative weight of the smaller-grain portion is higher. The TEM method is also used to measure the nanoparticle sizes, which are larger than those measured by the X-ray diffraction method. When the crystal size is smaller than 100 nm, the difference of grain sizes measured by X-ray diffraction and those by TEM is less than 20 percent.

In the experiment, the diffraction peak widths of (001) and (002), as well as (100) and (200) are used to calculate the particle size and microstrain dimensions along directions [001] and [100], respectively. the fact that under the same heat-treatment conditions $L_{[001]}$ and $L_{[100]}$ are nearly equal as shown in the experiment indicates that the crystal grains are essentially equilateral. Higher heat-treatment temperature results in larger grains. Moreover, the relationship between the grain size and the heat-treatment temperature meets the Arrhenius relation. The nanoparticle diameter is essentially determined by the crystallization temperature, not so much by the soaking time. Under the heat-treatment conditions of this experiment, the corresponding crystal size lies between 20 nm and 200 nm.

3. Changes of Soft-Mode Frequency and Axial Ratio c/a as Affected by Grain Size

The $PbTiO_3$ ferroelectricity belongs to the displacement type. The paraelectric-ferroelectric phase transition can be explained by the soft-mode theory of lattice vibration.[6] Burns et al.[7] believe that the soft optical mode that affects the paraelectric-ferroelectric phase transition is the E(1TO) mode. We used a Spex Type 403 Raman optical spectrometer with 5145 Angstroms radiation from an argon-ion laser as the light source, and measured the E(1TO) frequencies of $PbTiO_3$ nanoparticles of different sizes at room temperature. The results are shown in Table 1.

Table 1. Size Dependence of the Soft-Mode Frequency and the Ratio of c/a

Average size L_{hkl}/nm	Raman shift/cm^{-1}	c/a
Bulk	89[6]	1.0652[8]
200	85	1.065
115	85	1.064
70	82	1.064
50	81	1.064
30	78	1.062
22	71	1.059

Table 1 shows that the soft-mode frequency decreases with the decrease of the particle size. The temperature for ferroelectric phase change agrees with the "freezing" temperature of the soft mode, i.e., the temperature at which the soft-mode frequency approaches zero. Lower soft-mode frequency indicates closer proximity to the phase transition temperature. Hence, Table 1 concludes that smaller particles will have lower phase transition temperatures.

The phase transition of $PbTiO_3$ is the transition between the cubic crystal system (point group m3m) and the tetragonal system (point group 4mm). As the temperature approaches the transition point, the axial ratio c/a approaches 1. Table 1 lists the c/a values of the nanoparticles in different sizes. The values of c and a are measured with X-ray diffraction. The phenomenon wherein the c/a value decreases with smaller particle size indicates that the phase transition temperature of smaller nanoparticles is closer to room temperature, i.e., the phase transition temperature is comparatively low. This is another proof that the phase transition temperature decreases with the decrease of particle size. Due to the fact that the spontaneous polarization is in direct proportion to the c/a value, the decrease of particle size will reduce the spontaneous polarization.

4. Change of Specific Heat Peak by Particle Size

Differential scanning calorimetry of $PbTiO_3$ nanoparticles is conducted with a Perkin-Elmer Type DSC-2 thermal analyzer from room temperature to 550°C. The reference material is sapphire. The temperature is raised at the rate of 20K/min.

Figure 1 shows the relationship between the specific heat and the temperature of $PbTiO_3$ nanoparticles of different sizes. As the particle size becomes smaller, the position of the specific heat peak shifts toward that of lower temperature. In a ferroelectric substance, the specific heat peak is induced by the energy in connection to the buildup (or disappearance) of spontaneous polarization, which is one of the phase change phenomena of ferroelectricity. Figure 2 shows the relationship of particle sizes and the phase transition temperatures obtained from specific heat peaks.

Another characteristic of Table 1 is that the specific heat peak becomes lower and wider as the particle size is smaller. In fact, the peak area represents the phase transition heat ΔQ which is the energy buildup (or disappearance) from spontaneous polarization. Figure 3 shows that ΔQ decreases with the decrease of particle size. According to thermodynamics, the energy is in direct proportion to the square value of the magnitude of spontaneous polarization change at the phase transition temperature. It can be predicted that when the particle size is reduced to a certain degree, ΔQ will become zero, which means that spontaneous polarization ceases.

The fact that reduced particle size produces a wider heat peak indicates that phase transition of the small-sized particle samples takes place in a broader temperature range; in other words, the phase transition dispersiveness increases. This is probably due to imperfect crystallization of the particles. In addition, this observation can

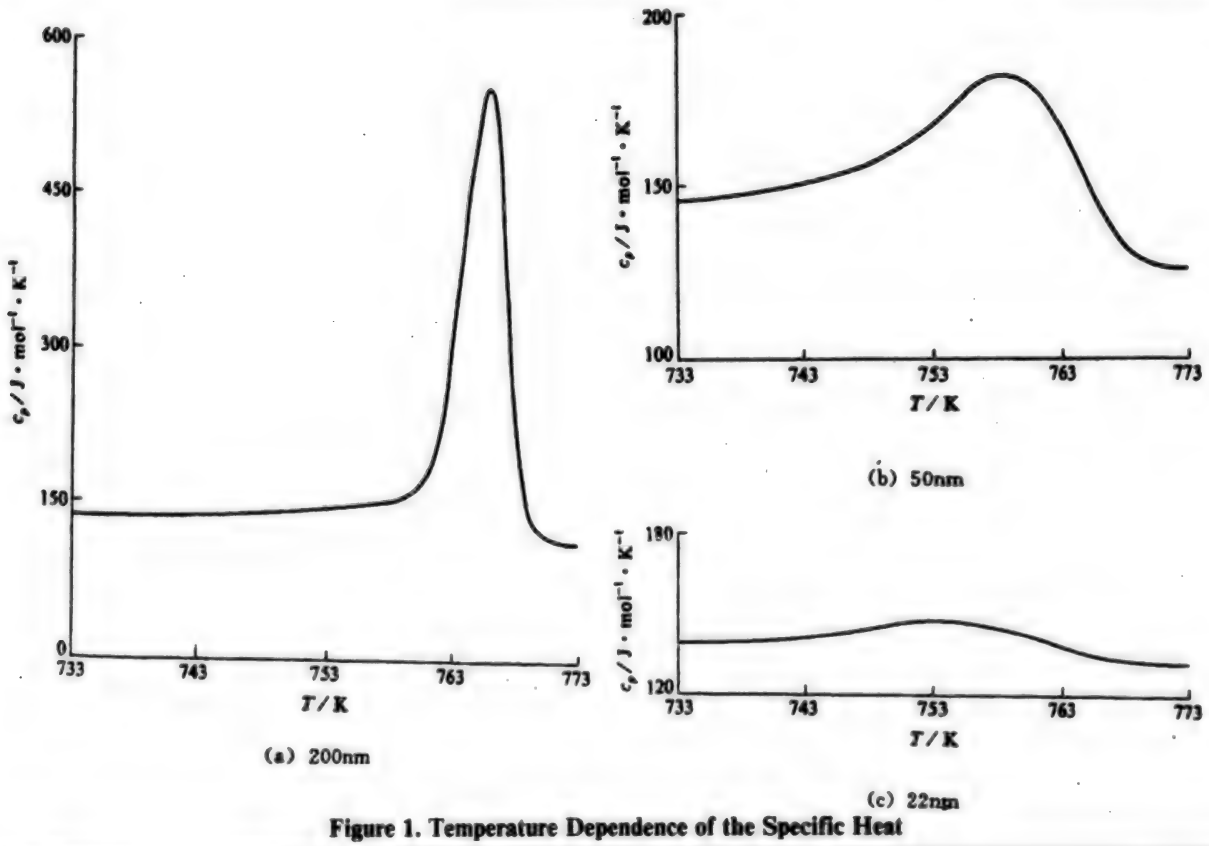

Figure 1. Temperature Dependence of the Specific Heat

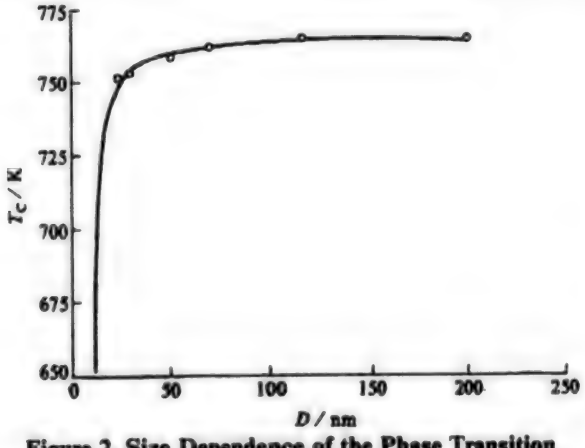

Figure 2. Size Dependence of the Phase Transition Temperature

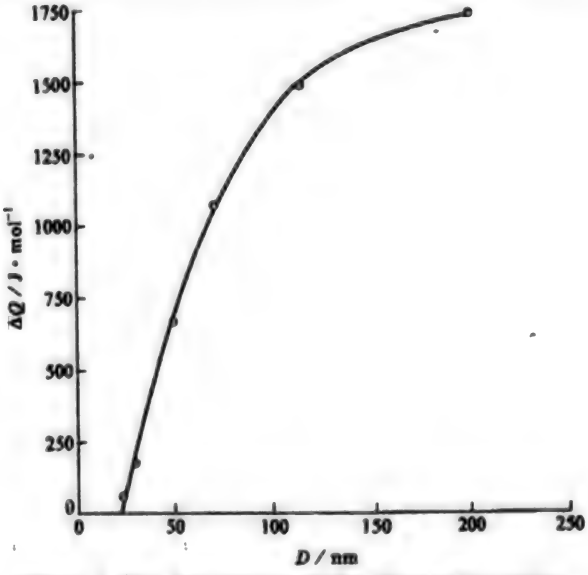

Figure 3. Size Dependence of the Heat of Transition

be further proved by the XRD spectra of $PbTiO_3$ which show that the spectra of smaller $PbTiO_3$ nanoparticles display higher background intensities and reveal non-crystalline cells.

The following empirical equation[2] is expressed by the solid line in Figure 2:

$$T_c(D) = T_c(\infty) - C/(D - 8.8)\ (K) \qquad (5)$$

This equation is derived by the least-squares approximation from the test data. In the equation, C = 256K-nm; $T_c(\infty)$ = 766K, which is the phase transition temperature of bulk $PbTiO_3$. From this equation, we have found that

when D = 9.1 nm, $T_c(D = 9.1) = 0$ K; therefore, $D_{crit} = 9.1$ nm is the minimum size of the particle possessing ferroelectricity.

Equation (5) was first suggested by Reference 2. In Reference 2, $T_c(D)$ is the temperature measured by Raman scattering when the soft-mode frequency approaches zero. In this investigation, $T_c(D)$ is the temperature of specific heat peak. The fact that test data collected from different experimental methods can nicely fit the same empirical equation indicates that the reactions both in Reference 2 and in this investigation follow the same mechanism. However, Reference 2 obtains 12.6 nm as the critical size D_{crit}; while this investigation obtains 9.1 nm. During the fitting process, we find that D_{crit} is sensitively dependent on the selection of the $T_c(\infty)$ value. Reference 2 selects 733K as $T_c(\infty)$, while this investigation selects 766K, because 766K has been adopted by most references.[9] Apparently, the differences among D_{crit} values are mainly because of the selection of different $T_c(\infty)$ values.

At present, there is no completely satisfactory theory[10] to explain the size effect on ferroelectric phase transition. We now explain it briefly from the angle of soft-mode image as follows: Ferroelectricity is essentially a long-range cooperative phenomenon. The soft-mode "freezing" is determined by the balance between the short-range force and the long-range Coulombic force.[6] For the optical transverse mode (soft mode) in a crystal with infinite size, the long-range Coulombic force is contributed by the summation of other dipoles in the crystal. To illustrate with electrical field E_s, the simplest situation is $E_s = (4\pi/3)P$, where P is polarization strength. When E_s is strong enough to overcome the short-range disturbance (tendency to cause disorder) effect, ferroelectricity can be established. For small-sized crystals, there are fewer of dipoles contributing to E_s, as a result, E_s becomes weaker. Besides, the boundary effect can no longer be neglected. Even in optical transverse mode, the depolarization field E_d is no longer zero. Just as with the short-range force, E_d also is a factor in destroying the dipole arrangement. When particle size is so small that E_s is not able to counterbalance the combined effect of short-range force and E_d, then ferroelectricity cannot be established even at low temperature. It is worth noticing that based on optical absorption and other tests, Reference 11 estimates that the length of the orderly ferroelectricity alignment in a ferroelectric body of perovskite type may vary from a few nanometers to dozens of nanometers. The critical size obtained in this experiment falls within this range. We should point out that the theoretical explanation of ferroelectric critical size is a very complicated and difficult task which should be thoroughly explored.

5. Conclusions

(1) $PbTiO_3$ nanoparticles have been prepared with the sol-gel method. Taking into consideration the instrument parameters and microstrain, the nanoparticle sizes are determined by the broadening of X-ray spectra. Their sizes range from 20 nm to 200 nm.

(2) As the particle size becomes smaller, the soft-mode frequency decreases; the axial ratio c/a becomes smaller; the temperature of specific heat peak drops and the specific heat peak turns lower and wider. These facts show that as the particle size decreases, the temperature for ferroelectric phase transition becomes lower; the spontaneous polarization diminishes; and the phase transition dispersiveness increases.

(3) The relationship between phase transition temperature and particle size coincides with the empirical equation (5), and the calculated critical size is 9.1 nm.

(4) That the phase transition temperature drops with the decrease of particle size can be explained with the soft-mode image. The decrease of particle size induces the weakening of the long-range Coulombic force of the dipole arrangement; hence, the long-range force is unable to counter the combination of the effect of depolarization field and the short-range force caused by the disturbance of the dipole arrangement.

References

1. Yao Xi, Zhang Liangyin, "Precision Composite Functional Materials," WULI [PHYSICS], 1992; 21:99 [in Chinese].

2. Ishikawa, K., Yoshikawa, K., Okada, N., "Size Effect on the Ferroelectric Phase Transition in $PbTiO_3$ Ultrafine Particles," PHYS. REV., 1988; B37:5853.

3. Uchino, K., Sadanaga, E., Hirose, T., "Dependence of the Crystal Structure on Particle Size in Barium Titanate," J. AM. CERAM. SOC., 1989; 72:1555.

4. Wilson, A. J. C., "X-Ray Optics," London: Methuen Press, 1949: 45.

5. Cully, B. D., "Elements of X-Ray Diffraction," 2nd Ed. London: Addison-Wesley Inc., 1978.

6. Cochran, W., "Crystal Stability and the Theory of Ferroelectricity," ADV. PHYS., 1960; 9:387; "Crystal Stability and the Theory of Ferroelectricity, Part Two: Piezoelectric Crystals," ADV. PHYS., 1961; 10:401.

7. Burns, G., Scott, B. A., "Lattice Modes in Ferroelectric Perovskites: $PbTiO_3$," PHYS. REV. LETT., 1970; 25: 167; "Raman Studies of Underdamped Soft Modes in $PbTiO_3$," PHYS. REV., 1973; B7:3088.

8. Joint Committee on Powder Diffraction Standards, Powder Diffraction File 6-452, Swarthmore, 1971.

9. Lines, M. E., Glass, A. M., "Principles and Applications of Ferroelectrics and Related Materials," Oxford: Clarendon Press, 1977: 248.

10. Maltani, M., Ayyub, P., Palkar, V., et al., "Limiting Long-Range Ordered Solids to Finite Sizes in Condensed Matter Physics," PHASE TRANSITIONS, 1990; 24 and 26:91.

11. Wemple, S. H., "Polarization Fluctuations and Optical Absorption Edge in $BaTiO_3$," PHYS. REV., 1970; B2:2679.

World's First Low-Cost Process for Making Kg-Class Metallic Nanomaterials Invented

94P60343A Beijing KEJI RIBAO [SCIENCE AND TECHNOLOGY DAILY] in Chinese 18 Jun 94 p 1

[Article by Yuan Xiaoyang [5913 2556 7122]: "China Invents New Technique for Fabricating Kilogram-Class Metallic Nanomaterials"]

[Summary] Beijing, 17 Jun—It has been learned from the Beijing General Institute of Nonferrous Metals (BGINM) that three BGINM Research Fellows—Li Yonghong [2621 3057 3163], Gao Yuzun [7559 1937 1415], and Zhang Taisong [1728 3141 1345]—have invented the world's first low-cost process for fabricating kilogram-class metallic nanomaterials. The BGINM chemical technique for fabricating these nanomaterials in kilogram-class amounts—quantities large enough to permit utilitarian production outside the laboratory—is opposed to the more expensive evaporation/condensation method. Applications for these nanomaterials include non-platinum-based catalytic converters, ultrafine metallic conducting resins, ultralow- temperature heat exchangers, and additives for making composite materials.

Study of High-Speed CVD for C/C Composite: High-Speed Directional Diffuse Technology

946B0108A Beijing GAO JISHU TONGXUN [HIGH TECHNOLOGY LETTERS] in Chinese Vol 4 No 2, Feb 94 pp 19-21

[Article by Luo Ruiying [5012 3843 4134], Yang Zheng [3799 1513], Qiao Shengru [0829 3932 0320], Yang Zunshe [3799 1415 4357], Kang Mokuang [1660 3106 3693], and Liu Yinglou [0491 2019 2869] of the Department of Materials Science and Engineering, Northwestern Polytechnical University, Xian 710071: "Study of Rapid Chemical Vapor Deposition of Carbon-Carbon Composite—High Speed Directional Diffusing Technology," sub-topic of a key basic research topic of the State's "Eighth 5-Year" Plan; MS received 25 Oct 93, revised 10 Dec 93]

[Text]

Abstract

A new technique to prepare carbon/carbon composite by high-speed vapor-phase deposition is developed. By means of the directional diffusion device in the deposition chamber and the directional pressure difference of the sample thickness, the hydrocarbon gas speedily and directionally diffuses into the sample and begins the deposition process. The test results show that the precipitation is rapid, and the final density of the sample is high and uniform.

Key words: High-speed directional diffusion, chemical vapor deposition, carbon/carbon composite.

I. Introduction

There are two methods to prepare carbon/carbon (C/C) composite: the resin (tar) method, and the chemical vapor deposition (CVD) method. The resin method is complicated; its products display drawbacks such as low density, inferior properties, tendency to crack, and lamination. The CVD method is simple; its products have uniform structure, high integrity, high density, and superior properties.[1] However, the CVD method is costly because it requires a long working cycle. Therefore, the main task, both here and abroad, is how to speed up carbon deposition, and reduce production time. The metallic coated carbon fibers can catalytically decompose the hydrocarbons, but only the inferior carbon blacks are deposited on the fiber.[2] Based on a large amount of exploratory experiment, this investigation has greatly improved the CVD equipment, and designed a new technique to prepare C/C composite. The equipment for the new method is simple to install, and easy to operate. Preparing C/C composites with the new technique takes less time, costs less, and is highly efficient.

II. Principle of Preparation Method

The process to deposit carbon on carbon fiber is as follows: The hydrocarbon gas dissociates into free radicals which then combine into active agglomerates. The agglomerates spread over the carbon fiber surface, and form nuclei that grow.[3] Increasing the precipitation rate requires the optimum combination of these three parameters: temperature, furnace pressure, and flow rate of the mixture of hydrocarbon and carrier gas. Even so, the vapor-phase precipitation rate will still be low; and precipitation time, long. Precipitation temperature is a much more sensitive parameter than that of furnace pressure and flow rate. Raising the precipitation temperature will undoubtedly increase the rate of hydrocarbon dissociation and the diffusion rate of the active agglomerates; and, consequently, increase the precipitation rate. However, the temperature effect on the chemical reaction rate is many times higher than its effect on the diffusing mass transfer rate.[4] Eventually, the concentration of the active agglomerates close to the sample surface becomes greater than that inside the sample; as a result, the agglomerates precipitate onto the surface before they can diffuse into the sample. This surface precipitation seals the paths by which the hydrocarbon gas flows into the sample, and the closed pores hinder interior densification. The furnace pressure is the sum of the partial pressures of the gas components (hydrocarbon, reaction residue, and carrier gas). The flow rate is the gas flow rate when the precipitation reaction is in active-state equilibrium. Excessive increase of flow rate and furnace pressure would still create the defects of the coated surface; it would also produce carbon graphite on the surface. If the gas directly diffuses into the sample body, causing dissociative combination and nucleation and growth, not only the precipitation rate can be increased, but the aforementioned defects can also be avoided. Based on this principle, under the optimum parameter combination, a precipitation chamber and a gas directional diffusion device have been designed. Based on the sample's inner and outer pressure difference and through the directional diffusion device, the low-temperature gas can rapidly diffuse into the sample body and then precipitate there.

III. Experiment and Results

The starting materials for the experiment are: 1K high-strength I-type polyacrylonitrile (PAN) plain carbon cloth made by Jilin Carbon Plant, propylene as precipitation gas, and nitrogen as carrier gas. For the experiment, two groups of samples are made (each group has two samples: for the large samples, outside diameter (OD) = 105 mm, and inside diameter (ID) = 20 mm; for the small samples, OD = 55 mm, and ID = 15 mm). One sample group is prepared by the differential pressure (DP) method and the other group by the high-speed directional diffusion (HSDD) method. Figure 1 shows the flow chart for the two samples prepared by the HSDD method.

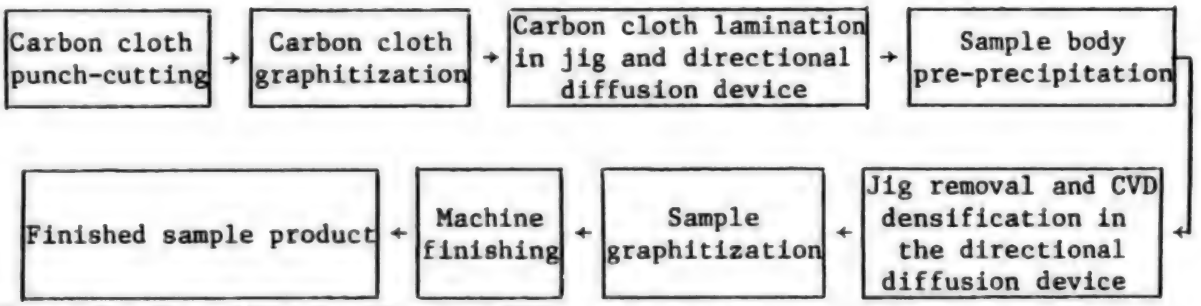

Figure 1. Flow Chart of High-Speed Directional Diffusion Technique

Table 1. Comparison of CVD Performance of DP Method and HSDD Method

Method		Precipitation time (h)	Final density (g/cm^3)	Sample surface coating area vs. total area (%)	Diametric density variation		Possibility for further densification	Carbon black area vs. total area (%)
					Sample density after removal of 10 mm surface thickness by turning (g/cm^3)	Density of the removed portion (g/cm^3)		
DP	Small sample	900	1.6	70	1.49	1.65	No	6
	Large sample	1100	1.4	85	1.30	1.48	No	8
HSDD	Small sample	500	1.75	0	1.75	1.75	Yes	0
	Large sample	600	1.70	0	1.70	1.70	Yes	0

Table 1 compares the results of the DP and HSDD methods. It shows that for the DP method, the sample surface has large blocks of precipitation carbon coating layers and small specks of carbon black, because the active agglomerates dissociated from the hydrocarbon gas concentrate more on the sample surface than on the sample interior. For further precipitation, after CVD densification, the sample must be machined to remove the surface coating and then treated with intermediate graphitization to remove the bottleneck-shaped closed pores. The process must be repeated many times, and the final sample density is still not high enough. The smoke-like carbon graphite dust has poor quality, and when they are sucked into the minute path openings in the sample body due to pressure differences, the sample cannot be further densified.

For the HSDD method, the hydrocarbon gas directionally diffuses into the sample body at high speed and then precipitates, and no surface coating nor carbon black forms, up until the density of the large CVD sample reaches 1.70; and that of the small sample, 1.75. Hence, no intermediate machining nor intermediate graphitization is needed (Figure 1). As a result, sample materials are economically used and the process is simplified. Furthermore, the precipitation process indicates that the precipitation rate within the sample body is high; precipitation time, low; and final sample density, high and uniform. Consequently, the HSDD method greatly increases the efficiency of the gas precipitation technique.

IV. Conclusion

For the first time in China, the HSDD method has been adopted to prepare carbon/carbon composites by gas precipitation. The process is simple and reliable, it reduces the precipitation time while increasing the precipitation efficiency. The final product has high density and superior properties at low cost. Doubtless, the HSDD process has a bright application future.

References

1. Wang Maozhang and He Fu, "Carbon Fiber: Manufacturing, Properties, and Applications," Beijing: Science Press, 1984: 486 [in Chinese].

2. Sugio Otani and Yuzo Sanada, translated by Zhang Mingda and Yang Zunying, "Elements of Carbon Engineering," Co-published by CAS Metals Research Institute and Lanzhou Carbon Plant, 1985: 68 [in Chinese].

3. W. Dele, K. Koetzlicker, H. Nickol, translated by Shi Xiaolo, "Thermal Decomposition of Carbon," Research Institute of Lanzhou Carbon Plant, 1983: 39 [in Chinese].

4. Fitzer, E., "The Future of Carbon-Carbon Composites," CARBON, 1987, 25(2): 170.

Microstructure, Interface of SiCp/Al Composites

946B0108B Beijing GAO JISHU TONGXUN [HIGH TECHNOLOGY LETTERS] in Chinese
Vol 4 No 4, Apr 94 pp 17-20

[Article by Geng Lin [5105 2651] and Yao Zhongkai [1202 1813 0418] of the Metal-Matrix Composite Research Office of Harbin Institute of Technology, Harbin, 150001, and Li Yichun [2621 5030 2504] of the General Research Institute for Nonferrous Metals, Beijing, 100088: "Microstructure and Interface of SiCp/Al Composites," funded by the Foundation of the State Key Laboratory for Metal-Matrix Composites of Shanghai Jiaotung University; MS received 18 Nov 93, revised 27 Jan 94]

[Text]

Abstract

The microstructure and interface of silicon-carbide-particle-reinforced aluminum alloy (SiCp/Al) composites made by squeeze-casting are studied. The results show that silicon carbide particles distribute uniformly in the composite. The amount of dislocation in the matrix is dense, and there is a small amount of stacking fault in silicon carbide particles. The interface bonding in SiCp/Al composite is perfect without the existence of reactants and holes. The absence of naked silicon carbide particle existing on the tensile fractured surfaces of SiCp/Al composites indicates that SiCp-Al interface is not broken during tensile fracturing of the composites, and that SiCp-Al interface produced by squeeze-casting has good interface bonding.

Key words: Silicon carbide, Aluminum, Composite Material, Interface

I. Introduction

In the early 1980s, a composite material with silicon carbide particle as reinforcing phase and aluminum alloy as matrix was prepared in the United States.[1] The composite has similar specific gravity, yet higher strength and rigidity as compared with aluminum alloy. Moreover, it has the good characteristics of high-temperature properties, abrasive resistance, and dimension stability as well as fabrication by conventional metallic processing methods.[1-4] SiCp/Al composite is being used more extensively owing to these characteristics.

SiCp/Al composite can be prepared by powder metallurgical method (P/M) or by squeeze-casting. Different methods will result in different microstructures and especially different SiCp/Al interface bonding. The interface bonding mode is the most important factor affecting the SiCp/Al composite properties; hence, an ever increasing number of research studies concentrate on the SiCp/Al composite interface.[6] Based on the microstructure research of SiCp/Al composites made by the squeeze-casting method, this paper investigates the SiCp/Al interface bonding, utilizing a transmission electron microscope (TEM) for microstructure study and scanning electron microscope (SEM) for fracture surface study. The research results offer significant theoretical guidelines for the analysis and improvement of SiCp/Al composite properties.

II. Material and Testing Method

The reinforcing materials used in this experiment are silicon carbide particles made by the Shenyang First Grinding Wheel Plant. The average particle size is 3.5 μm. The matrix material is industrial LDz aluminum alloy. Tables 1 and 2 show the physical properties of SiC particles and the chemical compositions of LDz aluminum alloy, respectively. The SiCp/Al composite is prepared by a squeeze-casting method. The particles occupy 35 volume percent of the material.

Table 1. Physical Properties of SiC Particles

Crystal type	Melting point (°C)	Density (g/mm^3)	Modulus of elasticity (Cpa)	Coefficient of thermal expansion (10^{-6}/°C)
Hexagonal	2735	3.25	57,000	4.3

Table 2. Chemical Composition of LDz Aluminum Alloy (wt/%)

Cu	Mg	Si	Cr	Fe	Zn	Ti	Al
0.50	0.83	1.06	≤0.20	≤0.50	≤0.20	<0.15	Balance

The particle configuration and distribution in the SiCp/Al composite, the dislocation density in the matrix alloy, and the SiC particle defects are studied with a TEM. The tensile fractured surface topography, as well as the relative compositions of Si and Al of certain zones on the fracture surface are studied and measured respectively with a SEM.

III. Results and Discussions

The squeeze-casting process to make SiCp/Al composite includes mainly the preparation of particle preform, and then the diffusion of molten aluminum alloy into the preform under a specified pressure. The SiC particle distribution uniformity in the composite depends on its distribution uniformity in the preform, which is determined by the preform preparation technique. The porosity and the SiCp/Al bonding mode of the composite are closely related to the squeeze-casting parameters. The TEM photo in Figure 1 shows that the SiC particles in the SiCp/Al composite used in this experiment display an irregular configuration and are uniformly distributed in the matrix. Besides, there is basically no hole in the composite material, and the bonding state in the interface is good.

Figure 1. TEM Photo: SiCp/Al Composite

TEM observation also reveals that dislocation distribution in the matrix of SiCp/Al composite is comparatively denser, as shown in Figure 2. The thermal expansion coefficient of the SiC particles in the SiCp/Al composite is about one-sixth that of the aluminum alloy. Hence, during cooling of the composite from high temperature to room temperature, large thermal stress is induced across the interface of the SiCp/Al. When the thermal stress is greater than the yield strength of the matrix alloy, the matrix alloy deforms plastically, which consequently increases the dislocation density. High dislocation density strengthens the matrix alloy. As a result, the composite strength is improved.

Figure 2. TEM Photo: Dislocation Density in SiCp/Al Composite Matrix Alloy

To further analyze the interface bonding state of the SiCp/Al composite, high-magnification TEM observations are conducted. As shown in Figure 3, the interface is very clean and no reactant phase nor segregated phase exists. Figure 3 also shows that a certain number of structural defects of stacking fault exist in the SiC particles. This structural defect will affect particle strength as well as the SiCp/Al interface bonding mechanism. On the one hand, the structural defects in the SiC particles make it easier for the aluminum in the matrix alloy to diffuse into the particles, which induces the diffusion bonding in the SiCp/Al composite interface. On the other hand, these structural defects would affect the particle surface structure, which in turn affects the crystallization of liquid aluminum on the particle surface during the composite preparation by squeeze-casting; and, consequently, this affects the SiCp-Al interface bonding mechanism in the composite. The interface bonding mechanism in the SiCp/Al composite made by squeeze-casting needs further study. And the stacking fault structural defect in the SiC particles as shown in Figure 3 has specific significance on the further study of the SiCp-Al interface bonding mechanism.

The interface bonding mode of SiCp/Al composite determines the interface bonding strength. At present, there is no preferable method to measure the SiCp/Al composite interface bonding strength. Indirect measurement is generally used. This investigation uses SEM analysis on the tensile fractured surface, and qualitatively analyzes the interface bonding strength of the SiCp/Al composite.

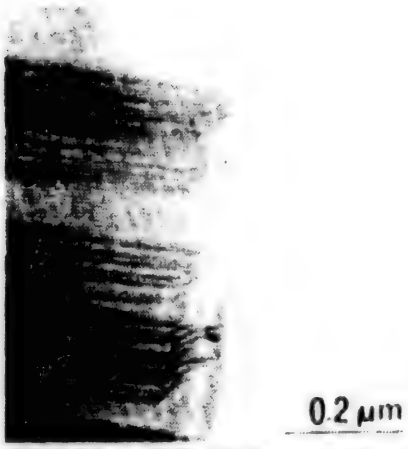

Figure 3. TEM Photo: SiCp/Al Composite Interface

Figure 4 shows the SEM photos of the SiCp/Al composite tensile fractured surface. Many imprints left by SiC particles after they were pulled away are shown on the fracture surface; however, there are no naked SiC particles on the surface. This indicates that during the process of tensile fracturing, the SiCp/Al interfaces have not been separated. The actual fracturing proceeds in the matrix. To further prove this, relative quantitative analyses of Si and Al are conducted at a selected few SiC particle imprint areas on the fracture surface (A, B, C, and D in Figure 4). Table 3 shows the results. The fact that certain amounts of both elements, Al and Si, exist at every imprint indicates that there actually were SiC particles and that the surface of each particle was covered with aluminum alloy. The different relative quantities of Al and Si at each imprint indicate that the thickness of the aluminum alloy covering each particle varies. The aforesaid illustrates that during the tensile fracturing of the SiCp/Al composite, the failure did not occur on the SiCp-Al interface, and the failure of the composite was caused by shear or by tensile fractures of the matrix in the neighborhood of the interface. From this observation, we can deduce that during the squeeze-casting process, the bonding strength between silicon carbide particles and aluminum alloy matrix is higher than the strength of the aluminum alloy matrix. The explanation of this phenomenon requires further research on the interface bonding mechanism of this type of SiCp/Al composite.

Table 3. Compositions of Selected Spots on Tensile Fractured Surface of SiCp/Al Composite

Point	A	B	C	D
Al (wt%)	35.79	39.45	45.30	23.72
Si (wt%)	64.21	60.55	54.70	76.28

IV. Conclusions

1. SiCp/Al composite prepared by a squeeze-casting process contains uniformly distributed silicon carbide particles of irregular shape. Holes are not observed in the composite. The interfaces have good bonding. No other reactant exists in the interfaces.

2. No naked silicon carbide particles exist on the tensile fractured surface. All the silicon carbide particles on the tensile fractured surface are covered with aluminum alloy of different thickness.

3. In the SiCp/Al composite made by the squeeze-casting method, the bonding strength between the silicon carbide particles and the aluminum alloy matrix is higher than the strength of the aluminum alloy matrix.

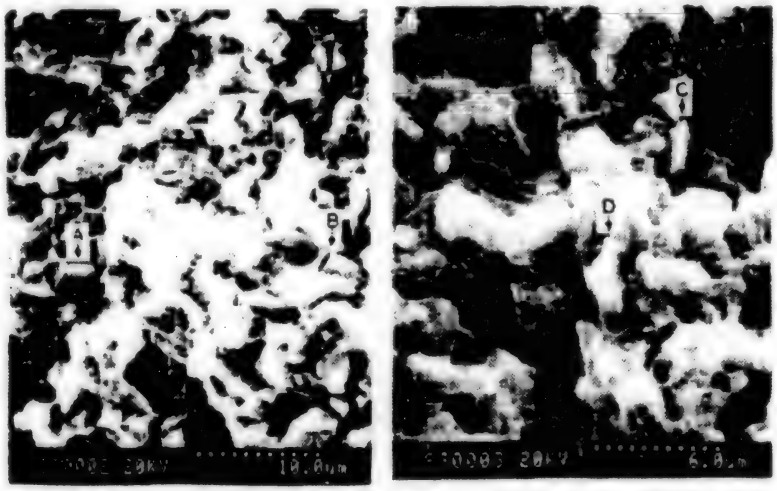

Figure 4. SEM Photo: Tensile Fractured Surface of SiCp/Al Composite

References

1. Li Yichun, "Study of the Dimensional Stabilization Technique of Particulate-Strengthened Aluminum Matrix Composite," Master's Thesis, Harbin Institute of Technology, 1991:3.

2. Arsenault, R. J. and Fisher, R. M., SCRIPTA METALLURGICA, 1983, 17:67.

3. Alpas, A. T. and Embury, J. D., SCRIPTA METALLURGICA, 1990, 24:931.

4. Cao Li, Wang Chuanying, and Shao Juling, Proceedings of Third Chinese Youth Materials Science Symposium, Dalian, 1991:419.

5. Prasad, S. V. and Rohatgi, P. K., JOURNAL OF METALS, 1987, 11:22.

6. Wang Chuanying, Cao Li, and Shao Juling, Proceedings of Third Chinese Youth Materials Science Symposium, Dalian, 1991:382.

Preparation of TiC-Ni_3Al Matrix Composites by SHS Technique

946B0093B Beijing GUISUANYAN XUEBAO [JOURNAL OF THE CHINESE CERAMICS SOCIETY] in Chinese Vol 22 No 2, Apr 94 pp 168-172

[Article by Mei Bingchu [2734 2671 0443], correspondent, and Yuan Runzhang [5913 3387 4545] of the Advanced Materials Research Institute, Wuhan University of Technology, Wuhan 430070: "Preparation of TiC-Ni_3Al Matrix Composites by Means of SHS Technique"; MS received 21 Nov 92]

[Text]

Abstract

The preparation of TiC-Ni_3Al composites from the four elements Ti, C, Ni, and Al by the SHS technique is investigated. The combustion temperature variation curves are measured. The results show that the combustion reaction temperature is high; its fluctuation is complicated and influenced by the TiC content. XRD and SEM are used to analyze the products of different compositions. The results show that through the SHS process, in the system where these four elements exist in a powder state, the designed TiC and Ni_3Al phases are the two stable phases. The synthesized products are porous, loose, and with cracks. The TiC crystals are fine and spherical powders.

1. Introduction

Since Walton and Poulos[1] synthesized refractory materials by the self-propagating high-temperature synthesis (SHS) technique, SHS has become one of the important research topics in the materials field. Hundreds of materials, including carbides, borides, intermetallic compounds, composites, etc., have been synthesized by the SHS method.[2,3]

In composite preparation, surface contamination and oxidation of raw powders are the principal factors affecting the final product properties.[4] For the TiC-Ni_3Al material system, particle properties (size, surface condition, etc.) of the ceramic phase (TiC) affect not only material properties, but also are crucial to the success or failure of the synthesizing process. The TiC-Ni_3Al composite is made from Ti, C, Ni, and Al by the SHS technique, based on the equation $Ti+C+3Ni+Al \rightarrow TiC+Ni_3Al$. Since TiC and Ni_3Al are made simultaneously at high temperature, there is the possibility that surface conditions will be greatly improved; thus particle surface contamination in the powder metallurgical process is avoided.[5]

This investigation adopts the Ti-C-Ni-Al system. It contains two violent exothermic reactions: $Ti+C \rightarrow TiC$, and $3Ni+Al \rightarrow Ni_3Al$. The intermetallic compound Ni_3Al has a certain distinctive high-temperature property; within a specific temperature range, its yield strength increases with the increase of temperature. Hence, the composite with the TiC and Ni_3Al phases is a good candidate for engineering structural material.[6] At present, cracks appear in the synthesized material. To obtain a solid material, an additional densification process (e.g., pressing) is required, which is a current research topic in progress.

2. Experimental Process

The raw materials used in this experiment are titanium, nickel, and aluminum powders with particle size of 30 μm, 10 μm, and 10 μm, respectively; and amorphous carbon powder (carbon black).

The powders are respectively weighed according to the following TiC and Ni_3Al chemical reaction:

$$w(Ti + C) + (1 - w)(3Ni + Al) \rightarrow wTiC + (1 - w)Ni_3Al,$$

where w is the mass content: 10 percent, 20 percent, 30 percent, 40 percent, and 50 percent, respectively. The raw material powders are measured according to calculated proportions, loaded into a ceramic container and mixed for 4 hours. The powder mix is removed from the container and then statically cold pressed (200 MPa) into a cylinder with a relative density of 50 percent. The pressed cylinder is then loaded into a SHS reaction device and synthesized with the bulk-heating ignition method (there are two SHS ignition methods: end-heating ignition, and bulk-heating ignition). The temperature parameters during the synthesizing process are measured, and the synthesized products are analyzed with XRD and SEM.

3. Results and Discussions

3.1 Reaction Temperature

Figure 1 shows the relationship of the system initial combustion temperature (ignition temperature) T_{ig} and

the maximum combustion temperature T_c versus the composition w. It shows that the T_{ig} temperature is independent of the system composition. The T_{ig} temperature (about 800°C)[6] is exactly the initial combustion temperature of the 3Ni+Al → Ni_3Al system. In the system composed of Ti, C, Ni, and Al elements, the main reactions are 3Ni+Al → Ni_3Al, and Ti+C → TiC. The ignition temperature of the latter is 1100°C.[3] Therefore, it can be assumed that the former reaction occurs first, causing the temperature to rise; then the latter reaction is ignited and the system temperature gradually increases until the reaction is completed. After that the system temperature gradually lowers to room temperature.

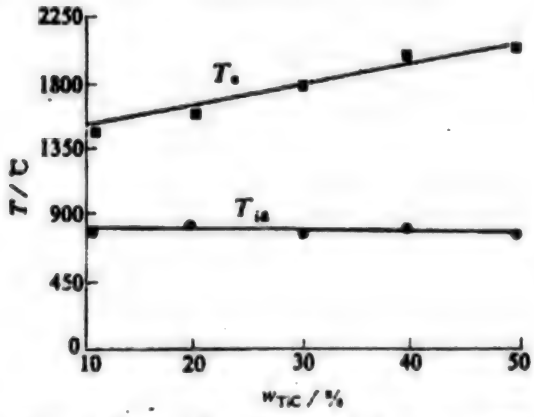

Figure 1. T_{ig} and T_c of TiC-Ni_3Al System vs. TiC Content

T_{ig}—Ignition temperature; T_c—Combustion temperature

The maximum combustion temperature T_c rises with the TiC content. Due to the fact that the free enthalpy of formation for TiC is -184 kJ/mol, and that for Ni_3Al is only -37.5 kJ/mol, the increase of TiC content means an increase of heat released from the reaction system, and consequently, the system temperature rises. Figure 1 shows that T_c is always above the melting point of Ni_3Al (1340°C), which explains why, during the combustion process, the metal phase is in the molten state. This factor is an indispensable condition for the preparation of dense composite materials.

Figure 2a shows that at the beginning of the combustion, the temperature rises very rapidly from room temperature to 1900°C, drops to about 1800°C, then instantaneously rises to the system's highest temperature (about 2000°C). Figure 2b is the temperature variation curve of the combustion wave front. These curve configurations indicate that the reaction proceeds in a very complicated manner; however, the phenomenon is beyond the discussion of this paper.

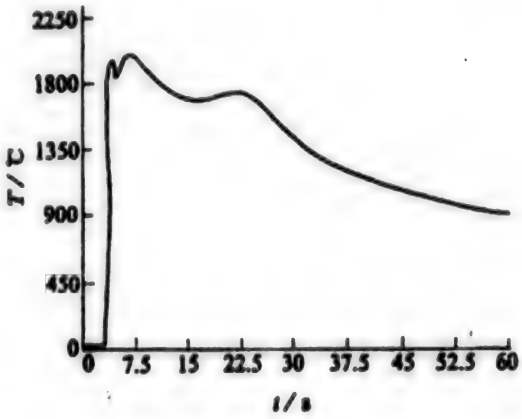

(a) Whole combustion

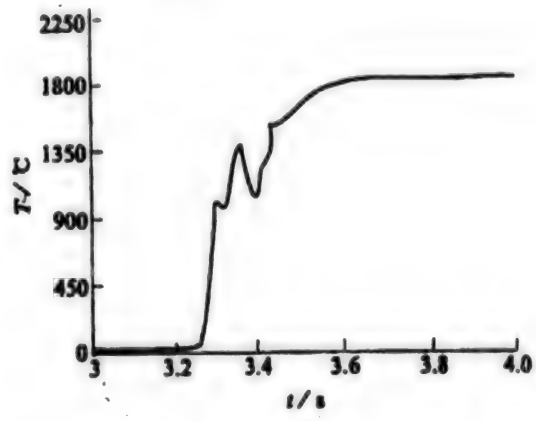

(b) Combustion front

Figure 2. Temperature Profile for the Combustion of 50% TiC + 50 % Ni_3Al

3.2 Morphology and Structure of Product

The synthesized products are porous and full of cracks. The porosity increases and the holes enlarge with the increase of the TiC content (Figure 3). The TiC particles are comparatively small, averaging about 3 μm; they are spherical in shape and appear to have been corroded (Figure 4).

The porous and puffy product is a drawback of the SHS technique. The causes of the puffy state and inconsistent densification are as follows: existing porosity after compacting; cracks caused by the internal and external temperature difference during the exothermic reaction; volume changes of the reactants; and the densification effect from the liquid phase during reaction.

(a) 10% TiC

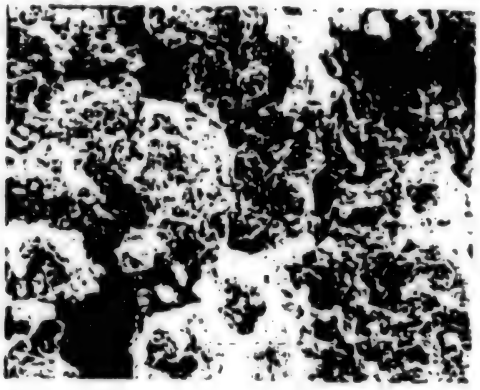

(b) 30% TiC

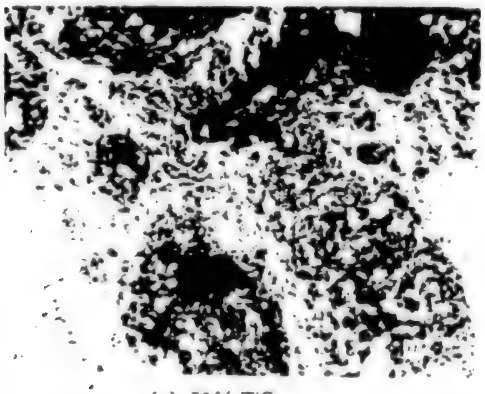

(c) 50% TiC

Figure 3. SEM Photographs of Products

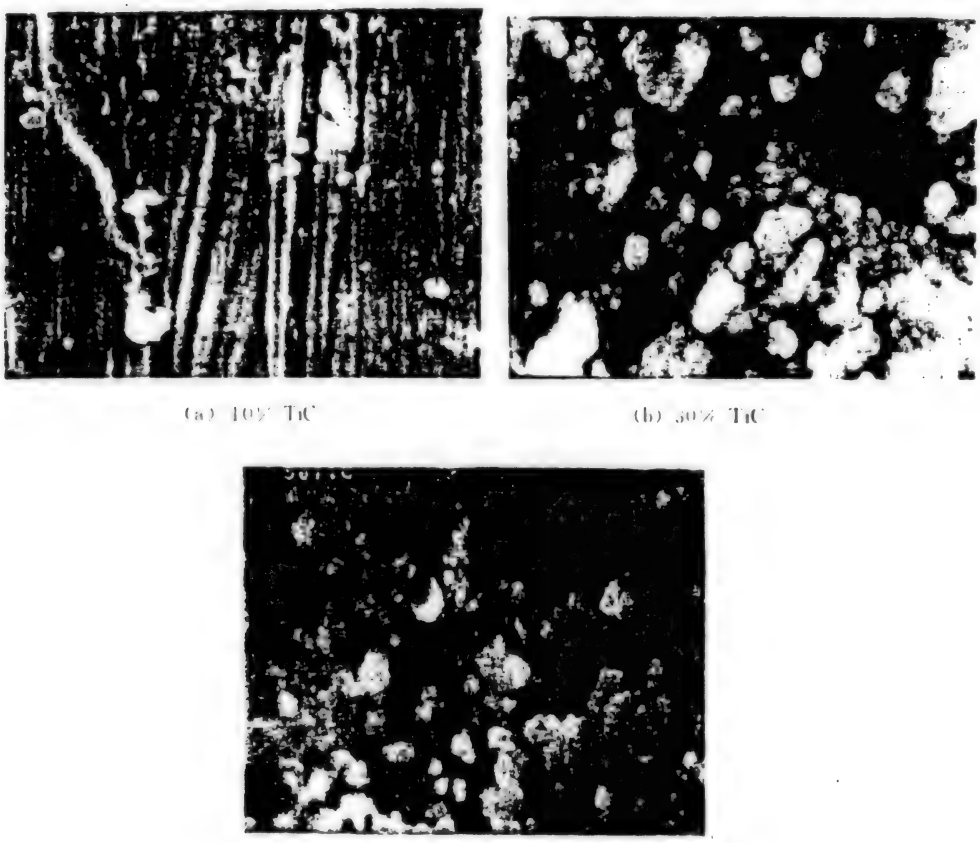

(a) 10% TiC (b) 30% TiC

(c) 50% TiC

Figure 4. Morphology of Synthesized TiC Particles, 2000 X

3.3 XRD Analysis

The XRD analyses of composite products with 10 percent, 30 percent, and 50 percent TiC, respectively, are conducted with a rotating target X-ray diffractometer (Figure 5). Figure 5 shows that the existing TiC and Ni_3Al phases are the same as the designed phases. This means that after the SHS process, the TiC and Ni_3Al phases are the two stable phases in the Ti, C, Ni, and Al quaternary system. Figure 5 also shows that the corresponding diffraction peaks change with the changing of TiC and Ni_3Al contents. The corresponding peak intensities also change accordingly. The intensities of TiC diffraction peaks become stronger when the TiC content is increased from 10 percent to 50 percent. The Ni_3Al peak intensities weaken when the Ni_3Al content is reduced from 90 percent to 50 percent, and the low angle peak intensities almost vanish at 30 percent Ni_3Al.

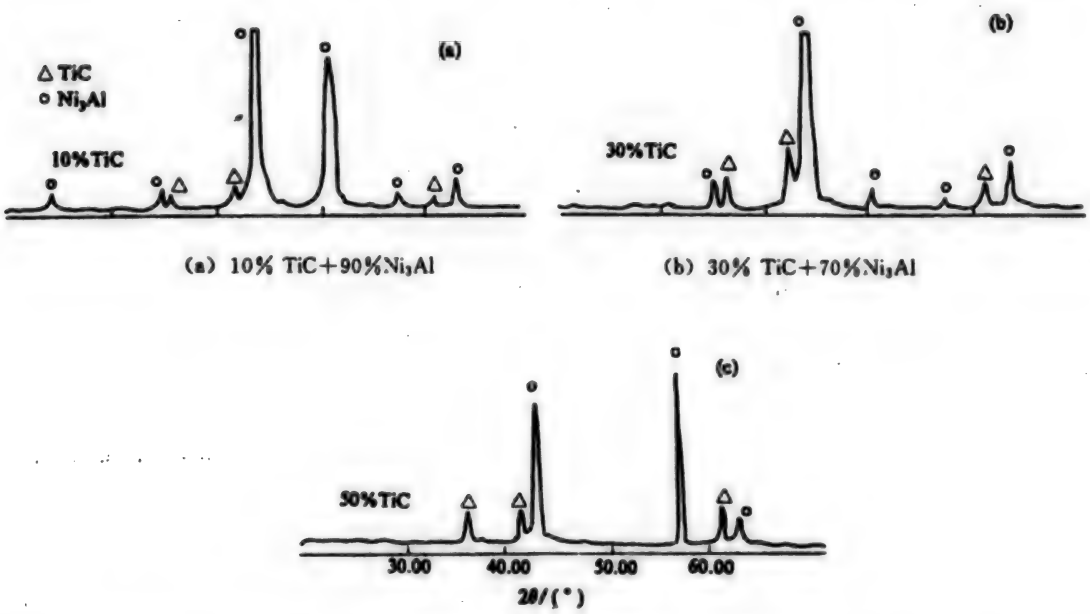

(a) 10% TiC+90%Ni_3Al (b) 30% TiC+70%Ni_3Al

(c) 50% TiC+50%Ni_3Al

Figure 5. X-Ray Diffraction Patterns of Products (With Different Compositions)

4. Conclusions

According to the properly calculated compositions of TiC and Ni_3Al, materials with only TiC and Ni_3Al phases can be synthesized from the four elements, Ti, C, Ni, and Al, by the SHS technique. The combustion temperature of this system is quite high. The content of TiC can vary from 10 percent to 50 percent; and the reaction temperature, from 1500°C to 2000°C. In this temperature range, the metal phase is in molten state which makes the dense TiC-Ni_3Al composite possible. The product is porous, puffy, and with cracks. To obtain a solid material, additional densification method has to be used. The synthesized TiC crystals are small, spherical, and look to be corroded. On this basis, it is inferred that TiC particles could have been segregated from the liquid phase.

References

1. Walton, J. D., Poulos, N. E., "Cermets From Thermite Reactions," J. AM. CERAM. SOC., 1959; 42:40.

2. Yi, H. C., Moore, J. J., "Review of Self-Propagating High-Temperature Synthesis (SHS) of Powder-Compacted Materials," J. MATER. SCI., 1990; 25:1159.

3. Holt, J. B., Munir, Z. A., "Combustion Synthesis of Titanium Carbide: Theory and Experiment," J. MATER. SCI., 1986; 21:251.

4. Adams, M. L., Kampe, S. L., "Characterization of Rapidly Solidified Ceramic Titanium Aluminide Powders," INT. J. POWD. MET., 1990; 26(2):105.

5. Kecskes, L. J., Niiler, A., "Impurities in the Combustion Synthesis of Titanium Carbide," J. AM. CERAM. SOC., 1989; 72(4):655.

6. Dunmead, S. D., Munir, Z. A., "Simultaneous Synthesis and Densification of TiC/Ni-Al Composites," J. MATER. SCI., 1991; 26:2410.

Aerospace

HK Aerospace Firm To Be Link to Overseas Market

40100076A Beijing CHINA DAILY (Investment & Trade) in English 6 Jun 94 p 2

[Article by Liu Weiling]

[Excerpts] China Aerospace International Holdings Ltd (CASIL), a Hong Kong-based subsidiary of China Aerospace Corp, is poised to become the Chinese aerospace industry's new window on the international market.

To expand the overseas market for China's aerospace products, CASIL hopes to establish branches in North America, Europe, South America and Australia in the near future, according to Wang Meiyue, its chairman and president.

The branches will be responsible for marketing, raising capital and gathering information.

CASIL is also exploring co-operation with investors from Japan, South Korea, Europe and the United States to establish manufacturing joint ventures, Wang said.

"We aim to make the company into an international conglomerate in five to 10 years," he said.

The company's major goal is to apply China's advanced aerospace technology to civilian use and help train management and sales personnel for China Aerospace Corp. The corporation is in urgent need of such skills as it enters the market economy.

Wang said, "We plan to base our future development mainly on the manufacturing of high-technology products such as programmed exchanges; big-screen, multifunctional colour TV sets; car alarm products; high-grade liquid crystal displays; fax paper; computers and satellite products."

The company already has a factory in Huizhou making telephone exchanges and intends to soon expand its annual production capacity to 1 million lines.

It is also considering joint ventures in Europe to produce colour TVs to crack into the European and American markets. [passage omitted]

To support the production of high-tech products, the company has established an aerospace science centre in Hong Kong that has recruited a strong team of technicians.

Similar centres are also planned for Shenzhen and Beijing to help China Aerospace Corp convert its advanced military products to civilian use, Wang said.

CASIL was established last year based on the old Hong Kong Conic Investment Co Ltd, which was taken over by China Aerospace Corp. By the end of 1993, the company had assets worth 1.7 billion Hong Kong dollars ($218 million).

Transfer of Aerospace Technology to Civilian Sector Still Needs 'Catalyst'

946B0123A Beijing JINGJI RIBAO [ECONOMIC DAILY] in Chinese 10 Apr 94 p 7

[Article by Guo Xiao [6753 2556]]

[Text] As the 'cold war' era came to an end, many developed countries actively increased their efforts to transfer aerospace technology to the civilian sector. For example, the U.S. Government has established and implemented various plans to promote the application of aerospace technologies for commercial use. Many of the U.S. aerospace technologies have been applied to areas such as medicine, public safety, energy, transportation, communications, manufacturing, and recreation; the cost-to-benefit ratio of such investment is as high as 1:14.

China is one of the more advanced countries in aerospace technology. Since establishing its aerospace industry 40 years ago, China has developed a series of advanced launch vehicles, and has successfully launched 35 different applications satellites and scientific research satellites; it is now in a position to compete in the international satellite-launch market. The latest achievements in China's aerospace technology have not only stimulated the development of other high-tech areas, but also promoted technological reforms and advancement in traditional industries. Since the 1980s, China's aerospace industry has made a concerted effort to transfer its technology to various commercial industries; it had developed thousands of high-tech equipment which are desperately needed for China's economic development, and durable consumer products which are needed to improve people's standard of living. However, technologies used by the civilian sector still account for only a small portion of the total accomplishments of the aerospace industry. The huge technical and economical potential of China's aerospace technology still has not been fully exploited.

Why is the transfer of aerospace technology to the civilian sector proceeding at such a slow pace? This was a topic of discussion at a recent conference on the application and promotion of aerospace technology held in Beijing. Representatives from different segments of the aerospace industry who attended the conference believe that the main reasons are the following:

First, the administrative system and operating system of the aerospace industry were established in the past primarily to develop military products and to carry out military plans; they are not effective in transforming scientific achievements into commercial products. Furthermore, there is a lack of overall policy to encourage the transfer of technological achievements.

Second, there is a lack of a unified plan and strong leadership to implement the transfer of aerospace technology to the civilian sector. Every research institution or factory implements its own plan either in the transfer of scientific achievements or technology development without coordinating with one another.

Third, many of the technological achievements cannot be produced on a large scale because the individual research organizations are not equipped for mass-production or do not have the capability to market the products.

Fourth, many of the efforts to commercialize military products were abandoned because the product supplier and receiver have conflicting interests and are unwilling to compromise or to invest funds for secondary product development or testing.

Fifth, most of the technologies of the aerospace industry are not protected in a legal sense because patents have not been applied; the phenomena of pirating of such technologies are wide spread. Also, a reasonable pricing structure has not been established; often the price of a product of technology-transfer is lower than the cost of research and development; clearly this affects the incentives of the technology-development organizations.

However, experts in the aerospace industry believe the future prospect of transfer of aerospace technology to the

civilian sector in this country is quite promising. Many advanced technologies such as remote-sensing and telemetry, space-based power supply, digital broadcast systems, use of solid-propellant rockets for weather control, petroleum extraction, fire prevention, mineral exploration, emergency rescue, and cable installation, earthquake monitoring from space, development of special medicines in space, material processing under micro-gravity conditions, satellite communications, etc., can potentially be used in various commercial industries. Application of these technologies will have an enormous impact on China's economic development. We must seriously address the immediate issues outlined above so the potential of transfer of aerospace technology to the civilian sector can be fully realized.

Beijing Aeronautical Technology Research Center Profiled

946B0119B Beijing GUOJI HANGKONG [INTERNATIONAL AVIATION] in Chinese
No 5, May 94 pp 51-52

[Article by Wu Qingrong [0702 1987 2837]: "Beijing Aeronautical Technology Research Center Moves On"]

[Text] Beijing Aeronautical Technology Research Center (BATRC) was founded in August 1958 with a mission to investigate the use and maintenance of aeronautical equipment. After 35 years of construction and development, it has become an influential, multi-disciplinary, comprehensive research institution in the maintenance of aeronautical equipment worldwide.

BATRC employs modern technology to upgrade and maintain equipment. It has considerable capability to perform research at a high level. It has developed technical expertise in the following seven areas: modification and upgrade of aeronautical equipment, lifetime study of aeronautical equipment, applied research on airborne equipment, technical analysis of accidents and failures, study of maintenance and testing techniques, study of equipment reliability and maintainability and aeronautical maintenance and repair engineering. In recent years, BATRC also developed significant technical know-how in inertial guidance and air traffic control. The prospect for further growth is very bright.

BATRC has over 50 laboratories and is equipped with modern instrumentation and equipment. It also has a strong technical staff that will meet any challenges. There are more than 400 technical employees, including over 100 senior engineers. There are not only technical leaders in every field but also experts in maintenance and repair as well.

In the past 35 years, BATRC has conducted a great deal of research on maintenance and repair of aeronautical equipment and obtained 571 accomplishments. It received 339 awards, including 51 national awards and 58 first and second place awards at the ministry level. Some of those accomplishments filled a void in China. Some are close to world class level. Some solved key technical issues in use and maintenance. Some are highly economically rewarding. In the past 35 years, a total of 710 papers have been published, including 35 presented and published in international conferences and journals.

In cooperation with other research institutes, factories and user units, BATRC has successfully modified a variety of airplanes for special applications in order to meet the needs of our government.

BATRC employed advanced technology and equipment to conduct fatigue test on an entire aircraft and scientifically determined the life and overhaul cycle of the aircraft and its weight bearing parts. It routinely repairs and maintains airplanes and engines to lengthen their useful lifetimes.

BATRC conducted hundreds of analyses of major aircraft failures and accidents. In some cases, it presented measures to prevent similar incidents from happening again. In some cases, it took direct action to put airplanes back in the air after they are grounded. It plays a critical role to ensure normal operation and flight safety. For instance, static electricity caused fire on a certain model of aircraft. After conducting a great deal of tests on the ground and in air, the root of the problem was found and preventive measures were taken to get rid of this problem completely. A paper discussing this accomplishment was well received in an international aeronautics conference. The technical strength of BATRC has been repeatedly demonstrated in failure analysis and incident inspection of accidents involving other countries.

BATRC systematically studied various maintenance-techniques and methods. It introduced a number of non-destructive instruments and techniques, over a dozen pieces of in-situ test equipment and an airborne engine monitoring system. Recently, an internal field radio failure diagnostic system was successfully developed for a specific model of aircraft on the basis of fuzzy logic. It is a comprehensive, intelligent system which significantly improves the level and accuracy of fault detection. This radically reforms maintenance procedures and enhances its protection capability.

BATRC is one of the early organizations in China involved in aeronautical maintenance research. Over the past 35 years, close to 100 papers were published. "Aircraft Maintenance in China" is the first paper in aircraft maintenance ever presented in an international academic forum. BATRC is responsible for writing and editing over 100 kinds of documents, including a series of technical regulations, engineering procedures, aircraft maintenance quality specifications, standards and maintenance data. The paper "Aircraft Maintenance Quality Standards" has become a specification for new aircraft maintenance design and was released as a military standard. BATRC's approach to maintenance is centered around reliability which has led to major breakthroughs in aircraft maintenance theory in China. It promotes the development of maintenance science and aeronautic maintenance reform.

BATRC will take full advantage of its personnel and technology and continue conducting research in aeronautic equipment maintenance and repair. In addition, it will actively pursue technology development and expand market development for its technical accomplishments. It will strengthen its research capability in order to create more opportunities in aeronautic engineering.

Biotechnology

World's First Attenuated Live Encephalitis Vaccine Developed

94P60290A Beijing JIAN KANG BAO in Chinese 13 May 94 p 1

[Article by Wang Suping [3769 5685 1627]]

[Summary] To date, China is the first and the only nation in the world capable of producing attenuated live encephalitis vaccine. The vaccine was developed by the Institute of Pharmaceutical and Biological Products Control in 1990. The product has already been put into large-scale clinical trials in high incidence areas such as Mengcheng and Guoyang counties. According to 1993 reporting, after immunization, morbidity of children aged from one to six years old dropped 53.35 percent—from 23.5 per 100,000 people to 10.99 per 100,000—and in Yongfeng County, Jiangxi Province, morbidity dropped from 15.36 per 100,000 people to 4 per 100,000. In the Dali area of Yunnan Province, among the 30,000 people under clinical observation, only two people who received the immunization became infected later. In contrast, 46 people in the unimmunized group were reported to be infected. The Rockfeller Foundation of the United States recently expressed interest in the product because of its effectiveness and agreed to provide modern production facilities for large-scale production and marketing.

New Bone Grafting Material Developed

94P60290B Beijing JIAN KANG BAO in Chinese 8 May 94 p 1

[Summary] A research team headed by Professor Hu Yunyu at the PLA Forth Medical University has developed a new material from ox bones to replace human bones in bone grafting. The team has been conducting heterogenic bone research since 1985. Researchers first treated the spongy ox bones with chemicals to produce non-antigenic vectors and also extracted bone-forming protein from the cortices of ox bones. They then combined the non-antigenic vectors and bone-forming proteins to produce bone substitute under special conditions.

Cloning of Hepatitis D Genome Said Successful

94P60290C Beijing JIAN KANG BAO in Chinese 20 Apr 94 p 1

[Article by Zheng Lingqiao [6774 7227 1564]]

[Summary] The CAS Research Institute of Virology has for the first time cloned the whole hepatitis D CDNA sequence from human sera. Under the guidance of Professor Zhan Meiyun, scientist Liu Shanlu first extracted the ribonucleic acid (RNA) from hepatitis D viruses that were obtained from sera of hepatitis D patients. Liu then used reverse transcription and polymerase chain reaction methods to clone the CDNA sequence. Recently, the world's two largest nucleotide genomic libraries—the European Molecular Biology Laboratory Database and the U.S. Genomic Library—have fed the Chinese-cloned CDNA sequence into their databases.

China Becomes World's Largest Vaccine-Producing Nation

94P60290D Beijing JIAN KANG BAO in Chinese 26 Apr 94 p 1

[Article by Zheng Lingqiao [6774 7227 1564]]

[Summary] China has become the largest vaccine-producing nation and largest vaccine market in the world. The nation is capable of producing over 1.2 billion doses of 21 vaccines including the six vaccines designated in the children's immunization plan. In the 1950s, China produced these vaccines against smallpox, rabies, Japanese encephalitis, forest encephalitis, typhus, pertussis, typhoid fever, diphtheria, tetanus, plague, brucellosis, and anthrax. In the 1960s, live polio and measles vaccines were produced. In the 1970s, epidemic encephalitis polysaccharide vaccines were produced. In the 1980s, blood-origin hepatitis B vaccine and live Japanese encephalitis vaccine were produced. In the 1990s, genetic engineering hepatitis B vaccine and live hepatitis A vaccines were produced. Currently, China is using new technologies to study and modify eight conventional vaccines. In order to expand sales of vaccines, China is also conducting R&D on 14 projects involving four types of new vaccines. This work includes research on polyvalence vaccine using recombinant vaccinia as a vector and an oral vaccine, adenovirus, as a vector.

Ciba-Geigy To Expand Business in China

40101009D Beijing CHINA DAILY [ECONOMICS] in English 7 Jun 94 p 2

[Article by Li Wen: "Ciba-Geigy To Expand Business in China"]

[Text] Guangzhou—Ciba-Geigy, a Swiss biological and chemical plant, is expanding its business in China by moving part of its manufacturing base from Europe to the mainland.

The planned move is a result of China's open and preferential policies, said the chief representative of Ciba-Geigy (Hong Kong) Ltd in Guangzhou.

And the steady development of the country's chemical industry is another reason for advanced technology and equipment to be transferred to China.

The move shows Ciba's long-term commitment to the huge Chinese market, despite several economic drawbacks, such as inconvertibility of the renminbi, said the representative.

And the company's latest investment in China, the establishment of an $11.6 million joint venture in Qingdao last month, demonstrates the pharmaceutical company's resolve to increase its investments in the country. The Qingdao venture is Ciba-Geigy's 11th project in China.

Last year, the group was given State permission to form a wholly-owned umbrella company in China.

The $10 million Ciba-Geigy (China) Ltd set up last year acts as a holding company for Ciba-Geigy's investments in the healthcare, agricultural, chemical and industrial sectors of the country.

Ciba-Geigy's South China business manager said that the firm has been slow in developing in this dynamic region partly because Guangzhou's chemical industry lags behind that of some northern areas.

"Ciba-Geigy has been growing fast in China in the past few years and the successful joint-ventures and township enterprises in the South are becoming our big customers," he said.

The company is actively seeking joint-venture partners to produce chemicals in South China.

Ciba-Geigy's current joint-ventures in China include the Beijing Ciba- Geigy Pharma Ltd, which manufactures anti-rheumatism and central nervous system drugs and the Shanghai Ciba-Geigy Animal Health Ltd, producing high quality animal health product, Shanghai Ciba Vision Contact Lens Company and Changzhou Toledo Electronics Scales, which manufactures high precision electronic balances and industrial and commercial scales.

Ciba-Geigy has offices in Beijing, Tianjin, Shanghai and Guangzhou, and plans to set up connections in other major cities such as Shenyang, Chongqing, Wuhan and Harbin.

Results in Genetic Research Said Fruitful

40101009C Beijing CHINA DAILY [SCIENCE/MEDICINE/ENTERTAINMENT] in English 3 Jun 94 p 5

[Text] China has reported new progress in genetic studies of anthel culture breeding and microbial genetics, with some results being applied in economic development.

To accelerate genetic study, scientists have extensively researched cell genetics, plant transfers of foreign genes and the development of species resources, molecular genetics and molecular biochemical mark.

In plant genetics, the "Jinghua No 1," developed by Beijing Plant Engineering Laboratory, has been hailed by Chinese and foreign scientists as the world's first anthel breeding of winter wheat. The new seed has been successful in 540,000 hectares of wheat.

About 10 wheat varieties and 22 rice varieties developed with anthel culture have been used in crops covering up to 2 million hectares, which boosted agricultural production.

The allo hexaploit secale cereal is another new result from the Chinese Academy of Agriculture Sciences, which raised per hectare cereal output by 40 to 60 percent above other conventional seeds. The product has been highly effective in cattle feeding with excellent quality in milk production.

A new soybean seed developed by the Institute of Genetic Research of the Chinese Academy of Sciences by applying chemical mutagenesis technology has been used in more than 200,000 hectares of crops since 1990, adding 100 million yuan ($11 million) in economic returns.

Meanwhile, new advances have also been scored in bio-organisms and medical genetics of human beings. The Chinese Academy of Medical Science has developed a unique way to detect antenatal genes by comparing two genes with hereditary diseases. The new way, which is applicable in different regions across China, is an easy, fast and accurate method to analyze antenatal genes.

The mutagenesis resistant effect of Chinese medicine is also a topic of research in Beijing University and Beijing University of Traditional Chinese Medicine.

New Diagnostic Method To Detect Cancer in Early Stage Developed

40101009B Beijing CHINA DAILY [SCIENCE/MEDICINE/ENTERTAINMENT] in English 3 Jun 94 p 5

[Article by Chen Qide]

[Text] A Chinese scientist has developed a new way to diagnose cancer before it becomes malignant.

The Alpha DNA Binding Protein (ADBP) method, developed by Associate Professor Lu Xinfa, detects cells, known as oncogenes, before they become cancerous.

And Lu has proved that three active oncogenes can lead to cancer if no proper dietary measures are taken.

Normally oncogenes can exist in a body for several years before developing into cancer.

During this method there will be no visible signs of the disease.

Although it takes a long time for cancer to develop, this is the first time that cancer can be detected at an early stage, said Lu, who works at the Institute of Infectious Diseases in Zhejiang Medical University.

By the time most hospitals diagnose the illness, the cancer is already well-developed. This makes it impossible to eliminate the disease completely.

Lu started his research into liver cancer in 1986.

Scientists believe that liver cancer results from hepatitis A, hepatitis B or C.

Research shows that between 65 and 95 percent of liver cancer cases develop from hepatitis.

Doctors analyze the Alpha Feto-Protein (AFP) in the patient's blood to diagnose liver cancer.

They believe that a person with 400 nanograms of AFP has contracted liver cancer. This method has a 70 percent accuracy rate.

But this system breaks down when applied to Chinese patients suffering from chronic hepatitis or liver cirrhosis. The AFP of these patients often exceeds 400 nanograms, even though they have not contracted cancer.

Clinical tests show that patients with cancer tissue measuring 4 centimetres can only live about four years after the operation.

But Lu claims that his ADBP method can more accurately diagnose whether a person has contracted liver cancer, and it does so several years before oncogenes become cancerous.

"This enables us to take preventative action to inhibit the growth of cancer," Lu said. And he claims his method has a 90 percent accuracy rate.

Zhang Hekang, 48, Zhejiang Province, contracted hepatitis in 1987. Four years later he was diagnosed as suffering from liver cancer.

Distressed, Zhang went to Lu for an oncogene examination. The result showed that oncogene activation rather than cancer.

The ADBP method can also be used to diagnose cancer of the lung, breast, cervix and thyroid.

Another patient from Hangzhou, Huang Kai, 71, was diagnosed in Shanghai with lung cancer. But Lu's diagnoses refuted the earlier diagnoses. Today Huang continues to enjoy a healthy life.

The DNA binding protein (DBP) method was advanced by experts from the University of California in the United States in the 1970s. American scientists believed that liver cancer patients had plenty of DBP. But they were unable to prove it.

Using the ADBP method, Lu discovered that healthy people had more DBP than liver cancer patients.

He believes that a person with activated oncogenes control the activation through dietary means.

He hopes his method will become a regular examination method.

Lu is confident that if used properly, this method will enhance health and prevent cancer.

His research has been boosted by a 60,000 yuan ($6,896) grant from the State Natural Science Fund.

The 60-year-old professor has been devoted to his research for nine years. And the results have passed provincial-level appraisal.

He is now searching for a vaccine which can prevent various cancers. Some samples have already been developed.

"Because of a lack of funds, we are unable to start production on a larger scale," he said.

He hopes to be able to work together with foreign counterparts to step up vaccine development.

Hangzhou To Become Base for Biotech Research

40101009A Beijing CHINA DAILY [BUSINESS WEEKLY-EAST CHINA] in English 30 May 94 p 5

[Article by Xiao Pei]

[Text] An international biotechnology park will be set up in Hangzhou, capital of Zhejiang Province.

It will become China's first base for research and development in biotechnology.

The park will use biotechnology to develop food, chemicals, agriculture and medicines. It also will be a centre for international trade, finance, tourism and training.

The overall planning of the park was approved last week in Beijing by experts from the State Science and Technology Commission, the State Planning Commission, the Ministry of Public Health and the Chinese Academy of Sciences.

Bioengineering is the most active field, with massive potential for high technologies. Experts predict that biotechnology will become the dominant industry in the next century. It is estimated that the world market for bioengineering products will exceed $100 billion by 2000.

The establishment of the base is a major step in speeding up the pace of applying bioengineering technology to commercial production, said Chen Yong, president of the Beijing Global Biotechnology Development Center. The center, a subsidiary of the Chinese Academy of Sciences, is responsible for the park's development.

Although China has made some achievements in bioengineering, few are used in mass production because of inadequate investment.

The park is intended to pool together the country's best biotechnology researchers and scientists.

It will maintain close co-operation with the Chinese Academy of Sciences, universities, research institutes and international organizations.

Foreign companies are welcome to invest in the park, said Chen.

After more than a year's inspection around the country, the center decided to build the park in Hangzhou because of its economic development, transportation and tourism.

The park will encompass 700,000 square metres in the Nanyang Economic and Technology Development Zone.

The total investment in building the park will be about 5 billion yuan ($575 million). Preparatory work began last June, and Chen said construction will be completed in four to six years.

By the end of the century, the total output of the park is expected to reach $5 billion and taxes and profits, $2.5 billion.

Computers

Efficient Implementation on YH Supercomputers of Library for Large Sparse Linear Algebraic Iterations

946B0092 Changsha GUOFANG KEJI DAXUE XUEBAO [JOURNAL OF NATIONAL UNIVERSITY OF DEFENSE TECHNOLOGY] in Chinese Vol 16, No 1, Mar 94 pp 86-91

[Article by He Xinfang [0149 2450 5364], Hu Qingfeng [5170 1987 0023], Wang Liping [3769 7787 5493], and Tian Zerong [3944 3419 2837] of the National University of Defense Science and Technology Computer Department: "Highly Efficient Implementation of Large Sparse Linear Algebraic Interation Library on YH Computer"; MS received 5 May 93]

[Text] **Abstract** This article discusses iterative algorithms, speedup methods, memory techniques, and parallel algorithms for large sparse linear algebraic equation groups. Combining with the features of vector machines and adopting effective program optimization measures, we developed scalar and vector library programs. The results of trial computations on YH [i.e. "Galaxy" supercomputer] systems indicate that the speed of large sparse linear algebra vector iteration libraries is substantially increased compared to scalar iteration libraries. When $N \geq 100$, the speedup is about 2 to 8 on a YH-1 machine and 2 to 7 on a YH-2 machine. When the number of iterations is increased, there is an even more significant increase in the speedup. The conjugate gradient (CG) acceleration method can effectively accelerate convergence and reduce the number of iterations by more than one-half.

Key terms: speedup, vector, scalar

Classification number: TP311, O241.6

Many scientific and engineering computations frequently pose the problem of solving large sparse linear algebraic equation groups. There are two types of methods for solving this type of problem, direct solution and iterative solution. Because the scale of the problem is generally rather large, a compressed memory format is often utilized. When the coefficient matrix is of a special class such as a band shape, block tridiagonal, or so on, the direct solution method and iterative solution method both can rather easily achieve parallel computation, but when the coefficient matrix is arbitrarily sparse, it is relatively difficult to achieve a parallel solution of its compressed memory format. Research on parallel algorithms for compressed memory formats when the coefficient matrix is arbitrarily sparse and the development of the corresponding vector or parallel computation applied software have important real significance and applied value for taking full advantage of parallel machines and improving the computational efficiency of this type of problem.

This article describes research on parallel algorithms as a basis for algorithm conversion and program optimization of a compressed memory format scalar linear algebra computation program when the coefficient matrix is arbitrarily sparse to develop a vector large sparse iteration library.

I. Basic Content

Large sparse linear equation group iteration libraries are mainly used when the coefficient matrix is generally sparse and symmetrically sparse, the opposite angle line element lightness occupies an optimum linear algebraic equation group that is solved using a Jacobi algorithm, successive overrelaxation method (SOR), symmetrical successive overrelaxation method (SSOR), RS algorithm, and so on. To accelerate convergence, different speedup methods are also employed for each type of algorithm, such as an adaptive Chebyshev (SI) speedup method and an adaptive conjugate gradient (CG) speedup method, and the use of a pre-processing conjugate gradient method for solution when the coefficient matrix is a block tridiagonal or band-shaped matrix. The entire library includes the JCG (Jacobi conjugate gradient) method, the JSI (Jacobi semi-iterative) method, SOR (successive overrelaxation) method, SSORCG (symmetrical SOR conjugate gradient) method, SSORSI (symmetrical SOR semi-iterative) method, RSCG (reduced system conjugate gradient) method, RSSI (reduced system semi- iterative) method, INCG (pretreatment conjugate gradient) method, and so on.

II. Compressed Memory Technique

Because the scale of the sparse linear algebraic equation groups encountered in practice is very large, a large portion of their coefficient matrix elements are zero, and non-zero elements generally account for 5 to 20 percent. Storing all of them takes a great deal of space, which would present substantial difficulties for solution. The algorithms in this library all employ row-and-column

pointer compressed storage techniques. Three one-dimensional number groups are used to store the non-zero elements in the original two-dimensional coefficient matrix A, with one real number group AP used to store the non-zero elements in A by row, an integer group JA to store the column number of the non-zero elements corresponding to AP, and another integer group IA used to store the row pointer, to store the first non-zero element in each row in the position of the one-dimensional number group AP. The program also contains several working number groups that are used for quick element access and parallel computation. The indirect access problem that is frequently encountered in a compressed memory format makes parallel computation inconvenient.

III. Parallel Algorithm Research and Program Optimization

Converting traditional serial computation sparse linear algebraic equation group iteration libraries into parallel computation vector libraries first requires research on parallel algorithms. We conducted systematic static-state analysis and a large amount of dynamic-state testing of the serial computation program in the original scalar library to find the core portions that affected the speed of the operations and then focused on the core portions in studying their parallel algorithms and effective implementation measures. This mainly involved the following areas:

1. In the iterative computations we frequently encountered basic core modules or program segments similar to sparse matrix multiplication, sparse matrix and vector multiplication, and solution of sparse vector scalar products. There were over ten of these modules in the iterative library, and some of the modules are repeatedly called in various algorithms. These modules involved a large amount of computing and took a great deal of time, with some of them accounting for over 80 percent of the amount of computing in one type of iterative algorithm. Thus, research on parallel computation and realization of this type of module is the key to increasing the speed of iterative operations. For example, the sparse matrix and vector multiplication module PMULT was called by several algorithms in this type of program:

```
SUBROUTINE PMULT(NN, IA, JA, AP, U, W)
INTEGER IA(*), JA(*)
REAL AP(*), U(NN), W(NN)
Asymmetrical sparse matrix and vector multiplication
DO 30 II = 1, N
IBGN = IA(II)
IEND = IA(II+1)-1
SUM = 0.
DO 10 JJ = IBGN, IEND
JAJJ = JA(JJ)
10 SUM = SUM + AP(JJ)*U(JAJJ)
30 W(II) = SUM
Symmetrical sparse matrix and vector multiplication
DO 40 II = I, N
40 W(II) = 0.
D0 70 II = 1, N
IBGN = IA(II)
IEND = IA(II+1)-1
UII = U(II)
WII = W(II)
DO 50 JJ = IBGN, IEND
JAJJ = JA(JJ)
W(II) = WII + AP(JJ)*U(JAJJ)
50 W(JAJJ) = W(JAJJ)+AP(JJ)*UII
70 CONTINUE
....
END
```

The problem of indirect access is encountered in the above module cycle and has a strong interrelationship with the computations so it is impossible to achieve parallel computation directly and the efficiency is very low. To achieve vector computation we convert the above module to:

```
Asymmetrical sparse matrix and vector multiplication:
DO 30 II=1, N
IBGN = IA(II)
IEND = IA(II+1)-1
IJ = IEND-IBGN+1
CALL GATHER(IJ, AA(1), U, JA(IBGN))
30 W(II) = SDOT(IJ, AA(1), 1, AP(IBGN), 1)
Symmetrical sparse matrix and vector multiplication:
DO 70 II = 1, N
IBGN = IA(II)
IEND = IA(II+1)-1
UII = U(II)
IJ = IEND-IBGN +1
CALL GATHER(IJ. AA(1), U, JA(IBGN), 1)
W(II) = SDOT(IJ, AA(1), 1, A(IBGN), 1)
CALL GATHER(IJ, AA(1), W, JA(IBGN))
```

```
DO 60 JJ = IBGN, END
60 AA(JJ-IBGN+1) = AA(JJ-IBGN+1) + A(JJ)*U(II)
CALL SCATTE(IJ, W, JA(IBGN), AA(1))
W(II) = WII
....
END
```

The AA(*) in the above program segment is an added temporary working number group, while GATHER, SCATTE, and SDOT are newly developed vector compilation modules (see reference [2]). After conversion, the modules completely achieve parallel computation, and when N=500 and M=250 (N is the sparse matrix rank and M is the half bandwidth of the sparse coefficient matrix, the same holding true below), the average time per call can be reduced to less than 1/11th of the original (see Table 1). Table 1 also lists the operating speedup for the seven other modules.

Table 1. Operating Speedup for Sparse Matrix Scalar and Vector Operation Modules on the YH-1 Machine

Module Name	N=500 M=250			N=800, M=400		
	Scalar t_s	Vector t_v	Speedup S_p	Scalar t_s	Vector t_v	Speedup S_p
PBBETA	1.615665	0.137923	11.71	4.127598	0.315211	13.09
PSSORI	1.559739	0.145936	10.69	3.970264	0.299818	13.24
PFSOR	0.7792339	0.072612	10.73	1.983419	0.149285	13.29
PVTBV	0.777925	0.070397	11.05	1.98324	0.145748	13.61
PMULT	0.778517	0.07048	11.06	1.987414	0.145625	13.65
UNSCAL	1.148798	0.094161	12.2	2.92409	0.217392	13.45
PJAC	0.777017	0.71966	10.8	1.98202	0.148433	13.35
PRSBLK	0.260512	0.029764	8.75	0.66327	0.061513	10.78

2. Conversion of serial algorithms, development of high efficiency vector compilation function modules.

It was pointed out above that sparse matrix compressed storage presents a large number of indirect access problems which pose many inconveniences for parallel computation. Achieving parallel computation first requires research on parallel indirect access technology and the development of parallel indirect access modules. For this reason, based on the various types of indirect access problems encountered in the iterative library, we developed the highly efficient vector indirect access subprograms GATHER and SCATTE:

GATHER(N, A, B, INDEX) has the function of achieving vector indirect access equivalent to A(I) = B(INDEX(IJ)), I =1, 2, ..., N.

SCATTE(N, B, INDEX, A) has the function of achieving vector indirect storage equivalent to B(INDEX(I) = A(I), I = 1, 2, ..., N.

Next, the program segments similar to solutions of scalar products encountered several times in the program segments such as the SUM = SUM + AP(JJ) * U(JAJJ) in the cycle above are solutions of scalar products. Thus, we combined the characteristics of parallel machines to make full use of vector function components and chaining techniques, cycle characteristics, hard instructions, and so on and used segmentation methods to develop vector compilation modules SDOT for highly efficient operation on the YH-1 and YH-2. SDOT can be called instead of program segments similar to scalar product solutions. The results processed in this manner effectively increase the operating efficiency of the entire library.

The operating time and speedup of the sparse matrix operation scalar and vector modules listed in Table 1 on the YH-1 machine are similar to those on the YH-2 machine. In Table 2, t_s and t_v are in units of seconds and the speedup $S_p = t_s/t_v$ with the symbols having the same meanings.

Table 2. Comparison of Vector and Scalar Library Operating Conditions When N=700 and M=250

Module Name	Number of Iterations	Scalar Library Operating Time (seconds)		Vector Library Operating Time (seconds)		Speedup	
		YH-1(T_{1s})	YH- 2(T_{2s})	YH-1(T_{1v})	YH-2(T_{2v})	YH-1(T_{1s}/ T_{1v})	YH-2(T_{2s}/ T_{2v})
Symmetrical JSI	49	37.83	13.59	10.94	3.271	3.46	4.15
Asymmetrical JSI	49	69.65	22.23	9.339	2.712	7.46	8.20
Symmetrical JCG	13	12.84	4.421	4.167	1.157	3.07	3.82
Asymmetrical JCG	18	30.40	9.434	5.694	1.473	5.34	6.40
Symmetrical SOR	38	49.44	15.88	10.58	3.055	4.67	5.20
Asymmetrical SOR	38	54.12	17.41	7.921	2.223	6.83	7.82
Symmetrical SSORSI	20	52.35	17.11	9.146	2.735	5.72	6.26
Asymmetrical SSORSI	20	87.95	26.14	14.13	4.128	6.22	6.33
Symmetrical SSORCG	10	36.86	11.72	8.398	2.373	4.39	4.94
Asymmetrical SSORCG	10	50.74	14.93	10.68	2.834	4.75	5.27
Symmetrical RSSI	21	28.25	9.089	6.071	2.017	4.65	4.51
Asymmetrical RSSI	22	33.47	10.52	7.865	2.114	4.26	4.98
Symmetrical RSCG	5	11.57	3.485	4.218	1.070	2.74	3.26
Asymmetrical RSCG	5	15.23	4.401	5.705	1.314	2.67	3.35

3. Program optimization

The optimization measures we adopted have the following points:

a. All cycles and expressions that can be described using vector statements are described using forced vectorized scalar statements.

b. Subprograms are inserted to convert several functional modules such as number group or vector operations, vector valuations and commutations, and other functional modules that are the primary modules and submodules usually called in the iteration library. They are inserted directly into the program segment that calls that module to achieve vector operations.

c. Cycle separation is carried out, which achieves conditional statement vectorization in the cycles. For example, for the program segment:

```
DO 50 I = IBGN, IEND
JAI = JA(I)
IF(JAI.GT.K) GOTO 40
TEMP2 = TEMP2-AP(I)*W1(JAI)
GOTO 50
40 TEMP1 = TEMP1-AP(I) * W1(JAI)
50 CONTINUE
```

Temporary working number groups AA(*) can be added to call the indirect access modules, converted into:

```
CALL GATHER(IJ, AA(1), W1(1), JA(IBGN))
DO 50 I = IBGN, IEND
AA(I-IBGN+1) = -AP(1)*AA(I-IBGN+1)
TEMP1 = TEMP1+CVMGT(AA(I-IBGN+1), 0, JA(I), LE, K)
50 TEMP2 = TEMP2+CVMGT(AA(I-IBGN+1), 0, JA(I), LE, K)
```

IV. Efficiency and Algorithm Analysis

To determine if the large sparse linear algebraic parallel iteration library operates accurately and reliably, we also developed a corresponding testing library when we developed the vector library that we used to test the accuracy of each of the algorithms and program operations, the operational efficiency under various types of conditions, and so on. The testing library was used to conduct a large number of data experiments. The results of the tests show that: all of the numbers of iterations for each of the algorithms in the vector library and scalar

library were completely consistent with the computed precision, but the vector library computation speed was faster and more efficient. The speedups of some of the algorithm vector library and scalar library were as high as 7 to 8. Table 2 lists the scalar and vector operating times, number of iterations, and speedups for each of the algorithms on the YH-1 and YH-2 machines for an N=700 and a half bandwidth M=250. Table 2 shows that as the number of iterations is increased the speedup increases. The conjugate gradient speedup method more effectively accelerated convergence than the Chebyshev semi-iterative speedup method, and that under normal conditions the conjugate gradient speedup method can reduce the number of iterations by more than one-half. Table 3 lists the library operation conditions for the vector library and scalar library on the YH-1 and YH-2 machines. The data in Table 3 show that the vector library has a faster operating speed and higher efficiency than the scalar library. When N=500, 600, ..., 1,000 and M=1, 100, 300 the speedup of the total operating times for the entire library (including the 14 algorithms and three bandwidths) averages 4.5 on the YH-1 machine and averages 5.1 on the YH-2.

Table 3. Comparison of Vector Library and Scalar Library Complete Library Operating Conditions

N	Scalar Operating Time (seconds)		Vector Library Operating Time (seconds)		Speedup	
	YH-1(T_{1s}	YH-2(T_{2s}	YH- 1(T_{1v}	YH- 2(T_{2v}	T_{1s}/T_{1v}	T_{2s}/T_{2v}
500	554.527	175.846	129.315	36.352	4.29	4.84
600	730.347	231.046	164.255	45.901	4.45	5.03
700	879.684	278.272	195.885	54.562	4.49	5.10
800	1033.62	327.995	228.55	63.626	4.52	5.16
900	1216.66	385.684	267.19	73.53	4.55	5.25
1000	1399.32	445.906	303.57	84.723	4.61	5.26

References

[1] D.M. Young and K.C. Jea, Conjugate Gradient Acceleration of Iterative Methods: Part II, The Nonsymmetrizable Case Rep CNA-163, Center for Numerical Analysis, University of Texas at Austin, 1980.

[2] D.M. Young, L. Hayes, and K.C. Jea, Conjugate Gradient Acceleration of Iterative Methods: Part I, The Symmetrizable Case Rep CNA-162, Center for Numerical Analysis, University of Texas at Austin, 1980.

[3] Li Xiaomei [2621 2556 2734] and Jiang Zengrong [5592 1073 2837], Bingxing Suanfa [Parallel Algorithms], Hunan Science and Technology Press, 1992, pp 303-307.

[4] Qinghua University Applied Mathematics Department, Xiandai Yingyong Shuxue Shouce, Jisuan Fangfa [Handbook of Modern Applied Mathematics, Computation Methods], Beijing Press, 1990, pp 364-423.

Digital Logic Design Expert System Unveiled

94P60344A Beijing KEJI RIBAO [SCIENCE AND TECHNOLOGY DAILY] in Chinese 16 Jun 94 p 1

[Article by Li Wei [2621 1792]: "Digital Logic Design Expert System Unveiled"]

[Summary] The University of Science and Technology for National Defense (USTND) has completed its State 863 Program project to develop an integrated digital logic design expert system. In this 4- year development project, USTND organically merged expert system methods with traditional CAD techniques for designing digital logic. This integrated expert system, built around 12 subsystems, is intended for design of devices up to 50,000 gates each, and contains a 240,000-line source program.

Neural Information Processing System Certified

94P60344B Beijing ZHONGGUO KEXUE BAO [CHINESE SCIENCE NEWS] in Chinese 24 Jun 94 p 1

[Article by Zhang Ling [1728 3781]: "Neural Information Processing System"]

[Summary] A parallel-processing "Neural Information Processing System" (NIPS) developed as an 863 high-tech project by a University of Science and Technology of China (USTC) Computer Science and Technology Department research group led by Prof. Chen Guoliang [7115 0948 5328] was recently certified in Hefei. This NIPS, built around nine Transputer chips, can simulate systems exceeding 50,000 neurons and processes over 500,000 neuron interconnection weights. Its main applications are image processing, speech recognition, and neural computing.

Lasers, Sensors, Optics

Latest Reports on Optical Computing

Optical Image Fuzzy Associative Memory

94P60297A Shanghai ZHONGGUO JIGUANG [CHINESE JOURNAL OF LASERS] in Chinese Vol A21 No 3, Mar 94 pp 216-219

[Article by Zhang Shuqun [1728 2885 5028] and Chen Caisheng [7115 1752 3932] of the Dept. of Electronic

Engineering, Xiamen University, Xiamen 361005: "Optical Image Fuzzy Associative Memory"; MS received 28 Jun 93, revised 30 Aug 93]

[Abstract] An optical method to implement a 2-D image fuzzy associative memory (FAM, first described by Kosko in ref. [8]) is proposed. By area-encoding fuzzy matrices, the max-min synthetic operation needed in an FAM is realized in a multiple imaging system. The FAM, composed of max-min neurons, is a neural network using Hebbian rules for learning. Experimental results are given.

Figures 1, 2, and 4, not reproduced, show three pictures of the area- encoding method for 5 mm x 10 mm elements of fuzzy matrices, a representation of a 4-D interconnection with a 2-D mask, and a photograph showing an input image, a mask, and an output image obtained with the system, respectively. Figure 3, a schematic of the implementation system, is reproduced below. There are no tables.

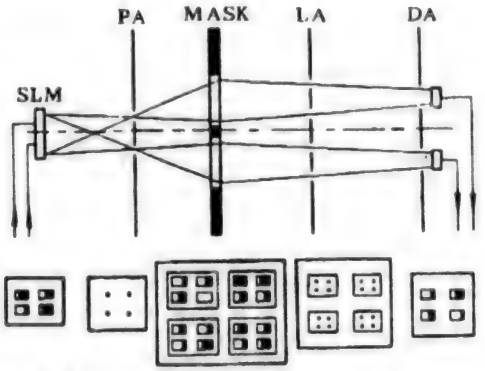

Figure 3. A Multiple-Imaging System for Implementing Image Fuzzy Associative Memory. PA: pinhole array; LA: lens array; DA: detector array; SLM: Spatial Light Modulator

References:

1. D. Psaltis, N. Farhat, OPT. LETT., 1985, 10:98.
2. T. Lu, S. Wu et al., APPL. OPT., 1990, 29:35.
3. B. Kosko, APPL. OPT., 1987, 26:4947.
4. C.C. Guest, R. Tekolste, APPL. OPT., 1987, 26:5055.
5. N.H. Farhat, APPL. OPT., 1987, 26:5093.
6. G.A. Carpenter, S. Grossberg, APPL. OPT., 1987, 26:4919.
7. A.T. Smith, J.F. Walkup, OPT. ENG., 1991, 30:1522.
8. B. Kosko, "Fuzzy Associative Memories in Fuzzy Expert Systems," ed. A. Kandel, Addison-Wesley, Reading, MA, 1987.
9. L. Liu, OPT. COMMUN., 1989, 73:183.
10. S. Lin, L. Liu, OPT. COMMUN., 1989, 73:268.

Full-Permutation Nonblocking Double Omega Interconnection Network

94P60297B Shanghai ZHONGGUO JIGUANG [CHINESE JOURNAL OF LASERS] in Chinese Vol A21 No 3, Mar 94 pp 220-224

[Article by Luo Fengguang [5012 7364 0342], Xu Jun [1776 6511] et al. of the National Lab. of Laser Technology, Huazhong (Central China) University of Science and Technology (HUST), Wuhan 430074: "Optical Implementation of Full-Permutation Nonblocking Double Omega Optical Interconnection Network for Optical Computing," supported by grants from State 863 High-Tech Program, NSFC, and the NDSTIC Basic Research Fund; MS received 7 Jun 93, revised 27 Sep 93]

[Abstract] The restrictions of a single Omega optical interconnection network are analyzed, and a method for optically implementing a full-permutation nonblocking 4 x 4 [i.e. 4-input, 4-output parallel-transfer] double Omega optical interconnection network is proposed. The optical circuit system consists of an Ar^{+3} ion laser, seven polarizing compound prism beam splitters, three quarter-wave plates, three step-reflectors, and three liquid-crystal spatial light switches.

Figures 1, 2, and 4, not reproduced, show a schematic of a 4 x 4 Omega interconnection network, a schematic of a 4 x 4 double Omega interconnection network, and photos of two kinds of output permutations, respectively. Figure 3, a schematic of the optical implementation system, is reproduced below. Table 1, not reproduced, lists the 64 permutations possible in the network with six control states and four outputs.

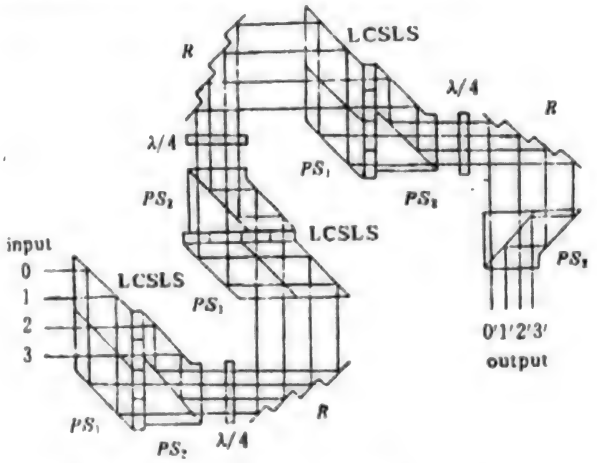

Figure 3. Light Circuit System of 4 x 4 Full-permutation Nonblocking Double Omega Network. PS_1, PS_2: polarizing compound prism beam splitters; λ/4; quarter-wave plate; R: step-reflector; LCSLS: liquid-crystal spatial light switch.

References:

1. Mingcui Cao, Fengguang Luo et al., APPL. OPT., 1992, 31(32):6817.
2. J. Jahns, M.J. Murdocca, APPL. OPT., 1988, 27:3155.
3. J. Jahns, OPT. COMMUN., 1990, 76:321.
4. T. Lang, IEEE TRANS. COMPUT., 1976, C-25:496.
5. D. Nassimi, S. Sahni, IEEE TRANS. COMPUT., 1981, C-30(5):332.
6. Ai Jun, Cao Mingcui, Luo Fengguang, Li Hongpu, GUANGZI XUEBAO [ACTA PHOTONICA SINICA], to be published.
7. K.M. Johnson, M.R. Surette et al., APPL. OPT., 1988, 27:1727.
8. Luo Fengguang, Cao Mingcui, Li Hongpu, Ai Jun, GUANGZI XUEBAO, 1992, 21(5):119.

Equivalent Optically Interconnected Perfect Shuffle/Exchange Network

94P60297C Wuhan HUAZHONG LIGONG DAXUE XUEBAO [JOURNAL OF HUAZHONG (CENTRAL CHINA) UNIVERSITY OF SCIENCE AND TECHNOLOGY] in Chinese Vol 22 No 3, Mar 94 pp 108-111

[Article by Luo Fengguang [5012 7364 0342], Cao Mingcui [2580 2494 5050] et al. of the National Lab. of Laser Technology, HUST, Wuhan: "Implementation of an Equivalent Optically Interconnected Perfect Shuffle/Exchange Network for Optical Computing," supported by grants from State 863 Program, NSFC, and the NDSTIC Basic Research Fund; MS received 19 May 93]

[Abstract] An optical implementation of an equivalent optically interconnected 8 x 8 perfect shuffle/exchange network for optical computing is described. A liquid-crystal spatial light modulator (LCSLM) is used as the optical exchange control device. The optically interconnected system consists of an Ar^+ ion laser light source, two polarizing Amici prisms (i.e. compound prism beam splitters), two beam splitters, the LCSLM, two total-reflection mirrors, a semi-transmitting/semi-reflecting lens, and a half-wave plate. Further application of this system requires miniaturization and semiconductor integration, such as development of symmetric self- electro-optic-effect devices (S-SEEDs) and large-numerical-aperture microlens arrays. The authors have fabricated a prototype GaP multi- step semiconductor microlens array with a single microlens aperture of 100 microns and a center spacing of 200 microns.

Figures 1, 2, 4, and 5, not reproduced, show a schematic of an exchange element, a schematic of an 8 x 8 perfect shuffle/exchange optical interconnection network, photographs of two output permutations, and a photograph of the GaP microlens array, respectively. Figure 3, a schematic of the optical implementation, is reproduced below. There are no tables.

References:

1. Yvonne A. Carts, "Optical Computing Nears Reality," LASER FOCUS WORLD, 1990, 26(3):53-54.
2. Johnson, K.M., Surette, M.R., Shamir, J., "Optical Interconnection Network Using Polarization-Based Ferroelectric Liquid-Crystal Gates," APPL. OPT., 1988, 27(9):1727-1732.
3. Haney, M.W., Levy, J.J., "Optical Efficient Free-Space Folded Perfect Shuffle Network," APPL. OPT., 1991, 30(15):2833-2836.
4. Cao Mingcui, Luo Fengguang, Li Hongpu, "Optical Perfect Shuffle- Exchange Interconnection Network Using Liquid-Crystal Spatial Light Switch," APPL. OPT., 1992, 31(32):6817-6819.

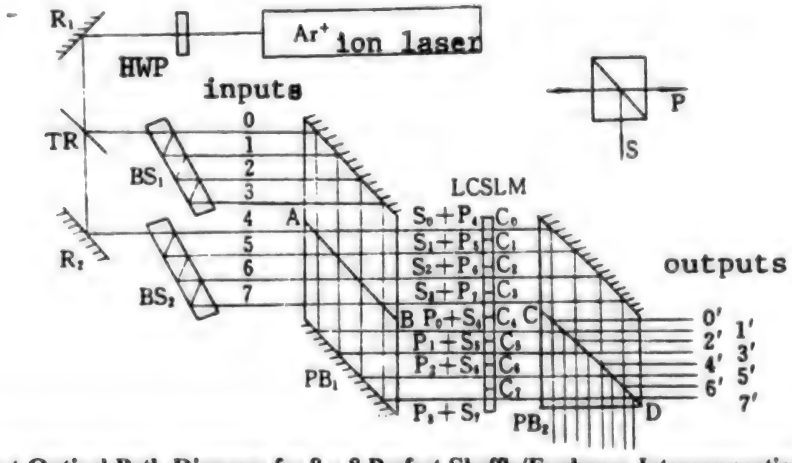

Figure 3: Equivalent Optical Path Diagram for 8 x 8 Perfect Shuffle/Exchange Interconnection Network. PB: polarizing compound prism beam splitter; BS: beam splitter; TRL semi-transmitting/semi-reflecting lens; R:total-reflection mirror; HWP: half-wave plate; CO-C7: LCSLM pixels; SO-S7: components of inputs after S-polarization; PO-P7: Components after P-polarization; A-B and C-D: surfaces coated with polarizing films.

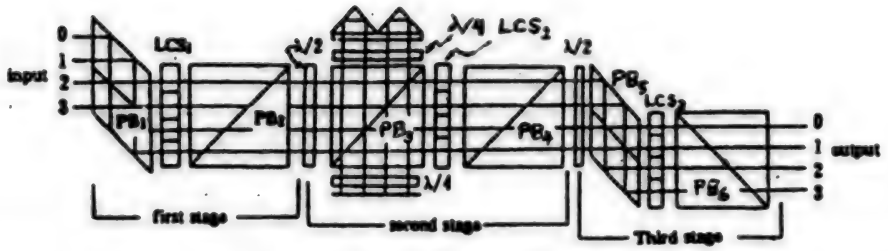

Figure 5. Schematic of Entire 3-Stage, 4-Port Nonblocking Banyan Switching Network. PB: polarizing compound prism beam splitter; LCS: liquid-crystal switching array.

5. Cao Mingcui, Li Hongpu et al., "Optical Hardware for the Perfect Shuffle Interconnection," OPT. COMPUTING AND PROCESSING, 1991, 1(1) :23-27.
6. Luo Fengguang, Cao Mingcui et al., "A New Omega Optical Interconnection Experimental System" [in Chinese], GUANGZI XUEBAO [ACTA PHOTONICA SINICA], 1992, 21(5):119-122.
7. Brenner, K.H., Huang, A., "Optical Implementations of the Perfect Shuffle Interconnection," APPL. OPT., 1988. 27(1):135-137.
8. Jewell, J.L., Mclall, S.L. et al., "Optical Computing and Related Microoptic Devices," APPL. OPT., 1990, 29(34):5050-5053.

Nonblocking Banyan Four-Port Switching Network

94P60297D Shanghai GUANGXUE XUEBAO [ACTA OPTICA SINICA] in Chinese Vol 14 No 4, Apr 94 pp 416-420

[Article by Li Hongpu [2621 3163 6225], Cao Mingcui [2580 2494 5050] et al. of the National Lab. of Laser Technology, HUST, Wuhan 430074: "Implementation of Nonblocking 4-Port Banyan Switching Network," supported by grants from State 863 Program and the NDSTIC Basic Research Fund; MS received 24 May 93, revised 3 Aug 93]

[Abstract] A new kind of nonblocking four-port Banyan switching network is proposed. Using conventional optical elements including six polarizing prism beam splitters, three liquid-crystal switching arrays, and various triangular prisms, quarter-wave plates, half-wave plates, and reflectors, this new network has been built and tested, and 24 switching functions have been realized.

Figures 1, 2, 3, 4, 6 and 7, not reproduced, show the following: a schematic of an 8 x 8 Banyan interconnection network, a schematic of a 4 x 4 nonblocking Banyan network, optical elements for implementing the first stage of the 4-port nonblocking Banyan network, the same for the second stage, a photograph of the four input ports, and a photograph of four different output permutations (corresponding to four of the possible 24 control states), respectively. Figure 5, a schematic of the optical implementation of the entire three-stage, 4- port nonblocking Banyan interconnection network, is reproduced below. Table 1, not reproduced, lists the 24 different switching functions (i.e., 24 different output permutations).

References:

1. J. Jahns, M.J. Murdocca, "Crossover Networks and Their Optical Implementation," APPL. OPT., 1988, 27(15):3155-3160.
2. J. Jahns, "Optical Implementation of Banyan Networks," OPT. COMMUN., 1990, 76(5-6):321-325.
3. M.J. Murdocca, A. Huang, J. Jahns et al., "Optical Design of Programmable Logic Arrays," APPL. OPT., 1988, 27(9):1651-1660.
4. Mingcui Cao, Hongpu Li, "Optical Hardware for Perfect Shuffle Interconnection," OPT. COMPUTING AND PROCESSING, 1991, 1(1):23-27.
5. Cao Mingcui, Li Hongpu, Luo Fengguang, "Optical Implementation of Perfect Shuffle/Exchange Omega Interconnection Network" [in Chinese], GUANGXUE XUEBAO [ACTA OPTICA SINICA], 1992, 12(12):1129-1134 [translated in full in JPRS-CST-93-010, 27 May 93 pp 19-22].
6. Karl-Heinz Brenner, A. Huang, "Optical Implementation of the Perfect Shuffle Interconnection," APPL. OPT., 1988, 27(1):135-137.
7. Krishnan Padmanabhan, Aran N. Netravali, "Dilated Networks for Photonic Switching," IEEE TRANS. COMMUN., 1987, COM-35(12):1357-1365.
8. R.A. Athale, S.H. Lee, "Development of an Optical Parallel Logic Device and a Half-Adder Circuit for Digital Optical Processing," OPT. ENGNG., 1979, 18(5):513-515.

Associative Memory with "Cat" Self-Pumped Phase Conjugator

94P60297E Shanghai GUANGXUE XUEBAO [ACTA OPTICA SINICA] in Chinese Vol 14 No 4, Apr 94 pp 421-424

[Article by Zhang Jingwen [1728 2529 2429], Zhao Hua [6392 2901] et al. of the Dept. of Applied Physics, Harbin Institute of Technology, Harbin 150001 and

Jiang Quanzhong [1203 0356 1813], Lu Xinliang [0712 2450 0081], and Chen Huanchu [7115 3562 4238] of the Institute of Crystal Materials, Shandong University, Jinan 250100: "Optical Associative Memory Using 'Cat' Self-Pumped Phase Conjugator," supported by grant from the High-Technology Committee; MS received 3 May 93]

[Abstract] An optical holographic associative memory using a "cat" self-pumped phase conjugator (16-deg-cut Cu:KNSBN [copper-doped potassium sodium strontium barium niobate] crystal, as opposed to the $BaTiO_3$ crystal used in the first "cat" self-pumped phase conjugator, developed by Feinberg[5]) as the thresholding feedback device and a low-absorpion, thin piece of Ce:Fe:$LiNbO_3$ crystal as the storage medium is presented. The crystal dimensions are 7.2 mm x 7.0 mm x 5.7 mm and the Cu-doping is 0.05 wt-percent. Experiments were conducted with an Ar-ion laser at four different wavelengths—514.5, 496.5, 488.0, and 476.5 nm, with 514.5 nm providing the best results. This cat self-pumped phase conjugator has a response of 150 ms, an imaging resolution of 50 pixels/mm, an object average light intensity of 56.5 mW/square cm for a reference light intensity of 2.42 W/square cm, and a conjugate reflectivity of 60 percent at an incident light intensity of 2.18 W/square cm. The complete image output can be addressed with less than 25 percent of the stored image.

Figures 1-5 and 7, not reproduced, show the following: a graph of reflectivity of the conjugator vs input light intensity, a photo of the phase-conjugate replica of a resolution chart, three photos showing how an input image undergoing severe phase distortion is restored in the conjugate output image, a graph of response time vs incident light intensity, a graph of diffraction efficiency vs full external cross angle of the two incident beams, and photos of complete and partial input images and the corresponding associative output images. Figure 6, the experimental set-up for implementing real-time associative memory, is reproduced below. There are no tables.

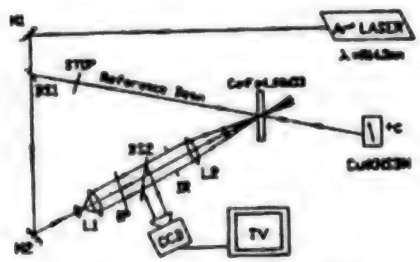

Figure 6. Experimental Setup for Real-Time Associative Memory: BS1, BS2: beam splitters; M1, M2: mirrors; L1, L2: lenses

References:

1. N. Farhat, D. Psaltis et al., "Optical Implementation of the Hopfield Model," APPL. OPT., 1985, 24(10):1469-1475.
2. H. Xu, Y. Yuan et al., "Implementation of Holographic Associative Memory with Dynamic Thresholding Device," OPT. COMMUN., 1992, 92(4- 6) :326-336.
3. Xu Kebin, Zhang Jingwen et al., "Real-Time Associative Memory Techniques and Devices" [in Chinese], GUANGZI XUEBAO [ACTA PHOTONICA SINICA], 1992, 21(5):73-80.
4. Wang Fan, Zhang Yimo, "Optical Associative Memory Using Self- Pumped Phase Conjugator" [in Chinese], GUANGXUE XUEBAO [ACTA OPTICA SINICA], 1992, 12(1):49-51.
5. J. Feinberg, "Self-Pumped, Continuous-Wave Phase Conjugator Using Internal Reflection," OPT. LETT., 1982, 7(10):486-488.
6. Yu Youlong, Jiang Zuohong et al., "Study of Self-Pumped Phase Conjugation Characteristics of Co:KNSBN Crystal" [in Chinese], GUANGXUE XUEBAO, 1992, 12(10):883-887.
7. S. Bian, J. Zhang et al., "Self-Pumped Phase Conjugation of 18- Deg-Cut Ce-Doped KNSBN Crystal at 632.8 nm," [journal title missing], 1993, 18(10):769-771.
8. Q. Jiang, Y. Song et al., "Mechanism of the Self-Pumped Phase Conjugator Using Cu:KNSBN," NONLINEAR OPTICS, 1991, 1(1):307-312.
9. Q. Jiang, X. Lu et al., "Enhanced Self-Pumped Phase Conjugation from 16-Deg-Cut Cu:KNSBN," APPL. OPT., 1992, 31(29):6299-6302.
10. J. Zhang, H. Xu et al., "Real-Time Double-Exposure Interferometry Using Self-Pumped Conjugator with Cu:KNSBN," OPT. COMMUN., 1992, 87(5/6) :263-266.
11. J. Zhang, H. Xu et al., "Real-Time Coherent Image Differentiation Using a Self-Pumped Phase Conjugator with Cu:KNSBN," to be published in APPL. OPT.
12. Zhang Jingwen, Sun Wanjun et al., "Very High Photorefractive Gain in Two-Beam Coupling with Thin Iron-Doped $LiNbO_3$ Crystal," CHINESE PHYS. LETT., 1993, 10(4):227-230.

Fabrication of Microlens Array Using Photosensitive Glass

94P60297F Beijing GUANGXUE JISHU [OPTICAL TECHNIQUE] in Chinese No 3, May 94 pp 19-20

[Article by Luo Fengguang [5012 7364 0342], Cao Mingcui [2580 2494 5050] et al. of the National Lab. of Laser Technology, HUST, Wuhan 430074: "Fabrication of Microlens Array Using Photosensitive Glass," supported by grants from NSFC, the 863 High-Tech Program, and the NDSTIC Basic Research Fund; MS receipt date not given]

[Abstract] A study of microlens array fabrication from photosensitive glass is presented. The glass is exposed using deep-UV light exposure for 5-20 min and heated through a thermal cycle (450-600 deg C, 600 deg temperature maintained for 30 min) with a hexagonal close-packed arrangement. A microlens array with a single-lens diameter of 400 microns, center spacing to lens diameter ratio of 1.2, and surface convexity of 9 microns has been fabricated. The experimental results indicate that the technique is applicable to fabrication of microlens arrays with single-lens apertures ranging from 50 microns all the way up to 600 microns.

Figures 1-3, not reproduced, show the following: a schematic of the formation of microlens structures from photosensitive glass, a drawing of the micronlens array surface, and a micrograph of a cross section of the microlens array, respectively. There are no tables.

References:

1. K. Iga, S. Misawa, APPL. OPT., 25 (1986):3388.
2. Masahiro Oikawa et al., JAPANESE J. APPL. PHYS., 20, 4 (1981), L296-L298.
3. Z.L. Liau et al., APPL. PHYS. LETT., 52, 22 (1988), 1859-1861.
4. Zoran D. Popovic et al., APPL. OPT., 27, 7 (1988), 1281-1284.
5. Kasra Rastani et al., APPL. OPT., 30, 11 (1991), 1347-1354.

Growth, Holographic Storage Properties of Ce: Fe: $LiNbO_3$ Crystal

94P60268A Beijing GUISUANYAN XUEBAO [JOURNAL OF THE CHINESE CERAMIC SOCIETY] in Chinese Vol 22 No 2, Apr 94 pp 129-133

[Article by Li Minghua [2621 6900 5478], Jia Xiaolin [6328 2556 2651], and Xu Yuheng [1776 3768 1854] of the Dept. of Applied Chemistry, Harbin Inst. of Technology, Bian Shaoping [6708 1421 1627] and Zhang Jingwen [1728 2529 2429] of the Dept. of Applied Physics, Harbin Inst. of Technology, and Liu Jinghe [0491 2529 0735] and Zhang Yi [1728 5065] of Dept. 4, Changchun Inst. of Optics and Fine Mechanics: "Study of Growth and Holographic Storage Properties of Ce:Fe:$LiNbO_3$ Crystal," supported by grant from NSFC; MS received 21 Apr 92]

[Abstract] Ce:Fe:$LiNbO_3$ crystal is grown by doping CeO_2 and Fe_20_3 into $LiNb0_3$. An oxidation or reduction treatment of the crystal is shown to be an effective way to change the relative concentrations of impurity ions with different valences and to improve the photorefractive properties of the crystal. An optical real-time associative memory employing a 10 mm x 10 mm x 2.9 mm sample crystal as a holographic storage medium and a 488-nm-wavelength Ar-ion laser as the light source has been implemented.

Figures 1-3 and 5, not reproduced, show the following: a graph of crystal transmissivity vs wavelength, a graph of measured gain coefficient vs angle between the two beams, a graph of measured diffraction efficiency vs angle between the two beams, and photos of experimental results (stored image, addressed image, output image) of holographic associative memory, respectively. Figure 4, the experimental set-up, is reproduced below. There are no tables.

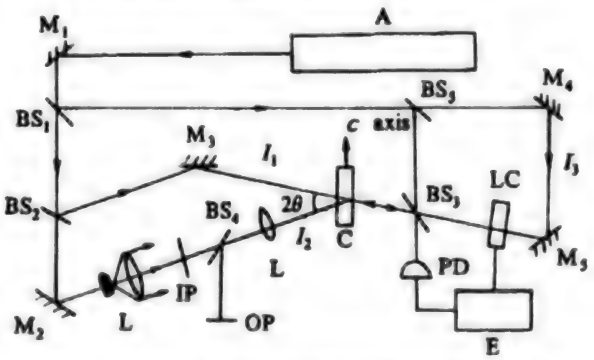

Figure 4. Experimental Configuration of Real-Time Holographic Associative Memory. A-Ar^+laser; M_1, M_2, M_3, M_4, M_5-Reflecting mirrors; BS_1, BS_2, BS_3, BS_4, BS_5-Beam splitters; C-Ce:Fe:$LiNbO_3$ crystal; L-Lens; LC-Liquid crystal electro-optic switch; PD-Electro-optic triode (i.e. photodiode); E-amplifier; IP-Input plane; OP-Output plane.

References:

1. Soffer, B.H., Dunning, G.J. et al., "Associative Holographic Memory with Feedback Using Phase-Conjugate Mirrors," OPT. LETT., 1986; 11(3): 118.
2. Zhang Hongjun, Dai Jianhua et al., "Application of Fe:$LiNb0_3$ Crystal Degenerative Four-Wave Mixing (DFWM) in Optical Image Processing" [in Chinese], WULI XUEBAO [ACTA PHYSICA SINICA], 1984;33(11):1593.
3. Wang Tianji, Fan Shaowu et al., "Real-Time Scattered Speckle- Displacement Interferometer Using Fe:$LiNbO_3$" [in Chinese], ZHONGGUO JIGUANG [CHINESE JOURNAL OF LASERS], 1985;13(5) :306.

4. Lu Tuansun, Liu Wenhu et al., "Real-Time Correlation Operations Using Fe:$LiNbO_3$ Crystal" [in Chinese], ZHONGGUO JIGUANG, 1984;12(1) :6.

5. Burke, W.J., Staeble, D.L. et al., "Volume Phase Holographic Storage in Ferroelectric Crystals," OPT. ENG., 1978;17(4):308.

Microelectronics

0.6-Micron $TiSi_2$ Polycide LDD MOS Process Studied, 31-Stage Ring Oscillator Fabricated

94P60333A Beijing BANDAOTI XUEBAO [CHINESE JOURNAL OF SEMICONDUCTORS] in Chinese
Vol 15 No 5, May 94 pp 361-366

[Article by Xu Qiuxia [1776 4428 7209], Gong Yiyuan [7895 5030 0337] et al. of the R&D Section, CAS Microelectronics Center, Beijing 100029: "Research on $TiSi_2$ Polycide LDD MOS Process"; MS received 12 Jun 92, revised 2 Nov 93]

[Abstract] Technologies for 0.6-μm $TiSi_2$ polycide LDD NMOSFETs [lightly doped drain n-channel metal-oxide semiconductor field-effect transistors] are studied. A 0.6-μm strictly anisotropic fine structure has been obtained by RIE [reactive ion etching]. Analytical results show that the TEOS [tetraethyl orthosilicate] SiO_2 film thickness and profile inclination angle are important factors affecting side-wall width, with optimum values of 350 nm, 88 deg., and 0.30-0.32 μm, respectively. A TiN/Ti compound layer is introduced between the Al and Si as a diffusion barrier, producing good thermal stability. The aforementioned technologies have been applied to a 19-step fabrication process successfully used to develop a 0.6-μm [channel length] $TiSi_2$ polycide LDD E/D MOSFET 31-stage ring oscillator, which has an average single-stage delay of 310 ps [picoseconds] (0.29 mW/stage) at an operating voltage of 5 V.

Figures 1-7, not reproduced, show a schematic of the LDD NMOSFET cross section, SEM and TEM micrographs of the device at various steps and with various changes in process parameters, and graphs of the I-V (current vs voltage) characteristic and breakdown voltage vs channel length. Table 1, not reproduced, lists various other device characteristics and parameters.

References:

1. K. Saito, T. Morase, S. Sato and U. Harada, Denshi Tsushin Rengo Taikai [in Japanese], 1978, p 220.

2. Xu Qiu-xia et al., J. VAC. SCI. TECHNOL., 1990, B8:1058.

3. G. Schatz and M. Kaufman, J. PHYS. CHEM., 1972, 76:3586.

4. C.J. Mogab and H.J. Levinstein, J. VAC. SCI. TECHNOL., 1980, 17:721.

5. Sang H: Dhong and Edward J. Petrillo, J. ELECTROCHEM. SOC., 1986, 133:389.

Chinese R&D of Microactuators Compared to U.S., Japanese Levels

94P60332A Beijing GAO JISHU TONGXUN [HIGH TECHNOLOGY LETTERS] in Chinese
Vol 4 No 5, May 94 pp 38-40

[Article by Cai Hegao [5591 7729 4108], Sun Lining [1327 4539 1337], and An Hui [1344 6540], Robotics Research Institute, Harbin Institute of Technology, Harbin 150001: "Piezoelectric/Electrostrictive Microactuators and Their Applications, Part 1 [of 2]"; MS receipt date not given. Cf. "Bionic Ultraprecise Planar Actuator, Controller" by same authors, abstracted in JPRS-CST-94-013, 25 Jul 94 p 20]

[Abstract] Worldwide trends in R&D of microactuators, especially the piezoelectric and electrostrictive types, are discussed. Microactuator applications in a variety of fields involving ultraprecise (submicron-class) positioning techniques—including precision machinery manufacturing, seismology, genetic engineering and medicine—are outlined, and the major types of microactuator operating principles are outlined. Chinese R&D of microactuators is compared with U.S. and Japanese levels in Table 1, reproduced below. Figure 1, not reproduced, shows a classification of piezoelectric/electrostrictive driver types.

Table 1. Submicron-Class Actuator Technology

Nation	Maker	Guide-way form	Drive mode	Run	Resolution (μ)	Displacement accuracy (μm)	Degrees of freedom	Application
United States	HP Company	Ball guide			0.008	0.016	X-Y	Electron-beam exposure machine
	NBS Company	Flexible bearing	Piezoelectric	50 μ	0.001		1	
	Micronix	Flexible bearing	Piezoelectric		0.02		6	X-ray exposure machine
	GCA	Elastic guide	Rectilinear		0.03		X-Y	Graphics generator
	BTL	Gas-float guide	Static friction			0.1	X-Y	Step-and-repeat camera
	Yosemite	Roller guide	Servomotor	100 mm	0.01	+/-0.01	X-Y	Electron-beam exposure machine
	Burleigh	Roller guide	Piezoelectric inchworm-style	25 mm	0.01		1,2,3,4	Electron-beam exposure machine
Japan	Hitachi, Ltd.	Flexible bearing	Piezoelectric	+/-8 μ		+/-0.05 μ	X-Y	Electron-beam exposure machine
	Tohoku University	Elastic guide	Electromagnetic			0.1	X-Y	Graphics generator
	Musashino	Elastic guide	Electromagnetic	+/-20 μ	0.01		4	X-ray exposure machine
	Musashino	Elastic guide	Electromagnetic, piezoelectric	+/-20 μ	0.03	0.1	6	X-ray exposure machine
	Fujitsu	Gas-float guide	Wedge-shaped block, screw	2 mm	0.03		X-Y	Mask alignment station
China	Shanghai Institute of Electrical Science	Ball guide	Piezoelectric	+/-6.4 μ	0.08		Y	Graphics generator
	MEI Institute 45	Elastic guide	Electrostrictive	20 μ	0.08		X-Y	Step-and-repeat camera
	University of S&T for National Defense	Flexible bearing	Electrostrictive	20 μ	0.1		1	Lathe microfeed
	Harbin Institute of Technology	Flexible bearing	Electrostrictive	20 μ	0.01	+/-0.05	1	Lathe microfeed
	Qinghua University	Ball guide	Wedge-shaped block, screw	300 μ	0.05	+/-0.25	X-Y-θ	Projection lithography machine
	Qinghua University	Elastic guide	Elastic reduction	10 μ	0.01	+/-0.2	X-Y	
	Qinghua University	Ball guide	Piezoelectric	2 μ	0.16		Y	Automatic stepper camera
	Harbin Institute of Technology	Flexible bearing	Electrostrictive	10 mm	0.01	0.5/0.05	X-Y	Robot micromanipulator

No references given.

Domestically Made Flat-Panel VFDs Compared With Imported Displays

94P60309A Beijing YIQI YIBIAO XUEBAO [CHINESE JOURNAL OF SCIENTIFIC INSTRUMENT] in Chinese Vol 15 No 2, May 94 pp 190-193

[Article by Ruan Shiping [7086 0013 1627] of the Display Systems Laboratory, Hangzhou University: "Analysis of Factors Involved in Low Brightness of Domestically Made Flat-Panel [Vacuum] Fluorescent Displays," supported by grant from NSFC; MS received Jun 92]

[Abstract] The key to the quality of domestically made flat-panel vacuum fluorescent displays (VFDs) is needed improvement in brightness. With such improvement, Chinese-made VFDs will be able to replace imported models. This paper compares the performance parameters—especially brightness—of domestically made VFDs with those of foreign-made models.

Figure 1, reproduced below, shows a schematic of the brightness measurement circuit for a VFD, while Figure 2, not reproduced, shows a graph of cathode emission efficiency vs. cathode grid spacing dcg. All four tables are reproduced below.

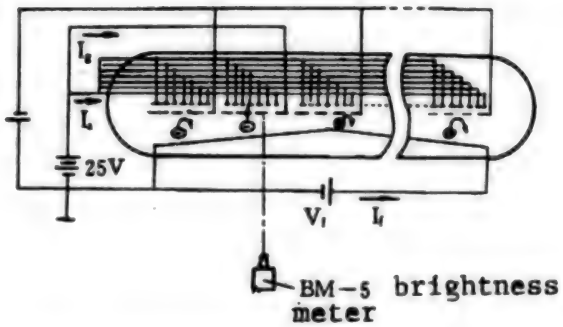

Figure 1. Schematic of Brightness Testing Circuit

Table 1. Structural Parameters of Domestically Made Multibit Flat-Panel Display Samples

Sample	No. of bits	dcg (mm)	dga (mm)	Character height (mm)	Stroke width (mm) (coating surface/anode)	No. of cathodes	Cathode spacing (mm)
Domestic 1	6	1.12	1.20	17.3	1.05	4	3.5
Doemstic 2	6	1.50	0.80	17.3	1.05	4	3.5
Domestic 3	12	0.93	0.93	16.5	0.90	4	4.7
Domestic 4	12	1.07	0.83	16.5	0.90	4	4.7
Domestic 5	9	1.95	0.95	9.5	0.90	2	5.3
Domestic 6	6	1.10	0.47	14.5	1.51/1.22	3	5.0

Table 2. Structural Parameters of Imported Multibit Flat-Panel Display Samples

Sample	Maker	Model No.	No. of bits	dcg (mm)	dga (mm)	Character height (mm)	Stroke width (mm) (coating surface/ anode)	No. of cathodes	Cathode spacing (mm)
Imported 1	FUTABA	B-BT-04A	13	0.85	0.40	7.0	0.57/0.83	2	3.5
Imported 2	NEC	FIP4B8B	4	0.80	0.60	4.8	0.70/1.10	3	2.8
Imported 3	NEC	FIP9C13	9	1.17	0.63	14.0	0.95	4	4.5
Imported 4	ITRON	FG159A2	15	1.07	0.60		0.86	3	2.7

Table 3. Comparison of Optoelectronic Parameters of Domestic and Foreign Samples

	Grid current Ig (mA)	Anode current Ia (mA)	Luminance L (cd/m^2)	Anode current density ja (mA/mm^2)	Light-emitting efficiency η_p (lm/W)	Anode-grid current ratio Ia/Ig
Domestic 1	2.50	3.20	0.940×10^3	0.078	1.58	1.28
Domestic 2	1.90	2.40	0.980×10^3	0.058	2.42	1.26
Domestic 3	2.20	3.60	2.420×10^3	0.098	3.08	1.64
Domestic 4	1.56	1.45	0.759×10^3	0.039	2.42	0.93
Domestic 5	1.32	1.06	1.164×10^3	0.052	2.80	0.80
Domestic 6	2.30	1.65	0.830×10^3	0.028	3.71	0.72
Imported 1	2.77	1.46	0.434×10^4	0.100	5.45	0.53
Imported 2	10.10	6.41	1.540×10^4	0.311	6.22	0.63
Imported 3	4.80	4.21	0.580×10^4	0.118	6.20	0.88
Imported 4	2.25	2.20	0.380×10^4	0.116	4.12	0.98

Table 4. Comparison of Cathode Emission Ability of Domestic and Foreign Multibit Flat-Panel Displays

	Heating voltage V_f (V)	Heating current I_f (mA)	Emission current I_c (mA)	Emission efficiency η_c (mA/W)		Heating voltage V_f (V)	Heating current I_f (mA)	Emission current I_c (mA)	Emission efficiency η_c (mA/W)
Domestic 1	2.70	170	29.2	63.6	Imported 1	4.35	52.2	40.3	174.1
Domestic 2	6.10	130	21.5	27.1	Imported 2	2.20	86.3	47.0	248.4
Domestic 3	5.40	160	51.5	60.2	Imported 3	4.90	150.0	83.0	111.6
Domestic 4	7.80	180	32.0	22.8	Imported 4	6.70	62.0	55.0	132.4
Domestic 5	7.47	64.7	20.1	41.6	$V_a = V_g = 25V$				
Domestic 6	4.50	98.7	22.0	49.5					

References

1. Tadashi Nakamura and Kentaro Kiyobashira, The NIKKAN KOGYO SHIMBUN Ltd., 1977, pp 4-9.
2. Takao Kishino, DENSHI KAGAKU [ELECTRONIC SCIENCE], Vol 3 (1983), pp 41-47.
3. Ruan Shiping, HANGZHOU DAXUE XUEBAO [JOURNAL OF HANGZHOU UNIVERSITY], Vol 16 (1989) No 2, pp 162-167.
4. Xin Xi, DIANZI YU YIBIAO JISHU, Vol 1 (1975), pp 1-11.

Wuxi Microelectronics Expansion Passes Acceptance Check

94P60345A Beijing JISUANJI SHIJIE [CHINA COMPUTERWORLD] in Chinese No 26, 6 Jul 94 p 1

[Article by Gao Lihua [7559 7787 5478]: "Wuxi Microelectronics Construction Passes State Acceptance Check"]

[Summary] The 1.043-billion-yuan Wuxi Microelectronics Expansion Project passed State acceptance check on 29 June. This project, with the China Huajing Electronics Group as general contractor and Germany's Siemens and Japan's Toshiba as contributors of process equipment, includes construction of an IC research center, expansion of a bipolar IC production line, and construction of a 2-3 μm MOS VLSI production line. The clean room, a dynamic class-10 (dust particles smaller than 0.12 μm) facility, not only meets 2-3 μm IC production requirements, it also meets those for 0.8 μm ICs. This production line has a front-channel monthly capacity of 16,000 wafers and a rear-channel packaging capacity of 20 million chips.

Nation's First LED Chip Production Line Operational

94P60345B Beijing ZHONGGUO DIANZI BAO [CHINA ELECTRONICS NEWS] in Chinese 11 Jul 94 p 1

[Article by Luo Laiping [5012 0171 1627]: "[Nation's] First Light Emitting Diode Chip Production Line Completed, Operational in Jiangxi"]

[Summary] Construction of the nation's first LED chip production line, at State-Run Plant 746 in Jiangxi Province, has been completed and the line is operational. Although China currently has a 1.5-billion-unit annual production capacity for LEDs, the LED chips themselves have so far been imported, at an annual State cost of almost US$10 million in foreign exchange. The new line, with equipment imported from the U.S., Japan, Britain, and Hong Kong, has an annual capacity of 240 million chips. Newly constructed plant area is 3000 square

meters, including a clean room of 800 square meters. Annual LED chip sales are expected to reach at least 12 million yuan, which will save the State $440,000 in foreign exchange.

Telecommunications

Newest Reports on Information Highway

AT&T Co-Hosts Telecom Clinic

40100085A Beijing CHINA DAILY in English 12 Jul 94 p 2

[Article by Liu Weiling]

[Text] Shanghai—In a move to help pave the way for China's information superhighway, U.S. telecom giant AT&T is launching a week-long seminar on advanced technology in China.

The seminar, which opened here yesterday and is expected to move to Beijing on Thursday, brings together more than 10 scientists from AT&T's Bell Laboratories and nearly 1,000 senior telecommunications and computer specialists throughout China.

Sponsored by the State Planning Commission and AT&T China Inc., the seminar will focus on recent advances in telecommunications technology and how they will influence China's market-oriented economy, according to John Mayo, president of Bell Laboratories.

"We see an opportunity for China to choose a technology path that will most directly move the country into the information age," said Mayo. "The opportunity is to leapfrog many of the older technologies that preceded today's advanced network systems and to make sure China benefits from the most advanced technology available."

To this end, Bell Labs plans to soon launch a research and development facility in China.

Although no further information about the planned branch is available, Mayo said Bell Labs will play a vital role in the development of China's telecommunications infrastructure.

The labs' activities in China will grow as AT&T's business here expands.

The high-profile visit from Bell Laboratories officials signals the company's intent on developing the Chinese market.

"Most of the technology AT&T is using was created at Bell Labs and is the same technology we intend to bring to our partners in China," Mayo said.

The seminar, also chaired by the State Science and Technology Commission, the Ministry of Posts and Telecommunications and the Ministry of Electronics Industry, covers a wide range of topics related to the so-called information superhighway.

Among the seminar presentations will be sessions on software, multi-media, silicon microelectronics, digital speech processing, network technology and architecture, scalable high performance computing, network management and wireless communications.

"The seminar will allow us to share a growing body of information about advanced communications technology with China's telecommunications experts," said William Warwick, chairman and chief executive officer of AT&T China, Inc.

"We want to deepen AT&T's contribution to developing a modern telecommunications infrastructure in China," he said. "And we want China to experience the same excitement over the arrival of the information superhighway as now exists in the United States."

AT&T is a global telecommunications and computer company with total revenue of $67.1 billion in 1993. It currently has nine joint ventures in China. Bell Labs is AT&T's research and development centre.

Communications Ministry To Build Info Highway

40100085B Beijing CHINA DAILY in English 20 Jul 94 p 1

[Article by Gao Jin'an]

[Text] China is speeding up its construction of a modern fibre-optic cable network.

It is the first step in the development of a nationwide information superhighway.

The network, comprising 22 trunk fibre-optic cables in addition to digital microwave lines and satellites, will be in place by the year 2000, according to sources from the Ministry of Post and Telecommunications.

It will serve "three gold projects"—the Golden Bridge Project for economic information, the Gold Card Project for financial exchange and the Golden Customs Project for foreign trade.

All provincial capitals, 330 prefectural cities and industrial cities will be plugged into the network.

The Xi'an-Chengdu and Beijing-Shenyang-Changchun-Harbin optical cables have already been installed and put into trial operation last month. And the 2,180-kilometre Xi'an-Lanzhou-Urumqi cable is expected to start its trial run next month, a ministry spokesman said.

At present, 38,660 kilometres of optical cables have become operational across the country.

In addition to the planned investment from the ministry and its local departments, $7 billion in foreign investment and loans will be used to complete the network by the turn of the century.

Over the past 10 years, more than $5.67 billion of foreign capital and loans has been used in the post and telecom sector.

The planned investment in the sector this year is 53.6 billion yuan ($6.2 billion).

In the first half of this year, 16.5 billion yuan ($2 billion) of fixed asset investments were used, most of them in trunk telecommunication projects, the spokesman said.

He announced that the ministry has met the target of its Eighth Five-Year Plan (1991-95) a year and a half ahead of schedule.

By the end of last month, the country's telephone exchange capacity had reached 48.1 million lines, exceeding the planned target by 100,000. And its long-distance telephone lines now number 533,000.

In the first six months of the year, 4.52 million new phones were added to the country's telephone network, bringing the country's total number of installed phones to 21.85 million.

But the waiting list for telephones has become longer as more and more families want to have their own telephones.

At the end of last year, there were 1.89 million applicants for telephones, the number soared to 2.18 million by the end of last month. And a total of 4.52 million applicants had their phones installed in the first six months of the year.

The ministry reported a sustained growth rate of 49.3 per cent in the post and telecom sector over the past six months, faster than the country's 11.6 per cent economic growth rate.

The turnover of the post and telecom business reached 30.34 billion yuan ($3.5 billion) over the past six months.

New Telecom Provider To Build Own Network

40100085C Beijing CHINA DAILY (BUSINESS WEEKLY) in English 25 Jul 94 p 1

[Article by Pei Jianfeng]

[Text] The newly launched China United Telecommunications Corp (China Unicom) plans to invest over 100 billion yuan ($11.56 billion) over the next five years building its own nationwide telecommunications network, according to Zhao Weichen, chairman of China Unicom.

By the year 2000, China Unicom hopes to increase the country's telephone coverage by 1 percentage point, provide 10 per cent of China's long distance telephone service, take 30 per cent of the mobile communications market and connect its network with the international network, he said.

China Unicom was set up to break the monopoly over China's telecommunications business held by the Ministry of Post & Telecommunications for decades.

To realize its goal, China Unicom is seeking wide-ranging co-operation with domestic and overseas partners, Zhao said.

Sponsored by the ministries of the Electronics Industry, the Power Industry and Railways, China Unicom has received investment from 13 large domestic companies including China International Trust and Investment Corp, China Everbright International Trust and Investment Corp, China Huaneng Group, China Resources Group and China Merchants Holdings.

Each of the 13 investors has invested 80 million yuan ($9.25 million) in China Unicom.

Many provinces, cities and large companies are eager to invest in China Unicom and become shareholders, Zhao said.

About 80 big-name overseas companies and financial institutions have initiated contacts to work with China Unicom.

Zhao said that China Unicom will take various measures to co-operate with foreign companies and organizations including borrowing, leasing equipment, contracting for engineering services and consulting.

He hopes that the government will allow China Unicom to make bold experiments in co-operating with foreign partners and introducing foreign funds.

There are more than 30 private telecommunication networks in the country including separate ones for the railroad industry, power industry, oil industry, radio and TV broadcasting industries, and the military.

China Unicom will first renovate and expand the railroad and power industry networks and link them with the existing public telecommunications network.

Other private networks will be welcome to join China Unicom to provide telephone services to the public, Zhao said.

China Unicom will also set up a nationwide mobile communications network that includes digital cellular mobile communications and paging.

A number of earth stations for satellite communications will be built around the country.

Zhao said that China Unicom will first set up its subsidiaries in Beijing, Shanghai, Guangzhou and Shenzhen.

Its local branches will be established gradually throughout the nation, he said.

Beijing-Taiyuan-Xian Fiber Optic Cable Trunk Line Construction Begun

94P60346A Beijing ZHONGGUO DIANZI BAO [CHINA ELECTRONICS NEWS] in Chinese 17 Jun 94 p 1

[Article by Jiang Guoqiang [1203 0948 1730]: "Beijing-Taiyuan- Xian Fiber Optic Cable Communications Construction Begun"]

[Summary] Construction of the 1710-km-long Beijing-Taiyuan-Xian fiber optic cable communications trunk line—a State Eighth FYP key project—has begun. This project, a critical part of the national digital communications network approved by the State Planning Commission, will interconnect 42 cities and county seats in Beijing Municipality, Henan Province, Shanxi Province, and Shaanxi Province.

Beijing-Wuhan-Guangzhou Fiber Optic Cable Trunk Line Construction to Begin Soon

94P60346D Beijing RENMIN RIBAO OVERSEAS EDITION in Chinese 19 Jul 94 p 1

[Article by Chen Bingguang [7115 3521 0342]: "Beijing-Wuhan Guangzhou Fiber Optic Cable Communications Trunk Line Construction Commencing"]

[Summary] Guangzhou, 16 Jul (XINHUA)—This writer has learned from authoritative sources that China is about to begin construction of the 3000-km-long, 600-million-yuan Beijing-Wuhan-Guangzhou high-capacity buried fiber optic cable communications trunk line, a State Eighth FYP key project. This trunk line, which will link up Beijing Municipality with Hebei, Henan, Hubei, Hunan, and Guangdong provinces, is being built in segments. Construction for the 500-odd-km-long, 125-million-yuan Guangdong segment, providing over 24,000 long-distance circuits, will begin this August. Construction for the remaining segments will begin in the near future and the entire cable is scheduled to be completed by 1999.

Shanghai Firm, AT&T to Jointly Construct Intelligent Buildings

94P60346B Shanghai WEN HUI BAO in Chinese 28 Jun 94 p 4

[Article by Qian Weihua [6929 4850 5478]: "Shanghai to Construct Intelligent Building System"]

[Summary] AT&T, via the retail firm Hong Kong Telecommunications, yesterday signed a technology cooperation agreement with Shanghai Chang Jiang Computer Systems Integration Company (SCJCSIC) to construct an intelligent building system in Shanghai. All of the computers in these buildings will be directly linked to an information center or networked directly into the [national] information highway. Several new 100-odd-story skyscrapers now being built in Shanghai will get this information technology. In addition, the Shanghai Telecommunications Tower, the Shanghai Jiaotong University S&T Tower, and the Chang Jiang Three Gorges HQ Tower have all contracted with SCJCSIC for construction or expansion projects utilizing AT&T's integrated wiring technology.

Three Gorges Development Corp. to Get "Intelligent Building" HQ

94P60344C Beijing JISUANJI SHIJIE [CHINA COMPUTERWORLD] in Chinese No 26, 6 Jul 94 p 1

[Article by Song Yi [1345 6146]: "Three Gorges Headquarters to Construct Intelligent Building"]

[Summary] China Chang Jiang Three Gorges Engineering Development Corporation has announced that it will construct an "intelligent building complex" for its new HQ. The building complex, whose structural wiring system will be jointly developed by the Chang Jiang Computer Group and Qinghua University, consists of a 33-story business information main tower and a 7-story "experts" tower, as well as a 4-story demonstration and exposition hall. The building complex will use AT&T's integrated voice/data wiring system for intra-tower communications, with fiber optic LANs for inter-tower communications and vertical backbones. The horizontal backbones will incorporate high-transmission-speed cable, supporting the current 10 Mbps [Ethernet] data and speech transmission rate and the coming 100 Mbps (FDDI [fiber distributed data interface]) data and image transmission rate, as well as ISDN traffic. Each information station within the building complex can be linked with the Chinapac national packet-switched public data network and thereby put on-line with stations in Beijing, Shanghai, Guangzhou, Chongqing and other cities.

Chongqing to Build 800-MHz Trunking Communications System

94P60346C Beijing ZHONGGUO DIANZI BAO [CHINA ELECTRONICS NEWS] in Chinese 4 Jul 94 p 3

[Article by Yu Ruming [0151 3067 2494]: "Chongqing to Build 800-MHz Trunking Communications System"]

[Summary] Chongqing Enterprise Development Ltd. is building an 800-MHz trunking communications system from imported equipment. This system, which will join an intelligent area trunking system made by the U.S. firm Motorola with SR-500 time-division multiple access (TDMA) digital microwave equipment made by Canada's SRT Company, is to be completed by 1996; it will consist of 15 base stations and 170 channels, and will provide services to 16,000 users in the greater Chongqing area. Services include analog and digital voice communications, fax, selective call-carrying (secure conversation), conferencing, and emergency/priority calling.

General Instruments Corp. Supplies DigiCipher Technology

40100089A Beijing CHINA DAILY in English 11 Aug 94 p 2

[Article by Wang Yong: "Instrument Supplier Nears Hi-Tech Deal"]

[Text] The U.S. General Instruments Corporation (GI) is close to a deal to supply its latest DigiCipher systems in China for the first time, it was revealed in Beijing yesterday. Negotiations between GI and the Chinese Ministry of Radio, Film and Television are under way, according to a source with the Boston-based Mascon Corporation, GI's China representative. A senior official from the ministry said digital compression technology, an advantage of the company, is a vital part of China's information superhighway.

Digicipher was developed by GI in the late 1980s and enhanced through 1993. It is an essential part of the all-digital system proposed for broadcast HDTV and for satellite and cable multi-channel digital television systems. "The ministry is studying the feasibility of setting up high-definition TVs, digital video and audio systems, and cable TV networks as part of the superhighway project," the official said.

As the world's leading supplier of bandwidth telecommunication systems, GI is competing with many other companies in the Chinese market, which has more than 1,000 cable TV stations. GI was a major participant at the '94 China Cable TV Show, which ended yesterday at the World Trade Centre in Beijing.

The DigiCipher I system, developed in 1992, allows up to 10 television services to be digitally compressed for transmission on a single satellite transponder. While the DigiCipher II system was initially designed to deliver digital television signals by satellite and cable to affiliates and subscribers, it can also transmit signals through microwave, fibre and asynchronous mode [i.e. ATM] networks.

Physics

Selective Photoionization of Isotopic Atoms via Pulsed Lasers

94P60308A Beijing WULI XUEBAO [ACTA PHYSICA SINICA] in Chinese Vol 43 No 3, Mar 94 pp 356-368

[Article by Dai Changjian [2071 7022 1696] of the Dept. of Physics, Zhejiang University, Hangzhou 310027 and Yu Changjiang [0060 7022 3068] of the Research Institute of Physical and Chemical Engineering of Nuclear Industry, Tianjin 300180: "Selective Photoionization of Isotopic Elements with Pulsed Laser Fields"; MS received 20 Mar 93]

[Abstract] Multi-step optical excitation and ionization techniques have proven to be useful in areas such as atomic spectroscopy [1], chemical reactions [2], and atomic vapor laser istotope separation (AVLIS) [3-4]. Furthermore, multi-step optical excitation dynamic processes [5] and interactions between different isotopes and continuous-wave (CW) laser fields [6-7] have been studied. CW laser fields, however, are characterized by difficult-to-control temporal characteristics and low excitation efficiency, leading to a high degree of nonlinearity in the separation medium—the plasma and ion processes become severely complex. Use of pulsed excitation sources can eliminate or greatly reduce these detrimental factors, and therefore has become a critical tool in AVLIS research [8]. In this paper, further study of interactions between pulsed laser fields and different isotopes (especially ^{235}U and ^{238}U) is conducted.

Specifically, the dynamics of isotopically selective interactions between the radiation of three pulsed lasers and atoms with a four-energy-level scheme are studied. Starting from the time-dependent Schrodinger equation with the rotating-wave approximation, the Sylvester theorem is applied to the dynamic equations associated with near-resonant and off-resonant excitations. Explicit expressions for the four-level occupation probabilities are obtained. The properties of coherent oscillations occurring in the atomic excitation processes with intense monochromatic lasers are explored in an analytic treatment. Conditions under which population inversion occurs are derived from near-resonant excitations. Finally, criteria for selecting the basic parameters for the pulsed lasers are also given.

Figures 1-3, reproduced below, show a model of the laser pulse series, an energy-level diagram for two different isotopic atoms, and a schematic of the displacement reflections of the laser beams in the reaction cavity, respectively. In Figure 1, Ω_1 is the intensity of the first excitation light, Ω_2 is the intensity of the second excitation light, and Γ is the intensity of the ionization light; τ_1, τ_2, and τ_3 are the pulse widths (approx. 100 ns) for the three lasers, with $\tau_1 \leqq \tau_2 \leqq \tau_3$ and pulse-series period $T = \tau_2 + \tau_3 + l$ (where l, the intermittent time of radiation of the laser field with respect to the atomic system, is about 10^5 ns). Additionally, λ (laser wavelength) is chosen to be 591.53 nm and uranium-atom evaporation temperature is about 2600 K. There are no tables.

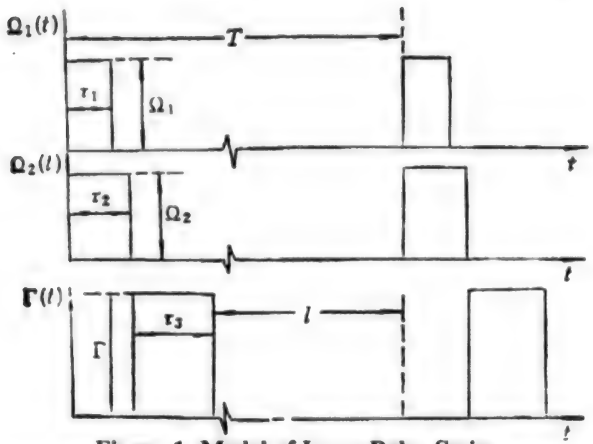

Figure 1. Model of Laser Pulse Series

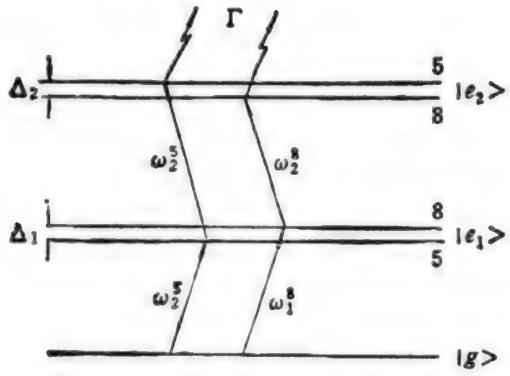

Figure 2. Energy-Level Diagram for Two Different Isotopic Atoms

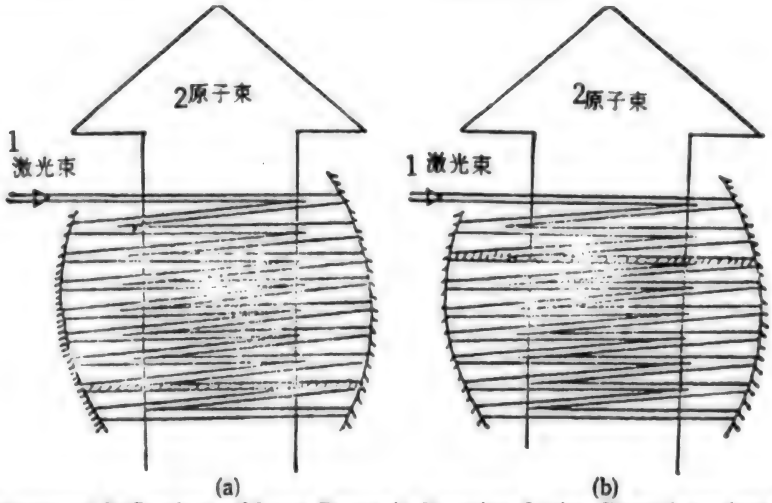

Schematic of Displacement Reflections of Laser Beams in Reaction Cavity. Shaded portions of atom beams represent different displacements for one group of atoms irradiated by a different series of laser pulses.

Key: 1. laser beam; 2. atom beam.

References:

1. T.F. Gallagher, J. OPT. SOC. AM., B4 (1987), 794.
2. J. Keller and J. Weiner, PHYS. REV., A29 (1984), 2230.
3. P.T. Greenland, CONTEMPORARY PHYS., 31 (1990), 405.
4. J.I. Davis and E. Rockower, IEEE J. QUANT. ELECTR., QE-18 (1982), 223.
5. Jiang Mengheng, Lin Fucheng, GUANGXUE XUEBAO [ACTA OPTICA SINICA], 11 (1991), 769.
6. N.V. Karlov et al., SOV. PHYS. TECH. PHYS., 28 (1983), 937.
7. Yu Changjiang, Wang Lijun, JILIN DAXUE ZIRAN KEXUE XUEBAO [JOURNAL OF JILIN UNIVERSITY, NATURAL SCIENCES EDITION], special issue (no 3) (1992), 763.
8. J.A. Paisner et al., APPL. PHYS., B46 (1988), 253.
9. D. Scarl et al., PHYS. REV., A24 (1981), 883.
10. W.L. Brogan, "Modern Control Theory," Prentice-Hall, Inc., New Jersey (1985), 224.
11. D. Kim et al., PHYS. REV., A41 (1990), 4966.
12. L.J. Rudziemski et al., eds., "Laser Spectroscopy and Its Applications," Decker (New York, 1987), 175.
13. P.L. Knight et al., "Concepts of Quantum Optics," Pergamon (New York, 1983).
14. J.R. Ackerhalt and B.W. Shore, PHYS. REV., A16 (1977), 227.
15. C.J. Dai, G.W. Schinn and T.F. Gallagher, PHYS. REV., A42 (1990), 223.
16. C.S. Chang and R. Schlier, PHYS. REV., A21 (1980), 872.

17. Y.R. Shen, "The Principles of Nonlinear Optics," Wiley (New York, 1984).

18. Noriaki Tsukada et al., PHYS. REV., A2l (1980), 1281.

Soft X-ray Lasing in Neon-Like Germanium Plasma Produced by Double-Pulse Laser of Lower Energy

40100087A Chengdu QIANG JIGUANG YU LIZI SHU [HIGH-POWER LASER AND PARTICLE BEAMS] in Chinese Vol 6 No 2, May 94 p 174

[Article by Huang Wenzhong, Zhang Qiren, et al. of the Southwest Institute of Nuclear Physics and Chemistry, P.O. Box 525-84, Chengdu, 610003 and Zhang Guoping, Sheng Jiatian, et al. of the Institute of Applied Physics and Computational Mathematics, P.O. Box 8009, Beijing, 100088 (MS received 6 Jan 94, revised 4 May 94)]

[Abstract] Soft X-ray 3s-3p lasting transitions originating from $J = 0$-1 and $J = 2$-1 in neon-like germanium plasma are observed at about 100J pump energy for the first time. The lasting plasma is produced by double-pulse laser with an interval of 350ps heating 10mm-long thin-film germanium targets. The line of 19.61nm ($J = 0$-1) is more intense than that of 23.63nm ($J = 2$-1), and the divergence angle is less than that of the latter.

Microwave Pulse Generation by Photoconductive Switching

40100087B Chengdu QIANG JIGUANG YU LIZI SHU [HIGH-POWER LASER AND PARTICLE BEAMS] in Chinese Vol 6 No 2, May 94 p 178

[Article by Yang Zixiang, Miao Tieying, et al. of the Institute of Applied Electronics, CAEP, P.O. Box 527, Chengdu, 610003 (MS received 25 Dec 93, revised 26 Jan 94)]

[Abstract] Conversion of energy from DC to RF has been demonstrated with an impulse-excited coaxial resonant cavity using picosecond optoelectronic switching techniques. A single pulse is capable of generating more than 140 RF cycles. Highest oscillations have been obtained at 952 MHz.

Particle Simulation of Dual-Beam Side-Shot Vircator

40100087C Chengdu QIANG JIGUANG YU LIZI SHU [HIGH-POWER LASER AND PARTICLE BEAMS] in Chinese Vol 6 No 2, May 94 p 228

[Article by Wang Zhixiong, Guo Yonghui, et al. of the Northwest Institute of Nuclear Technology, P.O. Box 69, Branch 15, Xi'an, Shaanxi, 710024 (MS received 13 Jul 93, revised 20 Nov 93)]

[Abstract] A dual-beam side-shot virtual cathode oscillator (SSVCO) model has been established and simulated by a 2.5-dimensional, fully electromagnetic, relativistic CIC particle simulation code WGCF. The simulations (including single-beam case) indicate: (1) the maximum average efficiency occurs for a fixed distance of the two anodes when the injected beam current J_0 is 1.2-2 times as large as the critical current J_c; (2) there is an optimum distance where the maximum efficiency is reached for a given ratio of J_0/J_c; (3) as compared with single-beam case, the microwave modes are purer, no direct current fields are coupled to output window and the central frequency expands wider; (4) oscillations still exist for J_0-J_c but d.c. fields are dominant. In addition, the power distribution functions with modes or frequencies and a new absorbing boundary condition have been derived.

Numerical Calculation of REB Diode, Experimental Research

40100087D Chengdu QIANG JIGUANG YU LIZI SHU [HIGH-POWER LASER AND PARTICLE BEAMS] in Chinese Vol 6 No 2, May 94 p 234

[Article by Zhang Dong, Yang Dawei, et al. of the China Institute of Atomic Energy, P.O. Box 275-7, Beijing 102413 (MS received 6 Aug 93, revised 9 Dec 93)]

[Abstract] A large-area diode (12cm x 75cm) using a single insulating structure without grading has been used in research on a hundred-joule KrF laser. The distribution of electric field lines and equipotential lines in this REB (relativistic electron beam) diode has been calculated and compared with experimental results. No flashover occurred when the electric field is less than 3kV/cm at the triple point (junction of lucite wall with metallic wall and a vacuum).

Performance Improvements of 3.3 MeV LIA

40100087E Chengdu QIANG JIGUANG YU LIZI SHU [HIGH-POWER LASER AND PARTICLE BEAMS] in Chinese Vol 6 No 2, May 94 p 254

[Article by Deng Jianjun, Ding Bonan, et al. of the Southwest Institute of Fluid Physics, P.O. Box 523, Chengdu, 610003 (MS received 27 Sep 93, revised 2 Dec 93)]

[Abstract] The 3.3MeV accelerator of Southwest Institute of Fluid Physics is a linear induction accelerator (LIA) whose electron-beam parameters are 2kA, 3.3MeV and 90ns, built in 1991. This accelerator was designed to drive the SG-I free electron laser. This paper describes briefly the accelerator and the SG-I FEL facility. Emphases will be placed on modifications to the pulsed-power system of the linac and beam conditioning section of the SG-I in order to satisfy the needs for FEL experiments. The beam current entering the wiggler has been increased. Beam quality and system reliability and stability have also been improved. Beam parameters have been given at different position. The two important parameters for FEL, beam emittance and energy spread, are 0.43 cm-rad and 1%, respectively. The beam current through the space and energy spread selector into the interaction region is about 950A. The ASE FEL output at

35 GHz frequency is about 100kW. Amplified FEL output of above 10MW power and gain of 20dB/m have been obtained.

Experimental Investigation of Large-area Diode for Hundred-joule KrF Laser

40100087F Chengdu QIANG JIGUANG YU LIZI SHU [HIGH-POWER LASER AND PARTICLE BEAMS] in Chinese Vol 6 No 2, May 94 p 259

[Article by Ma Weiyi, Wang Youtian, et al. of the China Institute of Atomic Energy, P.O. Box 275-7, Beijing 102413 (MS received 10 Sep 93, revised 7 Dec 93)]

[Abstract] Experimental investigation is described of a large-area diode for a hundred-joule-level KrF excimer laser pumped by an intense pulsed electron beam of 100ns. Using a 12cm x 75cm rectangular carbon felt cathode and an anode of 30μm-thick Al foil or 9 wires of 1.3mm diameter spaced 13mm from each other, total electron-beam energy higher than 8kJ is obtained at an electrode separation of 20-22mm, Marx generator voltage of 1.1-1.2MV, diode peak voltage of 620-670kV and diode peak current of 150-170kA. Maximum output energy of 106J is achieved for the KrF laser beam.

Lanzhou Heavy Ion Accelerator Achieves Maximum Design Targets

946B0119A Beijing ZHONGGUO KEXUE BAO [CHINESE SCIENCE NEWS] in Chinese 20 May 94 p 1

[Article by correspondent Song Wenjie [1345 2429 2638]: "Lanzhou Heavy Ion Accelerator Ion Beam Energy Reaches Maximum Targets"]

[Text] The Institute of Modern Physics of the Chinese Academy of Sciences announced that a 100 MeV O^{16} ion beam was successfully produced at 5:15 on May 3 on the Lanzhou Heavy Ion Accelerator at the Lanzhou National Accelerator Laboratory. This is the maximum energy design target of the Lanzhou Heavy Ion Accelerator. This achievement signifies the reach of a plateau in the operation of the accelerator.

It usually takes several years of operation before the maximum energy ion beam is generated for comparable accelerators in the world. Since its completion, Lanzhou Heavy Ion Accelerator is being modified as it operates. The original ion source was replaced by a new ECR ion source including a beam transport line and an axial injection system. Complete overhaul of the injector main coil and its constant current supply, deflector and its constant voltage supply, vacuum system and control system was made. A great deal of work was also done to perfect the RF and control system of the main accelerator. In addition, a direct pass-through ion beam and a radioactive strange nuclide secondary beam were completed. A series of technological upgrades significantly improved the performance of the accelerator and laid a solid foundation for achieving the maximum energy level. During the period, most of the equipment of the accelerator was operating at near maximum load. This is a rigorous challenge not only to the equipment but also to the technical level and operating experience of the technicians.

Lanzhou Heavy Ion Accelerator has provided a variety of heavy ion beams for research institutions and universities involved in nuclear physics, atomic physics, nuclear chemistry, biology and materials science. Significant results, such as the synthesis of Hg^{208}, a new nuclide, and the study of medium energy heavy ion collision, have been obtained to date. The accelerator operated for 3,500 hours last year which is the highest number ever. The successful production of the highest energy ion beam should enable us to expand the range and scope of experiments in the future.

National Developments

Figures in on Power Production for First Half of '94

94P60347 Beijing JINGJI RIBAO [ECONOMIC DAILY] in Chinese 7 Jul 94 p 1

[Text] The electric power industry experienced excellent growth for the first half of 1994. As of 20 June, the nation had generated 409.774 billion kilowatt-hours of electricity, an increase of 11.02 percent over the same period in 1993. Of this total, hydropower accounted for 67.23 billion kilowatt-hours, thermal power accounted for 337.01 billion kilowatt-hours, and nuclear power accounted for 5.534 billion kilowatt-hours.

From January through May, the nation's coal consumption rate for power production was 408.62 kilograms per kilowatt-hour, 3.75 kilograms per kilowatt-hour less than the same period in 1993. China's electric power enterprises actually sold 239.7 billion kilowatt-hours of electricity to earn 49.1 billion yuan which had a real tax value of 8.25 billion yuan. These figures represent increases of 7.8 percent, 34 percent, and 47.8 percent, respectively, over the same period of 1993.

In the first half of this year, the nation saw sustained growth in electric power output, maintaining a rate of increase of more than 11 percent. As a result of added hydropower capacity and good water storage levels at the first of the year, power output in the south showed a notable increase. Because of drought in much of the northern part of the country, power output was down compared to the same period of 1993. In May, the East China Grid reached its largest load—19.86 million kilowatts; this represented an increase of 2.78 million kilowatts, ranking this grid first among the country's five major power grids.

Closer Ties With French Power Up Electricity Industry

40100084A Beijing CHINA DAILY (Economics) in English 7 Jul 94 p 2

[Article by Chang Weimin]

[Text] Sino-French cooperation in power generating and the manufacture of electrical equipment is gearing up as a result of closer bilateral relations.

Executives from 20 big-name French firms, including Electricite de France and 100 Chinese corporate professionals, gathered for a seminar in Beijing yesterday.

French know-how and Chinese expectations for a rapid development of the power industry were discussed.

The seminar, to be continued in Shanghai next week, is being organized by China's Ministry of Power Industry and the China Electricity Council International.

A visit to China by French Minister of Industry, Posts, Telecommunications and Foreign Trade, Gerard Longuet, earlier this week, was regarded as a signal for warmer relations between the two countries.

The visit followed a visit to France by Chinese Minister of Power Industry, Shi Dazhen, earlier in the year.

Sino-French relations had been cool until early this year.

China, a huge market for power companies and electrical manufacturers worldwide, is being targeted by French power companies, said French government officials and corporate executives at the seminar.

French electrical equipment makers, who provided technology, equipment and services to more than 15 big Chinese projects, expect to manufacture equipment in China, said Antoine de Fleurieu, a manager of the French Electrical Equipment and Industrial Electronics Manufacturers' Association.

French companies will remain competitive in China, Fleurieu said.

China, which had installed 183 million kilowatts of generators by last year, needs to fix an additional 120 million kilowatts of machines by the year 2000.

In addition, powerful transmission systems in the country need to be renovated and linked to a national network. Increasing numbers of high-voltage lines and automatic distribution systems are to be installed.

All this makes China the largest market for electricity and electrical equipment in the world.

By the end of this year, 60 officials from China's electricity industry will have been trained in France.

Chinese participants will be able to attend a high-profile international technical seminar at the end of this year.

On Monday, the China Huaneng Group, a leading energy conglomerate in the country, signed a memorandum to purchase two 350,000-kilowatt generators from France for the Luohuang Power Plant in Sichuan Province.

Final negotiations for the project are under way, said French corporate executives. More than $90 million worth of electrical equipment was bought by China last year, compared with $127 million in 1990.

And the volume is expected to increase in the near future.

Outlook for Nation's Electric Power Summarized

94FE0617A Beijing ZHONGGUO DIANLI in Chinese No 4, 5 Apr 94 pp 62-63

[Article by Huang Xi [7806 2522] of the Institute of Water Resources and Electric Power Information: "Status and Development of China's Electric Power"]

[Excerpt]

1. Status of China's Electric Power Industry

Significant accomplishments have been obtained in the buildup of our electric power industry since the government was founded. Nevertheless, there was a lack of understanding on the critical and special role electric power plays in the economy. It is impossible to implement the idea to "build up electric power first" with limited investment provided by the government over the past 30 years. In the late 1970s, the government switched to a reform policy. A series of measures has been taken by the government and electric power authorities to raise capital for power plant construction. Especially in the last seven to eight years, the scale of power plants under construction continues to expand and the rate of basic construction has also picked up considerably. In 1987 the total added generator capacity increased by 10,000MW. In 1992 the record was broken to reach 15,000MW. In 1993, it is expected to increase by another 12,000MW (large and medium units only). Including smaller units, the total increase in capacity could reach 15,000MW again. We expect to generate 815 TWh of electricity in 1993, an increase of 9.4 percent compared to that of 1992. Even if electric power plant construction and production can increase at the above rates, the economy is also growing at a very fast pace. The long-term power shortage has not been alleviated. The "bottleneck" which started in 1970 has lasted for 23 years and is still with us. More than 20 percent of the production capacity in China cannot be put to use. Approximately 120 million people in rural areas still do not have electricity. This serious shortage of electric power not only hampers economic growth but is also inconvenient and prevents people from improving their standard of living.

The entire country is picking up its pace of reform and modernization. In his speech at the founding ceremony of the Ministry of Power Industry on 25 May 1993, Minister Shi Dazhen [0670 1129 2823] clearly laid out the objective to develop the electric power industry at an extraordinarily high rate at all cost. On 27 December 1993, in his report to the Electric Power Workshop, Minister Shi further clarified that "extraordinary growth" is to reform and overcome outdated rules and regulations that are obstacles to growth. "Extraordinary growth" not only involves quantity but also quality. It not only requires speed but also substance. It appears that the only way to solve the power shortage problem for a country that has 1.17 billion people is to immediately begin developing electric power at an extraordinary speed on the premise that our energy structure is centered around electricity. This clear objective is a conclusion of our experience in the past decades. It also agrees with the pattern followed by other industrialized countries around the world. It is not a short term measure to solve the power shortage problem. Instead, it is a long range plan that requires the hard work of several generations of people to modernize our country. Let us follow the rule governing socialist economy, take advantage of available opportunities, liberate our thinking and utilize various means to raise domestic and foreign capital to invest in the electric power industry in order to create the necessary condition for our industry to grow at an extraordinary rate.

2. Prospects for China's Electric Power Industry

According to economic statistics, China's GNP grew at an average rate of 13.9 percent per year between 1978 and 1991. The amount of electricity produced, however, only grew at an annual rate of 7.8 percent. There is a huge disparity between these two numbers. Compared to 1991, the 1992 GNP grew by 12.8 percent. However, the amount of electricity produced increased by only 10.3 percent. It is estimated that the rate of increase in electric power production will still lag behind that of economic growth by several percentage points, hence the urgency to develop electric power at an extraordinary rate becomes obvious.

After the First Plenum of the Eighth People's Congress, the economy will grow at an even faster pace. Up to the end of this century, the GNP will increase by an average of 8-9 percent per year. Reference [3] points out that during the plan period we must have different schemes to achieve three levels of standards to form a wide band, rather than a line. These three schemes must contain all possible scenarios that may occur during the plan period. To meet the projected GNP increase, the rate of growth of the electric power industry in China between 1993-2000 may be estimated at three levels, i.e., 8 percent, 9 percent and 10 percent. Therefore, by the end of this century, China will have a total installed capacity of 309, 332 or 358 GW. Over this eight-year period, 17,800, 20,700, or 23,900MW in new units must be installed every year.

In his report to the Electric Power Workshop last December, Minister Shi mentioned that the total installed capacity in China could reach approximately 300GW before the end of this century, which is an objective of one of the schemes described above. The present situation favors accelerated reform and growth. It is feasible to reach the 300GW in seven years, one year ahead of schedule in 1999, and accomplish the 332GW objective by the year 2000. In order to keep up with the rapid pace of economic growth and to alleviate the pressure on the electric power industry, as long as all factors are favorable, even the high scheme is also achievable.

In a report presented in the 15th World Energy Conference (WEC) in September 1992 in Madrid, Spain, a near-, medium- and long-range forecast for electricity demand worldwide was made. In 1990, 11,700 TWh of electricity was generated. Up to 2000, the average annual growth rate will be 3.5 percent. OECD (Organization of Economic Cooperation and Development) countries will grow at a rate of 2.4 percent, Middle East and European countries 2.3 percent, and developing countries 6.75 percent. By 2020, a total of 266,000 TWh of electricity

will be produced and the annual growth rate is 2.4 percent. As for the long range (2050), it is very difficult to predict because technology may cause drastic changes. Assuming that the amount of electricity produced in OECD and Middle East and European countries remains constant at 10,900 and 3,700 TWh, respectively, and developing countries are still growing at an annual average rate of 2.25 percent, then they will produce 23,400 TWh of electricity by 2050.

On the basis of the report mentioned above, by 2050, 38,000 TWh of electricity will be generated worldwide. It will grow at an average annual rate of 1.2 percent between 2020 and 2050. From the amount of electricity generated, it is possible to project that the total installed capacity worldwide will reach 3,990, 6,330, and 9,050GW in the years 2000, 2020, and 2050, respectively. The different growth rates for the near-, medium- and long-term clearly indicate the pattern that growth slows down when the base becomes large. In particular, it is difficult to predict how technology is going to evolve. Even by comparing results from methods such as elastic coefficient, product value consumption and simple product consumption and using a weighted approach, it is still very difficult to project electric power usage and production over the long term. Nevertheless, there is no doubt that technology and economic growth have a major impact. The degree of electrification continues to rise and energy conservation technology is becoming more and more effective. Since the 1960's, the ratio of the rate electric power consumption increase to that of GNP increase in developed industrialized countries, i.e., the elastic coefficient of electric power, generally shows a downward trend. This causes the rate of increase of electric power to slow down even quicker.

As mentioned earlier, by 2000 China will have 7.8 percent, 8.3 percent, or 9.0 percent of the total installed capacity worldwide if the growth rate is 8 percent, 9 percent, or 10 percent between 1993 and 2000, respectively. (It was 1.4 percent, 2.2 percent, 2.2 percent, 3.2 percent, and 5.0 percent for 1950, 1960, 1970, 1980 and 1990, respectively.) It will be at the same level as that of the USSR in 1989 (i.e., 333GW) which is a remarkable leap forward. In the first decade of the 21st century, China will have a larger electric power base and it will be hard to try to double it. On the basis of an annual increase of 6.5 percent, the total installed capacity will reach 580, 625, and 670GW by the year 2010 (corresponding to an annual increase of 27,100, 29,300, and 31,000MW, respectively). It will be close to that of the U.S. in the late 1980s. In the second decade of the 21st century, the total installed capacity will reach 900, 970, and 1,040GW by the year 2020 (corresponding to an annual increase of 32,000, 34,300, and 37,000MW, respectively). This corresponds to 14.2, 15.2, and 16.4 percent of the total installed volume worldwide, respectively. It will exceed that of the U.S. by a large margin. Many organizations now project a wide range of total installed capacity in China by 2020, such as 650, 710, 800, and 1,045 GW. Reference [3] also points out that 800GW by 2020 can basically meet the need for an economy which grows at 8 percent between 1990-2000 and 5 percent between 2000-2020. From the present standpoint, it will exceed 800GW by 2020 under the influence of the "extraordinary growth" guideline.

However, China has one-fifth of the population in the world. By 2020, even if its population only increases to 1.6 billion, the consumption of electric power per capita is still less than 3000 kWh. It is still lagging behind certain developing countries. On the basis of indicators such as GNP and electric power consumption per capita, it will take several generations for China to catch up with other countries. There is no doubt in our mind that a long range strategic mission for the electric power industry in China is to develop the industry at an extraordinary rate of growth.

Suggestions for Development of Clean Coal Technologies

946B0103A Shanghai DONGLI GONGCHENG [POWER ENGINEERING] in Chinese Vol 14 No 2, 14 Apr 94 pp 1-8

[Article by Zhang Mingyao [4545 0682 5069], Li Daji [2621 1129 7535], Cai Ningsheng [5591 1337 3932] and Xu Yiqian [1776 4135 6197] of Southeastern University]

[Excerpts]

1. Importance of Development of Clean Coal Technologies

Coal is China's major energy source. Approximately 76.1 percent (as of 1991) of our primary energy comes from coal. By the middle of the next century, coal will remain our major primary energy source (see Table 1).

Table 1. Proportion of Coal as China's Primary Energy Source

Year	Coal %	Oil %	Natural Gas %	Hydropower %	Nuclear %	New Energy %
1985	72.8	20.9	2.0	4.3	/	/
2000	approx. 70	19.5	4.0	6.0	2	/
2050	60-70	5	5.0	6.0	10-20	5

Coal also plays a leading role in the electric power industry, which is critical to China's economic growth. More than 70 percent of the installed capacity and electricity production comes from coal-burning thermal power plants. Table 2 shows a projection of electric power and energy production up to the year 2030. From Table 2, as the economy grows, the proportion of coal-generated electric power remains at 70 percent in 2015.

Table 2. Projection of Electric Power and Energy Production in China Up to 2030

Item	Unit	1990	2000	2015	2030
Total installed capacity	MW	125,000	240,000	500,000	1,040,000
Total coal-burning generator capacity	MW	90,000	187,000	350,000	
Electric power production	10^8kW h/a	6,300	12,500	26,000	54,100
Coal consumption rate to produce electricity	g/kW h	400	350	310	380
Total coal consumed for electric power	10^8 t/a	2.50	4.4	8.1	14.1
Total demand for primary energy source	10^8 t/a	10.0	14.6	21.8	30.7
Weight of electric power as primary energy source	%	26	30	37	46
Mean annual increase of electric power production	%	7.1	5.0	5.0	4.0
Mean annual increase in energy production	%	4.3	2.7	2.30	2.00
Weight of electricity from coal	%	approx. 70	approx. 78	70	60

Let us use the U.S. as an example. Its coal-burning power plants contribute approximately 50 percent of its total capacity. By 2010, the total installed capacity will reach 850,000-900,000MW. By then, coal will remain a dominant source to produce electricity.

Table 2 also shows that as production levels increase, the proportion of electricity as a primary energy source will rise. The ratio of coal consumed by the electric power industry to total coal production will rise from 25 percent in 1990 to 46 percent by 2030. This large-scale burning of coal will pose a serious threat to the environment if it is not properly managed. Most of the pollution associated with production nationwide is caused by the use of coal. It accounts for 90 percent of the SO_2, 70 percent of the NO_x, 70 percent of the dust and particulates and 71 percent of the CO discharged into the atmosphere. Since electric utilities are major coal users and they will use more coal in the future, this serious atmospheric pollution problem not only will endanger our environment and cause severe economic loss but also will adversely impact the rest of the world.

Furthermore, on the basis of known coal reserves, the sulfur content of our coal reserves is shown in Table 3. The average ash content of our power-generating coal is 27 percent. China also has a wide distribution of low-grade coal (high ash content and low thermal value). Therefore, clean burning of high-sulfur, high-ash content coal must be addressed.

Table 3. Sulfur Content in Coal in China

Sulfur Content	Proportion
< 1%	65-70%
1-2%	15-20%
> 2%	10-20%

The development of IGCC in China began in the mid-1970s under the direction of the State Science and Technology Commission. In 1986 the Taiyuan Heavy Machinery Factory successfully duplicated a 2.8 m diameter Lurgi fixed bed gasification furnace. It could process 120 tons of coal per day and produce 1,500 m^3/h of gas. Lintong Chemical Fertilizer Institute of the Ministry of Chemical Industry constructed a fluidized-bed water-coal slurry gasification pilot system that could process 36 tons of coal daily. Lunan Fertilizer Plant, Shoudu Steel Works, Xian Fertilizer Plant and Shanghai Coke Plant imported a total of eight Texaco gasification furnaces. Lanzhou Gas Company imported a pressurized fixed bed gasification furnace from Czechoslovakia and began to produce it in Dalian in a joint venture. Shanghai Design Institute of Power Generating Equipment and Accessories completed a study with GE on the use of low thermal value coal gas and a dual fuel regulating system for gas-burning turbines.

Many organizations have conducted feasibility studies on using IGCC for power generation, heating, and chemical production.

China began to work on PFBC-CC early. A comprehensive experimental study was underway at Southeastern University (Nanjing Institute of Engineering) in the early 1980s. In 1984 a 1MW thermal input experimental SEU-PFBC facility was constructed. Laboratory testing of PFBC was completed between 1986 and 1990. A long term evaluation of over 700 hours was conducted. To this end, the State Planning Commission officially listed PFBC-CC as a key national research project in the 8th 5-Year Plan in 1991. It is being conducted by Southeastern University in collaboration with over 20 organizations including Xuzhou Jiaan Power Plant under the jurisdiction of Jiansu Electric Power Bureau, Harbin Boiler Plant, Lanzhou Oil Refining Machinery Factory, Beijing Design Institute of China Petroleum Chemical Corporation, Xian Institute of Thermal Engineering and Petroleum University. A 15MW PFBC-CC pilot plant is being built at the Jia'an power plant. It is scheduled to be tested in 1995 and will serve as a demonstration commercial power plant in the 9th 5-Year Plan.

As for second generation PFBC technology, laboratory research is underway at Southeastern University, Shanghai Design Institute of Power Generator Equipment and Accessories and China Institute of Coal Research.

3. Recommendations on the Development of Various Advanced Power Generating Technologies

In conclusion, China should develop the following advanced clean coal burning technologies:

(1) IGCC Phase I

The maximum net efficiency in this phase of IGCC is approximately 40 percent. The condition is to integrate the separation unit to the gas turbine. The SO_2 scrubbing rate is 98 percent in this stage. NO_x is reduced by 90 percent. The sulfur scrubbed is a by-product as well. The level of investment for this kind of IGCC is at least 10 percent higher than that of a conventional power plant with a sulfur scrubber. Its operating cost will also be 10-20 percent higher. Therefore, the first generation IGCC is attractive purely due to environmental concerns. This is because developed nations further tightened their environmental protection targets. Even so, 40 percent net efficiency commercial IGCC power plants are still being validated. It won't be completed until the end of this century. Whether it can be used on a large scale depends upon further reduction of initial investment and operating cost.

As far as China is concerned, although environmental protection targets will also gradually be tightened, it is impossible to reach the level of developed nations immediately. In reference to the standards set by the U.S., in the 1970s, China won't reach that level by the end of the century, or even by 2010. China does not have the conditions to adopt IGCC technology on a large scale due to the following determining factors.

1) The environmental standards in China are not yet set to such a high level.

2) IGCC requires considerable initial investment, as well as a high operating cost.

3) Combustion power generation plays a key role (60-67 percent) in IGCC technology. Its investment is comprised of the following: coal processing 7 percent, gasification furnace 12-15 percent, heat exchanger 18 percent, wet dust removal equipment 3-5 percent, deacidification equipment 10 percent, power generating equipment (including combustion engine) 40 percent, and oxygen producing plant 12 percent. IGCC involves large gasification furnace, separation equipment and high temperature gas combustion engine. It will take a long time for us to make all the necessary equipment domestically.

4) An IGCC power plant is quite different from a conventional power plant. The former is more like a highly complex chemical plant. It will take some time to promote its use in the electric power industry.

(2) IGCC Phase II

Its unique feature is that its gasification furnace has an even higher thermal efficiency. Air or oxygen-enriched gas is used as the gasification agent. Sulfur and dust are removed from hot coal gas. The inlet temperature of the gas combustion engine is even higher (greater than 1300°C). It is an integration of an advanced coal gasifier and an advanced high temperature gas burning turbine. It will become a reality by 2010. Its net power generating efficiency will reach 45-47 percent. By then, IGCC will be truly attractive and commercially competitive.

To develop IGCC technology in China, it makes more sense to combine chemical production with the supply of heat, electric power, and coal gas. After taking chemical production into account, the initial investment and high production cost associated with coal gasification will no longer be an issue. On the other hand, the requirements for capital investment and production cost for coal gas to generate electric power are very stringent because conventional power plants are very economical. It is very difficult for new technology to compete with it.

(3) First Generation PFBC-CC

As discussed earlier, it will be practical by the end of this century or early next century. Its commercial goal is a 350 MWe power plant. It will be more advanced than the three existing commercial demonstration power plants in three areas: (1) reheated super-critical or sub-critical steam will be employed in the power generators, (2) desulfurization efficiency will reach 95 percent and Ca/S ratio will be further reduced, (3) NO_x removal technology (injecting ammonia into the smoke stack) will be employed to lower the NO_x level in the exhaust. These steps are taken to further improve environmental protection targets, lower initial investment and operating cost, and make it more competitive against conventional power plants.

(4) Second Generation PFBC-CC

It is projected that its commercial validation will be completed by 2005. It will enter the market between 2005 and 2010, approximately the same time frame as the second generation IGCC. This is because they share the same technological problems, i.e., high temperature ceramic filters to remove dust (or other high temperature dust removal technology) and high temperature gas combustion engines.

In view of the situation in China, commercialization of a PFBC-CC power plant may be earlier than an IGCC power plant because the system is relatively simple. It can compete with conventional power plants in the near term as far as initial investment and operating costs are concerned. More importantly, 80 percent of first generation PFBC-CC power plants use steam to generate electricity. In the second generation, more than 60 percent of the plants will use steam as well. It is more closely connected to the boiler and steam turbine industry already in existence. Its characteristics are also similar to those of conventional power plants. It is easier to develop because it is standing on a more solid foundation. As far as environmental protection is concerned, although it is not as good as IGCC, it can meet very stringent discharge standards. SO_2 and NO_x release levels are one-fourth the levels allowed by NSPS. In addition, another important factor is that PFBC-CC can use a wide range of coal. Conventional power plant technology is very mature. It is already very economically competitive. IGCC cannot replace it in the near future. However, it is clearly the right direction for future development.

4. Conclusions

1) IGCC is a major direction of development to achieve clean and highly efficient burning of coal to generate electric power.

2) Due to its superior environmental release targets and potential high efficiency, IGCC is the most attractive novel electric power generation technology. At the present stage, because of high initial investment and operating cost, it is not commercially competitive. It is expected that second generation IGCC will be technologically mature and commercially viable by 2010. In view of this fact, China should conduct research on relevant technology and construct pilot demonstration power plants to prepare for large scale development in the future. As for its current commercial use, it is more appropriate to combine chemical production with power generation (such as the Shanghai Coke Plant) to justify the high initial investment and operating cost.

3) The majority of PFBC-CC electric power generation is done with steam. Its development is closely dependent upon the boiler and steam turbine industry. The power plant operates more like a conventional power plant. It will be commercialized by the end of this century or early next century. The second generation will be even more attractive. We have built a solid base for its basic research. It also has a strong background in terms of hardware research and industrial backing. We should try to build a 100MW commercial validation plant either independently or as a joint venture in the 9th 5-Year Plan. At the same time, we should develop second generation PFBC-CC technology so that it can contribute to the clean burning of coal to generate electric power in China soon.

4) Both IGCC and PFBC-CC are clean coal burning electric power generating technologies. They have their advantages and are complementary to each other, rather than mutually exclusive. This is well recognized among experts worldwide.

5) Both IGCC and PFBC-CC involve the development of high temperature gas combustion turbines. China is very weak in this area. We must address this issue promptly.

References

1. Der, V.K. et al., The Marketing and Commercialization of MHD Power Systems, Proc. of the 11th Int. Conf. on MHD Electrical Power Generation, October 1992.
2. Li Jianye [2661 1696 2814], Status of IGCC Electrical Power Generation Technology, research report published by Shanghai Institute of Electric Power Generation Equipment and Accessories, 1993.
3. Jiao Shujian [3542 2885 2814], Development Trend of IGCC, RANQI LUNJI JISHU [GAS COMBUSTION TURBINE TECHNOLOGY], Vol 1, 1993.
4. Sun Zonghai [1327 1350 3189], Development of IGCC Abroad, MEI HUAGONG [COAL CHEMICAL ENGINEERING], Vol 1, 1993.
5. Jin Donglai [7246 2639 0171], New Development of IGCC Abroad and Some Recommendations, ZHONGGUO DIANLI [ELECTRIC POWER], Vol 3, 1993.
6. Proceedings of the 9th, 10th, 11th, 12th Int. Conf. on Fluidized-Bed Combustion, 1987, 1988, 1991, 1993.
7. He Peiao [0149 0160 2407]. A Novel PFBC-CC , RENENG DONGLI GONGCHENG [THERMAL ENERGY POWER ENGINEERING], Vol 6, 1992.
8. Anderson, J. et al., Principles and Design Philosophy for a 350 MWe PFBC Module, Proc. of the 12th Int. Conf. on FBC, 1993.
9. Pillai, K.K., Kyushu 350 MWe PFBC Sets the Trend in Japan, Modern Power System, April 1992.
10. Fan Congzhen [5400 1783 2182] et al., Experimental Investigation on NIT PFBC Test Facility for High Ash Coal, Proc. of the 9th Int. Conf. on FBC, 1987.

11. Zhang Mingyao et al., 500 Hour Test in Southeastern University's Pressurized Fluidized-Bed Combustion Facility, Proc. of the 11th Int. Conf. on FBC, 1991.

12. Zhang Mingyao et al., Design Concept of Jiawang PFBC-IGCC Test Facility, DONGNAN DAXUE XUEBAO [JOURNAL OF SOUTHEASTERN UNIVERSITY], Vol 5, 1992.

13. Sun W. Chun, Environmental Issues on the Use of Fossil Fuels in the United States, The 5th Int. Energy Conf., 1993.

14. Wheeldon, J.J., et al., Cost and Performance Improvements in Utility-Scale Bubbling PFBC Power Plants, Proc. of the 12th Int. Conf. on FBC, 1993.

15. Smock, R., Pressurized Fluidized-Bed Demonstration Units Operate Successfully, Power Engineering, Vol 97 No 3, 1993.

Foreign Investment Helps Ease Energy Bottleneck in Fujian

94FE0617B Fuzhou FUJIAN RIBAO in Chinese 30 Mar 94 p 6

[Article by Chen Yong [7115 0516]: "Foreign Investment Helps Ease Energy Bottleneck in Fujian"]

[Text] In order to ease the electric power bottleneck which chokes economic growth, Fujian has attracted a total of $800 million in foreign investment in the past few years to raise the total installed capacity in the province in the next seven years to 12 million kW.

To encourage foreign investment, Fujian is offering a number of incentives, including waiver of local income tax for all electric power plants built by foreign investors.

Last year, the Songyu power plant in Xiamen brought in $8.8 million in foreign investment to build the foundation for two generators with a combined capacity of 600,000 kW. An official contract was signed in Xiamen by a Hong Kong investor to invest $400 million to build two generator units at the Meizhou power plant with a combined capacity of 1.6 million kW. Design work has begun outside the country.

Other electric power construction projects under negotiation with foreign investors include the second phase expansion work at the Shaowu thermal power plant, a harbor power plant, three emergency diesel power plants in Xiamen, Jinjiang, and Xiamen, development of the Sanmingshaxi He and Upper Hangjinshan hydropower plant projects.

In the next seven years, Fujian will continue to construct a number of large electric power projects so that by the end of the century we will be able to generate 42 billion kWh of electricity. It is equivalent to 1300 kWh per person per year.

Fujian also plans to offer a number of near- to medium-term large electric power construction projects to foreign companies, including preliminary work at the Shanqian nuclear power plant in Huian, completion of the Shuikou hydropower stations, construction of the Manhuatan hydropower station in Yongding, the Qinshan hydropower station in Zhouning Muyang Xi, and Youxi Jiemian hydropower station, expansion of the Fuzhou power plant of China Energy Corporation and construction of the Zhangpu Gulei hydropower station.

Fujian is encouraging foreign investment in electric power construction so that electricity can be generated as early as possible to benefit the public. A foreign joint venture, stage 2 construction of the Pingtan thermal power plant, is under construction around the clock. The first 100,000-kW unit was brought on line at the end of March. The first-stage construction work for the Xiamen Songyu power plant has also been completed.

Work Begins on Main Portion of Three Gorges

94FE0617C Beijing RENMIN RIBAO OVERSEAS EDITION in Chinese 25 Apr 94 p 1

[Article by correspondent Shi Yongfeng [2457 0516 1496] and Jin Min [6855 2404] of the Xinhua News Agency]

[Text] The construction of a temporary lock begins on the left bank today. To date, three major projects in the main portion of Three Gorges have begun.

This temporary lock is constructed to ensure uninterrupted navigation along the Chang Jiang during the construction of the Three Gorges. The open channel on the right bank and temporary lock on the left bank are being built for navigation after the main waterway is cut off in 1997. During the wet season, the flow is greater than 25,000 cubic meters per second. When the open channel is not suited for navigation, the temporary lock will be the only means to ensure uninterrupted navigation on the Chang Jiang. This temporary lock is a class 1 single-lane lock. It can handle a 3000-ton vessel. The lock has a class-1 vessel lifting mechanism which can handle 3,500,000 tons each year in one direction. This is a highly complex project that involves difficult excavation on land and under water. It requires a maximum underwater excavation depth of 24 meters.

According to reports, two other major Three Gorges projects, the permanent lock and phase-1 construction of the powerhouse, broke ground on the 17th and 18th, respectively.

The navigation model experiment for the Three Gorges has been completed and a great deal of data was obtained. The Three Gorges Office of the State Council and the Ministry of Transportation held a meeting in Chongqing to discuss the navigation model experiments for the Three Gorges.

Power Network

Inner Mongolia—Hebei Transmission Line

946B0077B Hohhot NEIMENGGU RIBAO in Chinese 23 Feb 94 p 1

[Article by Wang Sheng [3769 3932]]

[Text] The 500,000-volt ultrahigh voltage transmission line from Fengzheng, Inner Mongolia, to Shalingze, Hebei, was completed last December. This transmission line was jointly built by the Shanxi Electric Installation Company, and the Inner Mongolia and Hebei Transmission/Transformer Installation Company.

This transmission line is the first ultrahigh voltage transmission line in the Neimenggu Autonomous Region and Ulanqab league. The total length is 180 kilometers and the installation was supervised by the Ulanqab power transmission engineering zone. Construction began in May 1993 and workers had to overcome a number of difficulties caused by complex geological conditions. Under difficult construction conditions, construction crews adhered to the schedule. The engineering quality was rated as superior in a joint quality evaluation.

This project is a major avenue for delivering power to Beijing.

Hydropower

700MW Generators for Three Gorges

946B0106A Chengdu SICHUAN RIBAO in Chinese 22 Apr 94 p 1

[Article by Xiang Datian [0686 1129 3944]: "A New Chapter in Hydropower History, Eastern Electric Motor Company Invests in Three Gorges Generators"]

[Text] Eastern Electric Motor Company obtained approval from the State Planning Commission to modify and expand the water turbine generators for the Three Gorges.

A total of 26 generators are scheduled to be installed at the Three Gorges. Each generator has a rated capacity of 700MW. The Three Gorges ranks number one in the world in terms of individual capacity as well as total capacity. A number of hydropower equipment manufacturers in the U.S., Japan, and France believe that the design and manufacture of the Three Gorges generators will mark a new milestone in the history of hydropower worldwide. Because of the size and weight requirements, all manufacturers must modify their manufacturing technology before they can build those generators for the Three Gorges.

Eastern Electric Motor Company is a major electric power generating equipment manufacturer in China. It produces 40 percent of the hydroelectric power generators manufactured domestically. Due to lack of capital to undergo technological upgrade, the company can only produce 600MW of hydroelectric generators per year which is not adequate to meet the demand of the Three Gorges. After expanding its capacity and improving its technology, Eastern Electric Motor can produce up to 2,000MW of hydroelectric generators annually, including two generator units for the Three Gorges. The State Planning Commission approved an investment of 670 million yuan for this expansion and technological upgrade project at Eastern Electric Motor Company.

In addition, Harbin Electric Motor Company and Tianjin Electric Generator Equipment Plant have also been given the go-ahead to expand and upgrade their facilities.

Prospects for Hydropower Development in Sichuan

946B0106C Chengdu SICHUAN RIBAO in Chinese 12 May 94 p 1

[Article by Cao Hong [2580 5725] and Xiong Dabin [3574 1129 2430]]

[Text] Sichuan has an enviable treasure. It has a reserve of 150 million kW of hydropower resources, or 5.3 percent of the hydropower reserve in the world and 26.8 percent of that in China. The amount of hydropower resource that can be developed is approximately 100 million kW, which is 24.2 percent of the total nationwide. It ranks number one in China.

Nevertheless, the fact is that while the rivers surge toward the east, only coal and oil are going in that direction. Only 6 percent of the hydropower resource in Sichuan is developed. Since the draught of 1970, electric power has been in short supply in Sichuan. The shortfall is as high as one-third of the total demand over this long period of time. This also ranks number one in the nation.

There is a strong contrast between the abundance in resources and shortage in electric power. The challenge we are facing is to take advantage of Sichuan's rich hydropower resources to solve its power shortage problem for good.

In 1986, after a survey of the Lancang Jiang in Yunnan and the Wu Jiang in Guizhou, over 60 experts were invited by the provincial government of Sichuan to survey the three rivers in Sichuan (the Jinsha Jiang, Yalong Jiang, and Dadu He). At the end of the tour, they wrote a report to the Central Government and the State Council to recommend the construction of a hydropower base in the southwest. They believe that the Jinsha Jiang may become the largest hydropower base in China, or even in the world, and that Sichuan is a potential "hydropower kingdom."

Most rivers in Sichuan have sufficient and steady flow. The rivers have large, but concentrated, drops, particularly the three rivers mentioned above. They have natural drops of over 2,000 to 3,000 meters. There are more than 1,400 rivers and streams in the province and a variety of hydropower stations can be constructed on these rivers across the province. Based on estimates, the amount of farmland flooded and number of people

displaced to generate 100 million kilowatt-hours of power annually in Sichuan are 34 percent and 35 percent of the national averages, respectively. Today, proposed sites of major hydropower plants are accessible either by highway or railroad. The distance of power transmission to load centers such as Chengdu and Chongqing ranges from 200 to 600 kilometers. If electricity needs to be delivered to central China, then it must travel 1,000 kilometers. Sichuan has the necessary conditions to develop hydropower.

From Sichuan's energy resource structure, 75.2 percent is in hydropower and 19 percent in coal. However, from the present production structure, 10.6 percent of the energy comes from hydropower and 75 percent from coal. Sichuan does not have much coal, it has 1.2 percent of the coal reserves in China. However, its coal production ranks number four in the country. Even so, the shortfall will continue to increase. By 2000, Sichuan will be short 25 million tons of coal. If coal must be shipped into Sichuan, the railroads won't be able to handle it.

In reality, hydropower is the answer for Sichuan. Economic development and realignment of primary energy resources nationwide also give us the opportunity to develop hydropower. However, the government also changed the way construction capital for hydropower is handled. Instead of direct government funding, it is loaned. Power stations are being built with capital raised from a variety of sources. Sichuan does not have the funds to do it by itself because it faces the challenge of a market economy.

In search for a way to develop hydropower, let us take a look at our neighbor, Yunnan. Yunnan has 90,000MW of hydropower resources developed. It ranks number two in China behind Sichuan. Less than 5 percent of it has been developed. Due to its limited financial resources, it is unlikely that Yunnan can develop any large-scale hydropower projects on its own. They accepted the recommendation of certain experts to use capital from the southeast coast to develop energy-related projects and to stimulate the economy in the southwest. In return, the energy produced in the southwest is going to be used to support economic growth in the southeast. Thus, inland and coastal areas mutually support each other to keep the economy growing. Yunnan took advantage of this opportunity and produced phenomenal results. In 1988, Yunnan provided incentives to attract Guangdong Province to invest in a joint venture to construct an 800,000 kW thermal electric power plant at Qujing. In 1992, Yunnan reached an agreement with Guangdong, the Ministry of Energy, and the National Energy Investment Corporation to construct the 4.2 million kW Xiaowan hydropower station. Yunnan provided 10 percent of the capital. Since 1993, Yunnan has delivered 900,000,000 kWh of electricity to Guangdong on a seasonal basis during the rainy season. Yunnan's goal is to turn the electric power industry into its second major industry, next to the tobacco industry.

Using external capital to develop its natural resources is an effective way for an under developed country or region to stimulate its economy.

The encouraging sign is that Sichuan has prepared a comprehensive hydropower development plan after repeated validation and modification. The provincial government issued a policy which requires us to focus on hydropower and limit thermal electric power as an ancillary source. The development of hydropower needs to be accelerated to raise the proportion of hydropower in the primary energy structure. As for the sites of hydropower stations, not only must we accelerate the construction of stations at Ertan, Baozhushi, Tongjiezi and Taipingyi and the cascades of the Baoxing He, we also have to speed up the early stage work at Tongzilin and the Nanya He cascade stations. In addition, we must actively pursue the construction of a number of large hydropower stations such as Pubugou to start at the end of the 8th or the beginning of the 9th 5-Year Plan.

In accelerating the pace of hydropower development in Sichuan, we face considerable difficulties. The major issue is a shortage of capital. Searching for capital and market is an approach under consideration. For example, Sichuan is seeking the joint development of the Jinsha Jiang with Yunnan and provinces in eastern and central China in order to realize the dream of delivering electric power generated in the west to areas in the east.

In terms of the mechanism for hydropower development, corporations will be set up along different river basins to develop a series of hydropower stations. Each corporation is owned by shareholders and operates as a business. The profit from the first power plant will be used to build the next one. This rolling over mechanism will speed up the pace of hydropower development.

We should try to have the comprehensive Sichuan hydropower development plan included in the national energy plan up to the year 2020 and also try to win preferential treatment by the government. Because the up-front preparation work is time consuming, there should be a higher budget for it to change the present situation which is not well prepared. People should also be relocated ahead of schedule.

Let us take this opportunity to develop our hydropower resource and convert this resource into products.

We are confident we can succeed.

Tianhuangping: 'Regulator' for East China Power Grid

946B0113B Hangzhou ZHEJIANG RIBAO in Chinese 1 Jun 94 p 7

[Article by Tang Huiching [0781 1979 0615] and Zhang Kecheng [1728 0344 6134]]

[Excerpts] In March of last year, a team of construction workers arrived at Tianhuangping, a hilly region in western Zhejiang Province, to begin construction of the Tianhuangping pumped-storage power station.

The Tianhuangping pumped-storage power station is located in the mid-section of the Tianmushan region in Anji County, near the center of the East China Power Grid. The key segments of the station include the upper and lower reservoirs, the water transportation system and the powerhouse. During the period of low demand such as at night, residual electricity is used to pump water from the lower reservoir to the upper reservoir, thereby "storing" the electrical energy in the form of potential energy. Then, during the daytime peak demand period, water from the upper reservoir is returned to the lower reservoir via the turbine generator, thereby converting potential energy back to electrical energy. The operation continues in this manner as this cycle is repeated indefinitely. The ratio between the amount of electricity used for pumping the water and the amount of electricity generated per year is 4:3. [Passage omitted]

It is estimated that by the year 2000, the peak load of the East China Grid will grow to 35.36 million kW; as the load increases, the differences between peaks and valleys are also expected to increase

A majority of the power facilities in the East China Grid have coal-fired generators which cannot be regulated easily to accommodate the rapid and frequent load variations.

To satisfy the need for regulating the load during periods of peaks and valleys and keeping the East China Grid operating efficiently, it is essential to construct a large pumped-storage power station for this region. [Passage omitted]

The Tianhuangping power station has six generators, each with a capacity of 300,000 kW, thus producing a total power generation capacity of 1.8 million kW; its maximum water head is 607.5 m. It is China's largest and highest-water-head pumped-storage power station. It is also rated one of the world's most advanced power stations in terms of the height of water head and power generation capacity.

The upper reservoir of the station is constructed by building a dam over the natural terrain of the Tianhuangping basin; the maximum capacity of the reservoir is 8.85 million cubic meters. The lower reservoir is constructed in the mid-section of the Dachi river at the foot of the Tianhuangping mountains, its maximum capacity is 10.08 million cubic meters. An equal portion of the two reservoirs is allocated for emergency power generation. Because the reservoirs occupy a relatively small area and there are no villages in the immediate vicinity, construction of the station will only cause minor flood loss, and no residents need to be relocated. The entire project is expected to take six and a half years.

Once completed, the Tianhuangping pumped-storage power station can supply 1.8 million kW of power to the East China Grid during the peak-demand period and can absorb 1.92 million kW of unused electricity during nighttime. In other words, it acts like a regulator that can improve the efficiency of electricity utilization for industries, agriculture and consumers located within the East China Grid.

Hydropower Development in Northwest Hubei

946B0131A Beijing RENMIN RIBAO OVERSEAS EDITION in Chinese 6 Jul 94 p 2

[Article by Yuan Zhenghong [5913 2973 3163] and Huang Xing [7806 5281]]

[Text] Three hundred and fifty-eight small and medium hydropower stations with a total of over 500 generator units and 1.10 million kW in installed capacity have been built by the Ministry of Water Resources, the Hubei Province and Yuanyang along the Han Jiang in places such as Yuanyang and Shiyan from Danjiangkuo to Baihe County in Shaanxi in northwest Hubei. They are capable of producing more than 5 billion kWh of electricity annually and are already connected to the central China power grid.

The development of hydropower in northwest Hubei helps stimulate production in areas covered by the central China power grid such as Henan, Jiangxi, Hubei, and Hunan. It also brings significant economic and social benefits to the middle and lower reaches of the Han Jiang in terms of flood control, irrigation, navigation and fish farming. According to our statistics, the GNP and tax revenue for the Yuanyang and Shiyan area in the Han Jiang basin in northwest Hubei are 17 billion and 600 million yuan, respectively. Compared to 1978, they correspond to an increase of 17.5 and 7 times.

The Han Jiang originates from the southern foot of the Qinling Mountains in Shaanxi. Over 6 million kW of water resources are available from its mainstream and tributaries. In the past, due to problems associated with transportation, technology, and lack of information, the water resources of the Han Jiang could not be developed and Yuanyang was a key poverty-stricken area. Recently, another 50,000 kW power station was built by the Danjiangkou Water Resources Hub Engineering Management Bureau using profits from earlier hydropower projects to tap the water resources of the mainstream of the Han Jiang.

Yuanyang is located in the remote northwest corner of Hubei. Over the years, Hubei and the water resources authority have handled hydropower development on the Han Jiang as a key industry. It has been developed in stages. A multi-faceted approach was used to raise capital from the government, different entities, individuals and businesses in a variety of forms to develop hydropower in the region. One hundred and forty-two towns and 90 percent of the villages and 85 percent of the rural residents now have electricity.

Xizang To Have 1 Million Kilowatts in Installed Capacity by End of Century

946B0131B Beijing RENMIN RIBAO OVERSEAS EDITION in Chinese 27 Jun 94 p 1

[Article by Zhang Dan [1728 0030] and Duo Qiuong [1122 4522], Xinhua News Agency]

[Text] According to authorities, Xizang will focus future development of its electric power industry on hydropower. Key hydropower stations will be constructed to expand its total installed capacity by 4- to 5-fold to close to 1 million kW by the end of this century.

The key project now under construction in Xizang is the Yamzho Yumco Lake pumped-storage power plant. After this 90,000 kW station is completed, the total installed capacity in Xizang will increase by 50 percent. Its first 25,000 kW unit will begin to generate electricity by the end of next year.

Another key hydropower station now under construction in northern Xizang is the 10,800 kW Chalong station in Naqu. It will begin to generate power next year.

In addition, we have the design of a series of stations, including the 16,000 kW Manla station in Rikazhe, the 20,000 kW Woka first-stage station in Shannan, and the 100,000 kW Zhikong station on the upper reaches of the Lhasa He.

Geothermal resources are abundant in Xizang. More than 600 geothermal sites are known to date, estimated to be able to accommodate approximately 800,000 kW of installed capacity. The 25,000 kW Yangbajain geothermal power plant near Lhasa is Xizang's largest power plant. Geologists are exploiting a 2,600-meter-deep geothermal layer in the Yangbajain area. Plans are to build a 50,000 kW geothermal in that area.

Pubugou: Another Massive Station on the Dadu River

94P60331 Chengdu SICHUAN RIBAO in Chinese 5 Jul 94 p 1

[Text] On 25 June, the preliminary plan for the Pubugou hydroelectric power station (total installed capacity: 3.3 million kilowatts) passed examination in Chengdu. The Pubugou hydropower station is located on the Dadu He above the already-constructed Tongjiezi and Gongzui hydropower stations. It will be Sichuan's next exceptionally large hydropower station following the Ertan project. Pubukou's reservoir will have a capacity of 5.177 billion cubic meters for a seasonal regulation capability. With a maximum height of 186 meters, its dam will be of the earth and rock fill variety. The below-ground powerhouse will be 290 meters long with a maximum excavation width of 32 meters and a height of nearly 69 meters. Because Pubugou has such a large reservoir capacity and good regulatory capability, it will greatly enhance the power-generating potential of the Gongzui and Tongjiezi hydropower stations. Although Pubukou is the same size as Ertan, its comprehensive benefits will surpass those of Ertan.

Thermal Power

Haibowan Power Plant Goes Into Commercial Operation

946B0077C Hohhot NEIMENGGU RIBAO in Chinese 23 Feb 94 p 1

[Article by Li Kexin [2621 0344 0207]]

[Text] On 28 February, the 100,000-kW No. 1 generator of the Haibowan Power Plant was officially put into commercial operation. Haibowan is the first stockholder-owned power plant in China's electric power system. The generator operated smoothly at peak output; all technical and economic performances have reached the highest level among generators of the same type.

Work began on the two 100,000-kW generators of the phase I construction at Haibowan on 24 April 1993. The No. 1 generator was completed four months ahead of schedule.

U.S.-China Joint Investment in Shanxi Power Plant

946B0077D Taiyuan SHANXI RIBAO in Chinese 13 Apr 94 p 1

[Article by Du Jucai [2629 1565 2088]]

[Text] With its two 50,000-kW generators completed ahead of schedule and in operation in the phase I construction project, the Hepo Power Plant in Shanxi recently broke ground for the construction of its phase II project of two 100,000-kW generators. The company is a U.S.-China joint venture with an investment of $110 million.

The U.S.-China joint-investment, Hepo Power Company, will be run independently. When the plant reaches a capacity of 300,000 kW, more than two-thirds of the electric power output will be delivered to Hebei Province via transmission lines put up by the company itself. This practice reduces intermediate steps and has been very beneficial for the economic system reform in the electric power industry.

Sichuan Develops First 330MW Generator Simulation System

946B0106B Chengdu SICHUAN RIBAO in Chinese 27 Apr 94 p 3

[Article by Xiao Su [1420 5685]: "Sichuan Develops First 330MW Generator Simulation System"]

[Text] A 330MW thermal electric power generator simulator has been developed by Sichuan Electric Industry Bureau and Asia Simulation Control System Engineering

Limited (Zhuhai). It passed a technical appraisal organized by Sichuan Science and Technology Committee in Chengdu on 10-13 April 1994.

Simulation is a rapidly advancing high technology developed in the past two decades. This comprehensive thermal electric power generator simulator is an extremely complex system engineering unit which integrates a number of high technologies, including simulation, computer, electronics, electrical engineering, thermal engineering, panel and instrumentation and modern multi media technology. It is used primarily for personnel training and scientific research for a large-scale thermal electric power generation plant. The Sichuan 330MW thermal electric power generator simulator is the first simulator developed independently in China by way of duplicating an imported thermal electric power generator simulator. It is also the largest thermal electric power generator simulator ever developed and placed in operation.

Ningxia Sets Record for Newly Installed Capacity

946B0084B Beijing RENMIN RIBAO OVERSEAS EDITION in Chinese 2 May 94 p 2

[Article by correspondent Sun Bo [1327 3134]]

[Text] In pursuit of the strategy of converting coal to electric power in the coal-rich Ningxia Hui Autonomous Region, the installation of new capacity reached its highest level in history last year, and the northwest was out front in extending rural electrification to village after village, raising per-capita utilization of electricity to 1,450 kWh, twice the national average, taking fourth place in the country. More new power plant projects will be underway soon, giving testimony to the vigor of electric power construction and development in Ningxia.

Ningxia has the resources needed for electric power development; coal, water, and open space, and coal and hydropower will be the mainstay industries for Ningxia's development. By the end of 1993, the total installed capacity for the region reached 1,714MW, and electric power output for the year reached 8.61 billion kWh.

Coal

Guizhou Set for Large-Scale Exploitation of Coal Resources

946B0084A Beijing RENMIN RIBAO OVERSEAS EDITION in Chinese 28 Apr 94 p 2

[Article by reporter Chen Zhiqiang [7115 1807 1730]]

[Text] Guizhou Province is working with the State to draw up a plan for a large-scale development of Guizhou's coal resources, and it is hoped that foreign interests will join in the development and construction, which includes thermal power plants and coal-chemistry projects.

Guizhou has more coal than the other provinces south of the Chang Jiang, including Guangdong, Fujian, and Jiangsu, and places fifth in the whole country. Since the early 1960s, China has spent 3.2 billion yuan to open up Guizhou coal resources, and has built a number of modern mine shafts. Last year, Guizhou produced over 45 million tons of coal, placing it ninth in the country.

Experts believe that a large-scale development of Guizhou's coal resources is the stratagem for adjusting the development of China's energy industry. At present, China's coal comes mainly from the north. China produced 1.14 billion tons of coal in 1993, only 300 million tons of which came from the south. That means China has to ship coal by rail, highways and canals from the north to guarantee needed energy for the burgeoning southeast coastal economy. "Shipping northern coal southward" increases the strain on China's already limited transportation capability, and many southern factories are often hindered in their production because of late coal shipments.

Experts note that Guizhou's neighbors, Guangdong, Guangxi, and Sichuan have serious coal shortages; for example, the two provinces of Guangdong and Guangxi run 100 million tons short of their needs in a year. Large-scale development of Guizhou's coal resources will relieve the transportation burden of "shipping northern coal southward," and Guizhou can provide the energy support that the south needs.

This year and next, Guizhou will be putting into operation a succession of key expansion and new-construction coal projects, and drawing up plans for a series of large-scale mines. In conjunction with that will be the construction of large-scale pit-mouth power plants and coal-chemistry projects to convert coal into electric power and to achieve a comprehensive development and utilization of coal. The early-stage preparations for an 800-million yuan casting coke project that will have an annual output of 400,000 tons, and an 80,000-ton methanol project have been completed, and plans are in the works for the 500MW Lamangzhai power plant and the 400MW Xiangshui power plant.

Guizhou plans to have a 60-million-ton coal-production capability by the year 2000, and over 100 million tons by 2020.

Authorities believe a rapid development of the transportation industry will be the springboard for development of Guizhou's coal resources, and in recent years huge national investments have been put into improving transportation conditions in Guizhou by totally electrifying the three railroad trunklines stretching from Guiyang into Yunnan, Sichuan, and Hunan, and upgrading the Guizhou to Guangxi line, which will rapidly increase the transport capability of Guizhou rail lines from the original 30 million tons up to 80 million tons. Work has also begun on the Nan (Ning) to Kun (Ming) rail line, which will lift the shipping capacity up to 40 million tons. The multi-track electrified rail line

that will reach from Zhuzhou, Hunan to Lupanshui, Guizhou, known as the "great western corridor," is in the initial stages of planning, and when that is completed the rail line carrying capacity will be up to 50 million tons.

Underground Gasification: 'Second Generation' Coal Mining Method

946B0101A Beijing ZHONGGUO KEXUE RAO [CHINESE SCIENCE NEWS] in Chinese 9 May 94 p 1

[Article by Gu Derun [6253 1795 3387] and Wang Jien [3769 4949 1869]]

[Text] A key national 8th 5-Year Plan project, an underground gasification pilot plant at the Xinhe Mine in Xuzhou, has been successfully put into operation. It is now steadily producing coal gas.

Underground gasification is a novel mining method that replaces traditional physical mining with chemical mining. Underground coal is converted to combustible gases in-situ. This is called a "second generation" mining method. Underground coal gasification has a bright future in China and this technology can be used to recover coal resources from abandoned mines. On the one hand, it is possible to turn an abandoned mine into a business that produces coal, electricity, and raw chemical materials. On the other hand, this technology can be used to exploit coal reserves that cannot be mined using conventional methods such as in thin layers or in complex geological environments. It also creates a way to exploit deep coal reserves in China.

Underground coal gasification technology has improved steadily and is attracting a great deal of attention. It has been employed in the field for years. However, conventional underground gasification technology has two unresolved issues: low thermal value and low gas production capacity. Hence, it is difficult to commercialize it. Professor Yu Li [0151 0500] of the China Mining University began to study this problem in 1984. On the basis of a review of the experience gathered worldwide, and specifically in reference to the fact that there are a large number of abandoned mines in China, a novel large cross-section, two-step gasification technique was developed. This creates a new way to commercialize underground coal gasification.

He successfully directed an on-site experiment at Mazhuang in 1987. In 1990, he began a pilot plant at Xinhe 2 which is a key 8th 5-Year Plan project. Our famous scientist Qian Xuesen [6929 1331 2773] is very interested in underground gasification and wrote Professor Yu several times to offer encouragement.

This plant experiment began on 23 March and will last 100 days. The maximum coal gas production rate per hour is 10,000 cubic meters and each cubic meter of gas contains approximately 1,500 kcal.

China's Coalbed Methane Resources and Their Exploitation

94FE0621 Beijing ZHONGGUO DIZHI [CHINA GEOLOGY] in Chinese No 4, 13 Apr 94 pp 15-18

[Article by Li Yuwei [2621 3768 0251] of the Ministry of Geology and Mineral Resources Petroleum Geology Institute]

[Text] For a long time, the methane in China's coal beds has been viewed as a dangerous material in underground coal mining, whereas by the 1980s in the United States coal bed methane had become an important energy resource that was placed into industrial development. Coal bed methane is a clean, convenient, and highly efficient energy resource. It is different from conventional natural gas in the areas of exploration and development and it is characterized by small investments and a high success rate. China has abundant coal resources and huge potential coal bed methane resources. This is an important realm for future energy resource development.

I. Coal Distribution Situation

Regarding the planar distribution of coal, China can be divided into three coal deposit zones—north, central, and south—on the basis of variations in the abundance of coal resources (the amount of coal resources available per square kilometer) and the geodesic structural position of coal-bearing basins.

1) North China relatively abundant coal deposit zone: This is located to the north of Yin Shan and includes the three provinces of Heilongjiang, Jilin, and Liaoning as well as eastern Inner Mongolia. This zone contains about 8 percent of China's total coal resources. It has a coal-bearing abundance of 5 to 10 million tons/square kilometer.

2) Central China abundant coal deposit zone: This is bordered on the north by Altay-Yin Shan and on the south by Kunlun Shan-Qinling, and is China's most abundant coal-bearing region with 86 percent of China's coal resources and a coal-bearing abundance of 5 to 10 million tons/square kilometer and as much as 50 million tons/square kilometer in local regions.

3) South China poor coal deposit zone: This zone is located south of a line from Kunlun Shan to Qinling and covers about one-half of China's total area, but it has relatively few coal resources, with only about 6 percent of China's total coal, and a coal-bearing reserve abundance generally from 500,000 to 1 million tons/square kilometer.

The North China relatively abundant coal deposit zone is also called the Northeast China-Inner Mongolia coal deposit region. The Central China abundant coal deposit zone is divided by Helan Shan into the Northwest China coal deposit region and the North China coal deposit region. The South China poor coal deposit zone is

divided by Longmen Shan-Daxue Shan into the South China coal deposit region and the Yunnan-Tibet coal deposit region.

Regarding the various geological periods in which coal resources were formed, there are 1) the early Carboniferous Cishui group and late Carboniferous Taiyuan group; 2) the early Permian Shanxi group and lower Shihezi group, and late Permian upper Shihezi group and Longtan group; 3) the early and middle Jurassic and late Jurassic-early Cretaceous coal system. The total coal reserves in these three periods account for 96.40 percent of China's proven reserves, whereas the reserves in all other coal accumulation periods are limited and only account for 3.60 percent of China's total (Figure 1).

China's largest amount of reserves are slightly metamorphosed coal, followed by highly metamorphosed coal, with relatively little moderately metamorphosed coal (meaning rich coal, coking coal, and lean coal). Rich coal accounts for 5.07 percent of projected reserves, coking coal for 2.89 percent, and lean coal for just 2.72 percent. These three types of coal account for 10.68 percent of total projected reserves. These three types of coal developed primary cleats and have excellent permeability, which are appropriate for extracting coal bed methane. This is one of the most important conditions for selecting regions for coal bed methane extraction.

The temporal and spatial distribution of China's different coal varieties have the following characteristics. In terms of periods, moderately and highly metamorphosed coal accounts for the largest proportion of the late Paleozoic and no brown coal has been discovered. While there is brown coal in the Mesozoic, it is slightly and moderately metamorphosed bituminous coal with highly metamorphosed bituminous coal and anthracite. The Tertiary has brown coal as well as slightly metamorphosed bituminous coal. In terms of regions, the area north of 38 degrees north latitude, including the Northeast China region and much of the Northwest China region, is brown coal and slightly and moderately metamorphosed bituminous. The North China region south of 38 degrees north latitude generated bituminous coal and anthracite with all degrees of metamorphism. Southwest China is mainly a region with reserves of moderately and highly metamorphosed bituminous coal, whereas Southeast China is predominantly highly metamorphosed bituminous coal and anthracite.

Statistical information on eruptive gas wells, among all of China's mines, show that the regional characteristics of the distribution of eruptive gas (methane) in China's mines is exactly the opposite of the distribution of coal resources. The South China and Northeast China regions are China's South China poor coal zone and North China relatively abundant coal zone, which have few coal resources but a high proportion of eruptive gas wells. In contrast, the North China and Northwest China regions are China's Central abundant coal zone development region with extremely abundant coal resources, but they have a very small proportion of highly eruptive gas mines (Figure 2).

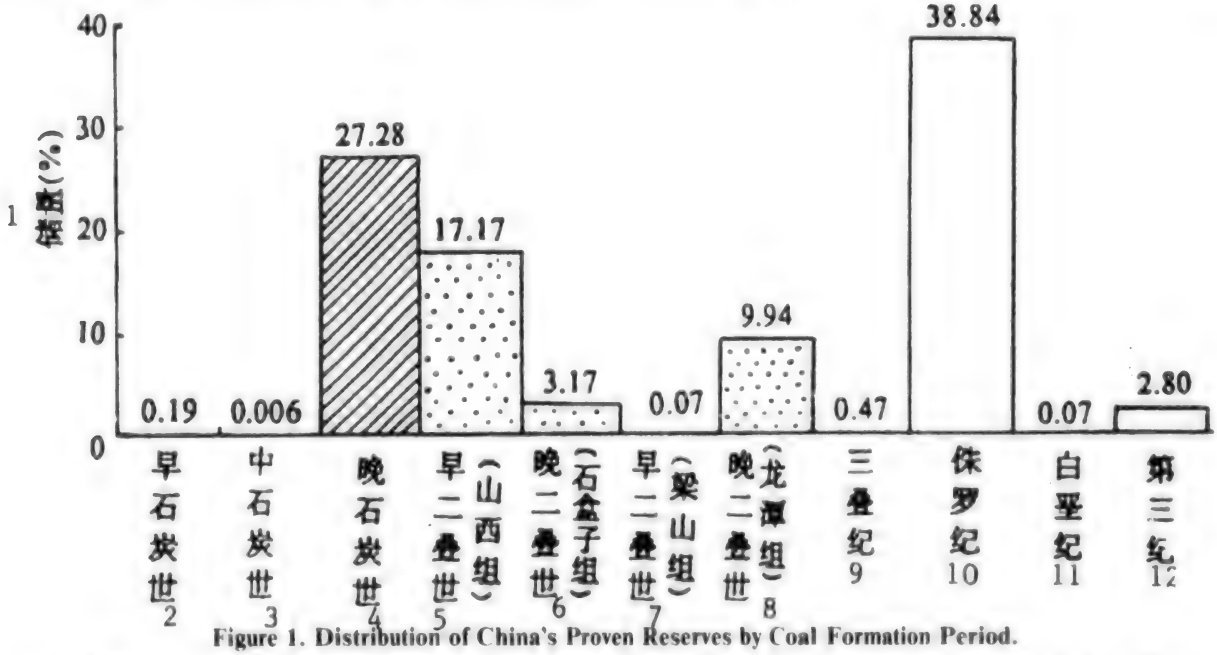

Figure 1. Distribution of China's Proven Reserves by Coal Formation Period.

Key: 1. Reserves (percent); 2. Early Carboniferous; 3. Middle Carboniferous; 4. Late Carboniferous; 5. Early Permian (Shanxi group); 6. Late Permian (Shihezi group); 7. Early Permian (Liangshan group); 8. Late Permian (Longtan group); 9. Triassic; 10. Jurassic; 11. Cretaceous; 12. Tertiary.

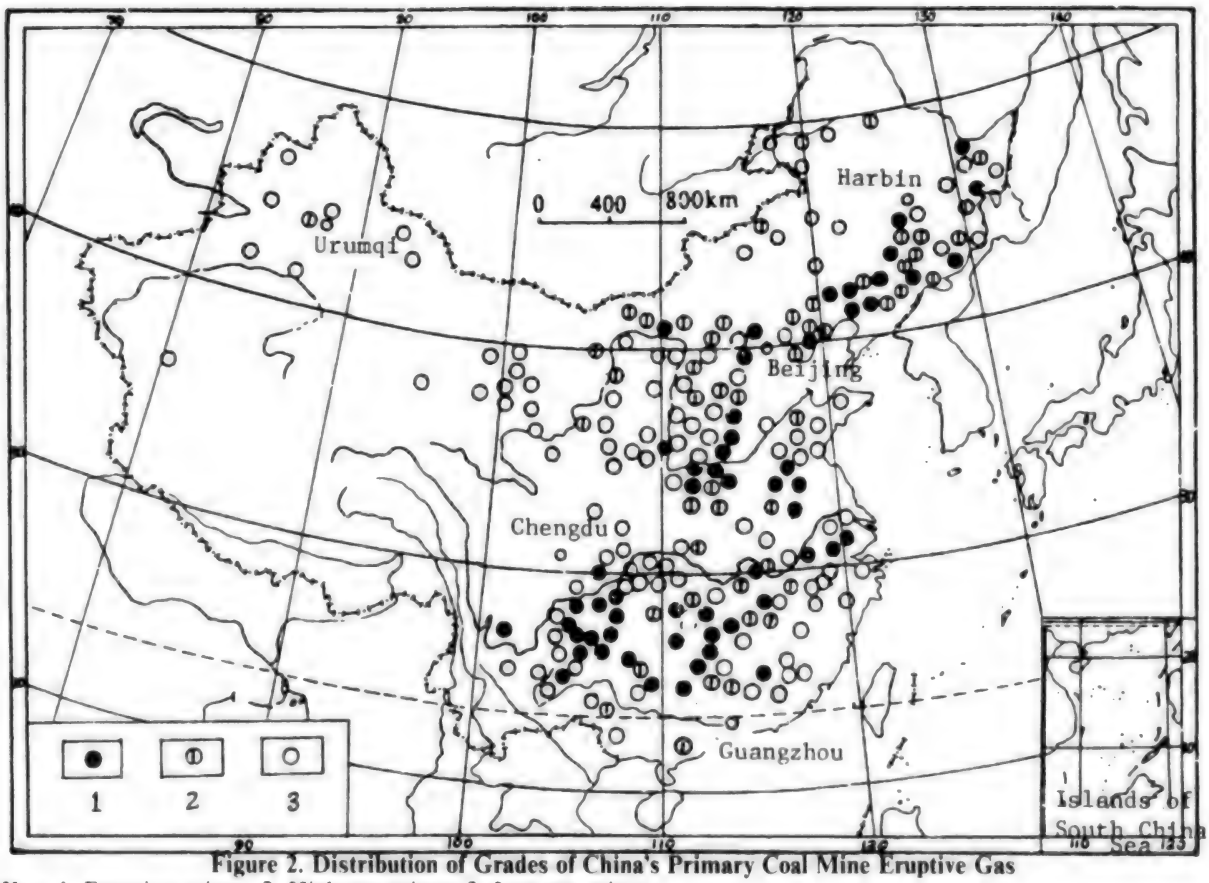

Figure 2. Distribution of Grades of China's Primary Coal Mine Eruptive Gas

Key: 1. Eruptive mines; 2. High gas mines; 3. Low gas mines

In summary, the temporal and spatial evolution of China's coal accumulation forces, the distribution of coal resources, and the distribution of coal metamorphism zones basically determine the fundamental configuration of China's coal bed methane resources and have a major impact on coal bed methane resource evaluation, prospecting and development deployments, and so on.

II. China's Projected Coal Bed Methane Resources

Using research done in a project to attack key state S&T problems during the Seventh 5-Year Plan by the Xi'an Branch Academy of the Central Coal Science Research Academy, the Monte Carlo simulation method was used for computations and a single coal system stratum in coal-bearing region was used as the basic computation element. Within the basic computation element, coal bed methane resource grades (divided into projected reserves and long-term projected reserves) and coal seam burial depths (divided into 1,000 meters and shallower, 1,000 to 1,500 meters, and 1,500 to 2,000 meters) are used as a basis for the demarcation of computation blocks.

The results of the computations show that the maximum value (with a 5 percent probability) for China's total coal bed methane resources are 25.24 trillion m^3 and the minimum value (with a 95 percent probability) is 10.6 trillion m^3. The representative value (the middle value with a probability of 50 percent) is 17.06 trillion m^3. Table 1 lists the coal bed methane reserves for each large coal deposit region.

Table 1. Brief Table of China's Coal Bed Methane Resource Distribution

Coal Deposit Region			Northeast China Coal Deposit Region	North China Coal Deposit Region	Northwest China Coal Deposit Region	South China Coal Deposit Region	National Total	Proportion of Each Resource By Grades
Proportion accounted for by each coal deposit region			1.6 percent	55.3 percent	33.6 percent	9.5 percent		
Coal Bed Methane Resources ($billion m^3$)	Projected	5 percent	101.195	851.685	199.176	508.146	1,660.204	4.2 percent
		50 percent	41.800	412.968	70.738	192.843	718.349	
		95 percent	21.934	146.962	9.952	63.213	242.061	
	Long-term Prospective	5 percent	282.826	11,078.812	1,085.704	2,192.922	23,639.64	95.7 percent
		50 percent	226.306	8,636.451	5,511.115	1,367.454	15,741.326	
		95 percent	193.429	6,073.477	3,186.751	904.792	10,358.449	
	Total Reserves	5 percent	394.129	11,929.897	10,218.991	2,701.070	25,244.087	
		50 percent	272.760	9,049.419	6,181.853	1,564.594	17,068.626	
		95 percent	218.336	6,220.439	3,196.709	967.985	10,603.463	
	Above 1,000 meters	50 percent	321.204	3,886.497	3,237.105	724.904	8,169.710	47.9 percent

III. Demarcation of Regions With Rich Coal Bed Methane Accumulations

The results of my computations for coal bed methane from the Xi'an Coal Science Academy and China Mining University allowed me to do a rough demarcation of regions with rich deposits of coal bed methane in China. I mainly took into consideration these factors: 1) The methane content of coal seams (usually from 8 to 15 m^3/ton of coal); 2) The category of the coal (because of the development of internal cleats in rich coal, coking coal, and lean coal, the permeability was no less than 1 md); 3) Total coal bed methane resources. Moreover, I gave consideration as appropriate to economic and geographic factors (such as proximity to cities, gentle topography, and convenience of construction).

Summarizing and analyzing the factors above, the regions that were determined to have rich deposits of coal bed methane are given in Table 2. While the Northwest China coal deposit region is extremely rich in coal bed methane resources and the total amount of resources and the amount of resources per unit of area are relatively high in the Junggar coal-bearing region, Turpan-Hami coal-bearing region, and Yili coal-bearing region, taking into consideration that the quality of their coal is low-grade bituminous coal and their economic and geographic factors, they temporarily will not be listed as regions with accumulations of coal bed methane.

Table 2. Regions of China with Rich Deposits of Coal Bed Methane

Coal-Bearing Region	Period	Coal Categories	Methane Content (m^3/ton)	Total Resources (billion m^3)	Resources Per Unit Area (million m^3)
Eastern Ordos coal-bearing region	C-P	Gas coal, rich coal, coking coal, lean coal	5.60 - 14.35	3,057.983	76.27
San Jiang-Muling He coal-bearing region	(J_3),E	Gas coal, coking coal	5.00 - 19.62	225.402	16.25
Liupan Shui coal-bearing region	E,T_3,(P_2)	Everything from gas coal to anthracite	2.00 - 26.19	782.384	80.67
Eastern foot of Taihang Shan coal-bearing region	C-P	Rich coal, coking coal, lean coal, poor coal, anthracite	4.39 - 40.28	126.374	43.64
Western Henan coal-bearing region	C-P	Long flame coal, gas coal, coking coal, poor coal	5.66 - 32.20	436.990	62.79
Huainan coal-bearing region	C-P	Gas coal, coking coal, lean coal	2.00 - 21.32	216.644	140.01
Central Ordos coal-bearing region	J_3,J_{1-2},C-P	Gas coal, long flame coal, rich coal, coking coal	5.00 - 8.00	3,277.457	32.94

Table 2. Regions of China with Rich Deposits of Coal Bed Methane (Continued)

Coal-Bearing Region	Period	Coal Categories	Methane Content (m^3/ton)	Total Resources (billion m^3)	Resources Per Unit Area (million m^3)
Xu-Huai [Xuzhou-Huai'an] coal-bearing region	C-P	Rich coal, coking coal, lean coal, poor coal	4.02 - 28.24	173.053	31.69
Huaying Shan-Yongrong coal-bearing region	$T_3(P_2)$	Long flame coal, rich coal, lean coal, poor coal	9.59 - 19.62	62.604	17.51
Bi Shui coal-bearing region	C-P	Rich coal, coking coal, lean coal, poor coal	2.50 - 26.20	1,259.272	61.77
Pingle coal-bearing region	T_3P_2	Everything from gas coal to anthracite	7.93 - 26.19	24.244	4.91
Western Shandong coal-bearing region	C-P	Everything from gas coal to anthracite	17.78 - 19.4	44.96	5.41
Chenzi coal-bearing region	$J_{1-2}T_3P_2$	Everything from gas coal to anthracite	4.24 - 26.19	13.295	9.19

Tables 1 and 2 contain data from the Xi'an Coal Science Academy

IV. Standards for Selecting Regions To Develop Coal Bed Methane

The quality of the conditions for doing geological evaluations of coal bed methane depend on reserves of coal bed methane and the permeability of coal seams. Moreover, they are also restricted by the hydrogeological conditions of groundwater, topography, economic and technical factors, and other conditions. Based on these factors, I conclude that the primary standards are:

1) The selected regions should have a resource foundation of coal bed methane that could be used for long-term commercial development.

2) The target coal beds have a large thickness (generally they should be greater than 2 meters), a broad distribution, stable coal seams, a high methane content in coal beds ($\geq$ 8m^3/ton of coal), appropriate burial (300 to 1,000 meters), and a gentle slope of coal bed occurrences (inclined $\leq$ 20°).

3) The coal beds should have a high permeability ($\geq$ 1 md). In a situation in which reliable permeability data are lacking, the following conditions can be considered: measurement by small coal samples, logging, and other methods; the coal medium is primarily rich, coking, and lean coal; small original ground stresses; relatively developed fissures.

4) The coal beds were subjected to relatively weak later period transformation, have no or only weak magmatic activity, and have relatively well-preserved original structures; the ground stress distribution of the coal beds and the rock strata above and below them is relatively stable and conducive to the use of pressure cracking techniques.

5) The hydrogeological conditions of the coal bed water are not complex and the strata positions above and below do not have large water surge strata or leaking strata.

6) They are near large cities, have a gentle topography, have good economic and technical conditions, and convenient construction.

V. Advances in Experimental Development of China's Coal Bed Methane

During the past several years, many departments in China have been extremely concerned with coal bed methane resources. The Ministry of Geology and Mineral Resources, Petroleum and Natural Gas Corporation, coal departments, and provincial, autonomous regions, and municipal governments have all organized forces for experimental development of coal bed methane. Moreover, several foreign companies have also invested in China to develop coal bed methane. For example, Amoco Corporation plans to select the Bi Shui Basin to conduct coal bed methane extraction experiments. With technical guidance from a United States company, Shenyang Coal Gas Company has drilled five coal bed methane extraction experimental wells in Hongyang Coal Field.

In all units involved in coal bed methane extraction experiments, the Ministry of Geology and Mineral Resources, North China Petroleum Geology has prepared specialized equipment and technical personnel for coal bed methane extraction. Since the Eighth 5-Year Plan, they have opened up four coal bed methane experiment regions at Huainan, Anyang, Liulin, and Chenghe. Among them, methane output after pressure cracking at the Coal Huai 1 mine reached 175 m^3/day. The recently built Coal Liu 1 mine has a daily gas output of 680.9 m^3.

In summary, China has abundant coal resources and enormous coal bed methane resources, and as soon as there are breakthroughs in coal bed methane extraction technology they will inevitably spur development of China's natural gas industry, especially in reducing the shortages of household gas for urban residents.

References

[1] Ministry of Coal Industry Capital Construction Department, Zhongguo Zhuyao Meikuang Kuangqu Tuji [Atlas of China's Primary Coal Mining Regions], 1988.

[2] Wang Xuzeng [3769 3563 2582], Zhongguo Meitian De Xingcheng Yu Fenbu [Formation and Distribution of China's Coal Fields], Science Press, 1992.

[3] Li Mingchao [2621 2494 3390] and Zhang Wuji [1728 0063 3444], Zhongguo Zhuyao Meitian De Qianceng Meichengqi [Shallow Strata Coal-Formed Gas in China's Primary Coal Fields], Science Press, 1990.

Oil and Gas

Joint Development of Northern Shaanxi Oil Resources

946B0077A Xian SHAANXI RIBAO in Chinese
15 Apr 94 p 1

[Article by He Dao [6320 7290]]

[Text] On April 13, an agreement to develop the oil resources in northern Shaanxi was reached between the People's Government of Shaanxi and the China National Petroleum Corporation. The agreement was signed by Deputy Governor Liu Chunmao [0491 2504 5399] for Shaanxi Province and Deputy General Manager Zhou Yongkang [0719 3057 1660] for the China National Petroleum Corporation. The signing ceremony was attended and addressed by Governor Bai Qingcai [4101 3237 2088].

The agreement follows:

(1) Oil and natural gas resources belong to the State and distribution rights reside with the State. Without permission, private parties or enterprises may not be allowed to engage in oil exploration activities. Various levels of government in Shaanxi should step up their oil protection effort and create a sound environment for oil and gas development.

(2) Northern Shaanxi is a historical region for China's revolution and Yanan is one of the high-priority assistance regions designated by the State Council. When the Changqing oil field embarks on oil exploration, local interests should be looked after. The crude oil produced in northern Shaanxi should be entered into the project, following State regulations. We recommend that oil from northern Shaanxi, after satisfying the consumption by the oil fields themselves, should be used first by existing refineries within Shaanxi.

(3) In order to accelerate oil development in northern Shaanxi and to reach the production goal of 3 million tons per year, the development of oil resources in northern Shaanxi must be planned uniformly and managed according to law. The relationship between the Changqing oil field and local organizations must be straightened out. Development priorities must be established and the development of major fields must be protected.

(4) A concrete agreement was reached regarding the mode of cooperation for the development of Pingqiao and surrounding areas.

(5) The China National Petroleum Corporation and the Shaanxi People's Government jointly established a Northern Shaanxi Oil Development Coordination and Leadership Group to address major issues in oil development.

(6) Recommend that the State Council adopt a supporting policy for the cooperative development of oil in northern Shaanxi.

Zhou Yongkang pointed out in his speech that the signing of the agreement has laid the foundation for achieving the target of 3 billion cubic meters of natural gas and 3 million tons of crude oil.

Modern Pipeline Planned for Sichuan Basin

946B0101B Shanghai WEN HUI BAO in Chinese
4 May 94 p 2

[Article by Zhou Zeshan [0719 3419 1472]]

[Text] China Petroleum and Natural Gas Corporation has decided to spend over 400 million yuan to build a fully automated modern gas pipeline with an annual gas delivery capacity of 2.7 billion cubic meters in a gas field in eastern Sichuan at the Datianchi tectonic belt. Preliminary engineering design has been completed and 60 kilometers will be completed by the end of the year.

The Datianchi tectonic belt is a major national natural gas field discovered in the 1980s. It covers Kaijiang, Liangping, Dianjiang and Changshou counties in Sichuan and contains approximately 87 billion cubic meters of reserves. Pilot production began in the early 1990s. It is a key natural gas reserve and production area in Sichuan in the Eighth and Ninth 5-Year Plan.

As for the pipeline, in addition to 170 kilometers of pipeline, it also involves the construction of four gas transport stations, seven valve chambers and five water removal stations. The pipeline employs a SCADA system to monitor, control and acquire data. It has the capability to display and record all relevant technical parameters centrally, alarm when necessary, pump gas, automatically shut off valves and semi-automatically clean the pipe. From the wellhead to the end of the pipeline, all we have to provide is minimal monitoring. There is no manual operation.

Dagang: New Life for Aging Oil Field

946B0113A Beijing RENMIN RIBAO OVERSEAS EDITION in Chinese 3 Jun 94 p 2

[Article by Man Xuejie [3341 1331 2638] and Cong Wenzi [0654 2429 3320]]

[Text] Tianjin (Xinhua)— After 30 years of development of the Dagang oil field, a decision has been made to shift the center of exploration from land to the off-shore region, thus bringing new life to this aging oil field.

Initial development of the Dagang oil field began in 1964. Over the past 30 years, the total area of exploration covered 18,000 square kilometers, and 13 oil and gas fields were developed; the total oil production reached more than 80 million tons and natural gas production reached 11.2 billion cubic meters.

Since the early 1990s, because of the increasing difficulty in finding new oil on land, it was decided to shift the center of oil and gas exploration from land to off-shore. The off-shore region of Bo Hai Bay is rich in oil and gas reserves, but the geology and terrain of this region are complex, and the load-bearing ability of the earth surface is poor, which makes exploration very difficult. In 1993, the Off-Shore Engineering Co. of the Dagang Petroleum Administration successfully built China's first off-shore platform near the Zhang Ju river in western Bo Hai Bay. In April of this year, oil and gas flows were discovered from this platform, thus creating new opportunities for off-shore exploration.

In response to China's need for off-shore exploration, which is designated as one of the key projects of the nation's "Eighth 5-year Plan," the Dagang oil field took on the responsibility of developing off-shore platforms and drilling equipment. In constructing a 3100 m^2, 13,000-ton platform capable of drilling more than 60 oil and gas wells, it used many new technologies such as prefabricating the platform structure on land, using hovercraft for transportation to the off-shore site, and building concrete anchors in the ocean for drilling. Currently, the Dagang oil field has become a multi-disciplined, integrated energy development center capable of oil and gas production, petroleum processing, mechanical manufacturing, research and design.

Development Stepped Up in Western South China Sea

946B0113C Beijing RENMIN RIBAO OVERSEAS EDITION in Chinese 8 Jun 94 p 1

[Article by Chen Bingguang [7115 3521 0342]]

[Text] Guangzhou, 7 June (Xinhua)—The China Offshore Petroleum Western South China Sea Corporation has made significant headway in the exploration of natural gas in the western South China Sea. Their strategy is to seek joint ventures with foreign companies but using domestic funds and domestic resources for exploration and development.

Investigations by both Chinese and foreign experts have shown that the Yinggehai and Southeast Qiong basin areas are rich in natural gas, with estimated reserves of 13.44 trillion cubic meters, which is about one-third of China's total natural gas reserves; the portion which is economically feasible for exploration is approximately 2.5-3 trillion cubic meters.

The discovery of natural gas in the western South China Sea has attracted the attention of many foreign petroleum companies. Since 1992, China has signed five new contracts for gas exploration with the U.S. companies ARCO and Esso. Currently, in conjunction with accelerated gas exploration activities, China is also working with the ARCO Co. and the Kuwait Overseas Petroleum Exploration Co. on a large-scale construction project at the Ya-13-1 gas field. The total cost of the project is $1.16 billion. According to the agreement, starting 1 January 1996, gas will be supplied to Hong Kong via under-sea pipelines for the next 20 years at the rate of 2.9 billion cubic meters per year; at the same time, gas will also be supplied to Hainan Province at the rate of 500 million cubic meters per year.

Since the beginning of this year, a multi-firm construction contractor that includes an Italian offshore construction company[1] and the European Ocean Engineering Co. have installed more than 700 km of undersea pipelines 28 inches in diameter between the mouth of the Pearl River and Yinggehai; the 70 km pipeline between the mouth of the Pearl River and Hong Kong is expected to be completed by August. This 800-km trunk line is the longest undersea gas pipeline in Asia. Installation of the 14-inch, 100-km pipeline between the Yinggehai platform and Sanya City of Hainan Island had also begun early this month.

According to plan, the western South China Sea region will have a natural gas production capacity of 10 billion cubic meters per year by the end of this century.

Footnote

1. Could be the offshore Construction Division of SHIPEM.

Headway in East China Sea Oil Exploration

946B0113D Beijing RENMIN RIBAO OVERSEAS EDITION in Chinese 7 Jun 94 p 1

[Article by Man Xuejie [3341 1331 2638]]

[Text] Tianjin, 6 June (Xinhua)—The first joint oil exploration project between China and the United States—the two-dimensional exploration of regional blocks 33/05 and 33/19 in the East China Sea—was completed yesterday.

These two regional blocks are located in an area more than 200 km east of Wenzhou, where the water depth is

approximately 100 m. In accordance with the exploration-risk agreement signed last year between the China National Offshore Oil Corporation and Texaco of the U.S., the exploration work will be performed by the No. 512 geophysical exploration ship of Zhonghai Geophysical Exploration Northern Co. The ship began operation in late March of this year, and within 67 days completed its 5300-km seismic survey task; it received high praise from foreign clients for the quality and efficiency of this operation.

East China Sea is an important oil exploration region recently developed by China's offshore petroleum industry; it covers 750,000 square kilometers of ocean. Since instituting its reform and open-door policy, China has completed over 150,000 km of seismic surveys in the East China Sea and completed the drilling of five pilot wells. Four of the wells showed signs of oil and gas, and more than 100 oil-bearing structures have been discovered.

During the period from June 1992 to June 1993, China solicited four rounds of competitive bids from foreign contractors to accelerate the exploration of 20 regional blocks in the East China Sea covering a total area of 72,800 square kilometers. More than 73 companies from 19 different countries responded, and 15 oil companies from 7 countries were selected to explore 18 of the regional blocks; the total exploration investment was $300 million.

Successful completion of the two-dimensional exploration of the 33/05 and 33/19 regional blocks will provide valuable scientific data for locating the first pilot well to be drilled in October of this year. It is expected that 20 pilot wells will be drilled by the end of 1996.

China National Petroleum Corporation Opens New Laboratory

946B0131C Beijing RENMIN RIBAO in Chinese 13 Jun 94 p 3

[Article by Jiao Nianyou [3542 1819 0645] and Zhang Hongmei [1728 3163 5019]]

[Text] A key scientific research project of the China National Petroleum Corporation, an "open laboratory for oil drilling technology," was recently completed at the Zhongyuan oil field. It also passed acceptance inspection by the ministry. The laboratory consists of a simulated experimental well, a ground process flow system, a real-time control and measurement system and an underground experimental system. These systems form a relatively comprehensive facility to perform research on techniques associated with mechanical oil drilling on a large scale. Its design, together with the completed full-size well shaft and underground test equipment, is the best in China in terms of scale, capability, and experimental conditions. Furthermore, as a whole, it is already at the leading edge worldwide. The research staff has made numerous innovations, including a four-shaft wellhead and synchronized four-shaft drilling technique, underground multi-point, real-time telemetry network and a variety of special underground tools.

Compared to similar facilities abroad, this comprehensive, multi-function high standard simulated production test site is very advanced in terms of scale and performance. This laboratory not only will serve all oil and gas fields in China but also will be open to the oil drilling technology market worldwide.

Prospects for Natural Gas Exploration in Yinggehai Basin

94FE0625A Chengdu TIANRANQI GONGYE [NATURAL GAS INDUSTRY] in Chinese No 2, 25 Mar 94 pp 14-20

[Article by Zu Jiaqi [4371 1367 3825], Western Nanhai Branch, China National Offshore Petroleum Corporation]

[Text] The Yinggehai Basin is a Cenozoic strike-slip extension basin with a northwestward orientation that developed above the Red River Geosuture line. It has an area of 11,300 square kilometers. It underwent rapid subsidence attended by high temperatures and contains chiefly marine sediments, with a thickness of more than 15,000 m, including thick, mature to highly mature hydrocarbon parent rocks. It has immense supplies of natural gas.

The basin's development includes some unique features. One very uncommon feature is the occurrence of four north-south oriented large shale-arch anticlinal zones that are associated with mud diapirism and cover an area of more than 1000 square kilometers. In addition, there is a large drape structure zone, a large combined turbidite body and structural trap zone, and a large coastal platform-margin combined reef and sandstone zone.

From the early Oligocene to the Pliocene, excellent reservoir strata developed in the basin, including coastal sand bars, delta river-channel sands, and turbidite fans, which are thick, cover a large area, and have consistent transverse properties. Within this region, the Meishan mudstone formation and the late Pliocene to Quaternary sediments, consisting of mud and clay sequences, form two regional caprock strata. Exploratory drilling has shown that abundant oil and gas occur in the region; there are both deeply and shallowly buried gas pools.

Prospecting for oil and gas in the Yinggehai Basin began in the early 1960s. Systematic exploration was carried on in the 1970s, and in the 1980s, joint exploration with ARCO (U.S.) and other organizations achieved major results. The discovery of the large Ya 13-1 gas field revealed the extensive occurrence of oil and gas in the basin.

Geologic Structure of the Region

The Yinggehai Basin is a Cenozoic strike-slip extension basin that developed on the Red River Geosuture line. It has an area of 11,300 square kilometers (Fig. 1) [1].

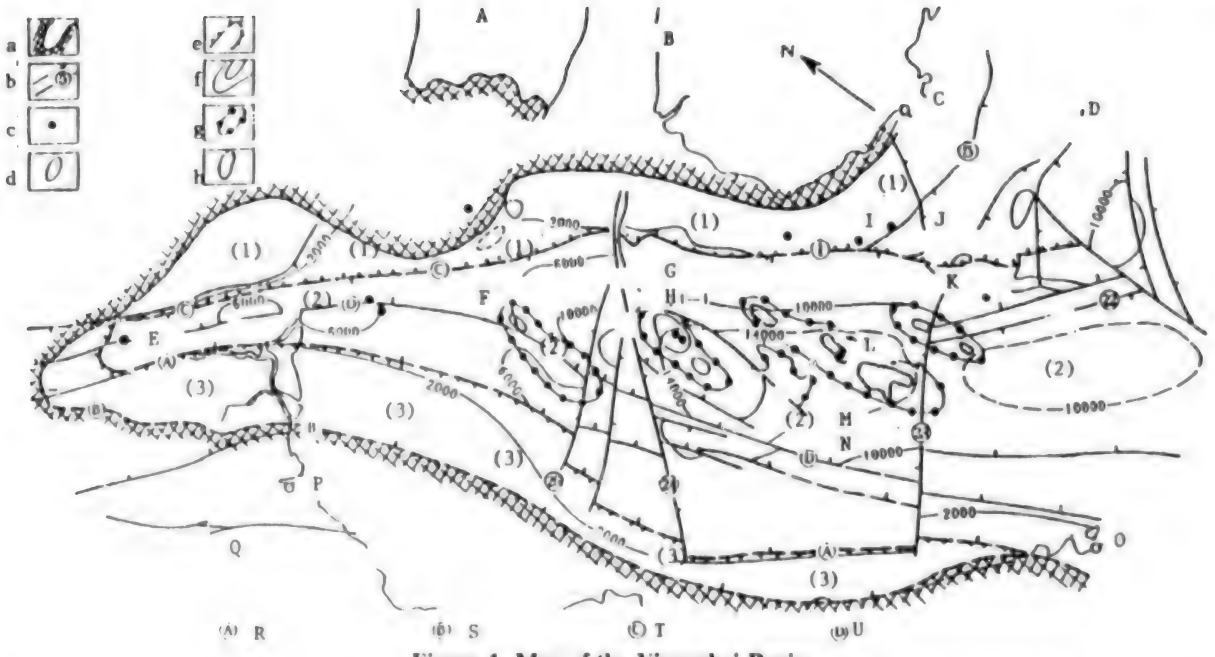

Figure 1. Map of the Yinggehai Basin

Key: a. Boundaries of basin; b. Faults, with numbers; c. Locations of wells; d. Local structures; e. Boundaries of top-level structural units; f. Cenozoic equal-thickness contours; g. Shale-arch anticline belts; h. Mud diapirs; A. Beibuwan Basin; B. Hainan Rise; C. Sanya; D. Jingdongnan Basin; E. Hanoi; F. Lingao shale-arch anticline belt; G. Dongfang shale-arch anticline belt; H. Dongfang 1-1; I. Ying 6 well; J. Ya 13-1 gas field; K. Ledong East shale-arch anticline belt; L. Ying 2 well; M. Le 8-1; N. Ledong shale-arch anticline belt; O. Danang; P. Thanh Hoa; Q. Kun-Song Rise; R. Black River Fault; S. Xiuli Fault; T. Lujiang Fault; U. Songhe Fault; (1)-(1)-(1) Northern slope zone; (2)-(2)-(2) Central depression; (3)-(3)-(3) Southern slope zone

The basin shows up on regional gravimetric maps as a northwest-oriented gentle positive gravitational anomaly. The Moho surface and the overlying sedimentary rocks produce lens-like reflections. The Moho surface is at a depth of 22 to 24 km in the sediments. The bottom of the basin is at a depth of 16 to 20 km and the base of the Tertiary sequence is at a depth of 12 to 17 km. Magnetometric maps show a magnetic body whose top is located at a depth of 15 to 17 km, and there is a faint set of closely spaced magnetic anomalies which cannot represent igneous intrusive bodies: most likely they are indicative of strong magnetization of Cretaceous sandstones and shales. The northwest-oriented strike-slip extension transformed the original northeast-oriented structure of the basin. It is inferred that at the end of the Paleocene, the basin was already controlled by the prevailing northwest-oriented tectonic stress. Two major faults, both with a northwestward strike, have developed on opposite sides of the basin. Their continuous, inherited development gradually ceased at the end of the Miocene. Fault 1, on the northeastern margin, can be traced for 126 km and has a maximum displacement of 4000 m; the displacement gradually declines to zero at the two ends. The other large fault, on the southwestern margin, developed symmetrically with Fault 1; it is called the Black River Fault. It is about 150 km long, with a displacement of 3000 to 4000 m. It extends northwestward to the mouth of the Red River in Vietnam, where it abruptly turns westward and continues outside the region. In the southwest, it runs to 17 21' N, near Danang, then makes a sharp turn toward the south. These two major basement faults appear to be sinistral strike-slip tension faults [2]. A small, hidden, NE-oriented normal fault that was generated along with them underwent inherited development during which it had a major influence on sedimentation.

The Yinggehai Basin is an inherited basin structure, oriented toward the northwest that contains primarily marine sediments. It joins the Hainan Rise on the northeast and the Kun-Song Rise on the southwest. It extends northwestward as far as the mouth of the Red River, but its northeastern boundary is indistinct. The north-south line passing through Sanya is provisionally taken as its boundary, so that everything west of the Ya 21-1 tectonic zone belongs to the basin. Within this region, the structure is rather uniform: the basin is bounded on two sides by the large faults, and its secondary structural units are the northern slope, the central depression, and the southern slope. We shall now discuss each of these structural units.

1. The Northern Slope

This is in essence a monocline dipping gently toward the southwest; it adjoins the Hainan Rise on the northeast and is bounded on the south by Fault 1. It covers an area of 20,000 square kilometers and contains Upper Tertiary sediments 1000 to 2000 m thick and a Lower Tertiary sequence 0 to 500 m thick. It is evident from numerous seismic sections and some drillhole data that in the region of Fault 1's hanging wall, the bedrock of the denuded ancient continental slope is overlain only by a series of transgressive neritic sandstones, which successively overlap each other toward the northeast, and a large sequence of clay sediments. The sea had already covered the zone of fault 1 by the Middle Miocene, and clusters and belts of Miocene reefs developed on the coastal platform along the southern margin of the ancient slope [3]. Data from the Ying 6 exploratory drillhole show that these reef bodies consist of a distinctive combination of unconsolidated sandstone and reef material in which the terrigenous sandstone and the reefs overlap longitudinally but are in contact transversally, producing excellent oil and gas reservoir conditions. The maximum thickness of the reef cores is 180 to 460 m.

Owing to changes produced by subsequent uplifting, the reef bodies are buried at depths from 1810 to 1520 m. In the west they are uplifted to a depth of 710 m. In the 1980s, at least 20 reef and sandstone complexes, with a total area of 564 square kilometers, were identified from seismic data. Moving eastward along the zone of Fault 1, one crosses Fault 5 and encounters the Ya 13-1 drape structure zone, with inherited development, whose axis is oriented toward the northwest. This structural zone is about 80 km long and 8 to 10 km wide and covers an area of 700 square kilometers. It has a closure of more than 360 m. It includes the Ya 13-1 North, Ya 13-1, Ya 19-1, and Ya 26-1 structural traps, which are excellently suited for the storage of oil and gas.

Exploratory drilling has shown that the Ya 13-1 structure is a large gas field, containing more than 100 billion cubic meters of gas. Its pay strata are primarily of Oligocene age. In the western part of the Fault 1 zone, there occur only a few fault-nose and draped anticline structures, including the Ling 9-1 and Lingao 17-1 structures.

2. The Central Depression

This depression contains chiefly Tertiary and Quaternary neritic and bathyal sediments with diverse sources of material. Their total thickness exceeds 20,000 m. They cover an area of 62,000 square kilometers. The depression is cut across from northwest to southeast by an occluded secondary NE-SW transform fault and is subdivided into the Hanoi Depression and the Yinggehai Depression (Fig. 1). During the course of its development, the Hanoi Depression was closer to the source of material; it covers a relatively small area of only 8000 square kilometers and consists largely of rivermouth clastic sequences, including Upper Tertiary sequences 5000 to 6000 m thick and Lower Tertiary sequences less than 1000 m thick. Toward the southeast, with passage into the Yinggehai depression, there is a gradual transition to bay, neritic, and bathyal sediments. The area of this depression is 54,000 square kilometers. The Upper Tertiary sediments are more than 12,000 m thick and the Lower Tertiary sediments about 7,000 m thick. Thick hydrocarbon-generating Middle Miocene plastic clay sediments occur in the central area of the basin. Under the excellent conditions of this region, with diverse sources of material, they are accompanied by large turbidite-sandstone bodies. The latest seismic data and successional analysis suggest that during the Early Miocene or later, the basin still contained thick delta-margin sandstones which promoted the development of very large deeply buried gas pools. This is a new exploration area that is currently attracting great attention.

In the Yinggehai Basin, recent high-resolution seismic data have shown the presence of four large shale-arch anticlinal belts, with a regular north-to-south *en echelon* arrangement. These anticlinal belts generally consist of two or three summits joined by saddles. They are 100 to 140 km long and 10 to 20 km wide and cover areas of 800 to 2000 square kilometers. This large anticlinal zone has developed since the Late Oligocene. The structures are simple, complete, and gently sloping (but become steeper at greater depths). Toward the flanks, the greatest slope is usually 7° to 8°, and there is no evident steep dipping and none of the buckling, upwarping, or overturning of strata that is associated with diapir necks. On the contrary, in the cores of these structures, the strata show a distinct inward dip, with a low-velocity seismically indistinct zone. There are many extension faults along the parallel axial lines. A dip is clearly evident at the south end of each anticline. The anticlines are uplifted toward the north, with a plunge of only 2° to 1°. In addition, the Tertiary sequences undergo uplifting and thinning out toward the north, and this is the key to identifying the trap areas. Some dispute now results from the fact that, during earlier mapping and interpretation of the seismic sections, many investigators interpreted the geophysical characteristics of the blurred zones in the axial areas of the anticlines as mud diapirs or piercement structures. Actually, there is no scientific basis for such an interpretation. Not only do the blurred zones in the seismic section involve low velocities (2200 to 2300 m/sec) and low densities, but in-phase axes can be traced intermittently in these zones, revealing a drop in velocity near the axis. These facts express the characteristics of the parent stratum, and no compelling evidence has been found to support the idea that as a result of underpressure, ascending mudstone pierced through several hundred meters of overlying strata. I believe that the objective interpretation of the indistinct zone is that in the deeply buried gas-generating stratum, as a result of dynamic effects, the natural gas moved along hidden tension faults and a dense network of microcracks in the brittle sandstone and shale strata, eventually accumulating in porous reservoir strata in the axial zones of these structures, where it formed a gas-filled zone. This interpretation is supported by recent evidence from many exploratory wells. The factors that gave rise to the

huge shale-arch anticline zone at the center of the basin were clearly complex. In general terms, in an inherited process that took place in the context of a strong northwest-oriented dextral strike-slip fold-producing force and the presence of structural ridges, in each sedimentation period from the Oligocene on, underpressured mudstones were subjected to an anomalous pressure as a result of high temperatures and pressures, which rapidly generated an immense buckling force (this force belonged only to the embryonic mud-diapir stage). By the combined effect of the above two kinds of force, a huge shale-arch anticlinal belt with the characteristics of the present-day Yinggehai region had essentially taken shape by the end of the Miocene and was completely formed by the end of the Pleistocene [1].

Large-scale river-channel sand body traps dating from the Upper Miocene to the Pliocene occur in the middle part of the central basin. They cover areas of 875 and 635 square kilometers and are 800 m thick. The sandstone bodies are surrounded by thick shales and are in direct contact with the oil-forming parent rock, which favors the development of large gas pools with lithologic traps.* In the eastern part of the basin there is a large zone containing a combination of turbidite sand bodies and structural traps that dates from the Miocene. The sandstone bodies are up to 346 m thick and are congruent with the Ledong 30-1 and Ya 35-1 sandstone bodies, having an east-west orientation, a total length of about 100 km and an area of about 700 square kilometers. Below them is a combination of Early Tertiary structural traps such as the Ya 35-1, Ya 28-1 and Ya 26-1 traps. The Ledong 30-1 well, at the western end of the large sandstone body, penetrates all strata from the Middle Miocene (Leshan) and passes through six layers of turbidite sandstone with individual thicknesses of up to 62 m and a total thickness of 226 m. Analysis of thin sections from the drillhole cores identified the material as fine-grained feldspathic sandstone. Electrical logging indicated an average porosity of 20-25 percent and an average permeability of 7.7 to 15.0 x 10^{-3} μ^2. The whole sequence penetrated by the well contained gas showings, with a total hydrocarbon content of 16.5 percent. The measurements eventually had to be terminated owing to a high pressure of 81.3 MPa at the bottom hole. Seismic analysis indicates that the middle segment of the turbidite sandstone body is at a depth of 3233 m and that the amount of natural gas in it exceeds a trillion cubic meters (not including the gas in Oligocene structures).

3. The Southern Slope

Seismic and drillhole data are lacking for this area. Based on regional geologic data, to the south of the major Black River Fault, the geology is similar to that of the northern slope zone, except that the source of material was primarily the granite-gneisses of the ancient Kun-Song land area of Vietnam, which probably had an adverse effect on the reservoir properties of the resulting sedimentary rock. This element of the basin has an area of about 31,000 square kilometers and consists primarily of a succession of marine facies that successively overlap each other and taper out toward the south. The thickness of the Lower Tertiary sequence ranges from 0 to 1500 m and that of the Upper Tertiary sequence from 1000 to 2000 m. There are few structural traps, and they are primarily of the monoclinal type. It is possible that coastal reefs occur along the hanging wall of the fault, and that a prismatic fault-block anticline belt similar to the Ya 13-1 feature occurs to the southeast along the fault, with highly favorable conditions for the storage of gas in the disjunction zone.

Hydrocarbon Parent Rocks**

In the continental slope basins of the northern South China Sea, the parent rock of known oil fields is primarily Eocene lacustrine shale of great thickness, with abundant organic matter. The parent rock of the gas-condensate fields of the neighboring Pearl River Delta basin is Oligocene bog shale with abundant organic matter from higher land plants. Because of the rapid subsidence of the Yinggehai Basin, its sediments are primarily of marine origin and have been subjected to high temperatures and pressures; thus, based on a comparison of the affinities between oil seepages and gas-field gas, an analysis of seismic and drillhole data, and special geochemical and biochemical hydrocarbon modeling, it is concluded that the thick Miocene Meishan shales are the principal parent rock. An even more striking fact is that the saturated hydrocarbons of this parent rock contain up to 90 percent of resins with a very high hydrocarbon generation potential, 2.7 times that calculated from the customary kerogen scale. In addition the parent rock is buried at a moderate depth of about 3000 m, which is optimum for hydrocarbon generation and migration. Group and isotopic analysis indicates that the renowned Yinggehai Village oil and gas seep, the petroleum gas from the Ya 13-1 gas field, and the Dongfang 1-1 natural gas were derived from the parent rock of the Meishan Formation.

The threshold oil generation depth for the Eocene and Oligocene parent rocks is 2400 to 5800 m, but in the central basin these rocks are buried at a depth of more than 6000 m; most of them, therefore, are below the threshold oil and gas generation depth and are now in the period of over-maturity. Thus, during their long history, the Eocene and Oligocene hydrocarbon parent rocks have made a significant contribution to the oil and gas of the region. In the eastern part of the depression, the Oligocene parent rock is less deeply buried and is capable of generating oil and gas. For the basin as a whole, these two sets of parent rock are still of secondary importance, but their contribution to the oil and gas of the basin is undeniable. Preliminary estimates (which do not include the Middle Eocene) are that the supply of natural gas in the region exceeds 10 trillion cubic meters.

The characteristics of the three sets of parent rock are discussed below.

1. The Miocene Meishan Formation

The Miocene formation is a group of dark-colored shales derived from semi-closed neritic and bathyal sediments, with an average thickness of nearly 1000 m and an average residual organic carbon content of 1.95 percent. Of the kerogen categories, they belong primarily to class II or to combined class II-III. The hydrocarbons generated by the thinnest resin bodies account for at least 90 percent of the total, and the hydrocarbon generating potential is extremely high, with a conversion rate of up to 100 percent. The actual amount of hydrocarbon generated is 2.7 times the kerogen-scale figure. Experiments modeling high-temperature hydrocarbon generation indicate an abnormally high gas generation rate of 182 to 506 m^3 per ton of TOC [total organic carbon], with gas as the primary product. The threshold depth of burial for hydrocarbon generation is 2800 m and the depth of peak hydrocarbon generation is about 3700 m. In their central part, the Meishan sediments have a thickness of about 3600 m; the top of the formation is buried at depths between 2300 and 4400 m, with an associated R_0 value of 1 to 4 percent; thus, it is at the optimum depth for gas generation and migration. Because bodies with abundant resin are the primary parent material for hydrocarbons in this formation, its hydrocarbon generation potential is extremely high. Since, in addition, its potential is chiefly for the generation of gas and condensate oil, if we assume a hydrocarbon generation potential twice that obtained by the customary estimation techniques, then its reserves of natural gas must be several trillion cubic meters, with immense potential.

2. The Oligocene Sequence

Oligocene parent rock is the principal parent rock of the Wenshan 9-2-1 oil and gas condensate field in the neighboring Pearl River Delta Basin and of the Ya 13-1 gas field in the Yinggehai Basin [4]. It consists of coastal bog sediments and its organic matter is primarily of kerogen classes II_2-III, with a large content of the remains of higher land plants. Its generation potential is primarily for gas-condensate. Its hydrocarbon generation potential is poor, ranging from 20 to 35 mg per g of TOC. It contains C_{29} stigmastane, an indicator of higher land plants, but for the most part its maturity level is in the condensate-oil and wet-gas window (R_0 from 0.6 to 1.66 percent). It has some gas generating potential.

The threshold hydrocarbon generation depth is 2600 m and the depth of peak hydrocarbon generation is 3700 m. The over-maturity threshold is 5800 m. Along the edge of the basin, this parent rock is either poor or lacking in organic matter owing to the shallowness of the water. In the central part of the basin it occurs at depths that are mostly in the transitional interval of hydrocarbon generation, and as a consequence, it is a minor parent rock in this region.

3. The Eocene Sequence

The Eocene parent rock consists of deep lake sediments. In this region, it is thought that they were generated only in the central depression. They are less than 3000 m thick, generally about 1000 m thick. They are rich in organic matter; their average organic carbon content is between 1.46 and 2.04 percent. The oil parent material is primarily of type I-II and is rich in algal remains, whose indicator compound is 4-methylsterane. In the oil window (R_0 from 0.6 to 1.5 percent), the oil generation zone is broad, and the oil generation rate is high; oil is the primary product. The hydrocarbon generation threshold depth is between 2400 and 2700 m. The peak oil generation and migration period is from the early Miocene on. Exploratory wells in the Yinggehai Basin have not yet encountered this interval; its sedimentation area is confined to the central part of the depression and is chiefly in the over-mature depth interval of 5800 m or more. Thus, in its evolution, this parent rock has made a contribution, but the extent of this contribution is still being investigated.

Reservoir and Caprock Conditions

From the Early Oligocene to the Pliocene, the Yinggehai Basin was covered by the sea, and the sources of material in all periods of sedimentation were primarily in the northwest Red River hydrographic system. In addition, watercourses arising in the ancient land areas of Hainan island to the northeast and the Kun-Song area to the southwest also carried large amounts of sediments into the basin. As a consequence, sand bars, delta river-channel sand bodies and turbidite fans developed extensively in all periods. The marine sandstones are thick, extensive, and laterally stable in their properties, with excellent reservoir strata. In particular, from the Oligocene to the Early Miocene, the thickness of the sediments is in the hundreds of meters; significantly, this also applies to the central part of the basin. Wells drilled in the Ya 13-1 gas field in the eastern zone have penetrated early Oligocene delta-margin sandstones with gas strata up to 154 m thick; the unimpeded flow volume of the natural gas is a maximum of 7.81 million cubic meters per day. In the Dongfang 1-1 gas-bearing structure in the western zone, the Upper Miocene Ying-Huang formation, with sandstone more than 150 m thick, has a porosity of 18 to 27 percent and a permeability of 10 x 10^{-3} μ^2, but the reservoir properties show great transverse variability. In the depth interval from 1284 to 1296 m, the Ying No. 2 well produces a gas yield of 33.5 x 10^4 m^3/day.

The Yinggehai Basin has two regional caprock sequences that cover the entire basin. The large-scale Middle Miocene marine transgression produced a set of neritic to bathyal shales 450 to 2000 m thick. The very thick mudstone stratum at the center of the basin, which is subject to a pressure deficiency, has developed fine-grained sandstone blocks and turbidite-sandstone bodies several hundred meters in size beneath this caprock sequence, and it is therefore well suited for the role of a large gas-bearing region. The Meishan caprock formation is the key to the development of the proven Ya 13-1

gas field. The Late Pliocene and Quaternary marine transgression extended even farther, and the resulting mudstone and claystone sequences, which are 8000 to 2200 m thick, again covered the entire basin. Drillhole data show that they are the regional caprock sequence for the Upper Miocene Ying-Huang oil- and gas-bearing formation.

As the net result of the excellent geological conditions described above, the main target sequences for regional-block oil and gas exploration wells are as follows.

1. In the Northern and Southern slope zones

The Upper Tertiary Meishan Formation is hydrocarbon parent rock. The Ying-Huang Formation is the principal natural gas target stratum, with an upper sandstone sequence and a lower combined reef and sandstone zone, and contains conventional oil; the Pliocene mudstone and the Tertiary claystone serve as caprock, and some biological gas is present.

2. In the Central Depression

The Lower Tertiary Lingshui Formation is the principal target stratum for oil and gas. The Upper Tertiary Ying-Huang Formation is a secondary target stratum for natural gas; commonly referred to as the "shallowly buried" gas stratum, it is buried at a depth 1000 to 2100 m.

The Lower Tertiary Yacheng Formation is a gas parent rock sequence. The Lingshui Formation and the Sanya Formation are the principal natural gas target strata, with normal pressures. The Ying 19-2 stratum has a pressure coefficient of 1.17 and the Ya 13-1 gas-bearing stratum has a pressure coefficient of 1.05. The Upper Tertiary Meishan Formation and the upper part of the Ying-Huang Formation serve as caprock, with pressure coefficients of 1.5 to 2.02.

The parent rock of the shallowly buried gas stratum is the Tertiary Meishan Formation and the lower part of the Ying-Huang Formation. The middle and upper zones of the latter formation or the reef material may function as reservoir rock. The Pliocene and Quaternary strata act as caprock.

Conclusions

The Yinggehai Basin is a gas-rich topographic basin that was formed by a northwestward strike-slip extension during the Cenozoic. It still retains a two-layered structure, consisting of a Tertiary fracture depression and a Late Tertiary depression. It underwent rapid subsidence attended by high temperatures and contains chiefly marine sediments, whose maximum thickness is 15,000 meters. They include extremely thick, mature to highly mature hydrocarbon parent rock with immense potential reserves of natural gas. In the center of the basin, tectonic stresses brought about mud-diapir activity and gave rise to four large shale-arch anticlinal zones, running from south to north and covering an area of more than 1000 square kilometers. These highly unusual structures are well suited to serve as natural gas reservoirs. In addition, there is a large drape structure zone, a coastal-platform margin reef belt, and a large turbidite sandstone and structural trap zone. The Ya 13-1 gas field, with more than 100 billion cubic meters of gas, has already been found in the drape structure zone. There have been major breakthroughs on the Dongfang 1-1 and Ledong 15-1 "shallow-stratum" structures in the shale-arch anticlinal zone, revealing excellent prospects for the discovery of large gas fields.

1. Principal Structural Belts with Conditions Favoring Abundant Gas Accumulation

a. The Ya 13-1 draped anticline belt. This consists of the Ya 13-1, Ya 13-1 north, Ya 19-1, and Ya 26-1 secondary structures. It is oriented toward the northwest, is 70 km long and 8 to 10 km wide, and covers an area of about 680 square kilometers. Most of the gas pools are deeply buried.

b. The Ledong shale-arch anticlinal belt. The principal structure is the Ledong 8-1 structure, which has both deep and shallow gas pools, with the latter predominant (there is a normal-pressure sequence from T_{40} to T_{60}). It consists of the Lingtou 19-1, Le 8-1, Le 14-1, and Le 14-2 secondary structures and covers an area of about 2000 square kilometers.

c. The Dongfang shale-arch belt. The main structure is the Dongfang 1-1 structure, which contains both deep and shallow gas pools and covers an area of about 1200 square kilometers.

d. The Lingao shale-arch anticlinal zone. The Lingao 20-1 structure is the principal structure, with both deep and shallow gas pools; it covers an area of about 1800 square kilometers.

e. The Ledong East shale-arch anticlinal belt. The principal structure of this belt is the Le 22-1 structure, which includes the 28-1 structure and contains both deep and shallow gas pools. It covers an area of about 400 square kilometers.

f. The Northern Slope reef and sandstone zone [3]. Seismic analysis indicates that the Middle Miocene coastal platform margin consists of reef clusters and belts. The core of the reefs has a maximum thickness of 180 to 460 m and is 120 km long. The zone is usually 6.5 km wide and it includes the reef core, reef bars, and reef foreslopes, covering an area of 916 square kilometers. The reef core has an area of 254 square kilometers and contains more than a billion cubic meters of gas. The Ying No. 6 well shows that it is a unique combination of unconsolidated sandstone and reef material. The mudstone caprock, several hundred meters thick, rests directly on this composite body. The combined lagoon-facies mudstone and reef body adjoins it on the north side, forming a lateral trap.

g. The Ledong combined turbidite-sandstone and structural trap belt. The large sand body is 346 m thick, 6-8 km wide, and about 100 km long, and covers an area of about 568 square kilometers. It dates from the Middle Miocene. Below it is a combination of Oligocene anticlinal structures (Ya 35-1, Ya 28-1, Ya 26-1).

2. Suggestions for Further Prospecting

a. The breakthrough on the main Ya 13-1 structure of the draped anticline belt demonstrated that structural belts of this type can have extremely abundant gas content. As a consequence, the construction of the Ya 13-1 oilfield has already begun, and it is expected to enter production in 1996. In addition, detailed exploration of the entire structural belt should move forward, providing control figures on the entire gas-containing area and identifying most of the reserves, so as to create the largest offshore gas field, with an annual output of nearly 10 billion cubic meters.

b. The large shale-arch anticlinal belt is the part of the Yinggehai Basin that is richest in gas. An exploratory well 5000 m deep should be drilled on each of the main structures, namely, the Le 8-1 and Dongfang 1-1 structures, in order to penetrate the deeply buried gas-bearing stratum. If a breakthrough is made, then more effective exploratory wells should be drilled. In addition, detailed exploration of shallow gas pools should be undertaken with a small number of wells on the major Dongfang 1-1 and Le 1-1 breakthrough structures, so as to quickly obtain a control figure for the natural gas reserves and to develop a second gas-producing area.

c. The combined reef and sandstone belt of the northern slope zone [3] represents yet another oil and gas pool type; its favorable characteristics include its closeness to shore, the shallowness of the water, and the relatively shallow depth at which the oil and gas pay strata are buried. An intensified seismic resurvey should be accompanied by initial drilling on the elevated No. 31082 reef body.

d. The Ledong turbidite-sandstone and structural trap zone is another new area with excellent prospects for the discovery of large gas-bearing areas. Chinese and foreign petroleum geologists consider this an especially promising area. Recently, the ARCO company drilled a 5000-meter well on the Ya 35-1 structure, at the east end of the large sandstone body. The Chinese geologists drilled a 4800-meter well on the Ya 26-1 structure, which is an elevation in the central area, and investigated the gas content of the sandstone body. The next step should be to intensify exploratory work. Strategic reconnaissance of these zones will further increase the supply of known large gas-bearing areas.

Footnotes

*Zhang Qiming [1728 0796 2494] and Hu Zhongliang [5170 1813 5328]. [Investigations of the Oil and Gas Content of the Yinggehai Basin; internal data], 1990.

**Zhang Quanxing [1728 3123 5281] and Li Li [2621 6849]. [New Advances in Research on Hydrocarbon Generation in the Yinggehai Basin], Western South China Sea Petroleum Company (internal data), 1992.

References

1. Zhang Qiming [1728 0796 2492] and Zhang Quanxing [1728 3123 5289]. The Yinggehai Basin, a Unique Oil- and Gas-Containing Basin. ZHONGGUO HAISHANG YOUQI [CHINA OFFSHORE OIL AND GAS], Vol 1 No 1, 1987.

2. Tang Xin [0781 9515]. Plate Structure of the South China Sea and Its Causative Factors. DIQIU WULI XUEBAO [JOURNAL OF GEOPHYSICS], Vol 24 No 4, 1981.

3. Zu Jiaqi [4371 1367 3825]. Prospects for Occurrence of Oil in the Reef Area of the Northern Slope of the Western Part of the Yinggehai Basin. ZHONGGUO HAISHANG YOUQI [CHINA OFFSHORE OIL AND GAS], Vol 2 No 3, 1988.

4. Zhang Quanxing. Oil and Gas Migration in the Ya 13-1 Oil and Gas Field. Ibid., Vol 2 No 2, 1988.

Nuclear Power

Conceptual Design of 200MW Nuclear Heating Plant

94FE0589A Chengdu HE DONGLI GONGCHENG [NUCLEAR POWER ENGINEERING] in Chinese Vol 14 No 4, 15 Aug 93 pp 289-295

[Article by Wang Dazhong [3769 1129 0022], Lin Jiagui [2651 1367 2710], Ma Changwen [7456 2490 2429], Dong Duo [5516 6995], and Zheng Wenxiang [6774 2429 4382] of the Institute of Nuclear Energy Technology, Tsinghua University, Beijing]

[Text]

Abstract

A number of advanced features, including natural circulation, integrated arrangement, self-pressurized performance, dual vessel structure, hydraulic control rod drive and passive safety systems have been incorporated into the nuclear reactor of NHP-200. This makes the NHP safe, reliable, simple and easily constructed and maintained.

The safety concepts, key design considerations, general description and main technical features of the NHP-200 are presented.

1. Introduction

The construction of the 5MW low-temperature nuclear heating plant at Qinghua University indicated that China's nuclear heating technology had reached

advanced world standards. The 5MW reactor has provided heating in three winters and was used in a number of significant experimental research projects. Experimental and operational results showed that the safety and reliability of the reactor were superior and the reactor had no adverse effects on the environment and the heating network. The heating utilization rate of the reactor has achieved 99 percent.

Today, 20 cities and enterprise units in China are in urgent need of nuclear heating in order to solve their energy shortage and environmental pollution problems. Some foreign countries also expressed interest in working with China and applying such nuclear reactor to the desalinization of sea water. Therefore, in order to realize commercialization of nuclear heating, it is vitally important and urgent for China to build a commercial scale nuclear heating demonstration reactor.

In recent years, while building the experimental 5MW low-temperature nuclear heating plant, China has also begun preliminary studies of large commercial nuclear heating plants. Plans to build a 200MW demonstration nuclear heating plant has been approved and the technology was made one of the high priority items in the Eighth 5-Year Plan. Today, the feasibility study of the 200MW NHP has been completed. Important results have been obtained in the experimental research of special equipment (such as the hydraulic drive mechanism for the control rod), and preliminary design work is underway.

In this paper, the design goals, safety concepts, key design considerations, general description, and main technical features are presented.

2. Reactor Type and Design Concepts

2.1 Reactor type and size

The selection of reactor type and size for the nuclear heating plant was determined mainly by the heating load requirement, the heating network condition, the economy of heating, reliability, and technical feasibility. The low temperature nuclear heating demonstration reactor shall be a light water reactor with an integrated design, natural circulation, self-pressurization and a dual vessel structure. The heating power will be 200MW and the design concepts are the same as that of the 5MW low-temperature nuclear heating reactor. Analysis shows that dual-vessel, low pressure, light water reactors are suitable heat sources on large and medium heating networks. The power range of a single reactor is roughly 100 to 500MW. Such reactors may also be used in electricity and heat co-generation, for industrial low pressure steam supply, and for sea water de-salinization and air conditioning.

The construction of a 200MW demonstration NHP and the development of 2x200MW commercial NHP should be significant for most cities in northern China and for salt water desalinization applications. NHP of this size is economically competitive, reliable, and technically feasible.

2.2 Design goals and safety requirements

The major issues in low temperature nuclear heating are safety and economy. As a demonstration device for commercial nuclear heating plants, the 200MW reactor must address these two intimately related issues. The design goals are therefore reliable, economical, and technically feasible.

Due to economical considerations, low temperature nuclear heating plants are usually built near populated areas; their safety requirements are therefore higher than that of nuclear power plants. Obviously, if one followed the traditional design concepts for nuclear power plants and devoted great resources to over-design and rely excessively on safety devices, then it would be not only difficult to realize the reliability goal, but the economic and technical feasibility goals would also be jeopardized because of increased construction and maintenance costs. Therefore, the reactor design has sound self-protection capability, that is, the safety operation of the reactor is achieved via internal mechanism and not through enabling means. Such design may simplify, even eliminate, the extensive and complicated safety devices in nuclear power plants. The design level of the components need not be elevated and may even be lowered in some cases. The heating system can therefore be simplified, the components will be easier to manufacture, the operation will be more reliable, and the economic competitiveness will be improved.

The general safety concept of the nuclear heating plant is to protect the health and safety of plant personnel and avoid over-exposure in the normal operation of the plant and in case of incidents involving design anticipated (or unanticipated) radiation level. The criterion is to ensure that no radioactive and environmentally hazardous materials exceeding the safety limit would escape the plant. To achieve this goal, the nuclear heating plant must satisfy the following basic safety requirements.

1) In any operation conditions, there must be reliable means for shutting down the reactor and for maintaining the reactor in a shut-down state.

2) There must be reliable means for dealing with residual heat expelled by the reactor core; the method should be passive in nature.

3) There must be reliable means to ensure that radioactive materials released to the heating network and the environment do not exceed a certain set limit.

4) There must be procedures to ensure that reactor core meltdown would not occur in any operating conditions. The emergency plan should be such that no evacuation of residents outside the plant zone would be necessary.

2.3 Design criteria

To satisfy the above safety principles and requirements, the design, manufacture, installation and operation of the nuclear heating plant must follow corresponding safety regulations, criteria, and standards.

Since there is not yet a complete regulation, standard or code for NHP in China and abroad, the design of the 200MW NHP should follow the pertinent sections of the established Chinese safety regulations for nuclear power plants; in addition, it should also satisfy the following basic design criteria:

1) The design of the nuclear reactor should ensure that over the entire life of the reactor it should have a negative reaction coefficient.

2) The residual heat of the reactor core should be expelled by natural circulation.

3) Establish an intermediate circuit so that the reactor cooling system and the heating network are separated.

4) Under design standard incidents, the surface of the fuel elements must not exhibit boiling phenomenon.

5) Under design standard incidents, the reactor core must be submerged in coolant at all times.

6) Under incident conditions beyond the design standards, there should be sufficient buffer time for the operators to take the appropriate actions to alleviate the incident results.

2.4 Classification of facilities

Buildings, systems, equipment and components in a nuclear heating plant may be divided into two major classes: safety-critical items and safety-noncritical items. Safety-critical items include the following three types of buildings, systems, instruments and components:

1) When they malfunction (including operating errors), it may lead to radiation over-exposure of the working personnel of the plant zone or surrounding residents.

2) They are used to prevent anticipated operating conditions from developing into an accident situation.

3) They are used for alleviating incident results.

Safety-critical items should be assigned a safety class based on their function. Corresponding design criteria, earthquake resistance capability and quality level can then be established to satisfy the safety requirements. Safety-noncritical items all belong to the non-safety class and their design should satisfy the regular quality standards.

Since there is not yet material classification criteria, standards, or guides in China or abroad, the design of NHP is based mainly on the relevant criteria, standards, and codes for nuclear power plants (such as the Chinese nuclear safety guide HAF0201, the EJ315-88 standard approved by the former Ministry for Nuclear Industry, and safety guide IAEA50-SG-D1 of the International Atomic Energy Organization). The classification and design standards also take in the unique features of a NHP.

3. Technology Basis

Research and development results obtained in the last few years on the technology of low temperature nuclear heating and the experience gained from designing, constructing and operating the 5MW reactor formed the sound foundation for building the 200MW nuclear heating demonstration plant.

3.1 Technological approach

A complete series of computer software was developed during the construction of the 5MW low-temperature nuclear heating reactor. This series included physics, thermodynamics, structural mechanics, environmental impact evaluation, transient and accident analysis, and FRA. Many of these software are internationally recognized advanced analysis tools. A series of advanced analysis models was also established in applying these software with the characteristics of the heating reactor. These models and software are totally applicable to the 200MW reactor. Advanced design and analysis tools are therefore available to satisfy the design requirements.

3.2 Reactor design

The main design characteristics of the heart of the 200MW nuclear heating plant—the reactor—include unitized design, full power natural circulation, self-stabilization of pressure, dual vessel structure, fuel containing gadolinium, hydraulic control rod drive and storage of spent fuel. These features are all common to the design of the 5MW low-temperature experimental reactor for heating. The reactor design can therefore draw on the experience of the 5MW reactor.

3.3 System layout

The system layout of the 200MW nuclear heating system is in principle the same as that of the 5MW low-temperature nuclear heating reactor. The system layout of the heating station is simpler and smaller. Therefore, there are no upsetting factors in the design of the 200MW heating station.

3.4 Manufacture of large scale equipment

Some of the key facilities and components of the 200MW heating station, such as the pressure vessel, safety vessel, and main exchanger, are larger than those of the 5MW experimental reactor and require more stringent specifications. However, China's current technology level should be able to handle the manufacture of such components.

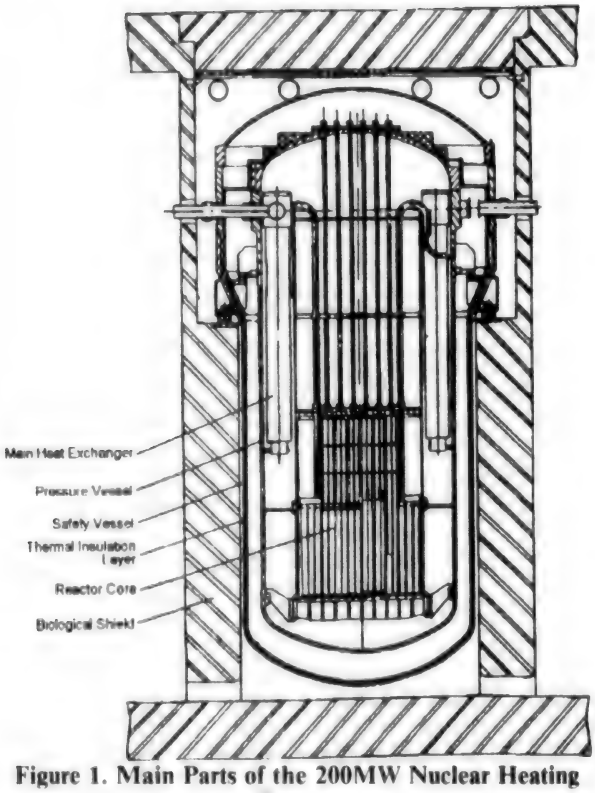

Figure 1. Main Parts of the 200MW Nuclear Heating Reactor

4. Overall Plan and Main Design Specifications

4.1 Overall plan and main parameters

The overall plan of the 200MW nuclear heating demonstration station is similar to that of the 5MW low-temperature nuclear heating experimental reactor. The design of the reactor uses a unitized layout, a full power natural circulation, self pressurization and dual vessel design. The main structure is shown in Figure 1. The main heat exchanger is located in the pressure vessel, the system pressure is maintained by the gas or steam space at the top of the vessel, the primary circuit has no circulation pump, and the circulation of the coolant relies on the density difference between the "hot zone" and the "cold zone" in the pressure vessel.

The reactor may be operated in two modes: the pressurized water mode and the microboiling mode. The latter mode can further elevate the natural circulation ability and the operating temperature; it can therefore produce low pressure saturated steam.

The safety vessel is in intimate contact with the pressure vessel and can endure the same pressure as the pressure vessel. The main heat exchanger uses U-shaped tubes for easier on-site inspection.

The reactor core is located at the bottom of the pressure vessel. In order to increase the driving force for natural circulation, there is a longer hydraulic lifting section (known as the "chimney") at the exit of the reactor core. Spent fuel is stored around the reactor. The reactor also uses a hydraulic drive for the control rod. In the primary circuit in the pressure vessel, the coolant flows through the core, absorbs the heat, and enters the main exchanger through the hydraulic lifter. The coolant transfers its heat to the water in the intermediate (second) circuit. Heat is output to the heating network (the third circuit) via the intermediate heat exchanger. The heating system therefore consists of three circuits—the first, second and third circuits. The reactor is not installed with an emergency core cooling system and the residual heat of the core is released to the final heat sink, the atmosphere. The secondary shut down method is in the form of a

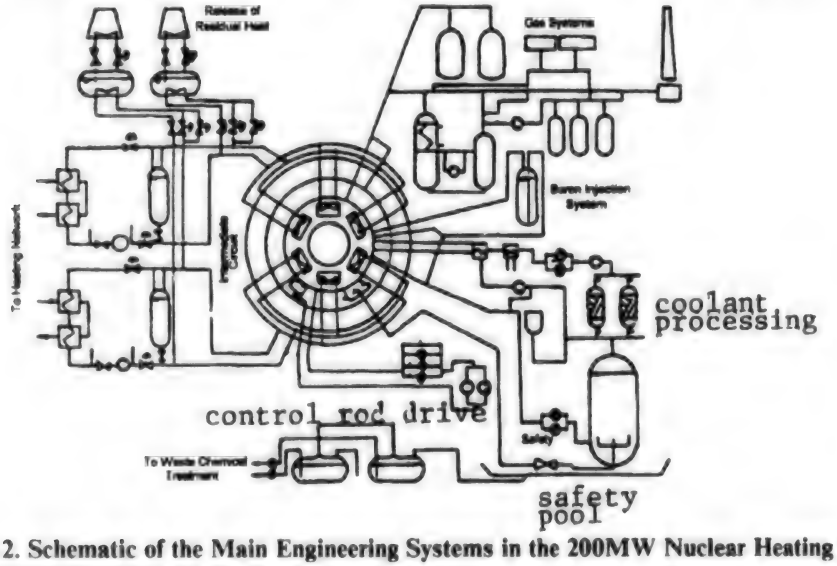

Figure 2. Schematic of the Main Engineering Systems in the 200MW Nuclear Heating Reactor

boron solution gravity feed system. The design of this system is based on the principle of in-mobility. In addition, there are also a few auxiliary systems.

The main engineering systems of the nuclear heating station are shown in Figure 2 and the main design parameters are listed in Table 2.

Table 2. Design Parameters of the 200MW Nuclear Heating Station

Nominal power of the heating station (MW)	200	200
Rated output power of reactor core (MW)	200	200
Rated output power of heating station (MW)	196	196
Operating pressure of reactor coolant (MPa)(1)	2.5	2.5
Entrance/exit temperature of reactor core (°C)	147/210	193.5/223.9
Operating pressure of intermediate circuit (pump entrance) (MPa)	3.0	3.0
Operating temperature of intermediate circuit (entrance/exit temperature of main exchanger) (°C)	90/140	130/195
Pressure of heating network (at two sides of central exchanger) (MPa)	0.9	0.9
Supply and return temperature of heating network (°C)	110/70	110/70(2)
Type of fuel assembly	12x12-3	12x12-3
Outer diameter of fuel rods (mm)	10.0	10.0
Type of control rod	Cross-shaped	Cross-shaped
Absorbent material of control rod	B_4C	B_4C
Material of combustible poisoning rod	Gd_2O_3	Gd_2O_3
Concentration of combustible poisoning rod %	3	3
Height of active zone of reactor core (m)	1.5	1.5
Equivalent diameter of first installed reactor core (m)	approx. 2.1	approx. 2.1
Zoned concentration of first load of fuel (%)	1.8/2.4/3.0	1.8/2.4/3.0
Initial fuel load (uranium metal) (tons)	12.6	12.6
Concentration of changed fuel (%)	3	3
Average unload consumption of equilibrium cycle (MW x d/t(U))	approx. 30000	approx. 30000
Average power density of reactor core (kWL^{-1})	38.6	38.6
Inner diameter of pressure vessel (m)	5.0	5.0
Net height of pressure vessel (m)	13.6	13.6
Number of main exchangers	6	6
Pipe specification of main heat exchanger	dia. 12x1	dia. 12x1

(1): All pressures quoted in table are absolute pressures.

(2): Under microboiling operating conditions, the reactor provides low pressure industrial steam in addition to heat.

The reactor and the associated auxiliary systems will be installed in the same building. Systems containing radioactive media will be concentrated in the underground or semi-underground of the building. In the zoning of the plant buildings and other systems, care was taken to minimize the contamination area in case of radioactive release. The design layout satisfied the access and transport requirements.

4.2 Key design considerations

The 200MW nuclear heating plant has all the advantages of the 5MW low-temperature nuclear heating experimental reactor. The key design considerations are described below.

1) The reactor has a unitized design, self-pressurization performance, and dual vessel structure. The first circuit of the reactor utilizes a unitized self-pressurization, and natural circulation design. With this design, the pressure vessel has no large diameter external pipes except a small number of small bore tubing. There are no large complex components outside the pressure vessel. This not only greatly reduces the probability for coolant leaks at the pressure boundaries, but also greatly reduces the seriousness in case there is a leak. Moreover, the safety vessel of the reactor is in intimate contact with the pressure vessel and is capable of withstanding a higher pressure. Even if there is a damage to the coolant pressure boundary in the safety vessel, the water level is guaranteed to cover the reactor core. These design considerations ensure that the reactor core will not be exposed under any circumstances. Therefore, there is no need for an emergency coolant system.

2) Natural circulation of coolant. The first circuit of the 200MW reactor has full power natural circulation of the coolant without the need for an external power. This design eliminated the primary circulation pump—a rotating part susceptible to damages, and improved the reliability of the cooling of the reactor. In the meantime, the most important safety system of the reactor, the residual heat release system, also uses natural circulation. Therefore, even if the reactor lost its external electric power source, it can still maintain normal cooling of the reactor core for a long time.

3) Reliable shut-down protection system. The control rod of the reactor uses a hydraulic drive system. The control rod does not extend beyond the pressure vessel and the working medium is the reactor coolant. The reactor uses a "fail safe" design principle; any interruption of the electric power, coolant flow, or pipe rupture will cause the control rod to fall. It is therefore inconceivable that this reactor can have a control rod jump out accident or other large reaction deviation accidents. Moreover, the reactor is also equipped with a non-kinetic boron injection system so that the reliability of the reactor shut down is elevated to an even higher level.

4) Installation of separation circuits. The heat transfer system uses a triple circuit design, that is, an intermediate circuit is installed between the primary circuit of the reactor and the heating network. The reactor coolant is therefore separated from the heating network. The operating pressure of the intermediate circuit is higher than that of the primary circuit. Together with a multitude of monitoring and separation devices, the leakage of radioactive water into the heating network is effectively prevented.

5) Low operating parameters and large thermal inertia. The operating pressure of the primary circuit of the reactor is about one-seventh of that of a pressurized water reactor. The volumetric power of the reactor core is less than one-half of that of a pressurized water reactor. Therefore, the fuel elements have a lower operating temperature and the rupture probability is correspondingly lower. In addition, the reactor contains a large amount of underheated water with a large heat capacity. Together with the triple circuit design, the changes of the process parameter are smoother even under transient or accident conditions.

6) The systems are simple to operate. For any design base incidents, the protection logic system generally triggers only two responses, namely, shutting down and opening the valve for releasing the residual heat. These reactions do not require operator intervention, which greatly reduces the possibility for operator's error.

5. Concluding Remarks

Based on the above description, the type and size of the reactor in the 200MW nuclear heating demonstration station are appropriate, the general plan is feasible, safety is assured, the technology is practical, and preliminary analysis shows that the heating plant is economically competitive.

Today the nuclear heating technology in China has entered the stage of industrial demonstration. With effort, the nuclear heating demonstration plant will surely be built. It will open up a broad future for low temperature heating nuclear reactors. This would give nuclear heating an important niche in future energy systems.

[Received May 13, 1992; revised April 10, 1993]

Wang Dazhong, male, 58, professor, graduated from engineering physics department of Qinghua University in Beijing in 1958 with a major in reactor engineering, presently director and chief engineer of the Institute of Nuclear Technology in Qinghua University.

Lin Jiagui, female, 59, professor, graduated from the Department of Dynamics, Nanjing College of Engineering, in 1956 with a major in thermodynamic devices, presently Deputy Director of the Institute of Nuclear Technology in Qinghua University.

Ma Changwen, male, 59, professor, graduated from the Department of Dynamics, Chongqing University, in 1956 with a major in electric generation, presently Deputy Chief Engineer of the Institute of Nuclear Technology in Qinghua University.

Inherent Safety Features of 200MW Nuclear Heating Reactor

94FE0589B Chengdu HE DONGLI GONGCHENG [NUCLEAR POWER ENGINEERING] in Chinese Vol 14 No 3, 15 Jun 93 pp 227-231, 255

[Article by Zhang Zuoyi [1728 0155 5030], Gao Zuying [7559 4371 3841], Wang Yansheng [3769 1750 3932] and Li Jincai [2621 6855 2088] of the Institute of Nuclear Energy Technology, Tsinghua University, Beijing]

[Text] All LOCA incidents for the 200MW nuclear heating reactor are analyzed in this paper. The analysis results show that the event sequences develop slowly and the reactor will automatically shutdown by means of the nuclear reactivity feedback of the moderator density. The reactor core is always covered with water. The 200MW nuclear heating reactor therefore has good inherent safety. In the event of loss of all heat sinks, the top of the reactor core will be uncovered with water after 51.6 hours. The frequency for this event is less than 10^{-12}/reactor year.

1. Design Features of the 200MW Heating Reactor

Figure 1 shows the cross sectional view of the 200MW heating reactor body. Thermodynamic and physical parameters of the reactor are listed in Table 1. Like the 5MW experimental heating reactor already in operation, the safety of the 200MW heating reactor is ensured by certain inherent, passive safety features. Unlike light water reactors, it does not require externally imposed safety devices such as the emergency cooling system. These passive mechanisms provide the reactor sound inherent safety characteristics and make it suitable for locations near cities.[1] The major safety features of the 200MW reactor are as follows:

(1) Full power natural circulation (shown in Figure 1)

After the reactor core heats up, coolant flows through the ascending tube and enters the upper cavity. Heat is released to the second circuit through six main heat exchangers arranged in an annular pattern. Cool water flows through the descending tube toward the bottom of the reactor core. The flow in the primary circuit is maintained by the density difference in the ascending and descending sections of the tube. This arrangement will eliminate all the accidents caused by the malfunction of the main circuit pump.

(2) The primary circuit has an integrated shell structure

The primary circuit is located inside a low pressure vessel. The vessel contains a large amount of coolant but has no large diameter outgoing main coolant pipes. All the outgoing pipes are concentrated at the upper part of the pressure vessel. This arrangement prevents any rupture of large diameter pipes like those in a pressurized water reactor.

(3) Dual shell pressure vessel

Outside the pressure vessel there is an adjacent safety vessel. All outgoing pipes from the pressure vessel have an isolation valve on each side of the safety vessel.

(4) The reactor core has a low power density and a negative moderator temperature reaction coefficient. The power density of the reactor core is about one-third of most PWR.

(5) The reactor has two independent passive residual heat cooling systems. Each system has an output power of 3MW and employs natural circulation. The residual heat can be unloaded as long as one of the systems is working.

(6) The operating pressure of the second circuit is higher than that of the primary circuit. This limits the discharge of primary circuit coolant to the second circuit in case of a broken heat exchanger tube.

Table 1. Major Parameters of the 200MW Nuclear Heating Reactor

Rated output power of reactor core (MWth)	200
Operating pressure of reactor coolant (MPa)	2.2
In/out temperature of reactor core (°C)	135/200
Primary circuit flow rate (kg/s^{-1})	705
Operating pressure of secondary circuit (MPa)	2.6
Operating temperature of secondary circuit (°C)	85/135
Height of active zone of reactor core (m)	2.1
Average power density of reactor core (kW/L^{-1})	27.6
Average linear power density of fuel rod (W/cm^{-1})	56.3
Maximum surface temperature of fuel rod (°C)	234
Maximum temperature of fuel block (°C)	987
Minimum DNBR of reactor core	2.86
Temperature coefficient of moderator ($°C^{-1}$)	-5.0×10^{-5}
Operating pressure of pressure vessel (MPa)	0.103
Operating temperature of pressure vessel (°C)	120

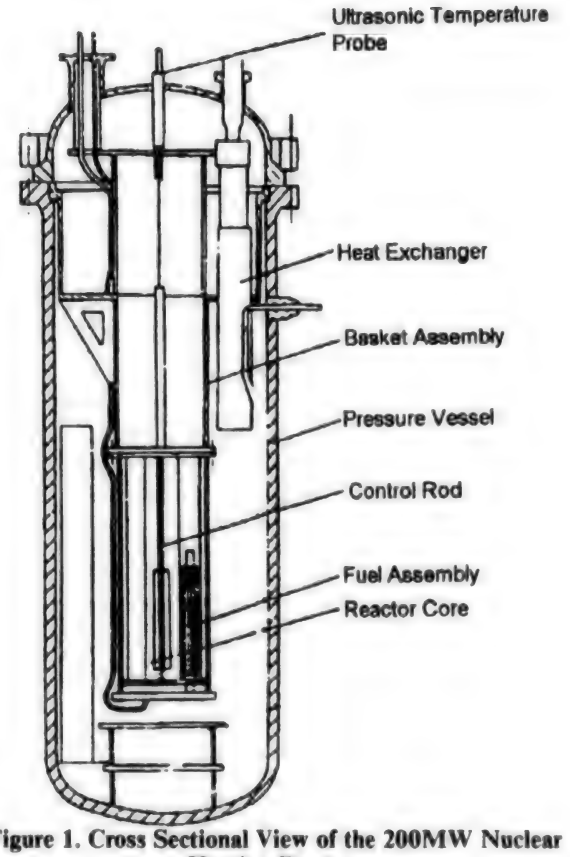

Figure 1. Cross Sectional View of the 200MW Nuclear Heating Reactor

2. Major Accidents of the Heating Reactor

When major ruptures occur to the main coolant pipe in most PWR, the reactor core will become exposed within a matter of tens of seconds and the surface temperature of the fuel elements will rise quickly. If the emergency cooling system was not activated immediately to spray water onto the reactor core, core melt-down will occur, with grave results of major radioactivity leak. The design concept of the nuclear heating reactor is to make the probability of core melt-down much lower than that of PWR even without elaborate emergency cooling systems. Based on internationally accepted standards, the probability of core melt-down can be totally eliminated so that the site of nuclear heating reactors may be located in the vicinity of cities.

As a very conservative assumption, the conditions that will prevent core melt-down are: (1) the reactor can be shut down safely under any circumstances, and (2) the core is always submerged in water. For the 200MW heating reactor, the core will always be submerged in water as long as the total water loss of the reactor vessel is less than 138.2 tons.

There are two types of causes for coolant loss and reactor core exposure. First, the heat output of the primary

circuit may decrease. When this happens, the increased pressure of the reactor vessel may cause the safety valve to open. Steam will then be released from the pressure vessel to the discharge tank. The second cause may be a major rupture in the primary circuit, which leads to a decrease of the total coolant. The most serious causes for coolant loss are: power outage and no boron injection by ATWS, rupture of boron injection tube, crack at the bottom of the pressure vessel, and safety valve stuck open.

In addition to accidents already considered in design standards, we considered cases of multiple malfunction and accidents not considered in the design standards. The probability for these accidents is extremely low, the purpose of the analysis is to show that, even under these extreme accidents, there will not be core melt-down. The multiple malfunction accidents considered are: (1) power outage, no boron injection by ATWS and safety valve stuck, (2) loss of all heat sinks (two residual heat systems, two secondary circuits, and water purification system all fail at the same time), (3) control rod water pipe broke and both stages of separation valves fail, and (4) boron injection tube broke ATWS.

3. Event Sequence Analysis

The purpose of event sequence analysis is to determine the maximum amount of water loss in an event. This is achieved through numerical simulation of the sequence of serious events described earlier that can lead to water loss from the reactor core. The computation uses the RETRAN-02 program[2] and makes detailed analysis of the events mentioned above.

3.1 Decrease of heat output from the primary circuit

3.1.1 Power outage, ATWS, no boron injection

This event refers to cases in which power outage or other reasons causes both intermediate circuits to be cut off, all control rods freeze up, boron water cannot be injected, and the shutdown function is lost. When this event occurs, the primary circuit loses its heat sinks, heat begins to accumulate in the heat exchanger and in the descending section, the natural circulation in the primary circuit goes down, the reactor core heats up, and the reactor power decreases because of the negative temperature feedback of the moderator. The heat given off by the fuel elements in the reactor core accumulates in the pressure vessel and causes the coolant temperature and the pressure to rise. At t = 146 sec, the safety valve first opens, but the valve reseats at t = 180 sec. At t = 701 sec, the reactor power drops to 8 percent of the rated value and the reactor shuts itself down. At 4000 seconds after the safety valve cycled eight times the heat power of the reactor becomes lower than the residual heat output power, the reactor core is constantly cooled and the safety no longer opens, hence the end of the event. Over the entire event sequence, the cumulative loss of water was 6 tons. Figures 2 and 3 show the event sequence.

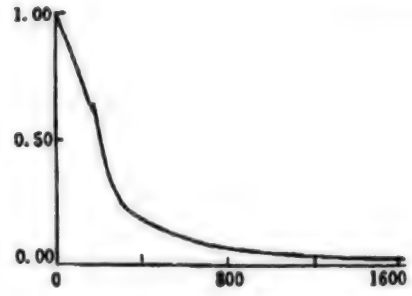

Figure 2.

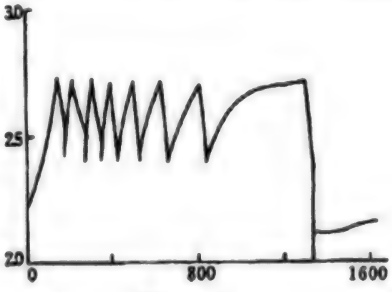

Figure 3.

3.1.2 Power outage, ATWS, no boron injection, and safety valve stuck open

This is the same situation as above but the safety valve is also stuck open. In the first 146 seconds after the secondary circuits are cut off, the temperature and pressure in the pressure vessel continue to rise and the safety valve opens to release steam to the outside. Since the average temperature of the reactor coolant is still higher than the reactor core exit temperature under normal operation, the reactor power begins to drop because of the negative feedback of the moderator temperature. After 670 seconds, the reactor power drops to 8 percent of the rated power and the reactor automatically shuts down. The sequence of events after this is the same as a safety valve stuck open; the maximum water loss is less than 35 tons. The positive reactivity in the later stage of the event brought upon by the temperature drop will be canceled by the bubbles formed after the reactor releases uncondensed gas. The reactor remains in the shut down state.

3.1.3 Loss of all heat sinks

We make the assumption of extremely rare multiple malfunctions that lead to simultaneous loss of both secondary circuits and both residual heat release systems, the loss of the water purification system, and the loss of all heat sinks of the reactor. The probability of such an event is extremely low. The event sequence may be divided into three stages: (1) the rise of temperature and pressure after the reactor shuts down, (2) the opening of the safety valve and the release of steam 2.47 hours after the incident, and (3) long term evaporation

while the pressure vessel is under normal pressure. After 51.6 hours, all the water above the reactor core exits would have evaporated and the liquid level would reach the exit of the reactor core.

The above analysis shows that, if no actions were taken in the first 51.6 hours after the reactor lost all its heat sinks, the liquid level in the pressure vessel would begin to fall below the top of the reactor. After two days and two nights, the residual heat generation would be 800kW. To ensure that the reactor core is covered by water at all times, the minimum flow rate of water replenishment is 1.3 t/h. A number of actions can be taken within the period of two days and two nights. For example, (1) start the reserve power source, (2) replenish the water in the reactor with the water replenishment system, (3) repair any one of the two secondary circuits, and (4) replenish the reactor water with a fire truck. The probability for exposing the reactor core is therefore small. Based on PRA analysis, this probability is less than 10^{-12}/reactor year. The event sequence curve is shown in Figure 4.

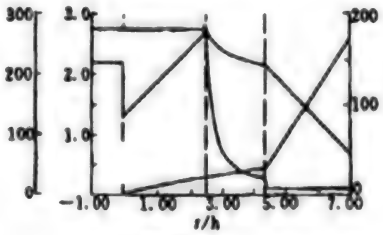

Figure 4.

3.2 Rupture events

3.2.1 Rupture of boron injection pipe

When the 50mm boron injection pipe ruptures, the liquid coolant in the pressure vessel will be released into the safety vessel. The liquid level will drop in the pressure vessel and the pressure will rise in the safety vessel. The reactor will undergo an emergency shutdown. After releasing liquid for 27 minutes, the liquid level in the pressure vessel will drop to the boron injection port. After that, the reactor will release steam. The two vessels will finally equilibrate at a pressure of 0.84 MPa until the steam is released. The amount of cumulated water loss from the pressure vessel during the event will be 97.4t.

3.2.2 Crack at the bottom of the pressure vessel

In the event of a 10cm^2 crack at the bottom of the pressure vessel, liquid coolant will be released into the safety vessel. This release will last for 5500 seconds until the pressure vessel reaches an equilibrium pressure of 0.92MPa. The total water loss will be 103.2t. The event sequence curves are shown in Figures 5 and 6.

3.2.3 Safety valve malfunctions and stays open

After the safety valve opens due to malfunction and becomes stuck open, steam and other uncondensed gas

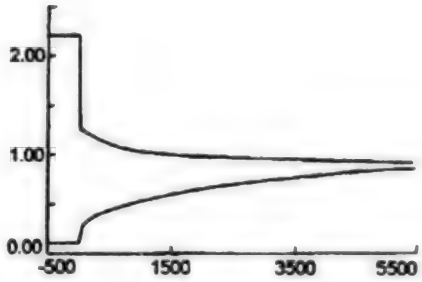

Figure 5.

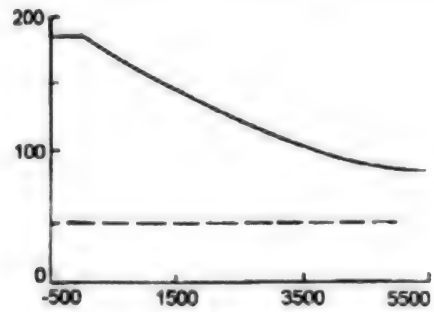

Figure 6.

in the pressure vessel will be released to the incident water tank outside the safety vessel. The heat carried out by the steam is equivalent to 15 percent of the rated power of the reactor. The temperature and pressure in the pressure vessel will continue to drop and reach the normal pressure after 4200 seconds. At the end of the release, the total water lost will be 22.7t.

3.2.4 Rupture of the hydraulic pipe for the control rod

After the rupture of the hydraulic pipe, liquid coolant is released to the large space at one atmosphere outside the safety vessel through a 100mm diameter rupture. After 3500 seconds, the temperature in the pressure vessel drops down to 100°C and the pressure reaches the normal pressure. At the end of release, 97.8 tons of water will be lost.

3.2.5 Rupture of boron injection pipe ATWS

Event analysis shows that 58 seconds after the rupture of the boron injection pipe, the top of the heat exchanger begins to become exposed. Subsequently, as the liquid level drops, the cross section of the flow from the upper cavity to the heat exchanger becomes smaller, the flow rate into the heat exchanger increases, and the circulation flow drops as the resistance increases. The temperature at the entrance of the reactor core remains basically unchanged. The reactor core heats up and the reactor power drops because of the reactive feedback of the moderator density. After 270 seconds, the reactor power

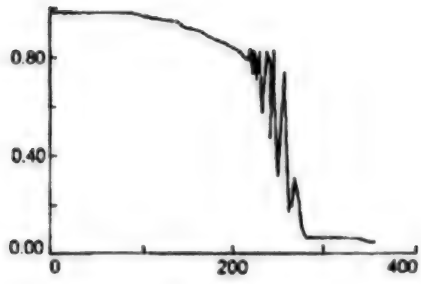

Figure 7.

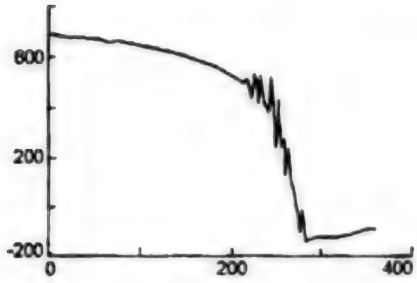

Figure 8.

drops down to 6.1 percent of full power and the reactor shuts down automatically. The curves of the shut down process are shown in Figures 7 and 8.

4. Conclusion

Event analysis shows that the 200MW heating reactor has good intrinsic safety due to the following main reasons: (1) The reactor can safely shut itself down automatically under the event conditions, (2) After the shut down, the enormous thermal inertia of the reactor makes the event evolve slowly. Even in the case of non-standard multiple malfunctions, there will be a relatively long period of time for taking appropriate actions.

Table 2 shows the analysis results for coolant loss events. Events responsible for coolant loss include the loss of heat sinks and pipe rupture. In the former, the cold end of the reactor's natural circulation will heat up, causing the driving force for natural circulation to decrease. This leads to a decreased flow rate and causes the reactor core to heat up. The reactor will automatically shut down due to the reactive feedback of the moderator density. In the case of a ruptured pipe, the liquid level in the pressure vessel drops, the resistance at the heat exchanger input increases, the circulation flow drops, and the reactor automatically shuts down due to the reactive feedback of the moderator density.

Table 2. Summary of Loss of Coolant Incidents

Event	Duration (sec)	Final Pressure (MPa)	Total Water Loss (t)	Amount of Water Above Core Exit (t)	Shut Down Charat.	Event Analysis
Power out, ATWS no boron inject			6.05	132.15	auto	IV
Power out, ATWS no boron inject safety valve stuck open		0.103	35.0	103.2	auto	non-std.
Loss of all heat sinks	51.6(h)	0.103	138.2	0.0	control rod fall	non-std.
Boron inject pipe rupture	4350	0.84	97.4	40.8	control rod fall	III
Crack at press. vessel bottom	5500	0.92	103.2	35.0	control rod fall	IV
Safety valve stuck open	4200	0.103	22.7	115.5	control rod fall	III
Rupture of hydraulic pipe for control rod	3550	0.103	97.8	40.4	control rod fall	non-std.
Rupture of boron inject pipe, ATWS		approx. 0.84	approx. 97.4	approx. 40.8	auto	non-std.

After the shut down of the reactor, there is a large amount of coolant above the reactor core exits. The latent heat of vaporization gives the reactor an enormous heat capacity. For a long period of time after the reactor shuts down (more than two days and two nights), the reactor does not need any external cooling. The reactor is in a sound state of cooling because the evaporation of the coolant absorbs the residual heat. Of all the events analyzed here, with the exception of losing all the heat sinks, the reactor does not require action and the reactor core will remain submerged in water for 51 hours. With two days and two nights to deal with the event, and considering that there are a number of remedial actions available, the probability of exposing the reactor core is less than 10^{-12}/reactor year.

References

1. Gao Zuying, Li Jincai and Qian Like. "5MW THR event analysis," Nuclear Power Engineering, 12(2), 14, (1991).
2. EPRI, RETRAN-02, A Program for Transient Thermal Hydraulic Analysis of Complex Fluid Flow System, NP-1850, 1981.

[Received August 12, 1992]

Zhang Zuoyi, male, 30, 1989 Ph.D. in reactor engineering, Qinghua University. Currently engaged in reactor engineering and safety research. Associate Scientist.

Gao Zuying, female, 56, 1965 graduate degree in reactor engineering, Qinghua University. Currently engaged in reactor engineering and safety research. Scientist.

Wang Yansheng, male, 36, 1985 Masters in Reactor Engineering, Qinghua University. Currently engaged in reactor engineering and safety research. Assistant Scientist.

Alternative Energy

Direction of Biogas Digester Development Analyzed

946B0121A Chongqing XIN NENGYUAN [NEW ENERGY SOURCES] in Chinese Vol 16 No 5, 5 May 94 pp 36-38

[Article by Zhu Jianxiang [2612 1696 3276], Hunan Rural Energy Office, Changsha]

[Text]

Abstract

This article describes the developmental direction of China's rural biogas digesters. The trend is toward small, high-efficiency, factory-produced units. The common features of small, high-efficiency biogas digesters are analyzed, with emphasis given to three representative models: upward flow float cover digester, diverted flow distributor type digester, and blocked flow automatic circulation digester.

Introduction

Biogas digesters in rural China play an important role for solving problems of energy shortage, environmental pollution, and agricultural ecology. Today there are about 5 million biogas digesters in China, with an annual output of more than 1 billion cubic meters of biogas. The great majority of these digesters are the Chinese-style hydraulic biogas digesters. Their low cost and compatibility with rural environment make them very popular in China and abroad. However, they also suffer from the following disadvantages: they require more sophisticated construction technology, their specific biogas output is low, their loading rate is low and the management of straw material is troublesome. Since the mid-1980s, China's biogas workers have been improving the biogas digester. Extensive research and demonstration has been carried out all over China and some superior models have emerged. These new models indicate the direction of biogas digester development in rural China.

The development direction is toward smaller, more efficient, factory-produced biogas digesters

In the last 10 years, as rural commodity economy developed in China, the promotion of biogas was also affected by the rules of the commodity economy. When the State cannot provide the biogas industry with substantial subsidies, the development must follow the rules of direct economic benefits. There are four factors that affect the direct economic benefits of a biogas system: first, the amount of biogas energy; second, the integrated utilization of the residual materials in biogas fermentation; third, investment in the biogas reservoir; and fourth, the management and operating costs of a biogas reservoir. The higher the efficiency in the comprehensive utilization of biogas and fermentation residue, and the lower the construction and management costs of the biogas pools, the more attractive and popular biogas will be. Farmers are therefore asking for the lowest possible construction cost for a biogas digester, a reduced digester volume, an improved digestive efficiency of the digester, reduced management need, and comprehensive utilization of the fermentation residue. In other words, they are asking for a new model of small, high-efficiency biogas digester to replace the current water pressure type of biogas digester. In addition, most of China's rural families use the biogas digester as an energy source and typically carry out the fermentation at ambient temperatures. The biogas digester needs only to be large enough to produce one day's gas consumption. The gas-producing efficiency of the new digester is much higher; volume reduction of home use biogas digesters is therefore a natural trend in their development.

A small, high-efficiency biogas digester can produce a greater volume of gas and requires a smaller volume to satisfy a given gas consumption. In recent years many research units, universities and colleges, and extension departments in China have conducted research on high-efficiency, small biogas digesters and have developed a number of models. In order to evaluate these devices uniformly, a national testing standard was formulated. On the other hand, farmers must also promote the biogas digester as a commercial product. In addition to the development of the small, high-efficiency digester, the digester must be easy to assemble and standardized. Factory production of small, high-efficiency biogas digesters has therefore become the development trend of China's rural usage of biogas.

As described above, China's development trend for the biogas digester is also a new direction internationally.

2. Current development status of China's small, high-efficiency biogas digester

A review of China's small, high-efficiency biogas digesters shows three mature and representative models: upward flow float cover digester, diverted flow distributor type digester, and blocked flow automatic circulation digester. Each of these models is described below.

2.1 Upward flow float cover digester

This model was developed by the Hunan Provincial Energy Resources Office and has been promoted nationwide. The volume of a single digester is 4 to 20 cubic meters.

The fermentation raw material enters the bottom of the anaerobic digester and the overflow material leaves from the top. Cotton-like high activity mud sinks under its own weight in the digester, providing a high level of active microbes in the digester. In addition, since the output device frequently stirs the mud at the bottom of the digester into the return flow, there is no thick sedimentation of mud at the bottom. These features greatly increased the digestive power and gas production rate of the device.

Experience shows that the upward flow digester has the following four advantages: 1) Its simple construction makes it easy and inexpensive to build; 2) It improves the gas production rate and digestive power under ambient temperature. At 10 to 15°C, the gas production rate reaches 0.20 to 0.30 $m^3/(m^3$ d). At 15 to 25°C, gas production reaches 0.30 to 0.60 $m^3/(m^3$ d). This rate is twice of that for a usual hydraulic type digester; 3) It improves the gas production rate and digestive power at low temperature. At a bath temperature of 10°C, the gas production rate using pig manure can be as high as 0.3 ^{3}3/(kg TS); and 4) It lowers the pressure in the digester, which makes construction easier and the service life longer.

2.2 Diverted flow distributor type digester

This type of digester was developed by the Biogas Office of Kunming Municipality. It uses human waste and animal manure as raw material for fermentation and has high gas production rate and raw material usage rate. It has been promoted in some provinces and cities in China.

This model retains the advantages of the hydraulic type digester and made the following improvements: 1) A grid is installed at the entrance to block off long fibers; 2) two flow-diverting plates are installed 450mm from the lower opening of the inlet; these diverters distribute the raw material input; 3) a blocking plate is installed 500mm from the lower opening of the output tube to retain the bacteria; 4) a hanging basket is installed under the top portal cover and at the middle of the digester; its main function is to fix the bacteria and remove floating material; and 5) the bottom of the digester tilts toward the output port at a 5-degree angle to facilitate the outward flow of fermented material.

2.3 Blocked-flow automatic circulation digester

This model was developed by the Chengdu Biogas Research Institute of the Ministry of Agriculture. It is suitable to use fecal material in this type of digester, which has been promoted in some regions in China. The digester structure has the shape of an elliptical cylinder. The top is a rectangular hydraulic cell. The input material goes through a straight pipe and the output material and waste are pushed out by a piston. The overflow liquid passes through the hydraulic cell and a reverse valve and is automatically recycled back into the digester. The reverse valve is a U-shaped tube and is installed near the inlet tube. The diameter of the U-tube is the same as that of the outlet tube so that the output device may be used for clearing the U-tube. By recirculating the liquid using the reverse valve, the bacteria are circulated. This allows the mixing of the bacteria with the new input material, which improves the digestive power and the material utilization.

Described above are four small, high-efficiency biogas digesters being promoted in China. Their design concepts all share the following characteristics:

First, in fermentation technology it is desirable to maintain the maximum amount of active bacteria in the digester. The uniform distribution of bacteria ensures good contact with the raw material and prevents the occurrence of "dead zones" or "short circuits" in the digester. This would solve the sedimentation and crusting problems in the digester.

Second, these models all have a relatively high gas production rate, a modest construction cost and sound direct economic benefits.

Third, the management and installation are simple, and the applicability is wide. These features make them easy to promote.

Foreign Broadcast Information Service (FBIS) and Joint Publications Research Service (JPRS) publications contain political, military, economic, environmental, and sociological news, commentary, and other information, as well as scientific and technical data and reports. All information has been obtained from foreign radio and television broadcasts, news agency transmissions, newspapers, books, and periodicals. Items generally are processed from the first or best available sources. It should not be inferred that they have been disseminated only in the medium, in the language, or to the area indicated. Items from foreign language sources are translated; those from English-language sources are transcribed. Except for excluding certain diacritics, FBIS renders personal names and place-names in accordance with the romanization systems approved for U.S. Government publications by the U.S. Board of Geographic Names.

Headlines, editorial reports, and material enclosed in brackets [ ] are supplied by FBIS/JPRS. Processing indicators such as [Text] or [Excerpts] in the first line of each item indicate how the information was processed from the original. Unfamiliar names rendered phonetically are enclosed in parentheses. Words or names preceded by a question mark and enclosed in parentheses were not clear from the original source but have been supplied as appropriate to the context. Other unattributed parenthetical notes within the body of an item originate with the source. Times within items are as given by the source. Passages in boldface or italics are as published.

SUBSCRIPTION/PROCUREMENT INFORMATION

The FBIS DAILY REPORT contains current news and information and is published Monday through Friday in eight volumes: China, East Europe, Central Eurasia, East Asia, Near East & South Asia, Sub-Saharan Africa, Latin America, and West Europe. Supplements to the DAILY REPORTs may also be available periodically and will be distributed to regular DAILY REPORT subscribers. JPRS publications, which include approximately 50 regional, worldwide, and topical reports, generally contain less time-sensitive information and are published periodically.

Current DAILY REPORTs and JPRS publications are listed in *Government Reports Announcements* issued semimonthly by the National Technical Information Service (NTIS), 5285 Port Royal Road, Springfield, Virginia 22161 and the *Monthly Catalog of U.S. Government Publications* issued by the Superintendent of Documents, U.S. Government Printing Office, Washington, D.C. 20402.

The public may subscribe to either hardcover or microfiche versions of the DAILY REPORTs and JPRS publications through NTIS at the above address or by calling (703) 487-4630. Subscription rates will be provided by NTIS upon request. Subscriptions are available outside the United States from NTIS or appointed foreign dealers. New subscribers should expect a 30-day delay in receipt of the first issue.

U.S. Government offices may obtain subscriptions to the DAILY REPORTs or JPRS publications (hardcover or microfiche) at no charge through their sponsoring organizations. For additional information or assistance, call FBIS, (202) 338-6735,or write to P.O. Box 2604, Washington, D.C. 20013. Department of Defense consumers are required to submit requests through appropriate command validation channels to DIA, RTS-2C, Washington, D.C. 20301. (Telephone: (202) 373-3771, Autovon: 243-3771.)

Back issues or single copies of the DAILY REPORTs and JPRS publications are not available. Both the DAILY REPORTs and the JPRS publications are on file for public reference at the Library of Congress and at many Federal Depository Libraries. Reference copies may also be seen at many public and university libraries throughout the United States.

END OF FICHE

DATE FILMED

27 Sep 94